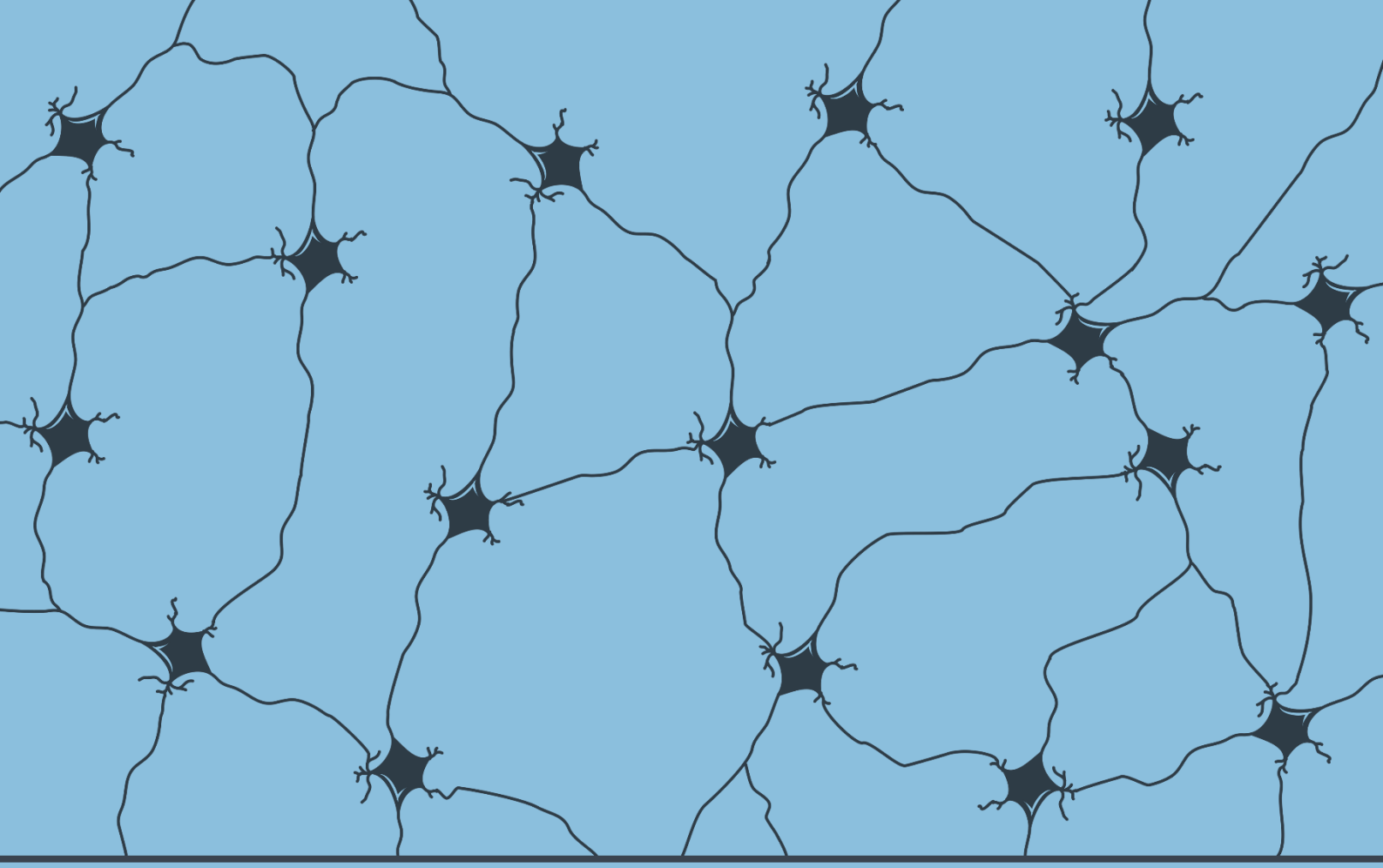

SYNAPTIC ALTERATIONS IN THE HIPPOCAMPUS OF AN ANIMAL MODEL OF PROGRESSIVE PARKINSONISM AND THE EFFECT OF DOPAMINERGIC TREATMENTS

Arantzazu Belloso Igueretegui

Doctoral Thesis

2022

eman ta zabal zazu

Universidad del País Vasco

Euskal Herriko Unibertsitatea

Synaptic alterations in the hippocampus of an animal model of progressive parkinsonism and the effect of dopaminergic treatments

Arantzazu Belloso Igueretegui

Directoras:

Dra. María Cruz Rodríguez Oroz

Dra. Ana Quiroga Varela

Memoria presentada para optar al título de Doctor
en Neurociencias por la Universidad del País Vasco

TESIS DOCTORAL

Donostia-San Sebastián, 2022

A mi familia

The research work presented in this doctoral thesis was developed at the Health Research Institute Biodonostia (IIS Biodonostia), the Center for Applied Medical Research (CIMA-Universidad de Navarra), and University of California Irvine (UCI) under the supervision of Dr. María Cruz Rodríguez Oroz and Dr. Ana Quiroga Varela, and was supported by a predoctoral grant from the Government of the Basque Country at 2016 call and by a grant for the mobility of predoctoral researcher staff from the Government of the Basque Country at 2019 call.

Acknowledgments

Me gustaría agradecer a todas las personas que me han apoyado de una u otra forma a lo largo de este camino.

En primer lugar, me gustaría agradecer a mis directoras. Mari Cruz, por darme la oportunidad de realizar esta tesis doctoral y destacar su potencial. Anna, por tu paciencia, tus consejos y por tu apoyo en los procesos de ensayo y error hasta dar con la combinación acertada. Gracias a las dos, sin vuestra ayuda este pequeño proyecto no hubiera salido adelante. También quiero agradecer a José Félix por su apoyo durante los primeros años de esta aventura y a Inma por ser siempre tan atenta.

A todos los compañeros del grupo de Parkinson, desde los inicios en Biodonostia, Leire, Haritz, Tatiana, Irene, Rosalía, Ana, por enseñarme todo lo que sabéis de neurociencias y más, por los buenos momentos en nuestro día a día, por las charlas en los cafés y las comidas. Belén, aunque no llegamos a coincidir codo con codo en Biodonostia siempre has estado ahí para ayudar en todo lo posible. Espero que por fin podamos celebrar como es debido todos los acontecimientos del grupo. No me quiero olvidarme del resto de compañeros del instituto, por todo lo aprendido con vosotros y por el maravilloso ambiente de compañerismo que se respira, ha sido un placer trabajar con vosotros.

De la etapa en el CIMA quiero agradecer en especial a Marta por todo su apoyo, su paciencia en las largas horas de confocal para conseguir la foto que lo cuadrara todo, y por sacarme una sonrisa en los experimentos perfectamente coordinados que parecían interminables. Al resto de compañeros del centro, en especial a los del 2.04 y 2.05, por alegrar el día a día y acogerme durante mis múltiples visitas.

También quiero agradecer a María, por su paciencia para analizar los resultados del PET. Los servicios de imagen y citometría del CIMA por resolver mis dudas y apoyarme a lo largo de los distintos experimentos.

Al grupo de proteómica de Navarrabiomed, Quique, Jokin, Mercedes, Karina, es un placer colaborar con vosotros.

I would like to thank Carl for accepting me in his lab at UCI MIND and giving me this amazing opportunity. Specially, I would like to thank Aleph for sharing his scientific knowledge, for his patience during those intense months, and for our musical exchanges. Andra, for our morning talks and weekend plans, over all, thank you for our friendship. I can't forget the rest of the group, Chris, Liqi, Nicole, Olivia, for making me feel part of these wonderful team.

Kuadrilla guztiari eskerrik asko, txikitatik bizi izan dugun guztiarengatik eta etorriko denarengatik. Naiz eta bakoitzak bide oso ezberdinak aukeratu ditugun beti hor egoteagatik, noizean behin nire txapak eta kezkak entzuteagatik eta elkarren artean dena errazagoa egiteagatik.

Como no podía ser de otra manera, aita y ama, por apoyarme a lo largo de este camino maravilloso, aunque un poco desconocido y en ciertas ocasiones complicado. Gracias por enseñarme los valores del trabajo y el esfuerzo para conseguir lo que uno se proponga. Al resto de la family, sobre todo izeba Arantza eta Pili, baita ere aitona, amona, izeba, osaba eta lehengusuak, eskerrik asko por interesamos por mis aventuras y regalarme unos momentos tan bonitos.

Eskerrik asko guztioi!

¡Muchísimas gracias a todos!

Summary

La enfermedad de Parkinson (EP) es el segundo trastorno neurodegenerativo más frecuente con una prevalencia global estimada de 6,1 millones de casos. La EP es causada por una degeneración gradual de las neuronas dopaminérgicas de la sustancia negra *pars compacta* (SNpc) y la consecuente depleción de dopamina en el estriado. Dicha disminución dopaminérgica da lugar a alteraciones en la fisiología de los ganglios basales, contribuyendo a la aparición de trastornos relacionados con el control del movimiento. Las manifestaciones clínicas más características de la EP son principalmente motoras, tales como el temblor de reposo, la rigidez y la bradicinesia. Histopatológicamente la EP se caracteriza por el depósito cerebral de cuerpos de Lewy y neuritas de Lewy, que son inclusiones intracelulares eosinofílicas que se encuentran en el citoplasma de las neuronas y neuritas, respectivamente. Estas inclusiones contienen agregados proteicos, siendo su principal componente la proteína α-sinucleina (α-syn). La agregación patológica de α-syn se ha descrito como uno de los mecanismos que contribuyen a la patogénesis de la EP, ya que una expresión elevada de α-syn por duplicaciones o triplicaciones del gen o diferentes mutaciones se han relacionado con la aparición y progresión de la enfermedad.

En este sentido, los depósitos anormales de α-syn junto con la pérdida neuronal asociada afectan a muchas otras regiones del cerebro, así como a otros sistemas de neurotransmisión como la acetilcolina, la noradrenalina o la serotonina, dando lugar a la aparición de manifestaciones cognitivas y conductuales de la EP o síntomas no-motores. Algunos de estos síntomas no motores, como por ejemplo la hiposmia o alteraciones del sueño entre otras, preceden en muchas ocasiones en años o incluso décadas a los signos motores (fase prodrómica o premotora). A lo largo de la progresión de la enfermedad, otros síntomas no-motores como el deterioro cognitivo leve o la demencia son bastante frecuentes, afectando negativamente a la vida diaria y contribuyendo al deterioro de la calidad de vida de los pacientes con EP.

El tratamiento farmacológico actual es sintomático y se centra en la reposición de dopamina mediante la administración del precursor de dopamina (L-DOPA) y/o agonistas dopaminérgicos como el pramipexol (PPX), actuando principalmente en los signos motores. Sin embargo, el uso prolongado de estos medicamentos se relaciona con la aparición de efectos secundarios como las discinesias (motor) o el trastorno de control de impulsos (TCI; no-motor).

El hipocampo es una estructura del sistema límbico ampliamente relacionada con los procesos de memoria y aprendizaje. Este núcleo también participa en el procesamiento de emociones, la toma de decisiones o el sistema de la recompensa mediante sus conexiones con otras estructuras del sistema límbico como la amígdala, la corteza prefrontal o el núcleo accumbens, respectivamente. En el hipocampo, la dopamina procedente de la vía mesolímbica

desde el área tegmental ventral (VTA) facilita los procesos de plasticidad sináptica promoviendo el almacenamiento de la memoria a largo plazo. Diversos estudios de imagen funcionales y estructurales han relacionado la disfunción y atrofia del hipocampo con problemas de memoria y progresión a demencia en pacientes con EP. Además, un incremento o una disminución de los niveles de dopamina en el hipocampo se ha asociado a la aparición de síntomas relacionados con la motivación en la EP tales como el TCI o la depresión, respectivamente. Sin embargo, los mecanismos subyacentes a la disfunción sináptica y la secuencia de los eventos patológicos, especialmente en el sistema límbico, continúa siendo una incógnita.

Por otro lado, la disfunción sináptica está emergiendo como uno de los eventos neurobiológicos tempranos y principales en el desarrollo de EP, apuntando a la sinapsis como clave en el inicio de la patología. Esto es debido a que la acumulación de la α-syn se produce principalmente en los terminales presinápticos, interfiriendo de manera directa en la maquinaria molecular a nivel sináptico y produciendo un malfuncionamiento en la liberación de neurotransmisores así como una pérdida de la conexión sináptica que darían lugar a la disfunción neuronal y la consecuente neurodegeneración, principalmente en las neuronas dopaminérgicas.

Es por ello que nuestra hipótesis plantea que la aparición de alteraciones cognitivas y conductuales en la EP está relacionada con una disfunción sináptica en el hipocampo causada por la acumulación de α-syn en las terminales presinápticas dopaminérgicas. Este fallo podría progresar hacia una degeneración de la vía mesolímbica dopaminérgica, que hasta cierto punto podría ser compensada por el tratamiento dopaminérgico. Así, las intervenciones terapéuticas tempranas centradas a revertir el fallo sináptico podrían prevenir o retrasar la degeneración dopaminérgica y evitar o aliviar los signos cognitivos y conductuales de la EP.

El objetivo general de esta tesis doctoral es estudiar la secuencia temporal de eventos sinápticos que tienen lugar en el hipocampo en un modelo experimental de parkinsonismo progresivo mediante la inoculación bilateral en la SNpc de un vector viral adenoasociado (AAV) que sobreexpresa la proteína α-syn humana (hα-syn) con la mutación A53T. Para ello, se ha realizado un estudio histológico de la vía mesolímbica donde se han caracterizado la SNpc y el VTA, así como el hipocampo a distintos puntos temporales post-inoculación (p.i.) de los AAVs: 1, 2, 4 y 16 semanas p.i. Además, se ha estudiado la evolución del comportamiento motor y cognitivo en los mismos puntos temporales. También se ha caracterizado la plasticidad sináptica (potenciación a largo plazo o LTP), y el efecto de dos tratamientos dopaminérgicos en la restauración de esa plasticidad en sinaptosomas aislados de hipocampo, en los estadios más tempranos de la expresión de hα-syn del modelo animal, antes de la aparición de manifestaciones

motoras. Asimismo, se ha llevado a cabo un el estudio proteómico mediante SWATH-MS en sinaptosomas aislados de hipocampo que nos ha permitido obtener una secuencia de procesos biológicos afectados a nivel sináptico. Finalmente, se ha realizado un estudio *in vivo* mediante tomografía por emisión de positrones (PET) para estudiar el metabolismo de la glucosa cerebral en el modelo de parkinsonismo con tratamiento crónico de PPX. El metabolismo de la glucosa es indicativo de la función sináptica debido a que la sinapsis es el compartimento celular fisiológicamente más activo de las neuronas.

Hasta la fecha, pocos estudios han analizado la degeneración dopaminérgica y la patología Lewy en el VTA y las consecuentes anomalías sinápticas que tienen lugar en el hipocampo. La mayoría de los estudios en modelos animales de parkinsonismo se han realizado utilizando modelos tradicionales mediante el uso de neurotoxinas que inducen una pérdida extensiva de las neuronas dopaminérgicas y carecen de un fenotipo progresivo, descartando su validez para estudiar la secuencia de eventos patológicos previos a la degeneración dopaminérgica. También se han realizado varios estudios en modelos animales transgénicos de genes asociados a la EP, particularmente, mediante la sobreexpresión de α-syn nativa o mutada. Sin embargo, la mayoría de los estudios se han centrado en la caracterización de la degeneración en la vía nigroestriatal, mientras que los pocos estudios centrados en el sistema límbico se han centrado exclusivamente en la caracterización cognitivo o conductual, así como en las alteraciones a nivel de plasticidad sináptica generalmente en estadios avanzados de la neurodegeneración dopaminérgica y/o expresión de la α-syn. Por tanto, falta una caracterización combinada tanto a nivel de VTA como del hipocampo desde el inicio de la expresión de α-syn y de la degeneración neuronal.

Los resultados del presente trabajo muestran que la inoculación bilateral del AAV-hα-syn en la SNpc produce una expresión progresiva de hα-syn en la SNpc y en el VTA desde la 1ª semana p.i., aumentando significativamente a la 4ª semana p.i. y manteniéndose a las 16ª semana p.i. Además, se observa una pérdida leve de neuronas dopaminérgicas del VTA desde la 1ª semana p.i. que se mantiene a lo largo del tiempo y precede a la pérdida observada en la SNpc, que no es significativa hasta la 4ª semana p.i. El VTA contiene principalmente neuronas dopaminérgicas, pero también otras poblaciones como neuronas GABAérgicas y glutamatérgicas. En el modelo animal AAV-hα-syn, hemos observado que la hα-syn se expresa no solo en las neuronas dopaminérgicas del VTA, sino también en neuronas glutamatérgicas del VTA que regulan la actividad local de las neuronas dopaminérgicas y también proyectan a regiones límbicas incluido el hipocampo donde modulan la plasticidad sináptica y la adquisición de memoria.

La hα-syn expresada en los somas neuronales de la SNpc y VTA se expande hacia las terminales axonales del hipocampo, observando hα-syn en el hipocampo desde la 1ª semana p.i., aumentando significativamente en la 4ª semana p.i. y manteniendo los niveles de expresión hasta la 16ª semana p.i. Dicha expresión se localiza principalmente en el giro dentado y en la región CA1 del hipocampo (las regiones de entrada y salida de la información del circuito interno del hipocampo) desde las etapas iniciales, expandiéndose hacia la región CA3 a partir de la 4ª semana p.i. Además, la hα-syn se encuentra dentro de las principales aferencias del VTA, colocalizando con las fibras dopaminérgicas principalmente en el hilio del giro dentado y la región CA1, con las fibras GABAérgicas en el hilio y la capa de células granulares del giro dentado, y ampliamente con las fibras glutamatérgicas a lo largo de todas las regiones del hipocampo.

Los animales AAV-hα-syn desarrollan una pérdida motora leve y una tendencia hacia un déficit cognitivo específicamente dependiente de hipocampo a la 4ª semana p.i. Asimismo, estos mismos animales muestran una inhibición de LTP en sinaptosomas del hipocampo desde la 1ª semana p.i., manteniéndose hasta la 4ª semana p.i. Por tanto, el fallo sináptico funcional es concomitante al inicio de la expresión de hα-syn en el hipocampo y a la degeneración dopaminérgica significativa en el VTA, precediendo el inicio de las manifestaciones motoras y cognitivas. La inhibición de LTP se asocia a una hiperexcitabilidad basal debida a un aumento de la expresión de los receptores postsinápticos AMPA. El agonista dopaminérgico PPX recupera parcialmente LTP a la 1ª y 4ª semana p.i. en los animales parkinsonianos, pero de manera interesante disminuye LTP en los animales controles. Por otro lado, la L-DOPA, precursor de la dopamina, recupera totalmente LTP a la 4ª semana p.i., pero no a la 1ª semana p.i., sin ejercer ningún efecto en los animales controles. El estudio de proteómica en la sinapsis hipocampal, muestra que en los puntos temporales más tempranos de la expresión de hα-syn en el hipocampo (1ª y 2ª semana p.i.), existe una desregulación significativa de los procesos de transporte intracelular asociados al citoesqueleto de actina y microtúbulos, además de alteraciones en el ciclo de las vesículas sinápticas, lo que en su conjunto podría alterar la liberación de neurotransmisores desde la terminal presináptica impidiendo una correcta comunicación neuronal y consecuentemente afectando a los procesos de plasticidad sináptica. En el punto temporal más avanzado (semana 16 p.i.), tras una prolongada expresión de hα-syn y una degeneración dopaminérgica leve y estable, se observa una desregulación de la homeostasis sináptica con alteraciones principalmente en la regulación del calcio, en la señalización a partir de receptores de membrana (especialmente receptores acoplados a proteína G inhibitoria), y alteraciones en la síntesis de proteínas, procesos biológicos clave para la función sináptica y el mantenimiento de los procesos de plasticidad sináptica a largo plazo.

Por último, el estudio *in vivo* del metabolismo de glucosa mediante PET en animales con tratamiento crónico con PPX muestra una reducción del metabolismo en el hipocampo anterodorsal únicamente en los animales con lesión dopaminérgica, aunque estén bajo el tratamiento dopaminérgico. Por tanto, los resultados obtenidos apoyan la relevancia que ejerce el deterioro de la función sináptica en el hipocampo, sugiriendo un posible papel en el desarrollo de signos cognitivos y conductuales asociados a la EP.

En su conjunto, los resultados de esta tesis doctoral muestran la importancia de la vía mesolímbica desde el VTA al hipocampo, destacando el fallo sináptico funcional temprano en el hipocampo y la afectación tanto de la vía dopaminérgica como la glutamatérgica en un modelo de parkinsonismo progresivo, lo que contribuye a la aparición de las alteraciones cognitivas. Los resultados de esta tesis doctoral abren la puerta a nuevas investigaciones que ahonden en su estudio para una posible intervención terapéutica temprana dirigida a dianas sinápticas a nivel funcional que podrían ralentizar y/o modificar el curso de las alteraciones cognitivas y conductuales desde las primeras etapas (antes de la lesión dopaminérgica clínicamente relevante).

Abbreviations

[^{18}F]-FDG	2-Deoxy-2-[^{18}F]-fluoroglucose
6-OHDA	6-hydroxydopamine
α-syn	α-synuclein
AADC	Aromatic amino acid decarboxylase
AAV	Adeno-associated viral vector
AMPAR	α-amino-3-hydroxy-5-methyl-4-isoxazolepropionic acid receptor
AP	Anterior-posterior
APP	Amyloid precursor protein
ATP	Adenosine triphosphate
a.u.	Arbitrary units
BPF	Bandpass filter
CA1-3	Cornu Ammonis 1-3
CAM	Cell-adhesion molecule
CaMKII	Calcium/calmodulin-dependent protein kinase II
cAMP	Cyclic adenosine monophosphate
CMV	Cytomegalovirus
CNS	Central nervous system
cLTP	Chemical long-term potentiation
COMT	Catechol-o-methyl transferase
CREB	Cyclic AMP-responsive element-binding protein
CSF	Cerebrospinal fluid
CT	Computed tomography
D1-5R	Dopamine receptors, subunits 1-5
DA	Dopamine
DAPI	4',6-diamidino-2-fenilindol
DAT	Dopamine transporter
DG	Dentate gyrus
DLB	Dementia with Lewy Bodies
DOPAC	3,4-Dihydroxyphenylacetic acid
DV	Dorsoventral
EPSC	Excitatory postsynaptic current
ER	Endoplasmic reticulum
EVV	Empty viral vector
FASS-LTP	Fluorescence analysis of single-synapse long term potentiation
FBS	Fetal Bovine Serum
FDR	False discovery rate
FL	Familiar location
FSC	Forward scatter
GABA	γ-aminobutiric acid
GAPDH	Glyceraldehyde-3-phosphate dehydrogenase
GluA1-4	AMPARs, subunits 1-4
GluN1	NMDAR, subunit 1
GluN2A-D	NMDARs, subunits 2A-D
GluN3A-B	NMDARs, subunits 3A-B
GPCR	G-protein coupled receptor

GPe	External globus pallidus
GPi	Internal globus pallidus
GWAS	Genome-wide association study
hα-syn	Human α-synuclein
HVA	Homovanillic acid
I/O	Input-output
ICD	Impulse control disorder
ICV	Intracerebroventricular
LB	Lewy body
L-DOPA	L-3,4 dihydroxyphenylalanine
LN	Lewy neurite
LPF	Long-pass filter
LRRK2	Leucine-rich repeat kinase 2
LTD	Long-term depression
LTP	Long-term potentiation
MAGUK	Membrane-associated guanylate kinases
MAO-B	Monoamine oxidase type B
MAPK	Mitogen-activated protein kinase
MCI	Mild cognitive impairment
mEPSC	Miniature excitatory postsynaptic current
mGluR1-8	Metabotropic glutamate receptors, subunits 1-8
ML	Mediolateral
MPTP	1-methyl-4-phenyl-1,2,3,6-tetrahydropyridine
MRI	Magnetic resonance imaging
n.a.	Not available
n.s.	Not significant
NAcc	Nucleus Accumbens
NAC	Non-amyloid component
NGS	Normal goat serum
NHS	Normal horse serum
NRS	Normal rabbit serum
Nrx	Neurexin
NL	Novel location
NMDAR	N-Methyl-D-aspartic acid receptor
OLT	Object location task
p.i.	Post-inoculation
PB	Phosphate buffer
PBS	Phosphate buffer saline
PBS-T	PBS with Triton X-100
PD	Parkinson's Disease
PDD	Parkinson's Disease dementia
PET	Positron emission tomography
PFA	Paraformaldehyde
PFC	Prefrontal cortex
PINK1	PTEN-induced putative kinase 1

PKA	Protein kinase A
PKC	Protein kinase C
PMT	Photomultiplier tube
PPF	Paired-pulse facilitation
PPX	Pramipexole
PSD	Postsynaptic density
RBD	REM sleep behavior disorder
REM	Rapid eye movement
ROD	Relative optical density
RT	Room temperature
SEM	Standard error of the mean
SDS	Sodium dodecyl sulfate
SLM	Stratum lacunosum-moleculare
SN	Substantia nigra
SNpc	Substantia nigra *pars compacta*
SNpr	Substantia nigra *pars reticulata*
SPN	Spiny projection neuron
SSC	Side scatter
STN	Subthalamic nucleus
SV	Synaptic vesicle
SWASH-MS	Sequential window acquisition of all theoretical mass spectra mass spectrometry
TARP	Transmembrane AMPAR regulatory protein
TBS	Tris buffer saline
TBS-T	TBS with Tween-20
TH	Tyrosine hydroxylase
vGlut2	Vesicular glutamate transporter 2
VMAT2	Vesicular monoamine transporter 2
VP	Ventral pallidum
VPS35	Vacuolar protein sorting 35
VTA	Ventral tegmental area
w	Week
WPRE	Woodchuck hepatitis post-transcriptional regulatory element
WT	Wild-type

Table of contents

Introduction

1. Parkinson's Disease

1.1. Epidemiology

Parkinson´s disease (PD) is the second most common neurodegenerative disorder with an estimated worldwide prevalence of 6.1 million individuals in 2016 (GBD 2016 Parkinson's Disease Collaborators, 2018), and an overall incidence of 40 new cases per 100,000 person-years (Hirsch et al., 2016). In Spain, the estimated prevalence of PD was 92,971 individuals in 2016 (GBD 2016 Parkinson's Disease Collaborators, 2018), and the incidence rate was 10 new cases every 100,000 person-year between 65 and 85 years (García-Ramos et al., 2016). PD is an age-related disease, with steadily increasing prevalence and incidence with age. The number of patients with PD worldwide has increased 2.4 times since 1990, which is partially explained by an increase in the number of older individuals (GBD 2016 Parkinson's Disease Collaborators, 2018). The number of cases with PD is expected to double by 2030, due to the increment in the current life expectancy of our society. This will lead to a high health system burden and socioeconomic repercussion, becoming this disorder a serious public health problem (Dorsey et al., 2007).

Numbers vary with sex, being the prevalence of PD 1.4 times higher in men than women (GBD 2016 Parkinson's Disease Collaborators, 2018). A protective effect of female sex hormones, a sex-associated genetic mechanism, or sex-specific differences in exposure to environmental risk factors might explain this male preponderance, although disparities in health care could also contribute (Cerri et al., 2019).

1.2. Neuropathology of Parkinson's Disease

1.2.1. Neurodegeneration of nigrostriatal dopaminergic system

The major pathological hallmark of PD is the selective and progressive neurodegeneration of the nigrostriatal dopaminergic neurons projecting to the striatum. Dopaminergic neurons located in the ventrolateral and caudal part of the substantia nigra *pars compacta* (SNpc; A9 area; Figure 1a) project their axons to the motor part of the striatum (rostral and dorsal areas of the caudate and putamen) (Björklund & Dunnett, 2007; Dickson et al., 2009). The progressive loss of dopaminergic neurons of the SNpc (Figure 1a-d) and the subsequent reduction of striatal dopaminergic innervation in PD patients causes a decrease in striatal dopamine (DA) concentration, which leads to a dysregulation of the basal ganglia circuitry and consequently, to the appearance of the cardinal motor signs of the disease (Dickson et al., 2009; Rodriguez-Oroz et al., 2009).

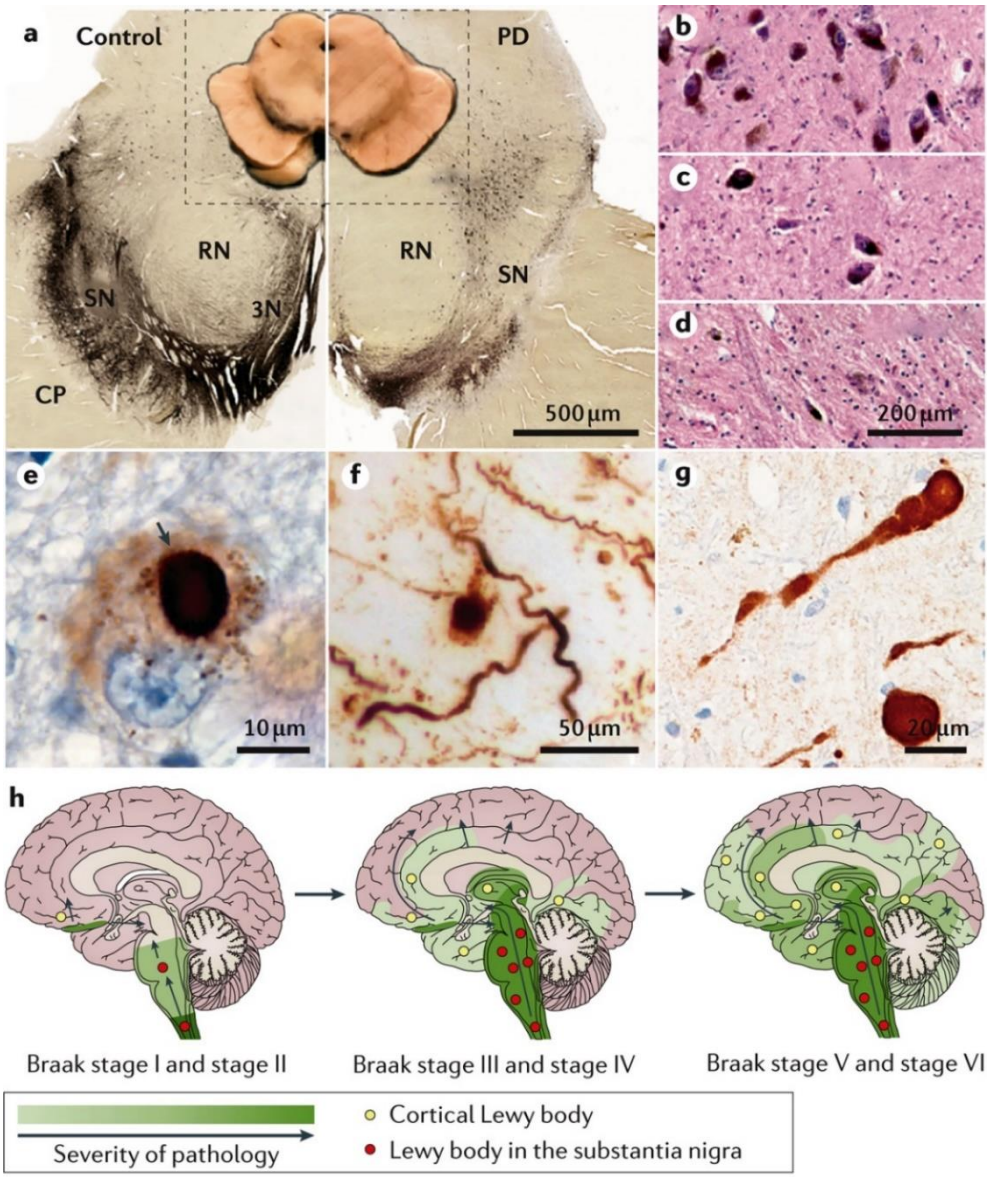

Figure 1. Neuropathological hallmarks of Parkinson´s Disease. A) Macroscopical and transverse sections of the midbrain upon immunohistochemical staining for tyrosine hydroxylase from a healthy control (left panel) and a PD patient (right panel). Selective loss of the ventrolateral parts of the SN is evident in the histological section of a PD patient. **B-D)** Hematoxylin and eosin staining of the ventrolateral region of the SNpc showing normal distribution of pigmented neurons in **B)** a healthy control, and diagnostically significant **C)** moderate or **D)** severe pigmented cell loss in PD. **E-G)** Immunohistochemical staining of α-syn shows the round, intracytoplasmic Lewy bodies (arrow in **e**), more diffuse, granular deposits of α-syn **(E-F)**, deposits in neuronal cell processes **(f)**, extracellular dot-like α-syn structures **(f)** and α-syn spheroids in axons **(g)**. **H)** The Braak theorized progression of α-syn aggregation in PD. α-syn inclusions occur in cholinergic and monoaminergic lower brainstem neurons in asymptomatic cases (Braak stage I and stage II), infiltrate similar neurons in the midbrain and basal forebrain in those with the motor symptoms of PD (Braak stage III and stage IV), and then are found later in limbic and neocortical brain regions with disease progression (Braak stage V and stage VI). From Poewe and coworkers (Poewe et al., 2017).

1.2.2. Lewy pathology

The other pathological hallmark of PD is the presence of concentric eosinophilic hyaline intracytoplasmic inclusions known as Lewy bodies (LBs) and Lewy neurites (LNs) that are found in the neuronal cell soma and processes, respectively (Lewy, 1912) (Figure 1e-g). The LBs are morphologically characterized for representing spherical cytoplasmic inclusions that show three different eosinophilic layers (nucleus, core, and halo). They are composed of misfolded or aggregated proteins that cellular degradation and reparation systems are not able to eliminate. The main component of these inclusions is the protein α-synuclein (α-syn), although other proteins such as ubiquitin and proteins of the neurofilament including TAU protein are also present (Irizarry et al., 1998; Spillantini et al., 1998). Interestingly, in a recent study LBs were found to wrap and encase vesicles, lysosomes, dysmorphic mitochondria, and disrupted cytoskeletal elements (Shahmoradian et al., 2019). LBs are mainly located in the dopaminergic neurons of the SNpc and the locus coeruleus, although they have also been observed in other brain structures like the basal nucleus of Meynert, hypothalamus, the dorsal raphe nucleus, the dorsal motor nucleus of the vagus, and pedunculopontine nucleus and even in limbic and neocortical brain regions (Braak et al., 2003; Sulzer & Surmeier, 2013). Thus, apart from nigrostriatal dopaminergic system pathology, extensive extranigral pathology is also observed in PD that leads to the dysregulation of other neurotransmitter systems such as noradrenergic, serotonergic, cholinergic, or glutamatergic systems (Barone, 2010; Sanjari Moghaddam et al., 2017), which may play a significant role in some of the non-motor symptoms of PD (Postuma et al., 2012; Schapira et al., 2017).

Lewy pathology has been hypothesized to progress in a stereotyped pattern throughout PD (Braak et al., 2003) (Figure 1h). Braak and coworkers performed α-syn immunohistochemistry in a large number of autopsy cases and suggested that toxic species of α-syn progressively reach different brain regions in a caudal-to-rostral direction that would explain the clinical-pathological progression of the disease. Based essentially on Lewy pathology, they suggested a six-stage scheme in which the pathology begins first at the olfactory bulb and the dorsal vagal nucleus and gradually follows an ascending course through the central brainstem that reaches the SNpc, culminating in widespread α-syn pathology at later stages and involving associative cortical regions.

However, Braak's hypothesis holds up for the majority, but not all the cases. On the one hand, it does not always correlate with the clinical severity or the neuronal loss (Jellinger, 2009). In addition, there are genetic forms of PD with clinical signs of the disease but no α-syn pathology (Schneider & Alcalay, 2017) and subjects with no signs of clinical PD but widespread α-syn

pathology (incidental PD) (van de Berg et al., 2012). On the other hand, aggregation of α-syn is not exclusive of PD, as it can be observed in other neurodegenerative synucleinopathies such as Dementia with Lewy bodies (DLB) and multiple system atrophy (Peelaerts et al., 2018).

1.3. Etiology

The mechanisms leading to neuronal degeneration in PD remain largely unknown. It is currently considered that the etiology of PD is likely to be a complex interplay among aging, environmental factors, and genetic predisposition (Pang et al., 2019; Simon et al., 2020).

1.3.1. Aging

Age is considered to be the main risk factor for developing PD. The prevalence and incidence of PD increase nearly exponentially with age and peak after 80 years (GBD 2016 Parkinson's Disease Collaborators, 2018; Hirsch et al., 2016). In addition, aging and PD share similar biological pathways. Dysregulation of oxidative stress, mitochondrial function, Ca^{2+} homeostasis, proteostasis, and neuroinflammation are involved in the natural course of aging, as well as in neurodegenerative processes such as PD (Hou et al., 2019; Vanni et al., 2020). During aging, the reduction in protein clearance systems is consistent with observations of increased levels of α-syn within nigral dopaminergic neurons (Chu & Kordower, 2007). Moreover, the vulnerability of dopaminergic neurons increases with age, making them more susceptible to silent toxics (Surmeier et al., 2017; Vila, 2019). Thus, the combination of aging and the pathological mechanisms associated with PD could lead to cellular stress and the onset of the disease.

1.3.2. Environmental factors

Environmental exposure to several factors also represents a risk factor for the development of PD (Ball et al., 2019). Neurotoxins such as 1-methyl-4-phenyl-1,2,3,6-tetrahydropyridine (MPTP) and pesticides like paraquat and rotenone have been associated with PD. Epidemiological studies show a 2.5-3 times higher risk of developing PD after exposure to pesticides (Pang et al., 2019). Moreover, these toxins have classically been used to model parkinsonism in animals, as they lead to dopaminergic neuronal cell death possibly by impairing mitochondrial functionality and increasing oxidative stress (Bové et al., 2005). Long-term exposure to several heavy metals such as iron, manganese, lead, and copper, have also been associated with an increased risk of developing PD. Heavy metals are essential cofactors for a variety of

biological processes, however, abnormally high levels can lead to oxidative stress, mitochondrial dysfunction, or protein misfolding, contributing to PD pathogenesis (Raj et al., 2021).

Interestingly, other environmental factors were associated with a decreased risk for developing PD. An inverse association has been suggested for cigarette smoking and coffee consumption, probably due to the effect of nicotine and caffeine on the central nervous system (CNS) (Noyce et al., 2012). Physical activity and vitamin E showed a protective effect on epidemiological and animal studies, as well as some drugs such as the non-steroidal anti-inflammatory ibuprofen or β2-adrenoreceptor agonists (Belvisi et al., 2020).

1.3.3. Genetic factors

Over the past 20 years, several causative genes and genetic risk variants have been associated with PD. To date, a total number of 23 loci and 19 causative genes have been identified, yet with a certain degree of heterogeneity regarding phenotypes, age-onset, and inheritance mode. It is estimated that about 5-10% of all PD cases are inherited, while the majority are idiopathic PD cases with unknown causes (Del Rey et al., 2018). Genetic studies have helped not only to identify genetic risk factors for PD development but also to elucidate the pathogenesis of the disease.

The first gene identified to be associated with inherited PD was *SNCA* (PARK1/4), which encodes the protein α-syn. Polymeropoulos and colleagues described for the first time a point mutation in the *SNCA* gene in a few families with adult-onset autosomal-dominant PD (Polymeropoulos et al., 1997). This finding led to the identification of α-syn as the main component of LBs (Spillantini et al., 1998). Since then, six pathogenic point mutations A53T, A30P, E46K, H50Q, G51D, and A53E have been associated with PD, all of which occur in the N-terminal amphipathic region (Cherian & Divya, 2020). Duplications (Chartier-Harlin et al., 2004) and triplication (Singleton et al., 2003) of the gene have also been described, with more severe clinical phenotype in patients with *SNCA* triplication than duplication, suggesting a dose-dependent association between disease severity and *SNCA* gene dosage (Chartier-Harlin et al., 2004). Moreover, genome-wide association studies (GWAS) have shown that single nucleotide polymorphisms in this gene increase the risk of developing sporadic PD (Campêlo & Silva, 2017), thus strengthening the role of α-syn in PD pathogenesis in both familial and sporadic cases of the disease.

Other PD-causative genes with an autosomal dominant inheritance include *LRRK2* (PARK8) and *VPS35* (PARK17). Mutations in *LRRK2* are the most common form of familial PD,

accounting for 1-2% of all PD cases. Several gain-of-function mutations have been identified to cause PD such as G2019S, N1437H, R1441C/G/H, Y1699C, and I2020T, with incomplete penetrance and dependent on age and specific mutation (Alessi & Sammler, 2018; Tolosa et al., 2020). Some of these mutations are highly prevalent in specific populations, such as the G2019S in the Ashkenazi Jews (Ozelius et al., 2006) and North African Berbers (Lesage et al., 2006), or the R1441G in the Basque Country where it accounts for 46% of all inherited PD cases (Ruiz-Martínez et al., 2010). *LRRK2* encodes the leucine-rich repeat kinase 2, a large multi-domain protein with GTPase and protein kinase activity involved in multiple cellular processes, including neurite outgrowth and synaptic morphogenesis, membrane trafficking, autophagy, and protein synthesis and phosphorylation (Rosenbusch & Kortholt, 2016). Recently, LRRK2 kinase activity has also been described to play a role in synaptic vesicle (SV) endocytosis (Arranz et al., 2015). In addition, *VPS35* encodes for vacuolar protein sorting 35 of the retromer complex involved in the retrograde transport from endosomes to the trans-Golgi network and recycling of cargo proteins such as membrane-bound receptors like glutamate α-amino-3-hydroxy-5-methyl-4-isoxazolepropionic acid receptors (AMPARs) or DA D1 receptors (D1Rs). Other cargo proteins of the retromer complex include degradative enzymes with lysosomal function, amyloid precursor protein (APP), and α-syn proteins (Rahman & Morrison, 2019).

Autosomal-recessive forms of PD include homozygous and heterozygous loss-of-function mutations in genes such as *PRKN* (PARK2)*, PINK1* (PARK6)*,* and *DJ-1* (PARK7). Although relatively rare among general PD populations, they account for a large proportion of early-onset PD (Cherian & Divya, 2020). *PRKN* encodes for the protein parkin, an E3 ubiquitin ligase, whereas *PINK1* encodes for PTEN-induced putative kinase 1, a serine-threonine protein kinase, both proteins involved in the elimination of damaged mitochondria through mitophagy (Ge et al., 2020). *DJ-1* is an oxidative stress sensor and antioxidant protein also suggested to act as a chaperone to prevent α-syn fibrillation through the chaperone-mediated autophagy (Dolgacheva et al., 2019). Furthermore, pathogenic mutations in other genes such as *ATP13A2*, *PLA2G6*, *FBXO7*, *VPS13C, DNAJC6*, and *SYNJ1*, have also been linked to autosomal recessive early-onset atypical parkinsonism. *ATP13A2* and *PLA2G6* have a lysosomal function (Bras et al., 2012; Lin et al., 2018), while *FBXO7* participates in the ubiquitin-proteasome system and mitophagy (Joseph et al., 2018). *VPS13C* is a protein involved in vesicular transport and mitochondrial maintenance (Lesage et al., 2016), and *DNAJC6* and *SYNJ1* code for auxilin and synaptojanin1, respectively, proteins involved in SV endocytosis (Nguyen et al., 2019).

In addition to PD-causative mutations, common genetic variants in several genes have been identified to increase PD susceptibility. In recent years, a high worldwide prevalence of

mutations in the gene *GBA*, encoding the lysosomal enzyme β-glucocerebrosidase, have been described in PD patients, ranging from 2% to 30% (Sidransky & Lopez, 2012). In homozygosis, *GBA* mutations cause recessive Gaucher's disease, a lysosomal storage disorder. *GBA* variant carriers exhibit a 5- or 10-fold greater risk of developing PD in heterozygosis or homozygosis, respectively, supporting the importance of protein clearance mechanisms in PD pathogenies (Behl et al., 2021). Other genes related to increased risk for PD include *MAPT* and *SH3GL2*, involved in microtubule formation (Cherian & Divya, 2020), and SV endocytosis (Nguyen et al., 2019), respectively.

Recently, epigenetic alterations have also been suggested to play a role in PD pathogenesis. Apart from genetic mutations, abnormal changes in epigenetic mechanisms such as DNA methylation, post-translational modifications of histones, chromatin remodeling, and small and long non-coding RNAs have been linked to PD (Rathore et al., 2021).

1.4. Pathogenesis

Despite the great progress in the understanding of the molecular basis of neurodegeneration in PD of the past years, the pathogenesis of the disease is not completely understood yet. PD is currently considered to be due to a combination of aging and abnormalities in several highly interconnected cellular mechanisms such as protein homeostasis, aggregation, degradation via ubiquitin-proteasome and lysosomal autophagy systems, mitochondrial function, oxidative stress, Ca^{2+} homeostasis, glutamate receptor-mediated neuronal excitotoxicity, synaptic dysfunction, and neuroinflammation. Epidemiological findings, pathological observations, and genetic discoveries have helped elucidate the role of these biological pathways in PD pathogenesis.

Genetic studies have established a direct link between PD and synaptic function, with some of the PD-causative and risk factor genes such as *SNCA*, *LRRK2*, *DNAJC6*, *SYNJ1,* and *SH3GL2*, involved in SVs trafficking and neurotransmitter release (Nguyen et al., 2019; Soukup et al., 2018). Furthermore, DA itself can contribute to PD pathogenesis. In normal physiological conditions, DA in the synapse is rapidly pumped into SVs through the vesicular monoamine transporter 2 (VMAT2) in order to prevent its cytoplasmatic oxidation into highly toxic quinones and reactive oxygen species production (Meiser et al., 2013). In PD patients, the activity of the VMAT2 is reduced (Pifl et al., 2014), which together with defective SV endocytosis can lead to cytosolic DA accumulation, oxidative stress, and mitochondrial and lysosomal dysfunction, contributing to neuronal toxicity (Blesa et al., 2015). Moreover, functional and structural studies in

humans and rodent animal models have shown that synapse loss and axonal degeneration precedes the death of the soma of dopaminergic neurons in the SNpc (Kordower et al., 2013; Wong et al., 2019). Thus, the synapse may be a key cellular compartment in early PD pathogenesis. Advances in the understanding of synaptic dysfunction in PD will be further detailed in the following sections of this doctoral thesis.

1.5. Clinical features and diagnosis

The first description of the disease was made by James Parkinson in 1817 in an essay entitled "*An essay on the Shaking Palsy*" (Parkinson, 1817). In this essay he observed a handful of people who showed resting tremor and gait disturbances in his daily walks in London, describing for the first time the motor signs of the disease. Currently, PD is clinically characterized by the presence of motor signs, such as resting tremor, rigidity, and bradykinesia (Jankovic, 2008; Postuma et al., 2015), also known as the cardinal signs of the disease. These signs appear due to the progressive loss of the dopaminergic neurons of the SNpc leading to dopaminergic denervation of the striatum (Dickson et al., 2009; Rodriguez-Oroz et al., 2009). It is estimated that these cardinal motor signs appear when there is about 30–60% of dopaminergic neuron loss together with a 70–80% loss of dopaminergic terminals and 50–75% neurite degeneration (Cheng et al., 2010). Since the original descriptions, the conceptualization and clinical spectrum of the disease continue to evolve, and nowadays, in addition to the motor signs, numerous non-motor manifestations are also recognized to be related to the neurodegenerative process of the disease (Postuma & Berg, 2019).

Classical diagnosis of PD occurs with the onset of motor signs (early-stage PD). However, the diagnosis is preceded in most cases by a prodromal phase of years or even decades characterized by specific non-motor signs (D. Berg et al., 2015; Postuma et al., 2012) (Figure 2). In this sense, several studies point that the neurodegenerative process of the SNpc could antedate in 12-14 years the occurrence of parkinsonian motor signs (Postuma et al., 2012; Postuma & Berg, 2019). Thus, this prodromal period could provide a potential temporal window to study pathological events leading to massive dopaminergic degeneration. In addition, during this period, a disease-modifying therapy, once it becomes available, could be administered to prevent or delay the neuronal degeneration and the development of the disease (Siderowf & Lang, 2012). Besides, over the course of the illness (mild and late-stage PD), there is an emergence of complications related to the progression of the neurodegeneration and the long-term dopaminergic treatment, including both motor and non-motor manifestations (Hely et al., 2005) (Figure 2).

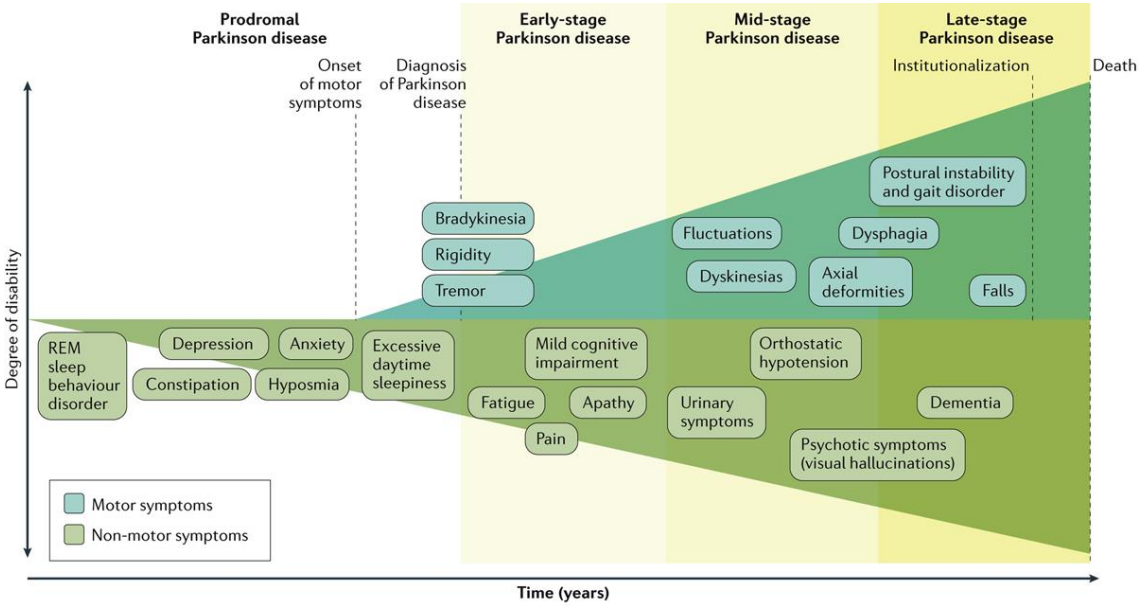

Figure 2. Clinical symptoms and time course of Parkinson's disease progression. Diagnosis of PD occurs with the onset of motor signs such as bradykinesia, rigidity, and tremor (early-stage PD). Diagnosis can be preceded by a prodromal phase of years or even decades, which is characterized by specific non-motor symptoms like REM sleep behavior disorder, constipation, depression, anxiety, hyposmia, and excessive daytime sleepiness (prodromal PD). Progression of the disease is driven by a combination of motor (postural instability and gait disorders, dysphagia, and frequent falls) and non-motor features (fatigue, pain, apathy, mild cognitive impairment, urinary symptoms, orthostatic hypotension, and dementia), along with long-term complications of the dopaminergic therapy (fluctuations, dyskinesia, impulsivity, and psychosis), causing clinically significant disability. From Poewe and coworkers (Poewe et al., 2017).

1.5.1. Motor signs

PD is clinically characterized by the presence of motor signs, such as resting tremor, rigidity, and bradykinesia (Jankovic, 2008; Postuma et al., 2015). The disease has usually an asymmetric onset, with unilateral signs in one limb. As the neurodegeneration progresses, they spread to the other ipsilateral limb, and, subsequently, the contralateral hemibody is affected. In addition, since the onset of the disease, axial involvement occurs in the form of facial hypomimia, decreased blinking, or hypophonia (abnormal weakness of the volume or timbre of voice) (DeMaagd & Philip, 2015; Postuma et al., 2015).

Resting tremor is present in about 70% of PD patients at the time of diagnosis, although most patients will develop this motor sign during the progression of the disease (Rajput et al., 1991). This tremor in PD occurs at rest when the majority of patients show a typical movement of

the fingers known as "pill-rolling" that consists of a tendency to join the thumb and index and perform semi-circular movements. Tremor increases with distraction maneuvers and disappears with the execution of voluntary movements with the affected limb or during sleep (Jankovic, 2008).

Rigidity is the persistent resistance and difficulty for passive movement of the joints of limbs, caused by an increased muscular tone or an excessive and continuous muscular contraction. The rigidity of limbs can be uniform or show increased or decreased tone and it increases when other body parts are moved or when talking (Jankovic, 2008).

Bradykinesia (slow execution of movements) and hypokinesia (reduction of movements) are the motor signs that mostly impair PD patients, as they interfere with the activities that require precise movement control. These motor signs consist of a difficulty to perform the whole movement process, from planning to execution, and encompass the loss of facial expressiveness, decreased arm swing when walking, or reduction of voluntary or automatic movements (Berardelli et al., 2001; Rodriguez-Oroz et al., 2009).

Other motor aspects that stand out in these patients not at the diagnosis, but later in the progression, are the gait disturbances and postural instability, which leads to impaired balance and frequent falls. PD patients present failure of postural reflexes, they walk with short steps, shuffling and with difficulty in the initiation, turning around, or approaching a destination (freezing of gait), being the latter a manifestation of more advanced stages of the disease. Other signs also frequent in the evolution of the disease are difficulty to swallow food (dysphagia) and speech disorders (dysarthria), which can be very disabling (Jankovic, 2008).

1.5.2. Non-motor signs

During the past decade, non-motor signs have gained importance. They are present to a variable degree throughout all stages of PD, some of them even before the onset of the cardinal motor signs (Postuma et al., 2012; Schapira et al., 2017) (Figure 2). During the prodromal phase, these symptoms can be characterized by impaired olfaction (hyposmia) (Doty, 2012), constipation (Fasano et al., 2015), neuropsychiatric disturbances such as depression, apathy, and hallucinations (Aarsland et al., 2009; Pagonabarraga et al., 2016), sleep-wake cycle disorders (Chahine et al., 2017) and rapid eye movement (REM) sleep behavior disorder (RBD) (Postuma et al., 2012). In the early stages of PD, it is frequent the presence of fatigue, and mild cognitive impairment (MCI) affecting early executive functions and working memory (Chahine et al., 2016; Delgado-Alvarado et al., 2016), apathy, and pain (Conte et al., 2013). As the disease advances, non-motor symptoms become increasingly prevalent and represent a substantial challenge in the clinical management

of these patients (Hely et al., 2005). Autonomic dysfunction, such as urinary incontinence, constipation, orthostatic hypotension (Pfeiffer, 2020), hallucinations, and other psychotic manifestations are common non-motor features in the late stages of PD (Ffytche et al., 2017). Dementia is also particularly prevalent, occurring in 83% of patients with PD at 8-12 years of disease evolution (Aarsland et al., 2017; Hely et al., 2005). In contrast to MCI, cognitive deficits in dementia are severe enough to impair daily life, such as social and occupational functioning, and personal care, independently of the motor and autonomic signs. Parkinson's disease dementia (PDD) is characterized by visual-spatial constructional deficits and recognition, semantic and episodic memory loss (Kehagia et al., 2010; Schapira et al., 2017). These non-motor symptoms directly contribute to the deterioration of the quality of life of PD patients. In fact, 28% of patients indicated in one study that non-motor abnormalities were more disabling than motor signs (Barone et al., 2009).

1.6. Pharmacological treatment

Lack of preventive or neuroprotective treatments makes the progression of the disorder unavoidable. Current clinical management is focused on the replacement of DA in order to alleviate the motor signs and improve the quality of life of PD patients (Schapira, 2009).

The DA precursor L-3,4-dihydroxyphenylalanine (L-DOPA) has been the gold standard treatment for PD since its discovery more than 50 years ago (LeWitt & Fahn, 2016). However, after prolonged periods of use, it is known to cause motor complications such as wearing off (reappearance of motor signs) and dyskinesia (involuntary movements) (Bastide et al., 2015; de Bie et al., 2020). Although these complications are still not completely understood, they are suggested to be related to non-physiological short-duration pulsatile stimulation of DA receptors due to the short half-life of L-DOPA. Several strategies have been developed to achieve dopaminergic stimulation in a more physiological manner, such as the addition of aromatic amino acid decarboxylase (AADC) as well as catechol-o-methyl transferase (COMT) inhibitors that prevent peripheral metabolism of L-DOPA, monoamine oxidase type B (MAO-B) inhibitors to prolong and increase synaptic DA concentrations, continuous drug delivery systems, or drugs with longer half-life such as dopaminergic agonists (Poewe et al., 2017; Schapira, 2009).

Dopaminergic agonists directly stimulate pre- and postsynaptic DA receptors, mainly targeting the DA D2 receptor (D2R) family, including D2R/D3R/D4R (Gerlach et al., 2003). With a longer half-life than L-DOPA, dopaminergic agonists induce a less pulsatile stimulation of DA receptors, markedly reducing the risk of inducing motor complications. However, the

improvement is usually partial and transient, and their long-term use is associated with the appearance of neuropsychiatric and behavioral side-effects such as impulse control disorders (ICDs) (Voon et al., 2017). In particular, dopaminergic agonists with high affinity for D3Rs, such as pramipexole (PPX), have been associated with ICDs (Voon et al., 2011a; Weintraub et al., 2010), probably through the abnormal activation of these receptors in the ventral striatum, overstimulating the brain reward system (Steeves et al., 2009). ICDs encompass a heterogeneous group of disorders and are described as the failure to resist a temptation, urge, or impulse that may be harmful to oneself or others. Classic ICDs include pathological gambling, compulsive shopping, hypersexuality, and binge eating among others (Weintraub & Claassen, 2017). These severe complications of the dopaminergic treatment can have a great impact on the personal, familial, psychosocial, financial, and quality of life of PD patients and their families.

Apart from pharmacological therapy, surgical options such as deep brain stimulation of the subthalamic nucleus also have an important role for a subset of patients with PD and help to reduce some motor signs such as stiffness, tremor, and slowness of movement, as well as motor complications (Rodriguez-Oroz, 2010). Recently, exciting cutting-edge approaches with less invasive technologies such as magnetic resonance-guided focused ultrasound for the treatment of motor signs in PD have been advanced (Martínez-Fernández et al., 2018).

Despite remarkable advances in the symptomatic treatment of motor signs of the disease, two major therapeutic challenges remain to be addressed. First, disease-modifying treatments to slow down or prevent the progression of neurodegeneration, and second, development of effective treatments for non-motor features of the disease as well as treatment-related complications.

2. Basal Ganglia and the Limbic System

2.1. Basal Ganglia

The basal ganglia are an interconnected group of grey matter nuclei located in the deep encephalon, comprising the striatum, globus pallidus with its external (GPe) and internal (GPi) segments, subthalamic nucleus (STN), substantia nigra (SN) with its *pars compacta* (SNpc) and *pars reticulata* (SNpr) portions, and the ventral tegmental area (VTA).

Anatomical and functional studies performed in the 1980s helped understand the organization of basal ganglia. Initially, five parallel circuits were described considering their cortical origin, including motor, oculomotor, dorsolateral prefrontal, lateral orbitofrontal, and anterior cingulate circuits (Albin et al., 1989; Alexander et al., 1986). All circuits share a similar structure as they originate in a cortical area that projects to the striatum, which in turn, connects to the output nuclei (GPi and SNpr) that project to the thalamus. Finally, the thalamus encloses the circuit projecting back to the cortical areas. According to their functions, these anatomic loops can be clustered into motor (motor and oculomotor circuits), associative (dorsolateral prefrontal and orbitofrontal circuits) and limbic (anterior cingulate circuit) circuits (Figure 3). The motor circuit connects primary motor and premotor cortices with the dorsal striatum, while the associative circuit connects the dorsolateral prefrontal cortex (PFC) and lateral orbitofrontal cortex with the striatum, and the limbic circuit connects the ventral striatum, also known as the nucleus accumbens (NAcc), with ventromedial PFC, medial orbitofrontal cortex, anterior cingulate cortex, amygdala, and hippocampus (Groenewegen, 2003; Groenewegen & Uylings, 2010). Importantly, the segregation of circuits is maintained within each nucleus of the basal ganglia, with dorsolateral areas implicated in motor functions, medial zones in associative processes, and the ventral ones in limbic functions (Figure 3). The motor circuit is implied in the refinement of motor functions, the associative circuit is involved in cognitive functions such as executive function and procedural learning, and the limbic circuit is involved in emotional processing (Rodriguez-Oroz et al., 2009).

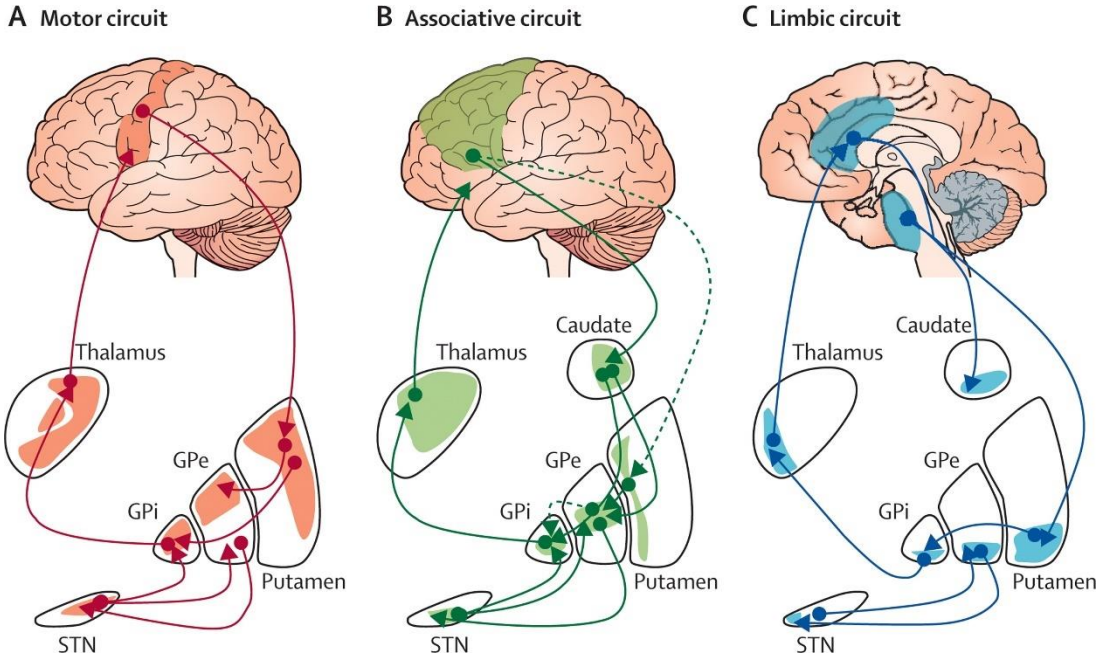

Figure 3. Anatomic and functional organization of the basal ganglia. The basal ganglia are divided into **A)** motor, **B)** associative, and **C)** limbic subregions, which are topographically segregated, as indicated by colored areas in red, green, and blue, respectively. Abbreviations: GPe, external globus pallidus; GPi, internal globus pallidus; STN, subthalamic nucleus. From Rodriguez-Oroz and coworkers (Rodriguez-Oroz et al., 2009).

2.1.1. Dopaminergic pathway: regulation of the basal ganglia

The SNpc and VTA are the major sources of DA in the brain. Based on connectivity and morphological studies, midbrain dopaminergic neurons are separated into dorsal and ventral tiers. Cells located in the dorsal part of the SNpc and VTA (dorsal tier) project to limbic and cortical areas as well as to some parts of the striatum, while neurons in the ventral part of the SNpc/VTA (ventral tier) innervate preferentially to the striatum (Bentivoglio & Morelli, 2005; Björklund & Dunnett, 2007).

According to the target efferent nuclei, midbrain dopaminergic neurons give rise to three main dopaminergic pathways: nigrostriatal, mesolimbic, and mesocortical pathways. The nigrostriatal pathway originates from the ventral tier neurons in the SNpc, and projects to the striatum. It is engaged in voluntary and automatic motor control and associative learning (dorsal striatum), and reward-related processes (ventral striatum). Dopaminergic neurons from the dorsal tier in the VTA project to the ventral striatum, septum, amygdala, and hippocampus through the mesolimbic pathway and participate in the regulation of reward-related processes. The mesocortical pathway also arises from the dorsal tier and innervates PFC, cingulate and perirhinal cortices involved in the regulation of executive functions such as working memory and attention

control (Arias-Carrión et al., 2010; Björklund & Dunnett, 2007). Because of the overlap between the mesolimbic and mesocortical pathways, they are often collectively referred to as the mesocorticolimbic system.

The SNpc contains dopaminergic neurons, which are enriched in neuromelanin, a byproduct of DA auto-oxidation and a natural pigment that gives the characteristic black color to this nucleus. The VTA contains not only dopaminergic neurons but also GABAergic and glutamatergic neurons. Dopaminergic neurons account for 60-70% of VTA neurons, while GABAergic and glutamatergic neurons account for 22% and 16%, respectively (H. J. Kim et al., 2019). The latter two neuronal populations send local projections to regulate the activity of dopaminergic neurons as well as long-range connections in parallel to dopaminergic neurons to cortical and limbic regions including NAcc, lateral habenula, PFC, amygdala, and hippocampus, most of which project back to the VTA (Adeniyi et al., 2020; Morales & Margolis, 2017; Ntamati & Lüscher, 2016; Taylor et al., 2014).

2.1.2. Motor circuit

The major input nucleus of the basal ganglia is the striatum. It receives glutamatergic projections from cortical and thalamic regions, and dopaminergic inputs from the SNpc and VTA (Joel & Weiner, 2000; Lanciego et al., 2012). Thus, the striatum acts as an integrative hub for glutamatergic and dopaminergic inputs assisting in the selection of appropriate behaviors through its outputs to downstream basal ganglia structures (Redgrave et al., 1999). GABAergic spiny projection neurons (SPNs), which comprise over 95% of total striatal neurons, are classically divided into two populations based on their output projection patterns and DA receptor expression profile, giving rise to the two main output projections of the striatum, the direct and indirect pathways (Burke et al., 2017; Gerfen et al., 1990). SPNs expressing mainly D1Rs represent approximately half of the SPN population and send dense projections to the GPi and SNpr, forming the direct pathway of the basal ganglia. By contrast, SPNs expressing mainly D2Rs project to the GPe, which sends inhibitory projections to the STN, constituting the indirect pathway. The STN sends glutamatergic excitatory projections to the GPi/SNpr, which are considered the main output nuclei of the basal ganglia, mainly projecting inhibitory inputs to the lateral region of the thalamus. Finally, the thalamus encloses the circuit projecting back glutamatergic excitatory inputs to the cortical areas. Thus, activation of the direct pathway disinhibits principal thalamic neurons leading to the activation of the motor cortex, facilitating motor action. By contrast, the activation of the indirect pathway ultimately inhibits thalamic neurons that lead to a lack of activation of the

motor cortex and consequently suppress motor behavior (Albin et al., 1989; Obeso et al., 2002) (Figure 4A).

The dopaminergic system plays a major role in the regulation of basal ganglia circuits. The release of DA at the striatum from nigrostriatal neurons plays a differential modulatory effect on the SPNs at the origin of both direct and indirect pathways (Gerfen, 2000). DA exerts its effects by binding to dopaminergic receptors, which belong to the G-protein-coupled receptor (GPCR) superfamily, specifically, D1Rs are coupled to stimulatory Gs and Golf G-proteins while D2Rs are coupled to inhibitory Gi/o subunits. Activation of D1Rs on the SPNs of the direct pathway exerts a facilitatory effect by increasing intrinsic excitability. On the other hand, activation of D2Rs decreases intrinsic excitability leading to an inhibition of the SPNs of the indirect pathway. Thus, the net effect of the dopaminergic innervation is a decreased inhibition of thalamic neurons and facilitation of inputs to the cortex (Gerfen & Surmeier, 2011; Obeso et al., 2002) (Figure 4A).

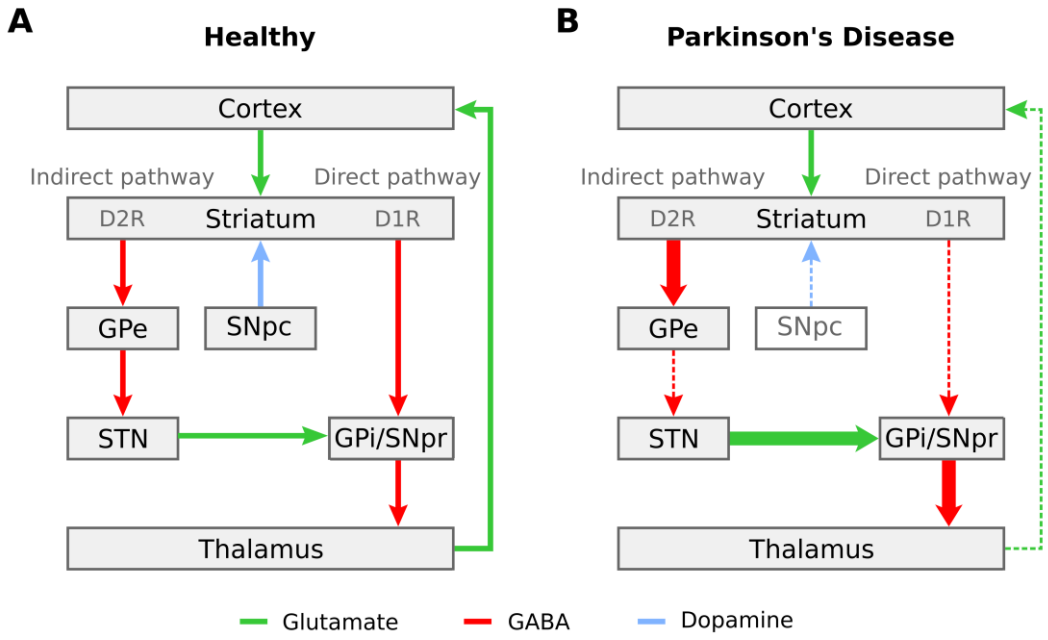

Figure 4. Basal ganglia circuitry. A) In a healthy state, dopamine modulates the basal ganglia motor circuit by activating the direct pathway through the D1Rs and decreasing the activity of the indirect pathway via D2Rs, ultimately disinhibiting thalamic neurons and favoring motor behavior. **B)** The degeneration of the nigrostriatal pathway in Parkinson's Disease leads to a potentiation of the indirect pathway coupled to a decreased activity of the direct pathway, ultimately inhibiting thalamic neurons and thus, suppressing motor activity. Green arrows represent excitatory glutamatergic projections, red arrows inhibitory GABAergic projections, and blue arrows modulatory dopaminergic projections. Abbreviations: GPe, external globus pallidus; GPi, internal globus pallidus; SNpc, substantia nigra *pars compacta*; SNpr, substantia nigra *pars reticulata*; STN, subthalamic nucleus.

2.1.3. Dysregulation of the motor circuit in Parkinson's Disease

The degeneration of the nigrostriatal pathway leads to an imbalance of the direct and indirect pathways of the motor circuit (Gerfen, 2000; Gerfen et al., 1990). Thus, it causes a decrease of the inhibition of the indirect pathway, reducing the activity of GPe and increasing the activity of STN, which in turn hyperexcites the GPi and SNpr. In addition, the direct pathway is hypoactivated increasing the activity of both GPi and SNpr. The hyperactivity of these nuclei leads to increased inhibition of the thalamus, reducing the stimulation of the motor cortex (Albin et al., 1989; Kravitz et al., 2010; Obeso et al., 2002) (Figure 4B).

Beyond the motor circuit, the anatomo-functional organization of the basal ganglia is particularly important to understand the pathophysiological mechanisms underlying the expression of clinical signs of PD. The initial loss of neurons in the ventral tier of SNpc, which leads to striatal dopaminergic denervation predominantly in the dorsolateral striatum (motor area), spreads progressively so the dopaminergic denervation reaches more medial and ventral areas (associative and limbic areas) (Figure 3). For this reason, motor deficits are the first signs of the disease, but executive dysfunctions or some neuropsychiatric disorders found in PD patients at different disease stages can be explained, at least partially, by the progressive dopaminergic deficit gradually altering both associative and limbic loops (Rodriguez-Oroz et al., 2009). Moreover, both the functional organization of basal ganglia nuclei and the gradual loss of the dopaminergic projections are also crucial when trying to understand the mechanisms underlying the side effects caused by dopaminergic drugs used for the treatment of motor signs in PD.

2.2. Limbic system

The limbic system is comprised of several interconnected cortical and subcortical structures. The circuit originally described by Papez in 1937 includes the hippocampus, fornix, mammillary bodies (hypothalamus), anterior nuclei of the thalamus, and cingulate cortex. Later on, in 1948, Yakovlev proposed that the amygdala, orbital and medial PFC, insula, and anterior temporal lobe play a crucial role in emotion and motivation. It was not until a few years later that MacLean proposed an integrative model for the limbic system based on Papez's and Yakovlev's previous work (Catani et al., 2013; Rolls, 2015) (Figure 5). Thus, two networks comprise the limbic system, one involved in the regulation of learning and memory processes based on the hippocampus and related structures, and another regulating emotion and motivation based on the amygdala and related structures. It has been suggested that memory and emotional systems comprise separate networks, as they involve largely different brain structures and connections

(Rolls, 2015). However, emotions are often part of episodic memories, and positive or negative events are better remembered than neutral events, supporting the interconnection between both systems. Furthermore, the amygdala and hippocampus are both anatomically and functionally connected (Fastenrath et al., 2014; Phelps, 2004; Y. Yang & Wang, 2017). Interestingly, both the hippocampus and the amygdala as well as cortical regions such as the PFC project to the NAcc, which is nowadays also considered part of the limbic system, linking basal ganglia to the limbic system (Rolls, 2015; Sesack & Grace, 2010).

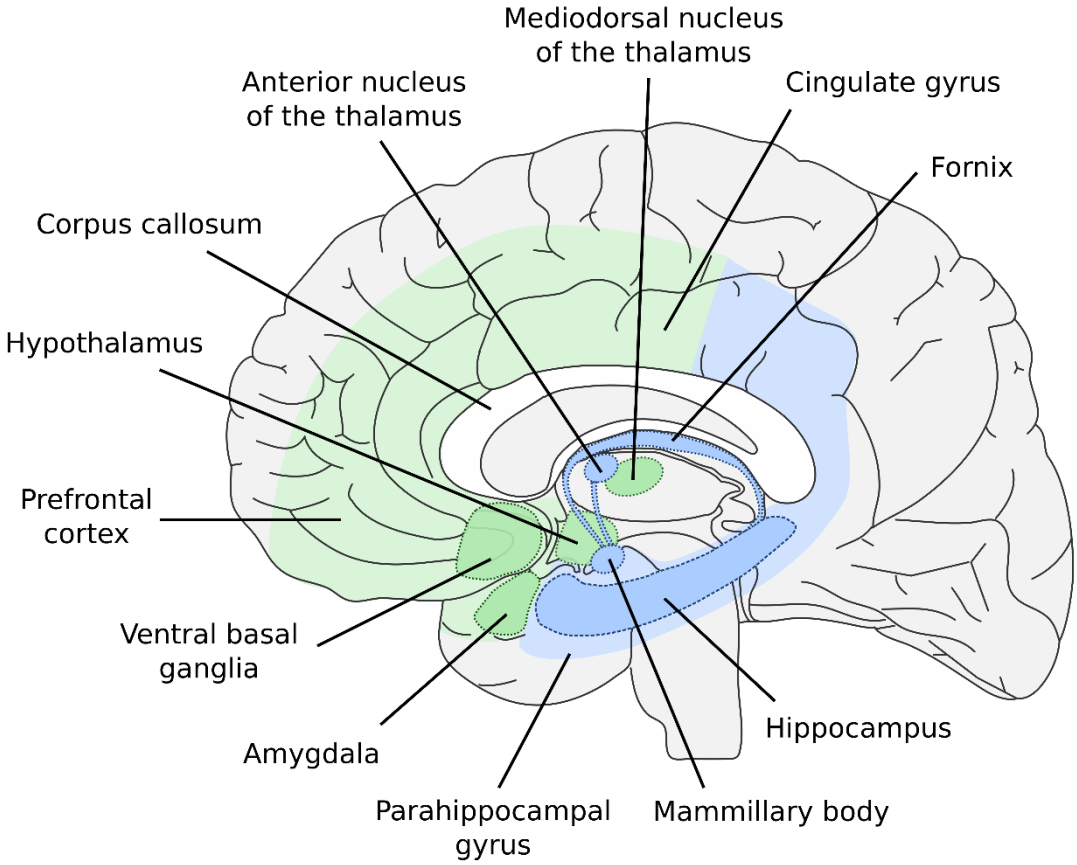

Figure 5. Limbic system networks. Blue areas show brain nuclei involved in learning and memory processes and green areas show brain nuclei participating in emotion and motivation processing. Adapted from Purves et al., 2004.

2.2.1. The hippocampus

The hippocampus has classically been related to learning and memory processes, as it is critical for the acquisition and long-term establishment of memories. It is particularly important for episodic memories, a type of declarative memory that is rapidly acquired and references to events in a specific time and place (Lisman et al., 2011; Squire et al., 2004). It has been suggested that declarative memory may participate in decision-making processes that require information processing, updating, and integration, allowing us to blend past experiences with future goals to drive appropriate behaviors and decisions. Thus, the hippocampus may participate together with the PFC, in behavior processing as well as executive functions such as the ability to switch between goals, planning, organizing, or decision-making (Gupta et al., 2009; Rubin et al., 2014). Furthermore, in the last years, the hippocampus has also been described to participate in reward-related processes and goal-directed behaviors, through its connections with the NAcc (Gauthier & Tank, 2018; LeGates et al., 2018), supporting the role of the hippocampus not only in memory and learning process but also in behavior.

The hippocampal formation consists of the dentate gyrus (DG), Ammon's horn, which is further divided into Cornu Ammonis 1 (CA1), 2 (CA2), and 3 (CA3), and the subiculum (Figure 6). These structures participate in the intrinsic circuit of the hippocampus, which is also known as the trisynaptic pathway. Afferent excitatory inputs enter the hippocampus through the perforant path and synapse with granule cells of the DG. The axons of these neurons give rise to the mossy fibers, which extend to the hilus of the DG and the CA3 region. When mossy fibers reach the CA3 region, make excitatory synapses with pyramidal neurons, which in turn project their axons through the Schaffer collaterals to the CA1 region. Finally, pyramidal neurons in the CA1 send efferent outputs to the subiculum and the entorhinal cortex, closing the hippocampal loop (Avchalumov & Mandyam, 2021; C. Schultz & Engelhardt, 2014). This hippocampal network was recently suggested to be regulated by the pyramidal neurons of the CA2 region through their broad connections with the CA3 and CA1 regions, although the exact mechanisms remain elusive (Lehr et al., 2021).

The main afferents to the hippocampus arrive through the perforant path and arise from the entorhinal cortex, which receives projections from association cortices, neocortex, olfactory bulb, and limbic cortex. Additionally, the hippocampus receives information from the mammillary bodies, thalamus, NAcc, medial PFC, septal nuclei, and basal forebrain through the fornix, while receives also direct afferents from the amygdala and contralateral hippocampus. Once the information has been processed in the hippocampus, efferent information projects back through the entorhinal cortex and fornix to the same areas that provided the initial input (Raslau et al.,

2015; C. Schultz & Engelhardt, 2014). Additionally, the hippocampus also receives modulatory direct innervation from midbrain dopaminergic neurons, serotonergic neurons from the raphe nuclei, locus coeruleus noradrenergic neurons, and cholinergic neurons from the medial septal nuclei.

Each subfield of the hippocampus is highly organized into different layers (Figure 6). The DG is divided into three layers: the molecular layer, granular cell layer, and hilus. The main excitatory neurons in the DG are granule cells, whose somas are densely packed in the granular cell layer. The dendrites of these neurons branch throughout the molecular layer where they make contact with afferent inputs from the perforant path, while the axons extend to the hilus and the CA3 region. The hilus contains inhibitory interneurons and excitatory mossy cells which project back to the molecular layer regulating granule cells drive towards the CA3 region. On the other hand, the three Ammon's horn subfields share a similar structure. The pyramidal cell layer contains the somas of pyramidal neurons, which are the main excitatory neurons. The basal dendrites of these neurons branch in the stratum oriens, while the apical dendrites branch into the stratum lucidum, stratum radiatum, and stratum lacunosum-moleculare (SLM). The stratum lucidum is only present in the CA3 region and contains the dendrites of pyramidal neurons that synapse with mossy fibers. Synapses of Schaffer collaterals with CA1 pyramidal neurons are contained throughout the stratum radiatum and stratum oriens. Inhibitory interneurons are scattered throughout all subfields and regulate the activity of surrounding inputs. Additional inputs arising directly from the entorhinal cortex through the perforant path or the temporoammonic pathway reach the SLM of the CA3 or CA1, respectively, where they synapse to distal apical dendrites of pyramidal neurons (Scharfman & Myers, 2013; C. Schultz & Engelhardt, 2014). Dopaminergic inputs arrive mainly to the stratum oriens and stratum radiatum of the CA1, although some innervation can also be found in the hilus and subiculum (Adeniyi et al., 2020; Edelmann & Lessmann, 2018; Lisman & Grace, 2005), while noradrenergic, serotonergic, and cholinergic innervations are widespread throughout the whole hippocampus (Awasthi et al., 2020; Frotscher & Léránth, 1985; Takeuchi et al., 2016).

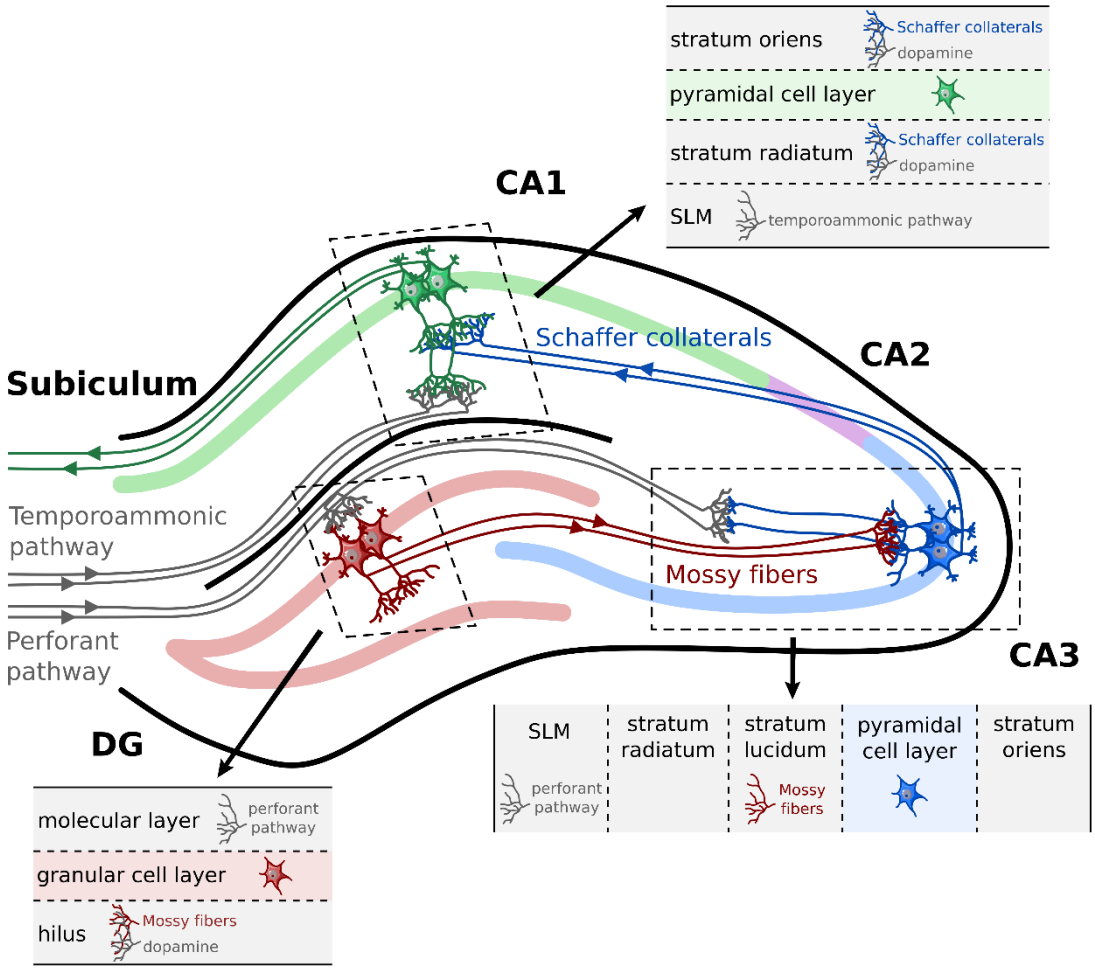

Figure 6. The hippocampus. Schematic representation of the main afferent and efferent pathways of the hippocampus as well as the intrinsic circuit of the hippocampus. The main projection neurons and their synaptic connections within the different layers are detailed for each hippocampal subfield.

2.2.2. Dopamine regulation of the limbic system

The mesocorticolimbic dopaminergic pathway projects to limbic and cortical structures including amygdala, cingulate gyrus, hippocampus, NAcc, olfactory bulb, and PFC, which in turn project back to the midbrain (Oades & Halliday, 1987). This system plays a key role in reward-related processes, as well as in learning and memory processes.

Inactivation of the VTA impairs memory acquisition and consolidation, as well as maintenance of long-term potentiation (LTP) in the hippocampus (Ghanbarian & Motamedi, 2013; Wisman et al., 2008), a process related to memory encoding that is modulated by DA (Jay, 2003; Lisman et al., 2011) (see section 3.2.2). It has been described that novel and reward stimuli activate dopaminergic neurons in the VTA (McNamara et al., 2014; Shohamy & Adcock, 2010). Indeed, the incorporation of new memories is facilitated by dopaminergic activity, enhancing learning

processes in animals (Lisman & Grace, 2005; McNamara et al., 2014) and humans (Knecht et al., 2004). Moreover, the prospect of receiving a reward improves long-term episodic memory for novel stimuli, in association with a coactivation of SNpc/VTA, striatum, and hippocampus (Adcock et al., 2006; Wittmann et al., 2005).

Lisman and Grace suggested that the VTA and hippocampus form a functional loop that detects novelty and uses this novelty signal to regulate the entry of behaviorally relevant information into the hippocampal long-term memory storage (Lisman & Grace, 2005). Novel stimuli reach the hippocampus, which compares the incoming information with stored memories to consider whether the stimulus is novel or not. A novel stimulus will drive an excitatory output from the hippocampus to the NAcc, sending inhibitory projection to the ventral pallidum (VP), and in turn, disinhibiting dopaminergic neurons of the VTA from the tonic inhibitory tone of VP GABAergic neurons. The activation of VTA neurons increases DA in the hippocampus, thus enhancing LTP in the CA1 region (Figure 7A). However, not all events may be sufficiently relevant to enter into long-term memory storage. Goal-directed motivation and salience information from other brain structures may regulate the entry of information into long-term memories, by reflecting the importance of the information. The combination of information may occur in the NAcc, where novelty information from hippocampal inputs converges with goal-dependent motivational signals from the PFC, activating VTA neurons when both signals coincide. What is more, dopaminergic neurons in the VTA could detect signal coincidence themselves, as they receive direct information from PFC, together with the aforementioned hippocampal-NAcc-VP inputs (Figure 7A). Thus, DA ensures that long-term memory only occurs for behaviorally relevant inputs.

Similarly, rewards and aversive stimuli may also activate VTA-hippocampal connections (Calabresi et al., 2013; Lisman et al., 2011; Shohamy & Adcock, 2010). During reward processing, the hippocampus and PFC compete for the activity of the NAcc (Goto & Grace, 2008), which in turn leads to increased activity of VTA neurons. The excitatory inputs from the hippocampus and PFC are modulated by different DA receptors in the SPNs of the NAcc, with postsynaptic D1Rs regulating hippocampal inputs and presynaptic D2Rs PFC inputs (Goto & Grace, 2005). Thus, rewards, by increasing DA release, facilitate hippocampal drives over PFC inputs helping to maintain behaviors that lead to that reward (Figure 7B). By contrast, the absence of reward decreases dopaminergic activity, facilitates PFC inputs, and reduces hippocampal inputs, which leads to increased flexibility to shift behavior towards better outcomes (Grace et al., 2007; W. Schultz, 2002).

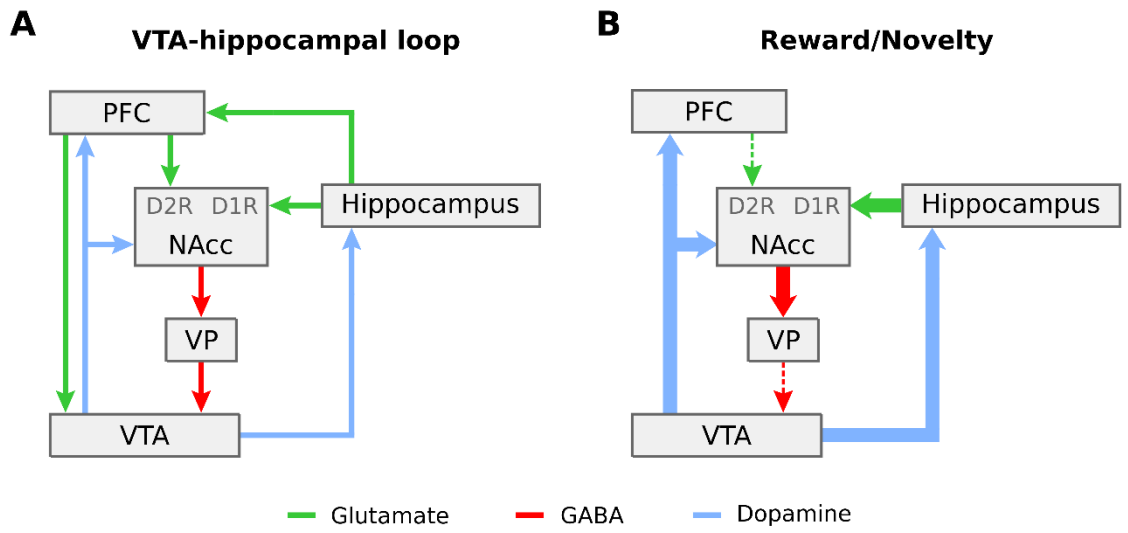

Figure 7. VTA-hippocampus loop. A) On the one side of the loop, the hippocampus processes stimuli to consider novelty. Novel inputs send excitatory signals to the NAcc, where the information combines with goal-directed motivation and salience signals from the PFC. Activation of NAcc sends inhibitory signals to the VP, which in turn inhibits VTA neurons. On the other side of the loop, activation of VTA increases dopamine release in target nuclei, including the hippocampus where dopamine potentiates LTP in the CA1 region, thus facilitating memory processing. **B)** During reward and novel stimuli processing, dopamine facilitates hippocampal excitatory inputs over the PFC inputs, potentiating dopaminergic activity in the VTA. Green arrows represent excitatory glutamatergic projections, red arrow inhibitory GABAergic projections, and blue arrows modulatory dopaminergic projections. Abbreviations: NAcc, nucleus accumbens; PFC, prefrontal cortex; VP, ventral pallidum; VTA, ventral tegmental area.

2.2.3. Dysregulation of the limbic system in Parkinson's Disease

Great effort has been made to understand the role of DA in limbic and cortical regions of the brain, as well as to unravel the pathophysiology behind the non-motor features of PD. Functional magnetic resonance imaging (MRI) studies have identified abnormal functional connectivity in PD patients since its earliest phase (Mishra et al., 2020; Sreenivasan et al., 2019). Recently, Caminiti and coworkers showed extensive axonal damage and loss of nigrostriatal pathway connectivity in early PD patients (Caminiti et al., 2017). Interestingly, in the same study, axonal damage was also reported in the mesolimbic system although to a lesser extent than in the nigrostriatal pathway. During this period, the dopaminergic treatment that restores DA in the denervated nigrostriatal circuit may overdose the mesocorticolimbic pathways (Cools et al., 2001). Indeed, functional and structural alterations in the mesocortical and limbic reward-related areas have been described in PD patients with ICD. Several positron emission tomography (PET) studies described reduced DA transporter (DAT) levels, indicative of dopaminergic degeneration, in the

ventral striatum of PD patients with ICD (Cilia et al., 2010; Navalpotro-Gomez et al., 2019; Voon et al., 2014) as well as reduced cortico-striatal connectivity (Carriere et al., 2015) and dynamic functional engagement of local connectivity involving the limbic circuit (Navalpotro-Gomez et al., 2020). Moreover, ICDs in PD are considered hyperdopaminergic disorders, with increased release of DA in the ventral striatum (Steeves et al., 2009), as well as overall increased activity of the brain reward system including the hippocampus, orbitofrontal cortex, and amygdala (Cilia et al., 2008). According to reward processing within the VTA-hippocampus loop, hyperactivity of the loop could potentiate hippocampal and mesolimbic inputs and facilitate particular responses or behaviors over others, leading to impulsivity (Calabresi et al., 2013) (Figure 7B). Moreover, reversal learning and decision-making processes in PD patients are worsened by dopaminergic replacement therapy (Frank et al., 2004). By contrast, neuropsychiatric symptoms such as depression, anxiety, and apathy, are considered hypodopaminergic syndromes, where a decrease in DA transmission would reduce mesolimbic and hippocampal activity, thus reducing motivation (Calabresi et al., 2013).

With the progression of PD, dopaminergic denervation gradually expands to limbic and cortical areas. Thus, an imbalance in DA transmission in the cortical and limbic systems may also be involved in cognitive impairment and dementia in PD. Structural MRI studies have described higher levels of atrophy in frontal, temporal, parietal, and occipital lobes as well as in the hippocampus, amygdala, caudate, putamen, and thalamus in PD patients with MCI and PDD compared to cognitively normal PD patients and control subjects (Martín-Bastida et al., 2021). Specifically, hippocampal atrophy has been associated with memory impairment and progression into dementia (Filippi et al., 2020; Jokinen et al., 2010; Kandiah et al., 2014; Mak et al., 2015; Pereira et al., 2013). Interestingly, other studies found hippocampal atrophy also in non-demented PD patients compared to healthy controls (Camicioli et al., 2003; Oh et al., 2021; Xu et al., 2020), even at early stages of PD without medication (Beyer et al., 2013; Brück et al., 2004). MCI in PD patients mainly affects executive functions, which depend on the connections between the dorsal striatum and the PFC, and are partially restored with DA replacement therapy (Kehagia et al., 2010; O'Callaghan & Lewis, 2017). On the other hand, PDD is associated with more severe deficits in executive function as well as visual-spatial constructional deficits and recognition, semantic, and episodic memory loss (Kehagia et al., 2010; Schapira et al., 2017). It has been described a greater loss of mesolimbic dopaminergic projecting neurons in PDD patients, as well as reduced gray matter in cortical regions, hippocampus, and striatum, and impaired connectivity between brain regions supporting executive function, attention, and memory (Gratwicke et al., 2015; Zarei et al., 2013). However, the role of DA in cognitive impairment related to PD remains largely unknown, and other neurotransmitter systems such as the cholinergic, noradrenergic, and serotonergic

systems, have been proposed to participate in the pathophysiology of non-motor features of PD. Of note, the spreading of Lewy pathology along with neurofibrillary tangles and β-amyloid plaques is associated with cognitive decline and dementia (Irwin et al., 2013; C. Smith et al., 2019).

3. Synapse and Synaptic Plasticity

3.1. The synapse

Santiago Ramón y Cajal proposed that neurons are not continuous throughout the body, they communicate with each other instead, an idea that contributed to the formulation of the Neuron Doctrine by Waldeyer in 1891 (Jones, 1999; Waldeyer, 1891). However, the term "synapse" was not introduced until 1897 by the neurophysiologists Foster and Sherrington (Foster & Sherrington, 1897). Synapses are now described as the intercellular junctions between a presynaptic neuron and a postsynaptic neuron (Südhof, 2012b). They are used to transmit signals between neurons in the CNS allowing an organized flux of information through the brain and are considered highly dynamic structures in terms of number, structure, molecular constituents, and functional properties (Lepeta et al., 2016).

There are two fundamentally different types of synapses: electrical and chemical synapses. In an electrical synapse, the cytoplasm of the presynaptic and postsynaptic neurons is connected by gap junctions, clusters of intercellular channels capable of rapid transfer of electric current. However, these synapses are not prevalent in the mammalian CNS. Chemical synapses are composed of a presynaptic terminal, the synaptic cleft, and the postsynaptic terminal and are based on the release of neurotransmitters from the presynaptic terminal and its detection by postsynaptic receptors, a process that requires a complex and tight regulation (Alcamí & Pereda, 2019; Purves et al., 2004) (Figure 8).

3.1.1. The presynaptic terminal

The presynaptic nerve terminal contains specialized secretory machinery that releases neurotransmitters by SV exocytosis in response to an action potential. By receiving an action potential, Ca^{2+} channels open, thereby allowing an influx of Ca^{2+} into the presynaptic terminal that promotes the assembly of the SNARE complex (Südhof, 2013). Ultimately, this molecular machinery will trigger SV trafficking from the closest pool, the readily releasable pool, to be tethered, docked, and fused to the presynaptic terminal called the active zone, for subsequent

release of neurotransmitters in the synaptic cleft (Südhof, 2012b; Südhof & Rizo, 2011). In addition to the SNARE complex, a subfamily of highly conserved small GTPases called Rab is implicated in intracellular trafficking of vesicles and the recruitment of SVs in the active zone (Binotti et al., 2016). After exocytosis, the SV membrane is retrieved from the synaptic cleft by endocytosis, either via clathrin-dependent slow or via clathrin-independent fast modes of endocytosis (Saheki & De Camilli, 2012). The SVs are locally loaded with neurotransmitters, hence being recycled to allow another round of exo-endocytotic membrane cycle. This mechanism allows the neurons to sustain a high firing rate without depletion of the SV pools (Gross & von Gersdorff, 2016; Saheki & De Camilli, 2012) (Figure 8). According to the type of neurotransmitter released, chemical synapses can be further classified into glutamatergic, dopaminergic, GABAergic, cholinergic, etc. (Purves et al., 2004). Of note, α-syn maintains neurotransmitter homeostasis by regulating different steps of this exo-endocytic cycle (Bridi & Hirth, 2018), as will be detailed in section 4.2.

3.1.2. The synaptic cleft

The synaptic cleft is the space between the pre- and the postsynaptic compartments. It contains cell-adhesion molecules (CAMs) involved in trans-cellular signaling and cell adhesion functions important for synapse formation, alignment of the pre- and postsynaptic compartments, and regulation of synaptic transmission (Südhof, 2018). CAMs are tethered to the pre- or postsynaptic membrane by a transmembrane domain or a glycosylphosphatidylinositol anchor and extend their extracellular domains into the synaptic cleft to interact with protein partners of the same or different CAM families. Additionally, CAMs can interact with non-adhesion molecules such as receptors, channels, and secreted factors as well as intracellular proteins, integrating into the presynaptic and/or postsynaptic machinery and organizing synaptic protein networks (Rudenko, 2017) (Figure 8). Several families of CAMs have been described to play a role in synapses, of which the Neurexin (Nrx) family has been extensively characterized (Südhof, 2017). Nrxs are encoded by three different genes (Nrx1-3) and expressed as long (α) and short (β) isoforms driven by alternative promotors, giving rise to thousands of isoforms in the brain. Nrxs are presynaptic CAMs that dynamically interact with several postsynaptic ligands such as neuroligins and leucine-rich repeat transmembrane proteins, as well as presynaptic and soluble adaptor proteins. Moreover, different Nrx isoforms have been described to affect synaptic transmission by controlling glutamatergic postsynaptic receptors at excitatory synapses (Dai et al., 2019).

3.1.3. The postsynaptic terminal

The postsynaptic terminal is specialized to receive the neurotransmitter signal and transduce it into electrical and biochemical changes in the postsynaptic cell, that may either excite or inhibit them, allowing further classification of synapses as excitatory and inhibitory synapses, respectively. The neurotransmitters bind to receptors that are concentrated at the postsynaptic membrane and are embedded in a dense and rich protein network known as the postsynaptic density (PSD). The PSD is a highly dynamic structure with varying molecular composition between different neuronal cell types and brain regions. Generally, it is comprised of anchoring and scaffolding molecules, cytoskeletal components, as well as receptors and enzymes involved in biochemical signaling pathways (Sheng & Kim, 2011) (Figure 8). Scaffolding molecules include membrane-associated guanylate kinases (MAGUKs), Shank and Homer protein families, which contain multiple protein-protein interaction domains (PDZ domains), while the most abundant protein is the enzyme Ca^{2+}/calmodulin-dependent protein kinase II (CaMKII), which plays an important role in the response to neural activity (Dosemeci et al., 2016). There are two major classes of neurotransmitter receptors in the PSD, metabotropic and ionotropic receptors. Metabotropic receptors are GPCRs, which upon binding of the neurotransmitter trigger a variety of downstream intracellular signaling pathways. Among others, DA receptors (D1-5), as well as metabotropic glutamate receptors (mGluR1-8), belong to this family. On the other hand, ionotropic receptors are ligand-gated ion channels involved in fast synaptic transmission. The binding of the neurotransmitter to the receptor triggers the opening of the channel, ultimately leading to changes in the membrane potential, which can be depolarizing (excitatory) or hyperpolarizing (inhibitory). In excitatory synapses, the most abundant ionotropic receptors are AMPARs and N-Methyl-D-aspartic acid receptors (NMDARs) (Beaulieu & Gainetdinov, 2011; Grubbs, 2008; Scheefhals & MacGillavry, 2018).

AMPARs are glutamate-gated ion channels that mediate the majority of fast excitatory synaptic transmission in the brain. Four subunits (GluA1-4) encoded by different genes assemble into tetramers to form the functional ion channel. Different subunit combinations confer unique cellular trafficking and biophysical properties to AMPARs. As such, GluA2-containing AMPAR insertion is rapid and constitutively active while GluA1-containing AMPAR insertion is slower and stimulated by neuronal activity. GluA2 subunit also confers Ca^{2+} impermeability to AMPARs due to a conversion of a glutamine residue into arginine in the channel pore (Shepherd & Huganir, 2007). In hippocampal CA1 neurons, GluA1/GluA2 and GluA2/GluA3 heteromers are the most common subunit combinations, with a small contribution of GluA1/GluA3 heteromers and GluA1 homomers (W. Lu et al., 2009; Wenthold et al., 1996). Moreover, single-channel properties and

synaptic expression of AMPARs are highly regulated by posttranslational modifications such as phosphorylation and palmitoylation, as well as the interaction with additional proteins known as auxiliary subunits such as transmembrane AMPAR regulatory proteins (TARPs) and the cornichon-like proteins CNIH2/CNIH3. These auxiliary proteins interact with scaffolding proteins of the PSD such as MAGUKs, stabilizing AMPARs to the cell membrane and targeting them to the PSD (Diering & Huganir, 2018).

NMDARs are ligand- and voltage-gated ion channels with high permeability for Ca^{2+}. They require the binding of glutamate, released from the presynaptic terminal, and the co-agonist glycine or D-serine, which are thought to be continuously present. Additionally, at resting membrane potential, NMDARs are blocked by Mg^{2+}, which upon depolarization of the postsynaptic membrane dissociates, allowing the opening of the channel (Hansen et al., 2018). Thus, NMDARs contribute only slightly to the postsynaptic response during basal synaptic activity but are crucial for the induction of long-term forms of synaptic plasticity (Citri & Malenka, 2008). Seven genes encode for the NMDAR subunits, one GluN1, four GluN2A-D, and two GluN3A-B, which assemble into heterotetramers to form the functional ion channel. Typically, GluN1 subunits, which are necessary for the proper assembly and surface delivery of NMDARs, associate with GluN2 subunits or a mixture of GluN2 and GluN3 subunits, which confer distinct biophysical properties. For example, GluN2A- and GluN2B-containing NMDARs have higher single-channel conductance and Ca^{2+} permeability, and are more sensitive to Mg^{2+} blockade than GluN2C- and GluN2D-containing receptors, while the incorporation of GluN3 subunits confers decreased Mg^{2+} blockade (Paoletti et al., 2013). In hippocampal CA1 neurons, GluN1/GluN2A and GluN1/GluN2B heteromers are the most common subunit combinations, with GluN2A-containing receptors being predominant during adulthood. Additionally, several posttranslational modifications such as phosphorylation at different subunits regulate functional properties and subcellular localization of NMDARs (Traynelis et al., 2010).

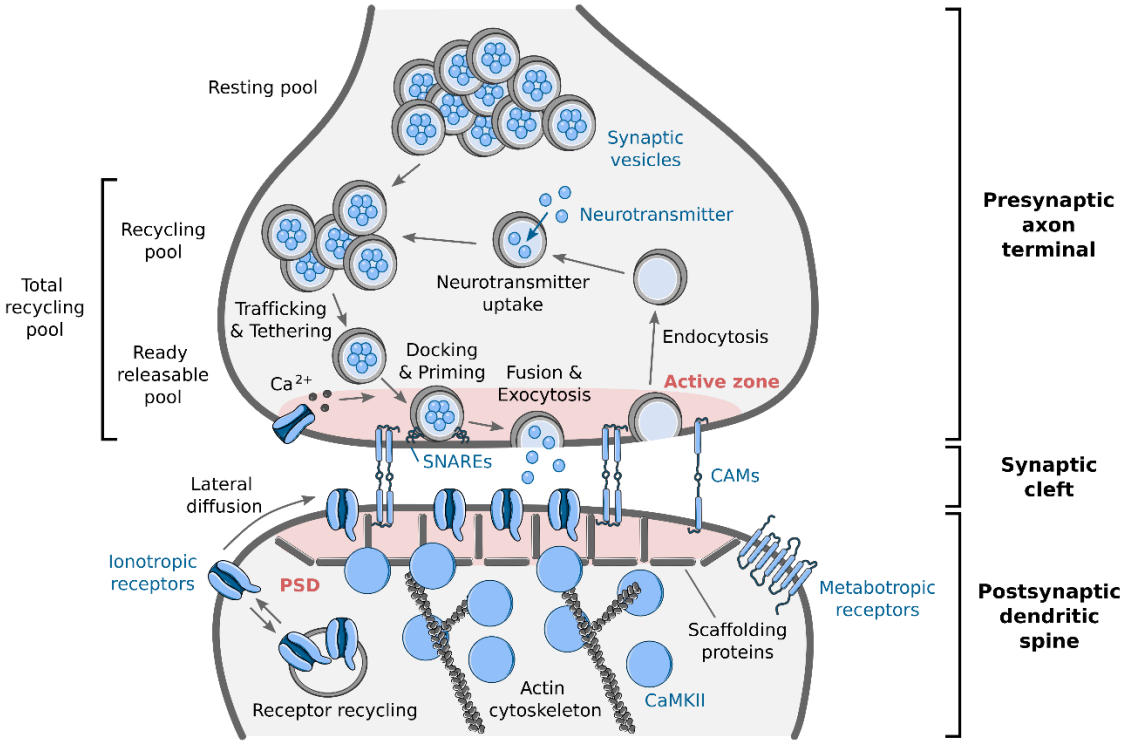

Figure 8. Structure of a chemical synapse. In the presynaptic terminal, the synaptic vesicle (SV) cycle regulates the release of the neurotransmitter. Upon an incoming action potential, voltage-gated Ca^{2+} channels open, allowing the entrance of Ca^{2+} into the presynaptic terminal. This activates molecular machinery including the SNARE complex proteins that recruit SVs from the proximal resting and recycling pools via trafficking and tethering to form the readily releasable pool. After docking and priming, the readily releasable pool of vesicles undergoes SNARE-mediated membrane fusion at the active zone, ultimately leading to neurotransmitter release into the synaptic cleft. After exocytosis, the SV membrane is retrieved to the presynaptic terminal via endocytosis, to be filled with neurotransmitter molecules and re-enter the exo-endocytotic cycle. In the synaptic cleft, CAMs tethered to the pre- or postsynaptic membrane interact with protein partners for the proper alignment of the pre- and postsynaptic compartments and the regulation of synaptic transmission. In the postsynaptic spine, neurotransmitters bind to ionotropic and metabotropic receptors that are embedded at the postsynaptic density (PSD). The PSD also contains scaffolding proteins, actin cytoskeleton, and signaling proteins, of which CaMKII is the most abundant enzyme. Receptors in the post-synaptic membrane are recycled by exo- and endocytosis cycles in extrasynaptic sites and subsequent lateral diffusion into the PSD.

3.2. Synaptic plasticity

Activity-dependent remodeling of synaptic efficacy and neuronal connectivity is a remarkable property of synaptic transmission and a characteristic of plastic events in the CNS. Synapses are extremely dynamic structures that are constantly being formed, eliminated, and reshaped. In fact, adaptive reorganization of neuronal connectivity, which allows the acquisition

of new information, both during development and in the mature brain, is based upon the strengthening of existing synapses, the formation of new synapses, and the destabilization of previously established synaptic contacts (Holtmaat & Caroni, 2016). Thus, synaptic transmission can be either enhanced or depressed by activity, and these changes span temporal domains ranging from milliseconds to hours, days, and presumably even longer (Citri & Malenka, 2008).

Short-term synaptic plasticity is the enhancement or depression of synaptic transmission lasting between a few milliseconds to several minutes. Observed in virtually all synapses, it is thought to play an important role in sensory input processing, transient behavioral changes, and short-lasting forms of memory (Citri & Malenka, 2008). Short-term synaptic plasticity depends on presynaptic mechanisms involving changes in the probability of neurotransmitter release after a transient increase of intracellular Ca^{2+} concentration in the presynaptic terminal (Zucker & Regehr, 2002).

Long-term synaptic plasticity is the activity-dependent modification of synaptic strength, lasting from hours to days. Excitatory synapses can be bidirectionally modified by different inputs, potentiating (LTP) or weakening (long-term depression, LTD) synaptic transmission (Citri & Malenka, 2008). These long-lasting forms of synaptic plasticity depend mainly on postsynaptic mechanisms with AMPAR insertion or removal from the synaptic membrane in LTP and LTD respectively, followed by new RNA and protein synthesis for long-term maintenance (Ho et al., 2011).

LTP was first described experimentally in the rabbit hippocampus by Bliss and Lomo in 1973 after applying a high-frequency stimulation at the perforant path resulting in a long-lasting potentiation of synaptic transmission (Bliss & Lomo, 1973). Several decades of research in the field have helped understand the characteristics and molecular mechanisms underlying the long-lasting strengthening of synapses confirming Hebb's theoretical model (Hebb, 1949) and describing the following characteristics of LTP: 1) cooperativity, where even though LTP cannot be generated with a single weak excitatory stimulus, simultaneous stimulation of several afferent axons may reach the threshold required to induce LTP; 2) associativity, where a weak input can be potentiated when it is activated in association with a strong input; and finally, 3) input specificity, where LTP can only be elucidated at the activated synapses, but not at adjacent synapses (Baltaci et al., 2019; Citri & Malenka, 2008).

Since the first description of LTP, several forms of long-lasting potentiation have been described at different brain regions and neuronal populations, trigged by different molecular mechanisms. The most extensively studied form of synaptic plasticity is NMDAR-dependent LTP

in excitatory synapses on the CA1 pyramidal neurons of the hippocampus, due to its relationship with long-term memory. This form of LTP depends on postsynaptic mechanisms, with the stimulation of NMDAR being a key step for LTP induction and subsequent AMPAR increase required for LTP expression. The activation of NMDAR has also been described to participate in the induction of LTP in other brain regions such as the striatum (Calabresi et al., 1992) and cortex (Liauw et al., 2005). On the other hand, presynaptic mechanisms have been described to participate in the induction and expression of LTP in other brain areas such as the synapses between the granule cells of the DG and the CA3 pyramidal neurons of the hippocampus (Nicoll & Schmitz, 2005). In these synapses, an overall increased influx of Ca^{2+} through different voltage-gated Ca^{2+} channels into the presynaptic terminal triggers the enhancement of glutamate release, crucial for LTP expression (Castillo, 2012).

3.2.1. NMDAR-dependent LTP

Glutamate release from the presynaptic terminal trigged by a massive entrance of Ca^{2+} after an action potential activates postsynaptic AMPARs allowing the entrance of cations and generating a postsynaptic excitatory response. If the response reaches a certain threshold, the postsynaptic membrane depolarizes, removing the Mg^{2+} blockade and allowing the activation of NMDARs as well. The entrance of Ca^{2+} through NMDARs rises intracellular concentrations of this ion, triggering several molecular signaling cascades. Overall, Ca^{2+} signaling leads to an increase in AMPAR activity through a direct increase in single-channel conductance and the recruitment of additional AMPARs to the synaptic membrane (Baltaci et al., 2019; Citri & Malenka, 2008). One of the most important steps in LTP induction is the activation of CaMKII by autophosphorylation following the binding of the Ca^{2+}/calmodulin complex. This step is sufficient and necessary for LTP induction as blockade or genetic deletions impair LTP, which are rescued by exogenous CaMKII enzymatic activity (Incontro et al., 2018; Lisman et al., 2012). CaMKII phosphorylates AMPARs increasing their single-channel conductance (Kristensen et al., 2011), and at the same time phosphorylates TARPs, enabling the exocytosis of AMPARs from endocytic reserve pools into the plasma membrane at extrasynaptic sites, and subsequent lateral movement of AMPARs within the plasma membrane to the PSD (Hayashi et al., 2000; Horak et al., 2014; W. Lu et al., 2010).

During the last years, CAMs are emerging as important regulators of AMPAR and NMDARs trafficking, synaptic targeting, and conductivity. It has been suggested that CAMs anchoring NMDARs to the PSD participate in LTP induction, while CAMs interacting with AMPARs participate in LTP maintenance by promoting their stabilization in the synaptic membrane (Keable

et al., 2020). Moreover, neural activity increases cell surface and synaptic levels of CAMs such as Nrx1β, NLGN1, and NLGN3 (Rudenko, 2017).

Activation of several kinases has also been described to participate in LTP maintenance and consolidation for hours or days during the so-called "late phase of LTP" (Baltaci et al., 2019). One of the key players in LTP maintenance is PKMζ, a constitutively active isoform of protein kinase C (PKC), which prevents AMPAR endocytosis and lateral diffusion away from the synapses (Sacktor, 2011). Additionally, activation of other kinases such as protein kinase A (PKA), CaMKIV, and mitogen-activated protein kinase (MAPK) is critical for the activation of key transcription factors such as cyclic AMP-responsive element-binding protein (CREB), and the signal transduction to the nucleus to sustain changes in gene expression for time periods extending beyond the initial stimulus (Ho et al., 2011). Indeed, this late phase of LTP depends on *de novo* protein and mRNA synthesis (Holt et al., 2019; Vickers et al., 2005). Moreover, several mRNAs can be found in dendrites, such as those coding for GluA1 and GluA2 subunits of AMPARs, and CaMKII, which are locally translated into proteins following LTP induction (Ju et al., 2004; Miller et al., 2002).

This functional strengthening of the postsynaptic response is accompanied by structural changes after LTP induction. In the presynaptic terminal, the active zone is enlarged, accompanied by a remodeling of SV pools, increasing and positioning recycled vesicles closer to the active zone (Bell et al., 2014; Rey et al., 2020). In the postsynaptic compartment, rapid enlargement of the dendritic spine is triggered, based on actin polymerization and regulated by Rho GTPases (Bosch et al., 2014; Murakoshi et al., 2011).

3.2.2. Dopamine: LTP modulator

DA exerts its effects by stimulating five different DA receptors (D1-D5), all of them corresponding to the GPCR superfamily. Based on their structural, pharmacological, and biochemical properties, DA receptors have been classified into two types. D1-like DA receptors include D1R and D5R, which are exclusively expressed postsynaptically and stimulate Gs/olf, promoting cyclic adenosine monophosphate (cAMP) production by adenylyl cyclase and the consequent activation of PKA signaling. On the other hand, D2-like DA receptors include D2R, D3R, and D4R, which are expressed both pre- and postsynaptically and stimulate Gi/o, decreasing adenylyl cyclase activity, and thus, PKA signaling (Beaulieu & Gainetdinov, 2011).

In the striatum, where the highest concentration of dopaminergic innervations exists, DA is required for the induction of both forms of long-term plasticity, LTP and LTD. In this brain nucleus, LTP induction depends on the activation of NMDARs as well as D1Rs, whereas D2Rs

negatively modulate LTP. By contrast, LTD induction in the striatum depends on mGluRs and requires the synergistic activity of both D1Rs and D2Rs (Calabresi et al., 1992; Calabresi et al., 2007). Interestingly, LTP and LTD require different levels of striatal DA. The injection of the neurotoxins 6-hydroxydopamine (6-OHDA) in rodents leads to a degeneration of dopaminergic neurons and the consequent depletion of DA in the striatum. Full depletion of DA completely abolished both LTP and LTD, however, partial DA denervation only impaired LTP maintenance without altering LTP induction or LTD induction and maintenance (Paille et al., 2010).

In the hippocampus, there is also ample evidence of DA modulating long-term synaptic plasticity processes. DA is required for long-term maintenance of both LTP and LTD in hippocampal slice preparations (Edelmann & Lessmann, 2018) as well as in freely moving rats (Lemon & Manahan-Vaughan, 2006). DA depletion after the injection of neurotoxins such as 6-OHDA and MPTP in rodents also affects the levels of this neurotransmitter in the hippocampus (Costa et al., 2012; Zhu et al., 2011). These animals present impairment in hippocampal LTP without deficits in basal synaptic transmission in electrophysiological *in vivo* recordings as well as in *ex vivo* hippocampal slices, which could be rescued with L-DOPA subchronic administration *in vivo* or bath application in *ex vivo* slices (Bonito-Oliva et al., 2014; Costa et al., 2012; Esmaeili-Mahani et al., 2021; Jalali et al., 2020; K.-W. Lu et al., 2017; Moriguchi et al., 2012; Pendolino et al., 2014; Zhu et al., 2011).

The role of DA in the late phase of LTP is thought to be mediated by D1-like receptors, as D1R/D5R antagonists (Lisman et al., 2011; O'Carroll & Morris, 2004) as well as genetic deletions of the D1R (Granado et al., 2008) or D5R (Moraga-Amaro et al., 2016) block LTP in the CA1 region of the hippocampus. Moreover, D1/D5 antagonists block the effect of L-DOPA in LTP recovery in 6-OHDA lesioned rats (Costa et al., 2012). Direct protein-protein interaction between NMDARs and D1Rs has been described, with D1Rs inhibiting NMDAR-mediated currents (Lee et al., 2002) and NMDARs enhancing surface expression and function of D1Rs in cultures hippocampal neurons (Pei et al., 2004). Activation of D1-like receptors has also been shown to increase AMPAR surface expression and synaptic transmission as well as local translation of the GluA1 subunit (W. B. Smith et al., 2005). Moreover, D1-like receptors activate adenylyl cyclase, rising cAMP levels and activating downstream signaling pathways including PKA and MAPK, which promote the expression of different genes related to synaptic plasticity (Granado et al., 2008; Huang & Kandel, 1995; Sarantis et al., 2009). Thus, coactivation of NMDARs with D1R/D5R may result in a synergistic downstream signaling activation critical for LTP maintenance. Additionally, some studies suggest that DA may also play a role in LTP induction, as D1/D5R agonists and antagonists enhance and

decrease the early phase of LTP, respectively (Otmakhova & Lisman, 1996), and genetic deletion of D1R also impair the induction of LTP (Granado et al., 2008).

Activation of D2-like receptors has also been implicated in LTP processes, as D2R antagonists and genetic deletions inhibit LTP in the CA1 region of the hippocampus (Frey et al., 1990; Rocchetti et al., 2015). In this region, D2Rs are mainly expressed in GABAergic interneurons (Puighermanal et al., 2015; Q. Yu et al., 2019), thus, it has been suggested that activation of D2Rs reduces GABA synthesis in the hippocampus (Steulet et al., 1990) allowing for LTP to occur (Wigström & Gustafsson, 1983). Although less understood, the D3Rs and D4Rs may also play a role in hippocampal LTP. Stimulation of D3Rs in the hippocampus has been shown to decrease GABAergic interneuron activity and, thus, stimulate glutamatergic activity (Hammad & Wagner, 2006; Swant et al., 2008), however, chronic treatment with the agonist PPX, which has greater selectivity for the D3Rs than D2Rs, has been described to inhibit LTP (Schepisi et al., 2016). The effect of D4Rs in hippocampal LTP is also controversial, with some studies showing facilitation of LTP (F. Guo et al., 2017), while others describe an inhibition (Navakkode et al., 2017).

3.3. Synaptic dysfunction in Parkinson's Disease

Synaptic dysfunction is emerging as one of the early and major neurobiological events in PD and several lines of evidence suggest that accumulation of α-syn in presynaptic terminals plays a central role in this process. In fact, numerous recent reports show aggregation of α-syn at synapses and, consequent alterations in synaptic function and structure confirm synaptic α-synucleinopathy as a primary event in the pathogenesis of PD (Bridi & Hirth, 2018; Calo et al., 2016; Ghiglieri et al., 2018). It has been proposed that the pathogenesis process underlying PD may feature a dying-back mechanism of cell degeneration, in which cell death is a consequence of early impairment of synaptic function and axon degeneration and retrograde progression of the pathology, as it has been described in other neurodegenerative diseases (Tagliaferro & Burke, 2016).

The first evidence that axons were affected in PD came from the study of Braak and coworkers. They demonstrated that α-syn inclusions were not only present in LB inclusions at the neuron soma, but also present in LNs and that the accumulation of α-syn at the axonal processes preceded that in cell bodies (Braak et al., 1999, 2003). Moreover, *post-mortem* studies have shown that nearly 90% of α-syn aggregates are located at synapses in the frontal cortex of other synucleinopathies (Kramer & Schulz-Schaeffer, 2007; Schulz-Schaeffer, 2010; Tanji et al., 2010) and significant synaptic pathology with almost complete loss of dendritic spines is observed at the

postsynaptic areas (Kramer & Schulz-Schaeffer, 2007; Zaja-Milatovic et al., 2005). These observations were confirmed by recent PET studies with the novel radiotracer [^{11}C]-UCB-J showing decreased synaptic vesicle 2A (SV2A) distribution in the SN and striatum as well as in several cortical areas since the early stages of PD (Matuskey et al., 2020; Wilson et al., 2020). Interestingly, nigrostriatal dopaminergic neurons exhibit particularly extensive unmyelinated axon arborizations with a large synaptic tree, which requires a great amount of energy and places them close to their maximum capacity (Pacelli et al., 2015; Pissadaki & Bolam, 2013). It has been proposed that in the presence of PD-associated risk factors, the highly branched axonal domain may be particularly vulnerable, triggering synaptic and cellular dysfunction ultimately leading to neurodegeneration (Wong et al., 2019).

With the progression of the disease, Lewy pathology spreads to limbic and cortical areas correlating with dementia in PD patients (Halliday et al., 2014). In a combined 2-Deoxy-2-[^{18}F]-fluoroglucose ([^{18}F]-FDG) PET and MRI study, cortical glucose hypometabolism was related to MCI in PD patients, which was replaced by atrophy or loss of volume of grey matter with surrounding areas of hypometabolism in patients with PDD (González-Redondo et al., 2014). These results suggest that hypometabolism in PD predates and is replaced by atrophy in a progressive and expanding manner as the cognitive state worsens. Since synapses are the physiologically most active compartments of neurons, hypometabolism would reflect a synaptic dysfunction that if it were maintained over time would lead to a loss of synaptic terminals and ultimately to neuronal degeneration, which would be detected as atrophy, representing two steps of the same process (González-Redondo et al., 2014).

Several synaptic proteins were found altered in the cerebrospinal fluid (CSF) of PD patients. Increased levels of SNAP-25 were described (Bereczki et al., 2017), as well as decreased levels of proteins related to neurotransmitter secretion (CHGA, SCG2, and VGF), synaptic plasticity (NPTX1), and endolysosomal autophagy system (AP2B1 and ubiquitin) (Lerche et al., 2021). Decreased CSF levels of the postsynaptic protein neurogranin were recently proposed as a biomarker for parkinsonian disorders including PD and PDD (S. Hall et al., 2020), however, other studies have reported increased (Bereczki et al., 2017) or even unchanged (Wellington et al., 2016) levels of this synaptic protein in CSF.

In addition, the expression levels of a range of proteins involved in synaptic transmission were found to be altered in *post-mortem* tissue from PD patients. A pathological study showed that in incidental PD brains (the presence of LBs without the clinical development of PD) there are already altered molecular events in the SN related to oxidative damage, suggesting that the pathological process precedes clinical diagnosis by years (Dalfó et al., 2005). In another study,

incidental PD brains at Braak stages I and II showed downregulation of Synapsin 2, complexin 2, and synphilin 1 gene expression and upregulation of synapsin 3, synaptophysin, synaptotagmin 2 in the SN (Dijkstra et al., 2015). A proteomic study in the SN of PD patients showed overexpression of proteins associated with the cytoskeleton, and downregulation of proteins involved in energy metabolism, mitochondrial function, intracellular transport, synaptic activity, and translation (Licker et al., 2014), while another study showed downregulation of proteins involved in the regulation of neurotransmitters and signal release processes in the SN, and related to synapse organization in the striatum (Xicoy et al., 2020). Recently, the lysosomal enzyme asparagine endopeptidase was found highly activated in human PD brains, particularly in the SN, where it cleaves hα-syn giving rise to smaller fragments prone to aggregation, which are present in LBs (Zhentao Zhang et al., 2017). In addition, fragmentation of the presynaptic protein SYNJ1 has been related to presynaptic dysfunction and dopaminergic neuronal vulnerability in *post mortem* PD brains. These fragments lack the phosphoinositide phosphatase activity and the ability to interact with other proteins, disrupting clathrin-mediated SV endocytosis and inducing presynaptic dysfunction, abnormal synaptic protein clustering, and dendritic spine degeneration (Zou et al., 2021). Apart from the nigrostriatal system, synaptic protein alterations have also been described in other brain regions of PD patients. In the hippocampus, a combined proteomic and stereological study showed altered synaptic proteins (CASKIN-1, TMEM163, REEP2, AHA-1, δ2-catenin, PHYHIPL, and α-1-syntrophin) in PD patients without overt hippocampal neurodegeneration (Villar-Conde et al., 2021). Additionally, a proteomic and ELISA study in PFC tissue from PDD patients, reflecting a more advanced PD stage, showed downregulation of various synaptic proteins (SV2C, NRGN, CBLN4, BDNF, GAP43, SNAP47, LRNF2, SYT2) (Bereczki et al., 2018). Together, these studies demonstrate synaptic impairment at the protein level in several brain regions across different stages of PD, suggesting that both motor and non-motor features are associated with impaired synaptic communication.

To sum up, synaptic alterations have been found to precede cell loss, thus, pointing to synapses as the primary region in the onset of pathology in PD. Moreover, synaptic alterations extend to limbic and cortical regions apart from the nigrostriatal system, which may contribute to the progression of the disease as well as to the development of non-motor signs. Thus, understanding the mechanisms of synapse alterations in PD may help find treatments to prevent synaptic loss and restore synaptic function before neuronal death, delaying PD progression and the onset of non-motor features.

4. α-Synuclein

4.1. Structure and location of α-synuclein

α-Syn is a small (14 kDa) intrinsically disordered protein, encoded by the *SNCA* gene (located in the 4q21.3-q22 chromosome) and belonging to the synuclein superfamily together with β- and γ-synucleins. It contains 140 amino acids divided into three regions, the N-terminal region (residues 1-60), the central region (residues 61-95), and the C-terminal region (residues 96-140) (Figure 9A). The N-terminal region is predicted to form amphipathic α-helices involved in membrane binding. These helices preferentially bind to lipids with acidic head groups, such as phosphatidylserine or phosphatidylinositol, and are stabilized by interactions with high-curvature membranes such as SVs. Several missense mutations (A53T, E46K, A30P) in this region have been found in familial PD, some of which affect membrane-binding properties. The central region is a hydrophobic non-amyloid β component (NAC) with a high propensity to form a β-rich conformation highly prone to aggregation. Transient intramolecular interactions between the N-terminal and C-terminal regions shield the NAC from aggregation when α-syn is in its unfolded native state. The C-terminal region is highly enriched in negatively charged amino acids, and similar to other intrinsically disordered proteins, has no defined secondary structure, facilitating the solubility of the protein. This region is subjected to multiple posttranslational modifications, which change the charge and structure of α-syn, affecting its binding affinity to other proteins and lipids (Longhena et al., 2019; Rosborough et al., 2017).

The expression and localization of α-syn are developmentally regulated. Although it is expressed in various peripheral tissues during human fetal development, in adults it is predominantly found in the nervous system and, for unclear reasons, in certain blood cells such as erythrocytes and platelets (Barbour et al., 2008).

In neurons, α-syn expression is induced following determination of neuronal phenotype and establishment of synaptic connections and lags behind the induction of other presynaptic proteins. It is initially detected throughout the soma and neuronal processes, but it eventually becomes predominantly localized at presynaptic terminals in the postnatal brain at several neurotransmitter systems. In this sense, *post-mortem* studies have shown that α-syn aggregates are located in synaptosomal protein extracts and that α-syn pathology prominently involves the synaptic compartments (Schulz-Schaeffer, 2010). Despite its ubiquitous distribution through many brain areas, α-syn pathology does not impact all brain sites of expression but rather shows a prevalent effect on selectively vulnerable sites such as the nigrostriatal dopaminergic system (C. Wang et al., 2016).

Under physiological conditions, α-syn is thought to exist predominantly as an unfolded soluble protein in the cytosol. Some studies with multiple biophysical approaches characterized α-syn tetramers with α-helix structure in the cytoplasm, suggesting a significant conformational plasticity of α-syn, highly dependent on its surroundings and interactions with other proteins and lipids (C. Wang et al., 2016). Upon membrane binding, the amphipathic N-terminal region of α-syn adopts an α-helix secondary structure, which is highly resistant to aggregation, and several α-syn proteins combine to form higher-order multimers (Burré et al., 2014). Thus, under physiological conditions, α-syn exists in an equilibrium between soluble unfolded species and membrane-bound helical multimers (Figure 9B).

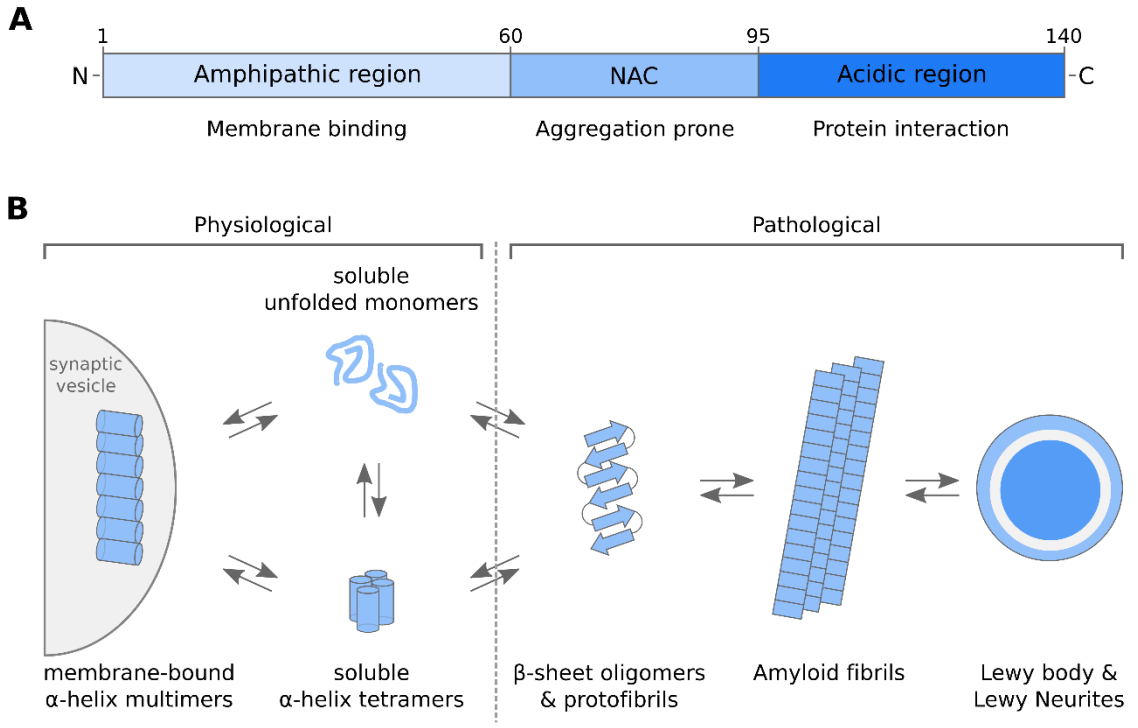

Figure 9. α-Syn structure and conformations in physiological and pathological conditions. A) Structure of α-syn with its main three regions and functions: the N-terminal amphipathic region involved in membrane binding, the central non-amyloid β component (NAC) prone to aggregation, and the C-terminal acidic region which participates in protein binding. **B)** Physiological and pathological conformations of α-syn. Under physiological conditions, α-syn is a natively unfolded monomer in dynamic equilibrium with soluble tetramers with an α-helical secondary structure and a membrane-bound state. Upon binding to highly curved membranes, such as synaptic vesicles, α-syn adopts an amphipathic α-helical structure, which is associated with multimerization. Under pathological conditions, soluble α-syn undergoes a conformational change and adopts a β-sheet secondary structure prone to aggregation, giving rise to α-syn oligomers and protofibrils that progress to insoluble amyloid-like fibrils that ultimately accumulate and form Lewy Bodies and Lewy Neurites.

4.2. Physiological function of α-synuclein

The function of α-syn in physiological conditions remains poorly understood. In light of its elevated morphological plasticity, α-syn has been proposed to behave like a hub protein, by interacting not only with the phospholipids of membranes but also with a variety of proteins (Burré et al., 2018; Longhena et al., 2019). α-Syn has been implicated in lipid homeostasis and membrane biogenesis, as well as in neurotransmission and synaptic plasticity, although the precise mechanisms remain unclear (Alza et al., 2019; Burré et al., 2018; Calo et al., 2016). On the one hand, both the absence and the overexpression of α-syn have been associated with disturbed lipid metabolism and aberrant lipid composition of membranes. Dysfunction of lipid signaling pathways has also been described, with decreased activity of enzymes such as phospholipase C, which is activated upon GPCR/Gq activation, and phospholipases D1 and D2, which play a role in neuronal cytoskeletal architecture and membrane receptor signaling, respectively (Alza et al., 2019).

On the other hand, α-syn increases the curvature of membranes (Varkey et al., 2010), and is preferentially localized to highly-curved small vesicles, such as ~40 nm SVs (Burré et al., 2018; Davidson et al., 1998). In line with these biochemical properties, it has been shown that α-syn participates in intracellular vesicle trafficking, probably by inhibiting the docking and/or fusion of vesicles to membranes, a process regulated by Rab proteins, a family of GTPases from the Ras superfamily (Gitler et al., 2008; M.-M. Shi et al., 2017). Furthermore, α-syn is thought to regulate neurotransmitter release by regulating the size, motility, and distribution of SV pools in the active zone of the presynaptic terminal (Scott & Roy, 2012; Vargas et al., 2017). In addition, α-syn can act as a chaperone molecule contributing to the assembly of the SNARE complex (Burré et al., 2010), and the subsequent SNARE-dependent docking of SVs to the plasma membrane (Lou et al., 2017), which are necessary for neurotransmitter release. However, α-syn does not participate directly in the fusion of the SVs with the plasma membrane and the release of the neurotransmitter (Lai et al., 2014). α-Syn has been associated not only with exocytosis but also with clathrin-mediated SV endocytosis (Vargas et al., 2014), supporting the role of α-syn in SV trafficking.

Additionally, α-syn plays an important role particularly in dopaminergic neurons by modulating synaptic DA levels. Direct interaction between α-syn and several proteins involved in DA metabolism have been described, such as the inhibition of tyrosine hydroxylase (TH), the rate-limiting enzyme of DA synthesis (Perez et al., 2002), as well as the VMAT-2 (J. T. Guo et al., 2008) and the DAT (Swant et al., 2011), involved in pumping cytosolic DA into SVs, and reuptake of DA from the synaptic cleft to the presynaptic terminal, respectively.

Together, these observations indicate that α-syn has an important role in maintaining neurotransmitter homeostasis by regulating SV fusion, clustering, and trafficking between the different SV pools, as well as in endocytosis and neurotransmitter reuptake and vesicle filling by interacting with neurotransmitter membrane transporters and other synaptic proteins.

4.3. Pathological role of α-synuclein

An increasing body of evidence from studies carried out in animal models and PD patients support the hypothesis that the processes underlying α-syn aggregation have a central role in the pathogenesis of PD (Calo et al., 2016; Ghiglieri et al., 2018). However, the molecular mechanism of α-syn structural transformation, the relation between different structural species and their functional and pathogenic roles in neuronal function and PD remains unknown.

Under pathological conditions, α-syn adopts a β-sheet amyloid conformation in contrast to the α-helix conformation found in physiological conditions. The β-rich conformations have an increased tendency to self-assemble into amyloid oligomers and fibrils, eventually leading to larger aggregates up to the size of an inclusion body (Burré et al., 2018) (Figure 9B). It has been proposed that α-syn oligomers and small fibrils play a key role in the neurodegenerative process by impairing cell function and leading to neuronal death. These toxic α-syn species negatively impact critical cellular processes such as mitochondrial function, endoplasmic reticulum (ER) stress, protein folding, protein degradation, axonal transport, and presynaptic function (Rosborough et al., 2017). The underlying triggers of α-syn accumulation and aggregation are unclear. A relative overproduction of the protein, mutations that increase misfolding or aggregation, as well as impairment of the ubiquitin-proteasome system and the lysosomal autophagy system involved in protein degradation, have been proposed as initial events in α-syn pathology (Poewe et al., 2017).

Moreover, α-syn oligomers and small fibrils not only cause cytotoxicity but may also propagate the neurodegenerative process from cell to cell. According to the prion-like hypothesis, toxic α-syn species can be transported intra-axonally to other brain regions and be released into the extracellular space, where they can be taken up by neighboring neurons. Those α-syn aggregates can have a seeding effect by recruiting endogenous unfolded α-syn proteins in the host cell and turning it into misfolded forms that will aggregate. Thus, initial α-syn misfolding in a small number of cells could progressively lead to the spread of α-syn aggregates to multiple brain regions over years or decades following the initial insult (Angot et al., 2010; Brundin et al.,

2010). This is consistent with Braak's hypothesis that α-syn pathology gradually engages more brain regions as the disease progresses (Braak et al., 2003).

5. Animal Models of Parkinsonism

Animal models are very useful tools to study the molecular pathogenesis of PD and provide valuable insight into potential new targets for disease intervention. The ideal animal model should be progressive and reproduce the histopathological, biochemical, and pathophysiological features associated with PD. However, as it occurs with other neurodegenerative diseases, PD has not been observed spontaneously in animals. Consequently, the main characteristic features of the disease have been imitated in experimental animals through the administration of different neurotoxic agents or drugs that disrupt dopaminergic neurotransmission or cause similar histopathological changes associated with PD (Van Kampen & Robertson, 2017).

The most commonly used animal models for the study of experimental PD are those resulting from exposure to neurotoxins such as 6-OHDA, MPTP, rotenone, and paraquat in rodents and primates. The PD toxin-based models cause an acute and rapid death of dopaminergic neurons and produce a DA loss phenotype without any progressing evolution of the pathology (Bezard et al., 2013). Of note, the administration of these toxins does not result in α-syn pathology. Although these traditional toxin-based models of PD have proved extremely useful in developing treatments for PD signs and in investigating side effects associated with DA replacement therapies, they do not model the molecular pathology of PD and consequently, have not succeeded in deepening into the neurobiological basis of the disease (Koprich et al., 2017).

Animal models based on PD-related genes have proven useful to unravel the function of specific proteins as well as to understand the neurobiology of the disease (Imbriani et al., 2018). Of note, because of the prominent role that α-syn plays in the pathology of PD, it represents a particularly appealing basis for animal models development (Benskey et al., 2016). These animal models based on PD-related genes, specifically α-syn, represent an ideal condition to explore subtle alteration of synaptic activity before neuronal degeneration occurs as they offer the possibility to follow the synaptic events at different time points along with the disease progression. To date, the vast majority of work on these animal models has been performed in rodents, although some research has also been performed in invertebrates (Drosophila and Caenorhabditis elegans; Surguchov, 2021) as well as in larger mammals such as non-human

primates, especially with α-syn-based models (Marmion & Kordower, 2018). These animal models can be subdivided into transgenic models of α-syn and other PD-related genes, models of exogenous α-syn by inoculation of fibrils or oligomers, and by viral vector-based overexpression of α-syn (Gómez-Benito et al., 2020; Imbriani et al., 2018; Koprich et al., 2017). The most relevant PD models in the studies of synaptic dysfunction will be described in the following section.

5.1. Transgenic models

Many transgenic mouse lines overexpressing wildtype (WT) or mutant human α-syn (hα-syn) have been generated to try to model *SNCA* missense mutations or multiplications described in PD. The majority of transgenic lines overexpressing mutant α-syn encode either A53T or A30P familial mutation. However, there are also double mutant transgenic lines that express both mutations, and a few express α-syn with modifications such as the C-terminal truncation of the last 20 residues (α-syn 1-120) (Koprich et al., 2017). One major difference between existing α-syn transgenic mice is the promoter used to control transgene expression, which includes mouse thymus cell antigen 1 (Thy1) promoter, human platelet-derived growth factor subunit B (PDGF) promoter, TH promoter, and the prion promoter (Prnp) (Garcia-Reitböck et al., 2010; Giasson et al., 2002; Masliah et al., 2000; Nemani et al., 2010; Tozzi et al., 2016; van der Putten et al., 2000). Bacterial artificial chromosome (BAC) models with upstream promoter elements have also been developed, often on a mouse *SNCA*$^{-/-}$ background, to drive expression of human *SNCA* at endogenous levels and to avoid potential confounding interactions with endogenous mouse α-syn (Janezic et al., 2013). The type of promoter used will determine the type of cells where α-syn transgene will be expressed.

Studies using these transgenic models have provided important insight into the synaptic alterations induced by α-syn. Experimental data show that the accumulation of toxic α-syn species causes a synaptic neurotransmitter deficiency that precedes cell death, pointing to synapses as the region of primary α-syn pathology in the cell. The release of DA from synaptic terminals is progressively impaired and is accompanied by defects in SV recycling and redistribution of SNARE proteins in synaptic terminals without changes in total DA content (Garcia-Reitböck et al., 2010; Janezic et al., 2013; Nemani et al., 2010). Thus, these studies suggest that dopaminergic dysfunction is not initially a direct effect of cell death or reduction of DA content, but is rather caused by functional impairment of neurotransmitter release at the synapse. Nevertheless, it remains unclear whether these functional disturbances lead eventually to anatomical degeneration as its temporal pattern has not been often studied.

Electrophysiological studies have shown altered synaptic plasticity in the striatum (Tozzi et al., 2012, 2016) as well as in the hippocampus (Costa et al., 2012; Nemani et al., 2010; Paumier et al., 2013; Singh et al., 2019; Teravskis et al., 2018) of several transgenic α-syn mice models (Table 1). Focusing on the hippocampus, the truncated hα-syn 1-120 transgenic model showed impaired LTP in the CA1 region in the absence of changes in basal synaptic transmission or DA content, although DA metabolite homovanillic acid (HVA) and noradrenaline levels were decreased (Costa et al., 2012). In the same animals, spontaneous DA release from synaptic terminals was unchanged while evoked DA release was decreased, in line with the studies suggesting impairment of activity-dependent neurotransmitter release. Furthermore, those animals showed hippocampal-dependent memory deficits before the onset of motor dysfunctions, which was rescued by subchronic treatment with L-DOPA. More recently, it was found a different degree of synaptic dysfunction depending on the α-syn form, with the A53T mutation leading to a more severe synaptic impairment than WT or A30P α-syn forms (Singh et al., 2019; Teravskis et al., 2018). Transgenic mice with the A53T mutation develop a progressive synaptic dysfunction with only decreased probability of neurotransmitter release (decreased frequency of miniature excitatory postsynaptic currents -mEPSCs-) at 3 months of age, that progressed into reduced synaptic strength (decreased AMPAR to NMADAR currents ratio), reduced postsynaptic AMPAR function (decreased amplitude of mEPSCs), and inhibition of LTP at 6 months of age. These synaptic deficits are accompanied by behavioral deficits, with impaired cognitive functions at 6 and 12 months but not at 3 months (Singh et al., 2019). WT and A30P α-syn only showed presynaptic impairment with decreased probability of neurotransmitter release, without postsynaptic or LTP deficits (Teravskis et al., 2018). Spatial memory was also unaffected by the expression of WT and A30P α-syn forms at 12 months of age (Singh et al., 2019). Thus, these results suggest that presynaptic dysfunction is a common feature among different α-syn forms, but the A53T mutation progresses to postsynaptic alteration as well, which is associated with hippocampal-dependent memory deficits. However, these studies were exclusively focused on the role of α-syn, and the integrity of the dopaminergic pathway nor the DA content were assessed.

Some studies also suggest that α-syn may decrease basal synaptic transmission. A transgenic hα-syn WT model showed a rightwards shift in the input-output (I/O) relationship within a range of stimulus intensities, which reflects a decrease in the efficacy of neurotransmitter release, as well as a decrease in the paired-pulse facilitation (PPF) (Nemani et al., 2010). Another study with the hα-syn A53T model found the same rightwards shift in the I/O relationship but increased PPF. These synaptic dysfunctions preceded the onset of memory deficits although were not associated with LTP impairment (Paumier et al., 2013). Additionally, a transgenic mice model

expressing the A30P mutation showed increased LTP in the CA3 region, where LTP depends on presynaptic mechanisms (Gureviciene et al., 2007), and enhanced basal synaptic transmission and impaired LTP in the DG, where LTP depends on the activation of NMDARs (Gureviciene et al., 2009).

Animal models based on other PD-related genetic mutations have also proven crucial for an improved understanding of disease mechanisms. Most common forms of familial PD are associated with gain-of-function mutations in the *LRRK2* gene. Several rodent transgenic models have been generated to overexpress WT or pathogenic variants of this gene (Seegobin et al., 2020). Transgenic mice expressing the G2019S mutation in the *LRRK2* gene show loss of bidirectional striatal synaptic plasticity with impaired LTP and LTD, which was associated with a change in AMPAR subunit composition with increased contribution of Ca^{2+} impermeable GluA2-containing AMPARs (Chou et al., 2014; Matikainen-Ankney et al., 2018). G2019S LRRK2 animals also show impaired LTD in the hippocampus (Sweet et al., 2015) as well as cognitive deficits with impaired long-term recognition memory together with motor impairment (Volta et al., 2015). Loss-of-function mutations in *PRKN*, *PINK1*, and *DJ-1* genes have been related to early-onset PD. Deletion of *PRKN* or *PINK1* genes has been associated with impairments in evoked DA release as well as LTP and LTD in the striatum (Kitada et al., 2007, 2009; Madeo et al., 2014). *PRKN*$^{-/-}$ animals showed memory deficits associated with hippocampal LTP impairment and increased basal levels of DA but no alteration in spontaneous or evoked release of neurotransmitters (Rial et al., 2014). By contrast, LTP was not impaired in the hippocampus of *PINK1*$^{-/-}$ animals, but there was an enhancement of presynaptic glutamate release (Feligioni et al., 2016). Genetic deletion of *DJ-1* also reduced LTP and completely abolished LTD in the hippocampus (Y. Wang et al., 2008).

Despite the valuable insight into the synaptic dysfunction induced by different forms and mutations of α-syn as well as other PD-related genes, most of the functional electrophysiological studies in transgenic mice models lack a proper characterization of the nigrostriatal system. Moreover, studies focused on histological characterization show that these animal models require prolonged periods of time for the development of pathological features. In α-syn transgenic models, α-syn pathology takes more than 6 months to develop, showing variability in the anatomical distribution of α-syn inclusions among different mice strains or gene promotors (Garcia-Reitböck et al., 2010; Janezic et al., 2013; Tozzi et al., 2016). In addition, dopaminergic neuronal cell loss is generally absent (Garcia-Reitböck et al., 2010; Giasson et al., 2002; Jagmag et al., 2016; Masliah et al., 2000; Seegobin et al., 2020; van der Putten et al., 2000) or takes more than 15 months to develop a mild 20-30% degeneration (Janezic et al., 2013; Xiong et al., 2018).

To sum up, transgenic mouse models possess strong construct validity, as they are based on human genetic data implicating mutations associated with PD. These models collectively exhibit some key features of PD, including α-syn inclusions, synaptic dysfunction in the nigrostriatal as well as in limbic and cortical regions, and non-motor symptoms, but show limited and inconsistent neurodegeneration on the SNpc, questionable motor signs, and prolonged time-course to develop pathology.

Table 1. Behavioral and electrophysiological studies performed in α-syn transgenic animal models.

Reference	Animal model			Behavior		Electrophysiology*		Biochemical and histological studies
	Species	Transgenic hα-syn	Time point	Motor	Non-motor	Region	Basal transmission and synaptic plasticity	
Singh et al., 2019 & Teravskis et al., 2018	Mice	WT	3-6 m	-	-	CA1	mEPSCs frequency ↓	Hα-syn n.s.
			12 m	-	Spatial memory n.s.	-	-	-
		A30P	3-6 m	-	-	CA1	mEPSCs frequency ↓	Hα-syn ↑
			12 m	-	Spatial memory n.s.	-	-	-
		A53T	3 m	-	Fear conditioning n.s.	CA1	mEPSCs frequency ↓	GluN1 n.s., GluN2A n.s., GluA1 n.s., GluA2/3, n.s.
			6 m	Locomotor hyperactivity	Impaired spatial memory and fear conditioning	CA1	AMPA/NMDA current ↓, mEPSCs amplitude, and frequency ↓, LTP ↓	Hα-syn ↑, GluN1 n.s., GluN2A n.s., GluA1 ↓, GluA2/3 ↓
			12 m	Locomotor hyperactivity	Impaired spatial memory	-	-	Hα-syn ↑, GluN1 ↑, GluN2A n.s., GluA1 ↓, GluA2/3 ↓
Paumier et al., 2013	Mice	A53T	2 m	n.s.	Anxiety and spatial memory n.s.	CA1	I/O curve shifted rightwards, PPF ↑, impaired LTD	Hα-syn ↑
			6 m	Locomotor hyperactivity	Anxiety n.s., impaired spatial memory	-	-	Hα-syn ↑↑
			9 m	-	-	CA1	I/O curve shifted rightwards; PPF ↑	-
			12 m	Locomotor hyperactivity	Decreased anxiety, impaired spatial memory	-	-	Hα-syn ↑↑
Costa et al., 2012	Mice	hα-syn 1-120	3-4 m	n.s.	Impaired context memory (rescued with L-DOPA)	CA1	LTP ↓, rescued with L-DOPA and D1-like agonist, but not with D2-like agonist	GluN2A ↓; [HVA] ↓, [NA] ↓; spontaneous DA release n.s., evoked DA release ↓
Nemani et al., 2010	Mice	WT	24-36 d	-	-	CA1	I/O curve shifted rightwards; PPF ↓; mEPSCs frequency ↓	Synapse density and SV density n.s.; SV clustering in the active zone ↓; PSD length ↑
Gureviciene et al., 2009	Mice	A30P	10 m	Exploratory activity n.s.	Spatial memory n.s.	DG	I/O curve shifted leftwards; LTP n.s.	Hα-syn ↑
			24 m	Exploratory activity ↓	Spatial memory n.s.	DG	I/O curve shifted leftwards; LTP ↓	Hα-syn ↑
Gureviciene et al., 2007	Mice	WT	4-5 m	-	-	CA3	PPF ↓; LTP ↑	Hα-syn ↑
		A30P	4-5 m	-	-	CA3	PPF ↓; LTP ↑	Hα-syn ↑↑

D: days; m: months; NA: noradrenaline; n.s.: not significant. *All electrophysiological studies were performed in *ex vivo* hippocampal slices from transgenic animals.

5.2. Models of inoculation of exogenous α-syn preformed fibrils/oligomers or LB containing tissue

Following the description of Braak, the hypothesis that α-syn spreads between interconnected anatomical areas have become an interesting way of modeling PD progression. Several models of α-syn spread that lead to degeneration have been developed, including intracerebral injection with LB containing tissue from *post-mortem* human brains or the injection with synthetic preformed fibrils or oligomers.

Recombinant α-syn fibrils induce the formation of inclusions that resemble LBs and LNs when added to primary neuron cultures or injected into different brain regions *in vivo* (Volpicelli-Daley et al., 2016). The inoculation of fibrils into the striatum induces a spatial and temporal pattern of neurotoxicity similar to the one observed in PD patients, with the presence of aggregated α-syn throughout the brain preceding loss of dopaminergic terminals and striatal DA, the subsequent death of SNpc neurons, and the corresponding motor impairment (Luk et al., 2012a, 2012b; Patterson et al., 2019; Paumier et al., 2015). By contrast, inoculation of fibrils in the SN was not associated with dopaminergic neuronal loss and motor dysfunction despite the widespread α-syn pathology (Masuda-Suzukake et al., 2013). Interestingly, α-syn inclusion formation occurs in brain areas distant from the injection site; when injected in the striatum they also appear in the hippocampus, cortex, midbrain, and other regions (Luk et al., 2012a; Paumier et al., 2015), which allows examining the impact of these aggregates on diverse neuronal populations. Thus, the potential to study the effects of α-syn pathology in multiple neurochemical systems and to model non-motor symptoms is an advantage of this model. This model has also been translated into non-human primates, providing a model of α-syn spread in an anatomical system closer to that of humans (Arotcarena et al., 2020; Chu et al., 2019; Recasens et al., 2014).

In this sense, most studies have been centered on the trans-synaptic propagation of α-syn and very few studies have been performed regarding synaptic alterations after the injection of these exogenous pathological α-syn forms. A study showed impaired DA release by *in vivo* amperometry recordings 10 days after the inoculation of hα-syn fibrils into the rat SN in combination with viral vector-mediated overexpression of hα-syn. These animals exhibited a reduction in DA release and reuptake rates in the striatum that was accompanied by progressive degeneration of dopaminergic neurons in the SN and impaired motor behavior over time (Thakur et al., 2017). Recently, electrophysiology recordings in slices from mice injected with fibrils in the striatum revealed dysfunction in synaptic transmission and plasticity. These animals exhibited LTP impairment in both populations of striatal SPNs by selectively targeting the GluN2A-NMDARs, with no detrimental effect on LTD (Durante et al., 2019). In line with these findings, incubation of

hippocampal slices with α-syn oligomers also showed increased neuronal excitability and impaired LTP (Diógenes et al., 2012; Ferreira et al., 2017; La Vitola et al., 2018; Martin et al., 2012; van Diggelen et al., 2019) (Table 2). The enhancement of basal transmission was shown to be mediated by the activation of NMDARs and the subsequent change in AMPAR subunit composition with an increased contribution of Ca^{2+} permeable GluA2-lacking AMPARs. Moreover, changes in basal transmission and synaptic plasticity were specifically associated with oligomeric species of α-syn, while monomers and fibrils did not impair LTP (Diógenes et al., 2012). Furthermore, intracerebroventricular (ICV) injection of α-syn oligomers, but not monomers or fibrils, impaired hippocampal-dependent memory in mice (La Vitola et al., 2018; Martin et al., 2012). Working memory was also impaired after the inoculation of WT-hα-syn fibrils or A53T-hα-syn fibrils directly in the hippocampus (Hu et al., 2016; Kasongo et al., 2020). Additionally, hα-syn fibril inoculation in the olfactory bulb of A53T transgenic mice but not WT mice induced a widespread α-syn pathology including limbic regions such as the hippocampus with hippocampal atrophy, neuronal loss and inflammation, which was accompanied by hyposmia, anxiety-like behavior, and memory impairment without motor dysfunction (Uemura et al., 2021).

One of the major drawbacks of the fibrils/oligomers model is the lack of knowledge about the spread of pathologic α-syn and the exact mechanism by which they induce endogenous α-syn to misfold (Carta et al., 2020). Although the progressive accumulation of aggregated α-syn in different brain regions over time may reflect a prion-like spread, the proposed cell-to-cell transfer remains controversial (Benskey et al., 2016). Additionally, it is important to highlight the great variability that exists in these models regarding the injection site (SNpc, striatum, olfactory bulb, ventricles, and combined models), the amount and type of fibrils or oligomers injected, and the animal species or strains used, which influence the development of neuropathology. Indeed, oligomers and fibrils present poor stability and a tendency to dissociate, not all the species hold the same toxicity, and the mechanisms of structure-related toxicity are still largely unclear. In addition, the animal species from which the α-syn is derived seems to be critical (Gómez-Benito et al., 2020; Luk et al., 2012a). Similarly, variability with the human brain extract model is also a critical problem, as there is no clear means by which different extracts can be benchmarked and thus how a reliable source can be developed to provide consistent quality for a robust animal model (Arotcarena et al., 2020; Recasens et al., 2014).

To sum up, most of the knowledge of the detrimental effects of α-syn oligomers and fibrils in the synaptic function come from *ex vivo* experiments, with few *in vivo* results pointing towards an impaired synaptic function preceding neuronal death. Moreover, although α-syn spread models induce a progressive pattern of pathology that resembles many PD features, they

currently represent models of a hypothesis (model of trans-synaptic spread of α-syn) rather than a disease, as they largely rely on the still controversial prion hypothesis. Further investigations and established guidelines for fibrils and oligomers preparation and injection protocols are required to characterize the robustness and reproducibility of this model and circumvent the great variability among different research studies (Koprich et al., 2017; Peelaerts et al., 2015), as they might be very valuable for evaluating therapies targeted at α-syn spread or blocking of seeding.

Table 2. Behavioral and electrophysiological studies performed in models of exogenous α-syn inoculation.

Reference	Animal model				Behavior		Electrophysiology		Biochemical and histological studies
	Species	hα-syn	Inoculation	Time point p.i.	Motor	Non-motor	Region	Basal transmission and synaptic plasticity	
Kasongo et al., 2020	Rat	WT Fibrils	Intrahippocampal injection	12 m	n.s.	Spatial memory n.s., impaired working memory	-	-	α-Syn aggregates in the hippocampus, without neuron degeneration in the hippocampus, SNpc and VTA
van Diggelen et al., 2019	Mice	WT Oligomers	Bath application*	-	-	-	CA1	LTP ↓	-
La Vitola et al., 2018	Mice	WT Monomers	ICV injection	10-15 d	-	Recognition memory n.s.	-	-	-
		WT Fibrils	ICV injection	10-15 d	-	Recognition memory n.s.	-	-	-
		WT Oligomers	ICV injection	10-15 d	-	Impaired recognition memory	-	-	No neuron loss in the hippocampus, synaptophysin n.s., PSD-95 n.s.
		WT Oligomers	Bath application*	-	-	-	CA1	LTP ↓	-
Ferreira et al., 2017	Mice	WT Oligomers	Bath application*	-	-	-	CA1	I/O curve shifted leftwards; LTP ↓	-
	Rat	WT Oligomers	Bath application*	-	-	-	CA1	I/O curve shifted leftwards; LTP ↓	GluN1 n.s; GluN2B ↑
Hu et al., 2016	Mice	A53T fibrils	Intrahippocampal injection	2 m	n.s.	Impaired working memory	-	-	α-Syn aggregates, inflammation ↑, apoptosis ↑
Martin et al., 2012	Mice	WT Oligomers	ICV injection	24 h	-	Cued fear conditioning n.s., impaired contextual learning	-	-	pCREB ↓, CREB n.s.
	Rat	WT Oligomers	Bath application*	-	-	-	CA1	LTP ↓	-
	Rat	WT Monomers	Bath application*	-	-	-	CA1	LTP n.s.	-
	Rat	WT Fibrils	Bath application*	-	-	-	CA1	LTP n.s.	-
Diógenes et al., 2012	Rat	WT Oligomers	Bath application*	-	-	-	CA1	I/O curve shifted leftwards; NMDAR-EPSCs ↑; GluA2-lacking AMPAR-EPSCs ↑; LTP ↓	Surface GluA1 ↑
		WT Monomers	Bath application*	-	-	-	CA1	LTP n.s.	-
		WT Fibrils	Bath application*	-	-	-	CA1	LTP n.s.	-

d: days; m: months; n.s.: not significant. *α-syn was preincubated in the recording chamber with *ex vivo* slices from healthy animals.

5.3. Adeno associated viral vector-based α-syn overexpression models

The development of gene delivery techniques using recombinant viral vectors has been very useful to address the need for animal models recapitulating the specific neuropathological processes of various neurodegenerative diseases. In this context, viral vector-mediated overexpression models for PD were developed using recombinant adeno-associated viral vectors (AAV) encoding either WT or mutant hα-syn inoculated in the SNpc (Bourdenx et al., 2015; Decressac et al., 2012; Kirik et al., 2002; Klein et al., 2002; Ulusoy et al., 2010). Recently, AAVs overexpressing hα-syn have also been inoculated in the olfactory bulb to model prodromal phases of PD (Niu et al., 2018), or in the PFC to model the cognitive dysfunction found in PDD and DLB (Espa et al., 2019; Wagner et al., 2020). AAVs use single-stranded DNA that integrates into the host genome and provides long-term expression in the transduced neurons, reaching up to 95% efficiency (Ulusoy et al., 2008, 2010) and thus, represent the current most used tool for preclinical studies (Koprich et al., 2017). Indeed, this model is also attractive as it can be applied in a broad range of animal species including rodents and non-human primates (Vermilyea & Emborg, 2015).

Several important considerations when using the AAV-hα-syn model that will influence the comparison among studies are the serotype, the promoter, inclusions of the woodchuck hepatitis post-transcriptional regulatory element (WPRE), and the type of hα-syn overexpressed. There are several serotypes of AAV vectors that have different propensities to transduce neurons in different brain regions (Carta et al., 2020; Ulusoy et al., 2010). The most efficient and extensively studied serotype for use in the SN is the AAV2, although over the last years new hybrid AAV serotypes which show increased transduction and spread of hα-syn have been implemented in this model (Decressac et al., 2012; Gaugler et al., 2012; Gorbatyuk et al., 2008; Oliveras-Salvá et al., 2013; Ulusoy et al., 2010). Specifically, AAV2/9 is the most efficient in hα-syn transduction (Bourdenx et al., 2015). Regarding the most common promoters to direct the expression of hα-syn, they include the hybrid cytomegalovirus (CMV), chicken β-actin (CBA), phosphoglycerate kinase (PGK), and human synapsin-I promoters. The latter provides neuronal-specific transgene expression, while the others provide a more ubiquitous expression. Furthermore, the inclusion of WPRE into the plasmid improves transgene expression levels (Decressac et al., 2012). On the other hand, the type of hα-syn overexpressed is also critical. Similar to transgenic mice, animal studies with different AAVs suggest that the A53T mutation is more toxic and prone to aggregate than either the A30P mutation or the WT form (J. Lu et al., 2015; Oliveras-Salvá et al., 2013; Peelaerts et al., 2015).

The key critical factors defining the successful outcome of AAVs for disease modeling are related to the quality, purity, and titer of the vector preparations. Since production, purification,

and titration methods vary between laboratories, it is often difficult to compare results between studies. The variability observed in the level of transgene expression and dopaminergic depletion will primarily depend on these critical steps (Ulusoy et al., 2008; Volpicelli-Daley et al., 2016). The purification procedure varies across studies and is crucial for obtaining a high yield of infectious AAVs that could cause non-specific toxic effects or immune reactions (Ulusoy et al., 2008). Determination of the titer or the number of viral genome copies is also critical, as the expression level is primarily determined by the titer. The amount of protein produced after transduction with AAVs may vary, but, typically, there is an approximately 2-4 fold increase in hα-syn levels compared to endogenous protein levels, similar to what might be caused by *SNCA* triplications in PD patients (Gorbatyuk et al., 2008; Volpicelli-Daley et al., 2016).

AAV-based overexpression of hα-syn (native or mutant) leads to a progressive loss of dopaminergic neurons in the SNpc (25-80% loss of TH^+ neurons), loss of terminals in the striatum (30-60% loss of TH or DAT markers), and motor impairment, although the extent of neurodegeneration and time course are variable (Bourdenx et al., 2015; Decressac et al., 2012; Koprich et al., 2010; Oliveras-Salvá et al., 2013; Ulusoy et al., 2010). The overexpression of hα-syn produces the formation of Lewy-like α-syn cytoplasmic inclusions and prominent axonal pathology with dystrophic morphology of presynaptic terminals, which develop early after vector injection and precede dopaminergic neuron cell loss (Chung et al., 2009; Decressac et al., 2012; Gaugler et al., 2012; Koprich et al., 2010; Lundblad et al., 2012; Phan et al., 2017). Moreover, DA levels, as well as its metabolites 3,4-Dihydroxyphenylacetic acid (DOPAC) and HVA, have been described to be decreased in the striatum (Decressac et al., 2012). Particularly, a reduction in DA reuptake rates was described in the striatum of AAV6-WT-hα-syn inoculated rats, which progressed into a reduction in evoked DA release before any significant loss of SNpc dopaminergic neurons (Lundblad et al., 2012). Another study using AAV2/6-WT-hαsyn suggested that reduced DA release corresponds to a decreased density of dopaminergic vesicles and dopaminergic synaptic contacts in striatal terminals at the ultrastructural level (Gaugler et al., 2012). Recent electrophysiological studies overexpressing AAV2/6-WT-hα-syn provide further evidence that α-syn overexpression leads to a failure in the striatal synaptic plasticity. Tozzi and coworkers showed that α-syn selectively blocks the induction of LTP in striatal cholinergic interneurons, without affecting SPNs, along with neuronal degeneration and decrease in motor activity (Tozzi et al., 2016). The same group has recently shown that during the acquisition phase of motor learning in the rotarod task, mice overexpressing hα-syn do not show the correct shift from LTD to LTP that control animals do, and demonstrate that this reorganization of cellular plasticity within the striatum is mediated by D1R and DAT (Giordano et al., 2018).

However, synaptic alterations in the limbic and cortical areas have been poorly characterized in AAV-based animal models. Delivery of AVV1/2-A30P-A53T-hα-syn into the olfactory bulb decreased spine density in several brain areas including the olfactory bulb, striatum, PFC, and hippocampus 12 weeks after the inoculation, which was accompanied by a decrease in TH^+ cell in the SN and a decrease in TH^+ fibers and DA and DOPAC content in the striatum (Niu et al., 2018). By contrast, inoculation of AAV2/6-WT-hα-syn into the PFC increased spine density in this area 10 weeks after the inoculation (Wagner et al., 2020). Despite the recent advances, there is a lack of functional studies assessing synaptic plasticity in limbic and cortical brain regions in association with the overexpression of α-syn in this animal model. So far, most of the studies are focused on the characterization of dopaminergic degeneration in the SNpc and the associated locomotor and behavioral alterations, with few studies assessing cognitive performance. Overexpression of α-syn in the SN has been associated with increased anxiety-like (Campos et al., 2013) and depressive-like behaviors (Caudal et al., 2015), impaired performance on a location recognition task (Crowley et al., 2018), and impulsivity (Jimenez-Urbieta et al., 2018).

Although the VTA plays a prominent role in behavioral and cognitive functions, few studies have assessed α-syn expression and neurodegeneration in this brain area. It has been described that dopaminergic neurons in the VTA are also transduced when the AAVs are inoculated in the SNpc (Caudal et al., 2015; Kirik et al., 2002). Moreover, expression of hα-syn leads to a loss of dopaminergic neurons in the VTA (30% TH^+ loss), although in a lesser stent than in the SNpc (43% TH^+ loss) (Caudal et al., 2015), which was accompanied by a variable loss of TH^+ innervation as well as dystrophic neurites in VTA target areas such as the NAcc and olfactory tubercle (Kirik et al., 2002). Direct delivery of AAVs overexpressing α-syn into the VTA has shown to induce a mild specific degeneration of dopaminergic neurons in the VTA without affecting neurons in the SNpc (Alvarsson et al., 2016; H. Hall et al., 2013), although one study found no degeneration in the VTA (Maingay et al., 2006). Furthermore, AAV6-WT-hα-syn inoculation into the VTA was associated with impaired emotional memory in the passive avoidance test, which is highly dependent on the amygdala and hippocampus, without alterations in sensorimotor function or any depressive-like behavior (Alvarsson et al., 2016). Spatial memory acquisition deficits were also found in AAV5-hα-syn inoculate rats, presumably due to an inability to develop an efficient search strategy (H. Hall et al., 2013). Direct delivery of AAV6-α-syn into the DG of the hippocampus has been related to impaired spatial memory and learning and increased anxiety-like behaviors (Mutluay et al., 2020). In those animals, although the inoculation was unilateral α-syn was found bilaterally, being more prominent on the injection side, but no neuronal loss was found in the hippocampus. By contrast, cognitive function was normal in rats inoculated with

AAV2/6-WT-hα-syn in the PFC (Espa et al., 2019) or when AVV6-WT-hα-syn were inoculated in the forebrain of neonatal rats, which induces the expression of α-syn preferentially in the cortex and striatum (Aldrin-Kirk et al., 2014).

Despite most of the behavioral studies have been performed with bilateral inoculations of the AAVs (Alvarsson et al., 2016; Campos et al., 2013; Caudal et al., 2015; Crowley et al., 2018; H. Hall et al., 2013; Jimenez-Urbieta et al., 2018) most of the studies focused on the histopathological characterization have been carried out with unilateral inoculation (Chung et al., 2009; Gaugler et al., 2012; Lundblad et al., 2012; Mutluay et al., 2020; Phan et al., 2017; Tozzi et al., 2016), where compensatory mechanism from the unaffected side could take place. On the other hand, although evidence shows that synapses are the primary site of pathology in α-synucleinopathies, most studies using the AAV model have been primarily focused on cell death and there is a lack of studies focused on the active functional α-syn pathology that interferes with normal synaptic physiology. Studies focused on the temporal pattern of synaptic abnormalities that take place before and during the onset and progression of the dopaminergic degeneration in motor and limbic areas would give valuable insights into the precise synaptic mechanisms that take place on the prodromal phase of the disease as well as disease progression and would allow us to implement new pharmacological approaches.

Summarized, targeted overexpression of hα-syn in midbrain dopaminergic neurons using AAV reproduces many of the characteristic features of PD as it is accompanied by abnormal accumulation of hα-syn leading to aggregation, cellular, biochemical, and synaptic pathologies, neuroinflammation, dopaminergic system degeneration, and consequent motor and non-motor impairment that develop progressively over time. Thus, this model represents the current most used tool for preclinical studies as it offers a robust tool for the study of the neurobiological basis of the disease and its progression as well as for the preclinical evaluation of new therapies that could help to slow or halt its development.

Hypothesis and aims

Our hypothesis is that the onset of cognitive and behavioral alterations in PD are related to a failure of the synaptic function in the hippocampus due to the accumulation of presynaptic α-syn aggregates in dopaminergic terminals, which would progress to neurodegeneration of the mesolimbic dopaminergic pathway and that, to some extent, would be counterbalanced by dopamine replacement therapy. In addition, synaptic enhancers at early phases of the neuropathological process could prevent or delay the mesolimbic dopaminergic neurodegeneration, preventing or ameliorating cognitive and behavioral manifestations.

The main objective of this doctoral thesis is to elucidate the temporal sequence of synaptic alterations in the hippocampus associated with α-syn overexpression and dopaminergic degeneration in a rat model of progressive parkinsonism. Additionally, the synaptic function will be tested under the effect of two dopaminergic drugs.

The following specific objectives were established:

- To determine the temporal sequence of hα-syn overexpression in the hippocampus and its relationship with the dopaminergic degeneration in the SNpc and VTA.
- To study the early stages of the motor behavior and hippocampal-dependent memory performance associated with the overexpression of hα-syn.
- To assess the temporal sequence of synaptic plasticity and the effect of the two standard dopaminergic drugs (PPX and L-DOPA) in isolated hippocampal synapses by fluorescence analysis of single-synapse long-term potentiation (FASS-LTP).
- To analyze the temporal sequence of synaptic protein expression patterns in isolated hippocampal synapses by proteomics approach.
- To evaluate brain glucose metabolism after chronic PPX treatment by [^{18}F]-FDG PET.

Materials and methods

The most relevant antibodies and buffers used in the different experiments of this doctoral thesis are detailed in the annex section.

1. Development of the animal model of parkinsonism

1.1. Animals

Adult male Sprague-Dawley rats weighing about 300 g at the beginning of the experiment (Charles River Laboratories, France) were used. Animals were housed in standard conditions of temperature and humidity (70% humidity, 22ºC), kept on a regular 12 h light/dark cycle, and allowed to *ad libitum* access to food and water. All experimental procedures were approved by the ethics committee for animal research at Biodonostia Health Research Institute (CEEA16/11; ANIMA4-002; San Sebastian, Spain), CIC biomaGUNE (FOR-EP-03-0414; San Sebastian, Spain), and CIMA-Universidad de Navarra (108-17; Pamplona, Spain) and were carried out following the guidelines of the Spanish Government (RD53/2013) as well as European Union Council Directive (2010/63/EU). All efforts were made to avoid and/or alleviate animal suffering and to reduce the number of animals.

1.2. Viral vectors

Recombinant AAVs with 2/9 serotypes were custom ordered from the core facility of production of AAVs of the University of Bordeaux (Bordeaux, France). Each vector was driven by a CMV promoter and transgene expression was enhanced using a WPRE.

1.3. Experimental groups

The cross-sectional study designed involved two experimental groups:

- **AAV-hα-syn:** Animals inoculated with the viral vector AAV2/9-CMV/α-synA53T, encoding for the hα-syn protein with the A53T mutation (Titer: 3.9 x 10^{13} genomic particles/milliliter).
- **AAV-EVV**: Animals inoculated with the viral vector AAV2/9-CMV/EVV, which are empty capsids of the AAV with no overexpression of transgenes (empty viral vectors; EVV) and representing the control group (Titer: 1 x 10^{12} genomic particles/milliliter).

Each experimental group was subdivided into multiple independent subgroups of rats according to the final evaluation time point post-inoculation (p.i.) of the viral vector: 1 week (w),

2 w, 4 w, 16 w, and 20 w. The time points selected for each study are explained in the following section.

For the histological characterization and proteomics study 1, 2, 4, and 16 weeks p.i. were chosen to evaluate the temporal pattern of the alterations from the beginning of hα-syn overexpression in the hippocampus to the establishment of the dopaminergic lesion. For the behavioral evaluation (motor and cognitive) and FASS-LTP study, animals were studied at 1 and 4 weeks p.i. in order to assess the initial phases of hα-syn overexpression. For the PET, the study was carried out 20 weeks p.i. of the AAVs, once the dopaminergic lesion was established (16 w p.i.) and following a chronic treatment (4 w) with the dopaminergic drug PPX, as described in previous studies (Jimenez-Urbieta et al., 2018). A representation of the different studies performed is summarized in Figure 10.

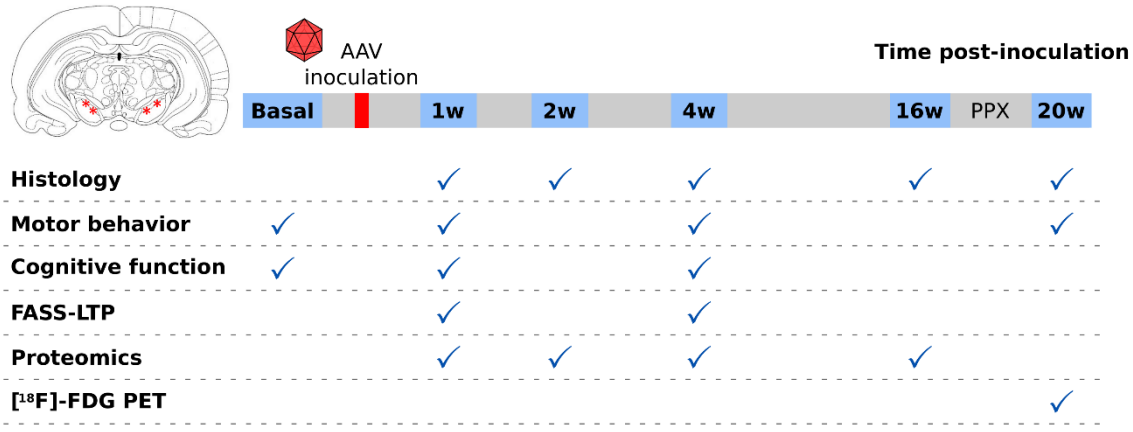

Figure 10. Experimental design. Representation of the viral vector inoculation sites (bilaterally in the SNpc, red asterisks) and experimental design for the different studies with the final evaluation time points after the inoculation of the AAVs.

1.4. Stereotaxic surgery

Rats were anesthetized with isoflurane in oxygen-enriched air (4% induction and 2-2.5% maintenance) and placed on a stereotactic frame (Stoelting Co.). The head was fixed with the ear bars and with the incisor bar positioned -3.3 mm below the interaural line. A sagittal incision was made in the skin and the periosteum was carefully separated to locate the cranial sutures. The coordinates where the AAV was inoculated were calculated from Bregma (the anatomical point on the skull at which the coronal suture is intersected perpendicularly by the sagittal suture) as the origin for anteroposterior (AP) and mediolateral (ML) axis, and related to dura as the origin for dorsoventral (DV) axis. Two small holes were drilled in the animal's skull with a dental drill. The AAVs were bilaterally inoculated in two points (1 µL per site) in each SNpc using a Hamilton

syringe (10 µL, Neuros #1701RN, Hamilton Company) connected to an infusion pump at a rate of 0.2 µL/min (4 µl of total volume/animal). The coordinates used were: 1) AP: -4.9 mm, ML: +/- 2.2 mm, DV: -7.7 mm; 2) AP: -5.4 mm, ML: +/- 2.0 mm, DV: -7.7 mm, from Bregma according to the Atlas of Paxinos and Watson (Jimenez-Urbieta et al., 2018; Paxinos & Watson, 1998). Upon completion of inoculation, the needle was maintained in place for 1 min to allow the solution diffusion away from the injection site and it was slowly retracted from the brain. Finally, the skin was sutured and the evolution of the postoperative was controlled to avoid any complication.

2. Histological characterization

2.1. Brain tissue collection

Animals (n = 4-5/group and time point) were deeply anesthetized with a mixture of oxygen and isoflurane (5%), sacrificed at the corresponding time points (1, 2, 4, and 16 weeks p.i.), and perfused transcardially with 0.1 M phosphate-buffered saline (PBS) followed by 4% paraformaldehyde (PFA). Brains were rapidly removed and post-fixed in the same fixative solution for 24 h, and then cryoprotected in 30% sucrose. Serial coronal sections (40 µm thick) were obtained on a freezing microtome (SM2010R, Leica Biosystems) and were stored in a cryoprotectant solution at -20°C until their use.

2.2. Immunohistochemistry

Immunohistochemistry was performed on coronal free-floating sections to assess the integrity of the nigrostriatal pathway by TH staining in the SNpc/VTA and DAT staining in the striatum, as well as to assess the overexpression of hα-syn in the SNpc/VTA and hippocampus. Every sixth section throughout the entire SNpc/VTA was selected for TH immunostaining, while three sections were used for the hα-syn and DAT immunostainings. Different protocols were optimized for the analyses of each protein and are described in the following section. In each experiment, negative controls with the tissue incubated without the primary antibody but including the secondary antibody were performed.

Sections were washed in 0.1 M PBS and endogenous peroxidase was quenched in 3% H_2O_2 in PBS for 10 min at room temperature (RT). Sections were washed in PBS and preincubated in a blocking solution to inhibit unspecific staining and allow for tissue permeabilization, according to the different protocols:

(I) DAT: 10% normal rabbit serum (NRS) and 0.4% Triton X-100 in PBS (PBS-T) incubated for 1 h at RT.

(II) Hα-syn: 10% normal horse serum (NHS) and 0.2% PBS-T incubated for 1 h at RT.

(III) TH: 4% NHS and 0.3% PBS-T incubated for 30 min at RT.

Afterward, sections were incubated overnight with their corresponding primary antibody:

(I) Goat anti-DAT with 4% NRS in 0.2% PBS-T incubated at RT.

(II) Mouse anti-hα-syn with 10% NHS in 0.2% PBS-T incubated at 4°C.

(III) Mouse anti-TH with 1% NHS in PBS incubated at RT.

The following day, after washing in PBS, sections were incubated with their corresponding biotinylated secondary antibody:

(I) DAT: anti-goat with 4% NRS in 0.2% PBS-T for 1 h at RT.

(II) Hα-syn: anti-mouse in 0.2% PBS-T for 1 h at RT.

(III) TH: anti-mouse in PBS for 1 h at RT.

Afterward, all sections were washed and processed with the avidin-biotin-peroxidase complex diluted in PBS (1:100, Vectastain ABC kit, Vector Laboratories, #PK4000) for 1 h at RT. Finally, the signal was revealed with 0.05% 3,3'-diaminobenzidine tetrahydrochloride (DAB; Sigma-Aldrich, #D5905)/H_2O_2 solution for 4 min. All stained sections were mounted on glass superfrost slides, air-dried overnight, dehydrated in ascending alcohol concentrations for 5 min (70%, 95%, 100%), cleared in xylene for 10 min, and coverslipped with the mounting medium (DPX, Panreac, #255254.1610).

All incubations were performed in agitation to facilitate a homogeneous penetration of immunoreagents. More details of the nature, origin, and dilution of the primary and secondary antibodies are available in Table 7 and Table 8 of the annex section.

2.3. Optical microscopy and quantitative analysis

All images for quantification of DAT, hα-syn, and TH stainings were acquired with an Aperio CS2 digital pathology slide scanner (Leica Biosystems).

2.3.1. Quantification of DAT immunoreactivity in the striatum and hα-syn immunoreactivity in the SNpc, VTA, and hippocampus

In order to quantify the representative surface expression of DAT in the striatum and hα-syn in the SNpc, VTA, and hippocampus, 3 representative sections for each animal and time point of the striatum (approx. AP: +1.60 mm, +1.00 mm, and -0.26 mm from Bregma according to stereotaxic atlas; Paxinos & Watson, 1998), SNpc/VTA (approx. AP: –5.30 mm, –5.60 mm, and –6.00 mm from Bregma according to stereotaxic atlas; Paxinos & Watson, 1998) and hippocampus (approx. AP: -3.30 mm, -3.80 mm, and -4.16 mm from Bregma according to stereotaxic atlas; Paxinos & Watson, 1998) were analyzed. Images were converted to 8-bit greyscale images and each brain structure was delimitated according to the stereotaxic atlas (Paxinos & Watson, 1998). Relative optical density (ROD) of grey levels of DAT and hα-syn immunoreactivity were obtained using ImageJ software (NIH) according to the following formula (Tatulli et al., 2018; Vermilyea et al., 2019):

$$ROD = log \frac{basal\ grey\ level}{signal\ grey\ level}$$

The mean ROD values were averaged across all animals for each group and time point.

2.3.2. Quantification of TH$^+$ cells in the SNpc and VTA

TH$^+$ neurons in SNpc and VTA were determined by the unbiased stereological method using an Olympus Bx61 motorized microscope (Olympus) equipped with a DP71 digital camera (Olympus) connected to an XYZ stepper (H101BX, PRIOR) and driven by CAST Visiopharm software (Visiopharm). The optical fractionator method (West, 1999) was used to estimate the total number of TH$^+$ cells in the SNpc and VTA of each animal, as previously described (Jimenez-Urbieta et al., 2018; Rodríguez-Chinchilla et al., 2020). To sum up, this method is designed to provide estimates of the total number of neurons from thick sections sampled randomly with a systematic randomly sampled set of unbiased optical dissectors covering the entire nucleus. Thick sections provide the opportunity to observe cells in their full 3D extent and thus, allow for easy and robust cell classification based on morphological criteria. The optimal sampling parameters were determined previously in a pilot study (Jimenez-Urbieta et al., 2018) including a few animals to determine the number of sections to be analyzed and the number of optical dissectors within the sampled sections. Based on the tissue thickness and distribution of TH$^+$ labeled neurons the optimal size of the optical dissectors employed was 4538.03 µm^2 with an x-y-step length of 213 µm and the dissector height was set to 20 µm (Drøjdahl et al., 2010). The estimation criteria to obtain an efficient stereological design was minimum counting of 150-200 neurons to ensure covering 10%

of the total of the SNpc or VTA for each hemisphere and animal according to the Gundersen method (Gundersen & Jensen, 1987; West, 1999).

A total number of 7 sections per animal covering the entire rostrocaudal extent of the SNpc and VTA (AP: between -4.30 mm and -6.72 mm from Bregma according to stereotaxic atlas; Paxinos & Watson, 1998) were quantified. The SNpc and VTA of each section were delineated using a 4x scanning objective (Olympus) employing external structures used as reference (Paxinos & Watson, 1998). Once the boundaries of the nuclei were delimited, TH^+ cell counting was performed using a 100x oil immersion objective (Olympus). A positive cell was defined as a nucleus covered and surrounded by the corresponding TH immunostaining and the size and shape criteria of the somas were kept uniform throughout the study. Only the somas that were located inside the counting frame or those that touched the inclusion lines were included in the quantification. All somas that were out of the grid or on the bottom and left edges were discarded.

Estimation of the total number (N) of TH^+ cells in the SNpc and VTA was calculated indirectly using the following equation:

$$N = \sum Q \times \frac{t}{h} \; x \; \frac{1}{asf} \; x \; \frac{1}{ssf}$$

Where ΣQ is the total number of counted particles, t is the average thickness of each section, h is the height of the optical dissector, asf is the sampling fraction of the area and ssf is the sampling fraction of the sections. Estimated populations for the SNpc and VTA of each hemisphere were averaged across all animals for each group and time point (Gundersen & Jensen, 1987; West, 1999).

2.4. Immunofluorescence

Triple immunofluorescence staining was performed on coronal free-floating sections containing the VTA to confirm the presence of hα-syn in dopaminergic (TH^+) and glutamatergic ($vGlut2^+$) neurons. Also, several double immunofluorescent stainings were performed on coronal free-floating sections containing the hippocampus to elucidate the dopaminergic (TH^+), glutamatergic ($vGlut2^+$), or GABAergic ($GABA^+$) nature of hα-syn^+ fibers in the hippocampus. In each experiment, negative controls with the tissue incubated without the primary antibody but including the secondary antibody were performed.

Sections were washed in 0.1 M PBS and subsequently incubated with 0.3% PBS-T for 10 min at RT to permeabilize the tissue. After blocking with 10% normal goat serum (NGS) for 1h at

RT, sections were incubated overnight with the corresponding primary antibodies in PBS at 4ºC. The next day, sections were washed three times in PBS followed by incubation with their corresponding secondary fluorescent antibodies for 1 h at RT. Cell nuclei were counterstained with 4',6-diamidino-2-fenilindol (DAPI; 1:10000; Invitrogen, #D1306) diluted in PBS for 15 min at RT. After two washing steps with PBS, all sections were mounted on glass superfrost slides, air-dried overnight, and coverslipped with Vectashield mounting medium (Vector Laboratories, # H-1400).

All incubations were performed in agitation to facilitate a homogeneous penetration of immunoreagents. More details of the nature, origin, and dilution of the primary and secondary antibodies are available in Table 7 and Table 8 of the annex section.

2.5. Confocal microscopy

Fluorescent images were acquired with a Zeiss LSM 800 laser scanning confocal microscope (Zeiss) with a Plan-Apochromat 63x/1.4 numerical aperture oil-immersion objective. Fluorescence was visualized by combining the following laser set for the triple immunofluorescence of the VTA: λ = 405-488-561-633 nm; and for the double immunofluorescences of the hippocampus: λ = 405-488-561 nm. Image acquisition parameters were optimized for each marker. Images of the VTA (approx. AP: -5.30 mm from Bregma according to stereotaxic atlas, Paxinos & Watson, 1998), and dorsal hippocampus (approx. AP: -3.80 mm from Bregma according to stereotaxic atlas, Paxinos & Watson, 1998) were acquired using ZEN Imaging Software (Zeiss). The image size was 1024 x 1024 pixels with a field of view of 101.41 x 101.41 µm.

3. Behavioral tests

All behavioral tests were performed before the inoculation of the AAV (basal) and at the final time point assessed (1 or 4 weeks p.i.; n = 8/group and time point). Prior to behavioral tests, animals were handled by the experimenter for three days for familiarization with the handling procedure and test environment, and to avoid handling-induced anxiety.

3.1. Stepping Test

The adjusting stepping test was used for *in vivo* monitoring of the motor impairment induced by dopaminergic degeneration (Bido et al., 2017). Rats were held by the experimenter with one hand fixing the hind limbs and slightly raising the hind part above the surface. With the

other hand, the experimenter fixed one of the upper limbs, and the animals were slowly moved sideways over a distance of 90 cm, in approximately 5 seconds, firstly in the forehand and then in the backhand directions. The sequence of testing was always the right paw forehand and backhand adjusting stepping followed by the left paw in the forehand and backhand directions. The test was repeated twice for each animal each session and the average values of the number of adjusting steps in both directions with each forepaw were considered in the analysis.

3.2. Open Field Test

Spontaneous locomotor activity and anxiety-like behaviour were assessed with the open field test. The apparatus consisted of an open arena (90 cm length x 90 cm width x 40 cm height) where animals were left to explore freely for 15 min, and the activity was video recorded. An experimenter blind to the group and time point analyzed the data obtained in the recordings. Ethovision XT software (v13; Noldus) was used to analyze total distance traveled (cm), total velocity (cm/s), and the time spent moving (%) as a measure of locomotor activity, as well as time spent in the center (%) of the arena as a measure of anxiety-like behaviour. Data recorded at 1 and 4 weeks p.i. were normalized to basal behaviour and represented as a percentage to basal.

3.3. Object Location Task

The role of the hippocampus appears to be critical for the spatial and temporal components of recognition memory (Barker & Warburton, 2011), thus, we used the object location task (OLT), a spatial version of the object recognition task, to assess specifically the function of the hippocampus.

The OLT was performed in the same arena as the open field, with additional visual cues placed on the walls of the arena.

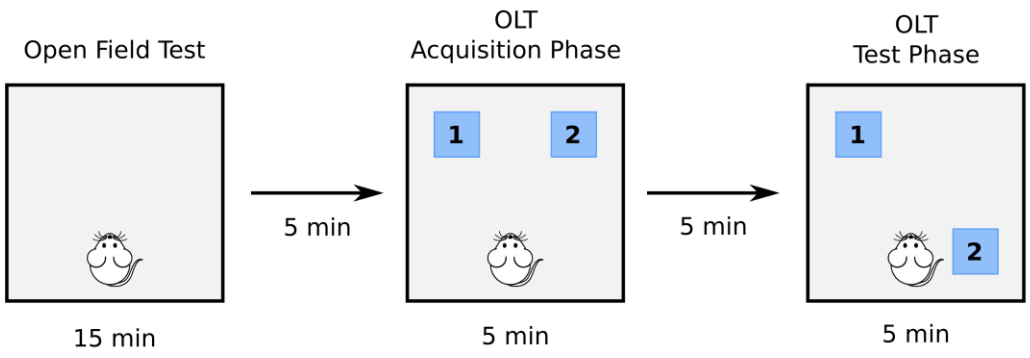

Figure 11. Open field test and object location task (OLT).

The OLT comprised three successive phases with an intertrial time of 5 minutes between phases (Figure 11). The performance of the open field test (15 min) was considered as the first phase or habituation phase. In the second phase or acquisition phase, rats were allowed to explore two identical objects (1 and 2) placed in the far corners and equidistant in the arena (10 cm away from the walls), for 5 min. Shortly thereafter, animals were returned to their cages for 5 min. For the third phase or test phase, object 1 was maintained in the same location (familiar location; FL), while object 2 was moved in diagonal to object 1 (novel location; NL), and animals were allowed to explore the arena for 5 min. The phases were recorded using a camera mounted above the arena. Between the phases, the arena and objects were cleaned with 70% ethanol to minimize olfactory cues (Denninger et al., 2018).

An experimenter blind to the group and time point scored for the amount of time spent sniffing the objects using Ethovision XT software; which consists of the animal directing its nose towards the object at a distance of 2 cm, discarding any other behaviour. In the test phase, time spent exploring the object on the FL and NL (%) were measured, as well as total exploration time (s), total distance traveled (cm), and velocity (cm/s). Animals exploring the objects for less than 10 seconds were discarded.

4. Fluorescence Analysis of Single-Synapse Long Term Potentiation

LTP was assessed by flow cytometry in freshly isolated single synaptosomes after a chemical stimulation of LTP (cLTP) and, fluorescent staining of presynaptic Nrx1β and postsynaptic GluA1 (Figure 12). The FASS-LTP experiments with hippocampal synaptosomes were carried out as previously described (Prieto et al., 2017) with the collaboration of Dr. Cotman's lab at the UCI MIND Institute (Irvine, CA, USA).

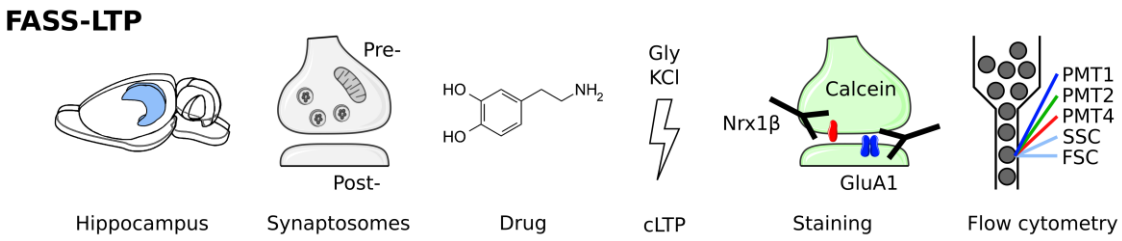

Figure 12. **Fluorescence Analysis of Single-Synapse Long Term Potentiation (FASS-LTP) workflow**. cLTP: chemical long-term potentiation; PMT: photomultiplier tubes; SSC: side scatter; FSC: forward scatter.

4.1. Brain tissue collection

Animals (n = 8/group and time point) were sacrificed by CO_2 inhalation at the corresponding time points (1 and 4 weeks p.i.). Brains were rapidly removed from the skull, and hippocampi and midbrains of both hemispheres were carefully dissected. Hippocampi were processed for synaptosome isolation and FASS-LTP, while midbrains were immediately frozen in dry ice and stored at -80ºC for further confirmation of hα-syn expression by western blot.

4.2. Synaptosome isolation from rat hippocampus

Hippocampi were rapidly dissected and transferred into a microfuge tube containing 1.5 mL of sucrose buffer. All the material was pre-cooled on ice, including sucrose buffer, microfuge tubes, grinder, and pestle. To homogenize the tissue, hippocampi were chopped and immediately homogenized with 6-8 strokes of the pestle while keeping the grinder on ice (clearance: 0.15-0.25 mm). Samples were transferred into microfuge tubes and centrifuged (1200 x *g* for 20 min; 4°C) to obtain the supernatant S1 containing the cytoplasm and membranous structures which was divided into three microfuge tubes containing the same volume. Two of the microfuge tubes were used for the FASS-LTP protocol, while the third microfuge tube was cryopreserved on sucrose buffer at -80ºC.

Samples containing supernatant S1 were centrifuged (12000 x *g* for 20 min; 4°C) to obtain the supernatant S2 containing the cytoplasm and pellet P2 enriched in synaptosomes. The supernatant S2 was discarded and pellet P2 was resuspended by carefully pipetting with either 1.5 mL of extracellular solution or cLTP solution. Synaptosomes were incubated in a cell culture dish (30 mm) for 10-15 min at RT and agitation for the recovery of membrane potential. BCA Assay was run to determine the protein concentration of the samples (see section 5).

4.3. Nuclei and mitochondria isolation from rat liver

Together with the brain dissection, the livers were also extracted and immediately frozen in dry ice and stored at -80ºC. Livers were used to isolate cell nuclei and mitochondria in order to have biological size standards for setting the size gate for synaptosome selection in the flow cytometer.

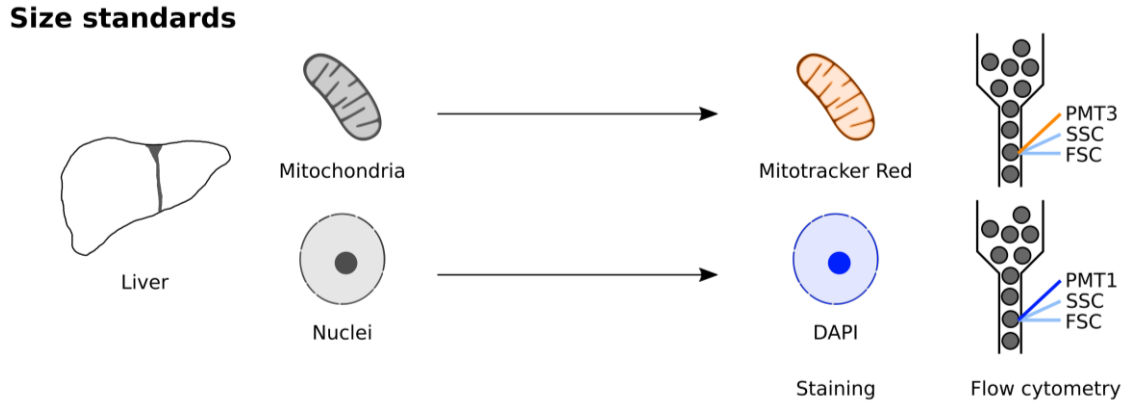

Figure 13. Workflow for isolation of size standards for flow cytometry. PMT: photomultiplier tubes; SSC: side scatter; FSC: forward scatter.

For nuclei isolation, livers were slowly thawed on ice until complete defrost and homogenized manually (clearance: 0.15-0.25 mm) in buffer A. Samples were centrifuged (600 x *g* for 10 min; 4°C), supernatant S1 containing the cytoplasm portion was discarded and the pellet P1 was resuspended in ice-cold buffer A, and centrifuged (600 x *g* for 10 min; 4°C). Supernatant S2 (debris) was discarded, and pellet P2 containing crude nuclei was resuspended in ice-cold buffer B. Samples were divided into 1.5 mL microfuge tubes and centrifuged (16000 x *g* for 30 min; 4°C) to obtain a pellet P3 containing isolated nuclei (Nagata et al., 2010).

For mitochondria isolation, livers were homogenized in buffer C. After the first centrifugation step, pellet P1 was discarded, while supernatant S1 was centrifuged (7000 x g for 10 min; 4°C). Supernatant S2 (cytoplasm) was discarded, and the pellet P2 containing membranous structures was resuspended in ice-cold buffer C and centrifuged again (7000 x g for 10 min; 4°C). Supernatant S3 was discarded, and pellet P3 containing isolated mitochondria was resuspended in buffer C (Frezza et al., 2007). Protein concentration was quantified by BCA Assay (see section 5).

4.4. cLTP stimulation

The following experimental conditions were tested for each animal:

- Synaptosomes in extracellular solution, with PPX (10 µM; Sigma-Aldrich, #A1237), L-DOPA (30 µM; Sigma-Aldrich, #D1507-5G) or vehicle, without glycine and KCl stimulation (basal condition)
- Synaptosomes in cLTP solution, with PPX (10 µM), L-DOPA (30 µM) or vehicle, with glycine and KCl stimulation (cLTP condition)

All the material and samples, including extracellular, glycine, and KCl solutions, and flow cytometry tubes were incubated for 5 min at 37ºC to reach physiological temperature. After the recovery of membrane potential, 30-75 µg of synaptosomes were transferred into flow cytometry tubes and the corresponding drugs (PPX or L-DOPA) or vehicle (water) were added and incubated for 10 min at 37ºC. Subsequently, the glycine solution was added to cLTP solution containing tubes, while the same volume of extracellular solution was added to basal condition tubes. All samples were incubated for 15 min at 37°C. In order to stimulate the depolarization of the presynaptic terminals, KCl solution was added to cLTP condition tubes, while the extracellular solution was added to basal condition tubes. All tubes were incubated for 30 min at 37°C. Stimulation was stopped with ice-cold 0.1 mM EDTA in PBS and samples were blocked with 5% fetal bovine serum (FBS; Gibco, #10500-064) in PBS before the staining. Tubes were chilled on ice and immediately centrifuged (2500 x *g* for 10 min; 4°C). The supernatant was discarded, and the pellet was resuspended with gentle agitation while samples were kept on ice.

4.5. Fluorescence staining of surface GluA1 and Nrx1β

After stopping the depolarization and blocking, resuspended synaptosomes were incubated in agitation with primary antibodies anti-GluA1 and anti-Nrx1β (Table 9, annex), and 100 nM Calcein AM (eBioscience™, #65-0853-39) for 30 min at 4°C. Calcein AM is a membrane-permeable non-fluorescent substrate metabolized by intracellular esterases turning it into a membrane-impermeable and fluorescent Calcein. Properly sealed and functional synaptosomes retain the fluorescent staining intracellularly once cleaved by esterases. Afterwards, samples were washed with ice-cold 5% FBS and centrifuged (2500 x *g* for 10 min; 4°C). The supernatant was discarded, synaptosomes were resuspended, and incubated with the corresponding secondary antibodies conjugated to Brilliant Violet 421 and Alexa Fluor 647 (Table 10, annex), respectively, and 100 nM Calcein AM for 30 min at 4°C in agitation and darkness. After one last washing step

with ice-cold PBS, synaptosomes were resuspended in PBS and stored protected from light at 4°C until analyzed in the flow cytometer.

4.6. Fluorescent staining of mitochondria and nuclei

Isolated mitochondria and nuclei were defrosted, brought to physiological temperature, and transferred to flow cytometry tubes. Mitochondria (150-200 µg) were incubated with 25 nM Mitotracker Red CMXRos (Invitrogen, #M7512) for 30 min at 37ºC, while nuclei (150-200 µg) were incubated with DAPI (1:10000; Invitrogen, #D1306) for 10 min at RT. After the corresponding staining, samples were washed with PBS and centrifuged (2500 x *g* for 10 min; RT). The supernatant was discarded, samples were resuspended and stored protected from light at 4°C until analyzed in the flow cytometer.

4.7. Flow Cytometry

Flow cytometry enables the measurement of optical and fluorescent characteristics of single-cell/particles (synaptosomes, mitochondria, nuclei). Samples were acquired using a FACSCanto II System (BD Biosciences) equipped with a 405 nm solid state diode violet laser, a 488 nm solid state blue laser, and a 633 nm helium-neon red laser. Relative size and granularity were determined by forward scatter (FSC) and side scatter (SSC) properties, respectively, and the fluorescence was detected with the following photomultiplier tubes (PMTs), and bandpass filter (BPF) and long-pass filters (LPF): Brilliant Violet 421 and DAPI PMT1 (BPF 450±50 nm), Calcein AM PMT2 (BPF 530±30 nm; LPF 502), Mitotracker Red CMXRos PMT3 (BPF 585±42 nm; LPF 556), and Alexa Fluor 647 PMT4 (BPF 660±20 nm) (Figure 14). FSC, SSC, and fluorescent signals were collected using logarithmic amplification. Small fragments and debris were excluded by establishing an FSC threshold (gain = 500), and a total of 50,000 size-gated particles were collected and analyzed for each sample (event rate: ~500/s).

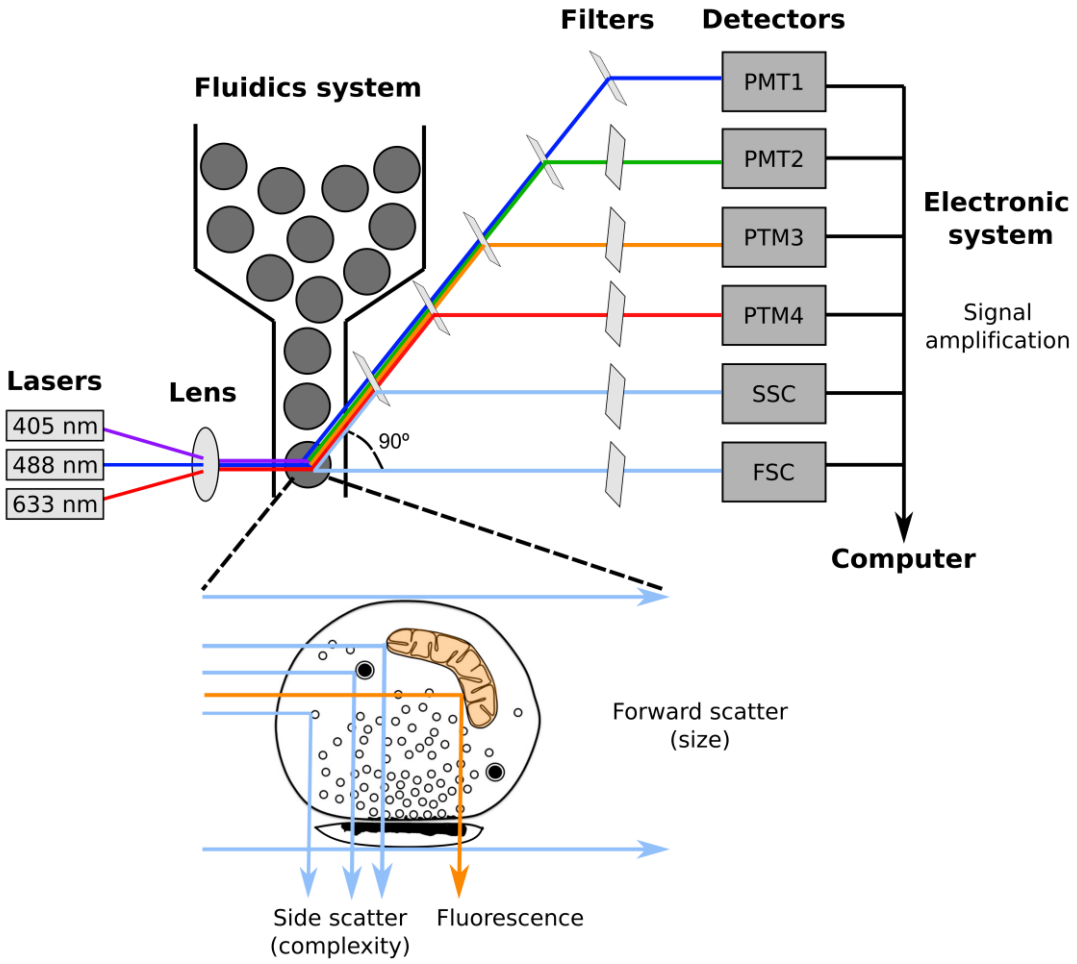

Figure 14. **Components and light scattering properties of flow cytometry.** When the laser strikes a particle it scatters the light, which is collected by several lenses, and optical mirrors and filters that separate and direct specific wavelengths into the appropriate detector. Two types of light scattering occur, forward scatter (FSC) and side scatter (SSC). FSC light results from the collection of diffracted light along the same axis as the laser beam, and it is proportional to the area or size of the particle. SSC light results from the collection of reflected light at approximately 90 degrees to the laser beam, and it is proportional to the cell granularity and intracellular complexity. Fluorescent emissions are also collected at approximately 90º angle. Light scatter and fluorescence signals are then converted into a voltage pulse using photodetectors, such as photomultiplier tubes (PMT). Finally, the electronic system collects, amplifies, and sends the information to a computer.

4.8. Flow cytometry analyses

FlowJo software (v10; FlowJo, LLC) was used to analyze the flow cytometry data. First, considering FSC and SSC parameters, particles ranging from ~0.75 to 3 µm were selected, corresponding to synaptosomes (Prieto et al., 2017). Isolated rat mitochondria (~0.5 µm), and nuclei (~8 µm) were used as size standards (Figure 15).

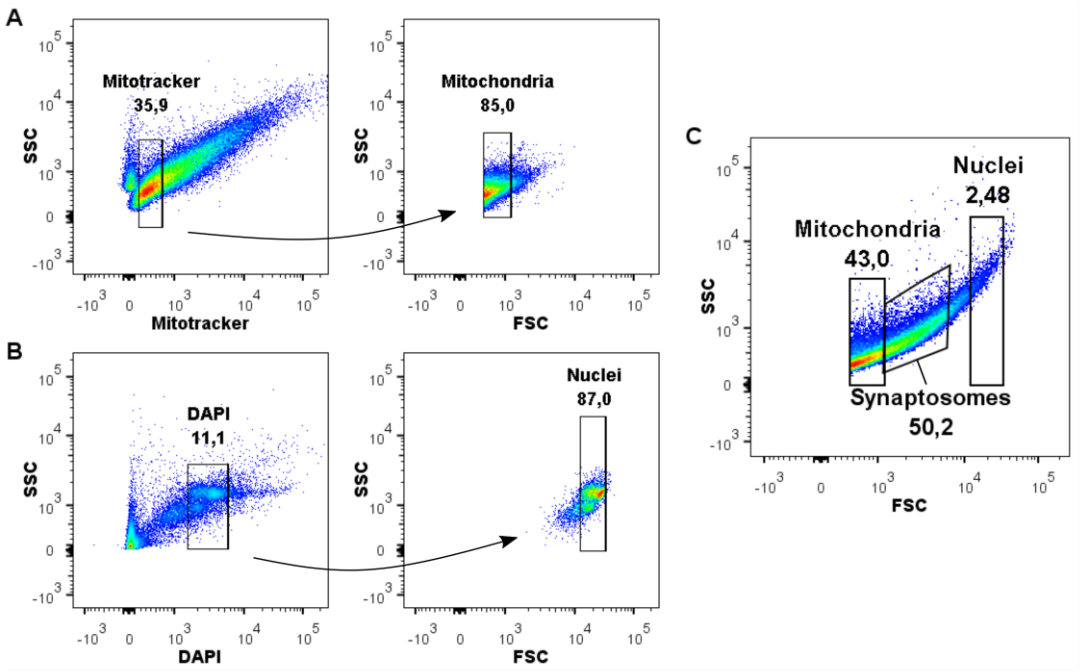

Figure 15. **Size-based analysis of flow cytometry data**. **A)** Selection of "mitochondria" size gate based on Mitotracker staining in mitochondria isolated from liver. **B)** Selection of "nuclei" size gate based on DAPI staining in nuclei isolated from liver. **C)** Representation of "mitochondria" and "nuclei" size gates in synaptosomes isolated from brain, and selection of "synaptosomes" size gate.

Second, considering FSC-H and FSC-A parameters, doublets and big aggregates were excluded and single events were selected for further analysis (Figure 16A). For a given cell/particle, each signal is represented across the time, where the maximum scattered light or fluorescent signal is achieved as the cell/particle reaches the center of the laser beam, decreasing the signal until baseline before the next cell/particle arrives. Thus, the resulting graph is defined by its area (A), height (H), and width (W) (Figure 16B). Disproportions between these parameters can be used to identify doublets and bigger aggregates, with twice the area and width for the same height (Figure 16C).

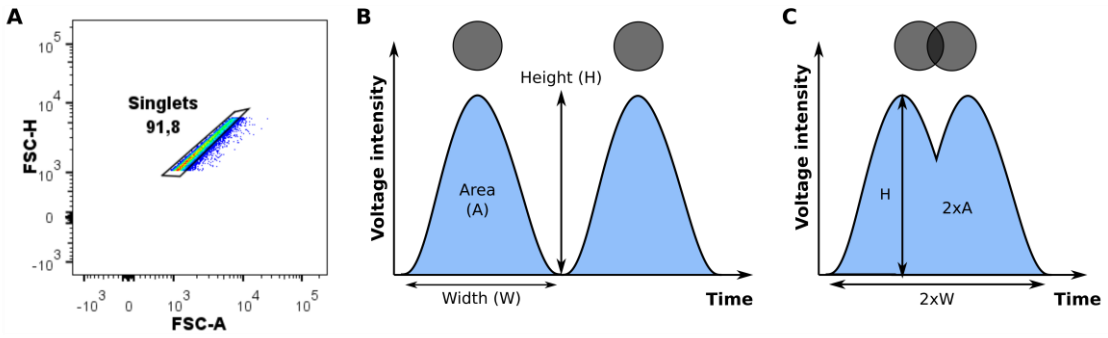

Figure 16. **Single particles ("singlets"). A)** Selection of single particles. **B)** Flow cytometry signal representation of well separated single particles and **C)** overlapping particles (doublets). A: area; H: height; W: width.

Next, fluorescence-based gates were set based on standard immunostaining controls to differentiate background fluorescence from the signal. These controls consist of 1) synaptosomes incubated with no Calcein AM nor primary or secondary antibodies to discriminate fluorescence of the sample itself; 2) synaptosomes incubated only with Calcein AM to establish the background levels of this fluorescent marker; and 3) Fluorescence Minus One (FMO) staining controls with all the primary and secondary antibodies, and calcein staining except for one primary antibody, to establish the background staining levels for GluA1-Alexa Fluor 647, or Nrx1β-Brilliant Violet 421.

After selecting synaptosomes based on size, and giving consideration to the staining controls, Calcein AM positive events were selected, corresponding to functional synaptosomes. Finally, GluA1 and Nrx1β single-positive populations were selected, and the "Make and Gate" Boolean analysis tool was used to evaluate the double-positive population (Figure 17A-B). For a visual representation, GluA1 and Nrx1β stainings were plotted on the same graph, and a quad gate was used to separate double-negative (left, bottom), single-positive for GluA1 (right, bottom) and Nrx1β (left, top), and double-positive (right, top) populations. An increase of GluA1/Nrx1β double-positive population in cLTP samples compared to the basal condition was considered as indicative of cLTP (Figure 17C).

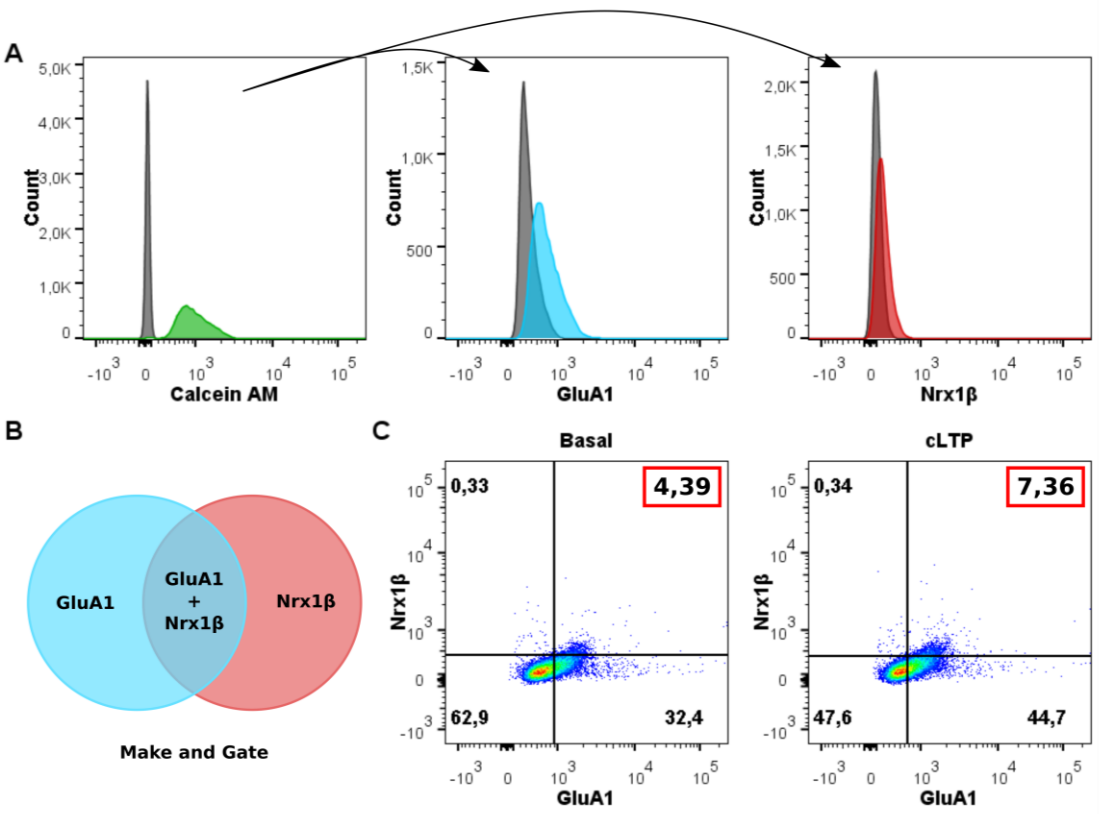

Figure 17. **Fluorescence-based analysis of flow cytometry data**. **A)** Single positive stainings for Calcein AM (green), GluA1 (blue), and Nrx1β (red), and the corresponding negative controls (grey) for each staining. **B)** Make and Gate Boolean analysis of GluA1/Nrx1β single- and double stainings. **C)** GluA1/Nrx1β stainings in basal and cLTP conditions, highlighting the double-positive population (right, top).

5. Protein quantification

The protein concentration of each sample was measured using the BCA protein Assay (Thermo Fisher Scientific, #23227). Ascending concentrations of bovine serum albumin (BSA) standard solutions were used to build a standard curve and unknown protein concentration samples were tested. After incubation of samples with 200 µL of AB solution (A:B, 50:1) for 30 min at 37°C, the absorbance of each well was measured at 560 mm wavelength in a spectrophotometer (SPECTROstar Nano, BMG LABTECH). All standards and samples were tested by triplicate and mean values were calculated.

6. Western Blot

6.1. Midbrain homogenate extraction

To confirm the presence of hα-syn, midbrain homogenate extracts from the same animals of FASS-LTP experiments were used. Midbrains were slowly thawed on ice until complete defrost and 450 µL of 2% sodium dodecyl sulfate (SDS) buffer was added to each sample. Samples were homogenized by 2-3 strokes in a Dounce Glass (clearance: 0.0013 – 0.0635 mm) followed by 12 up and down strokes with a syringe with a 26 GA needle. Samples were transferred to microfuge tubes, sonicated for 2 min, and left resting on ice for 20 min. Finally, samples were centrifuged (15900 x *g* for 13 min; 4°C) and the supernatant was collected and stored at -80ºC.

6.2. Western blot

Eighteen µg of protein were mixed with loading buffer 4x and lysis buffer and denatured at 95°C for 10 min. Each well of the gel was loaded with 20 µL of sample and electrophoresis was run in 4-15% Mini-PROTEAN®TGX Stain-Free™ Protein Gels (Bio-Rad, #4568083) at constant 120 mV for 60-90 min and home-made electrophoresis buffer. Protein Marker VI (10 - 245) prestained (Panreac, #A8889) was loaded as a molecular weight marker. Once proteins were separated according to their molecular weight, proteins on the gel were transferred to PVDF membranes (0.45 µm pore size) using the Trans-Blot Turbo RTA Mini PVDF Transfer Kit (Bio-Rad, #1704272). Transfer sandwich was mounted following the instructions of the manufacturer and run in the Low MW program of the Trans-Blot Turbo System (5 min at a constant 1.3 A up to 25 V).

When transference was completed, the membrane was cut and the membrane piece corresponding to hα-syn molecular weight was incubated in 4% PFA (Electron Microscopy Sciences) for 30 min. After 3 washing steps with Tris Buffer Saline (TBS) with 0.1 % Tween-20 (TBS-T) for 10 min, membranes were incubated with blocking buffer (5% skim milk in TBS-T) for 1 h at RT in agitation. For the detection of glyceraldehyde-3-phosphate dehydrogenase (GAPDH; loading control) in the upper membrane piece, fixation was omitted. After the blocking step, membranes were incubated with the corresponding primary antibody anti-hα-syn or anti-GAPDH (Table 11, annex) in blocking buffer overnight at 4°C in agitation. The next day, membranes were washed twice with TBS-T for 10 min and twice for 5 min, and afterward, incubated with the corresponding HRP-conjugated secondary antibody (Table 12, annex) in blocking buffer for 1 h at RT in agitation. Membranes were washed with TBS-T twice for 10 min, once for 5 min, and the last one for 5 min with only TBS. Membranes were revealed with chemiluminescence using

Immobilon Western HRP Substrate Classico (Sigma-Aldrich, #WBLUCO500), and immediately visualized with the ChemiDoc MP system (Bio-Rad).

7. Quantitative proteomics by SWATH-MS

The proteomic study of hippocampal synaptosomes was carried out with the collaboration of the group led by Dr. Joaquín Fernandez and Dr. Enrique Santamaría from the Clinical Neuroproteomics laboratory at Navarrabiomed Health Research Institute (Pamplona, Spain).

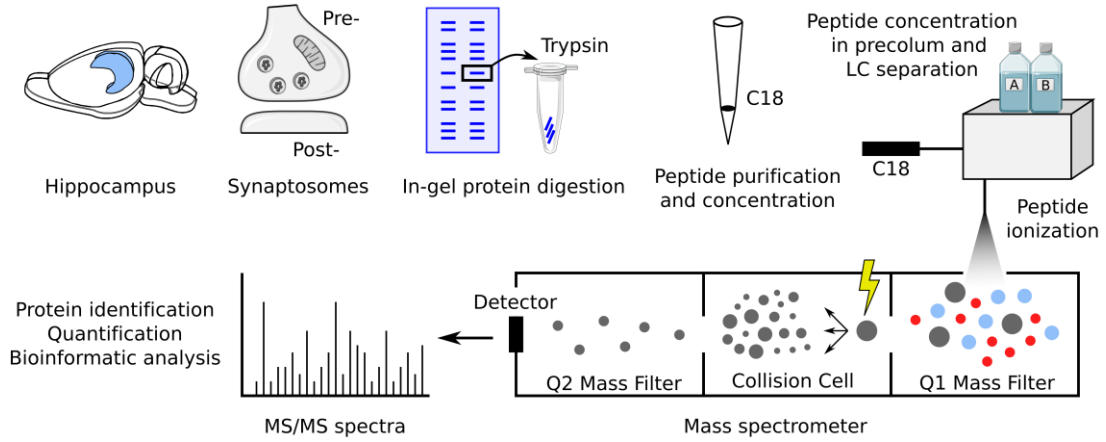

Figure 18. Proteomic study workflow.

7.1. Brain tissue collection and synaptosome isolation

Animals (n = 5/group and time point) were rapidly anesthetized with a mixture of oxygen and isoflurane (5%) and sacrificed at the corresponding time points (1, 2, 4, and 16 weeks p.i.). Brains were rapidly removed from the skull, and hippocampi were carefully dissected. As described in section 4.2., hippocampi were homogenized in buffer D and centrifuged to obtain the supernatant S1, containing the cytoplasm and membranous structures. To maximize sample recovery, the pellet P1 was centrifuged again and supernatant S1' was mixed with the S1, while P1' pellet was discarded. The mixture (S1 and S1') was centrifuged (11600 x *g* for 12 min; 4ºC), and the supernatant S2, containing the cytoplasm, was discarded and pellet P2, enriched in synaptosomes, was resuspended in 700 µL of buffer D. In order to purify synaptosomes, resuspended samples were added on top of the same volume of buffer E, and centrifuged (12000

x *g* for 1 h; 4ºC) to create a sucrose gradient. After the centrifugation, different phases were separated, and the interphase, corresponding to synaptosomes, was transferred into a microfuge tube. Finally, samples were sonicated for 10 s at medium power (Sonopuls HD2070 Bandelin).

7.2. Sample preparation and protein digestion

Synaptosomes were homogenized in lysis buffer, centrifuged (100000 × *g* for 1 h; 15 °C) and protein concentration was measured by Bradford assay (Bio-rad). A pool of all samples was used as input for generating the sequential window acquisition of all theoretical mass spectra–mass spectrometry (SWATH-MS) assay library. To increment the proteome coverage in-gel digestion was applied. Protein extracts (30 µg) were diluted in Laemmli sample buffer and loaded into a 0.75 mm thick polyacrylamide gel with a 4% stacking gel cast over a 12.5% resolving gel. The total gel was stained with Coomassie Brilliant Blue and 12 equal slides from the pooled sample were excised from the gel and transferred into 1.5 mL microfuge tubes. Protein enzymatic cleavage was carried out with trypsin (Promega; 1:20, w/w) at 37 °C for 16 h as previously described (Shevchenko et al., 2006). Purification and concentration of peptides were performed using C18 Zip Tip Solid Phase Extraction (Millipore). The peptides recovered from in-gel digestion processing were reconstituted into a final concentration of 0.5 µg/µl on MS buffer before mass spectrometric analysis.

7.3. LC-MS/MS analysis for spectral library generation

MS/MS datasets for spectral library generation were acquired on a TripleTOF 5600+ mass spectrometer (Sciex) interfaced to an Eksigent nanoLC ultra 2D pump system (Sciex) fitted with a 75 µm ID column (Thermo Scientific 0.075 × 250 mm, particle size 3 µm and pore size 100 Å). Before separation, the peptides were concentrated on a C18 precolumn (Thermo Scientific 0.1 × 50 mm, particle size 5 µm and pore size 100 Å). Mobile phases were 0.1% formic acid in water (A) and 0.1% formic acid in acetonitrile (B). Peptides were eluted in a linear gradient of buffer B from 2% to 40% in 120 min. The column was equilibrated in 95% B for 10 min and 2% B for 10 min. During all processes, the precolumn was in line with the column, and flow was maintained all along the gradient at 300 nl/min. The output of the separation column was directly coupled to the nano-electrospray source. MS1 spectra were collected in the range of 350-1250 m/z for 250 ms. The 35 most intense precursors with charge states of 2 to 5 that exceeded 150 counts per second were selected for fragmentation using rolling collision energy. MS2 spectra were collected

in the range of 230–1500 m/z for 100 ms. The precursor ions were dynamically excluded from reselection for 15 s.

7.4. Database search and results processing of assay library

MS/MS data acquisition was performed using AnalystTF 1.7 (Sciex) and spectra files were processed through ProteinPilot v5.0 search engine (Sciex) using ParagonTM Algorithm (v.4.0.0.0) (Shilov et al., 2007) for database search. To avoid using the same spectral evidence in more than one protein, the identified proteins were grouped based on MS/MS spectra by the Progroup™ Algorithm, regardless of the peptide sequence assigned. False discovery rate (FDR) was performed using a non-linear fitting method (Tang et al., 2008), and displayed results were those reporting a 1% Global FDR or better.

7.5. SWATH-MS

Individual protein extracts (20 µg) from all experimental groups were subjected to in-gel digestion, peptide purification, and reconstitution before mass spectrometric analysis as previously described. For SWATH-MS-based experiments, the TripleTOF 5600+ instrument was configured as described by Gillet and coworkers (Gillet et al., 2012). Using an isolation width of 16 Da (15 Da of optimal ion transmission efficiency and 1 Da for the window overlap), a set of 37 overlapping windows was constructed covering the mass range 450–1000 Da. In this way, 2 µl of each sample was loaded onto a trap column (Thermo Scientific 0.1 × 50 mm, particle size 5 µm and pore size 100 Å) and desalted with 0.1% trifluoroacetic acid at 2 µl/min for 10 min. The peptides were loaded onto an analytical column (Thermo Scientific 0.075 × 250 mm, particle size 3 µm and pore size 100 Å) equilibrated in MS buffer. Peptide elution was carried out with a buffer B linear gradient as previously described, and eluted peptides were infused in the mass-spectrometer. The Triple TOF was operated in swath mode, in which a 0.050 s TOF MS scan from 350 to 1250 m/z was performed, followed by 0.080 s product ion scans from 230 to 1800 m/z on the 37 defined windows (3.05 s/cycle). The collision energy was set to optimum energy for a 2 + ion at the center of each SWATH block with a 15 eV collision energy spread.

7.6. Label-free quantitative data analysis

The resulting ProteinPilot group file from library generation was loaded into PeakView® (v2.1, Sciex) and peaks from SWATH runs were extracted with a peptide confidence threshold of 99% confidence (Unused Score ≥ 1.3) and FDR lower than 1%. For this, the MS/MS spectra of the

assigned peptides were extracted by ProteinPilot, and only the proteins that fulfilled the following criteria were validated: (1) peptide mass tolerance lower than 10 ppm, (2) 99% of confidence level in peptide identification, and (3) complete b/y ions series found in the MS/MS spectrum. Only proteins quantified with at least two unique peptides were considered.

7.7. Bioinformatic analysis

The identification of significantly enriched structural complexes and biological processes from the deregulated proteins in synaptosomal fractions was performed using Metascape (Zhou et al., 2019). For the generation of the different heatmaps, after the identification of all statistically enriched terms (structural complex: GO/KEGG terms; biological process: GO/KEGG terms, canonical pathways, hallmark gene sets), cumulative hypergeometric p-values and enrichment factors were calculated and used for filtering. The remaining significant terms were then hierarchically clustered into a tree based on Kappa-statistical similarities among their gene memberships. Then, a 0.3 kappa score was applied as the threshold to cast the tree into term clusters. The term with the best p-value within each cluster was selected as its representative term and displayed in a dendrogram. The heat map cells are colored by their p-values and grey cells indicate the lack of enrichment for that term in the corresponding list. The interactomes of human and rat α-syn were obtained from the curated Biological General Repository for Interaction Datasets (BioGRID: https://thebiogrid.org/; Oughtred et al., 2019). The synaptic ontology analysis was performed using the SynGo platform (https://syngoportal.org/; Koopmans et al., 2019). The "brain expressed" background set was selected, containing 18,035 unique genes in total, of which 1104 overlap with SynGO annotated genes. For each ontology term, a one-sided Fisher exact test was performed to compare differential datasets and the "brain expressed" background set. The result is shown in the "p-value" column. To find enriched terms within the entire SynGO ontology, a multiple testing correction using FDR was applied (q-value column).

8. *In vivo* positron emission tomography

8.1. Dopaminergic drug treatment

PET scans were carried out with animals under dopaminergic drug chronic treatment with PPX. Once the dopaminergic lesion was established after 16 weeks p.i. of the AAVs, animals were treated chronically for 4 weeks with the dopaminergic agonist PPX (0.25 mg/kg/day; subcutaneous; A1237; Sigma-Aldrich, St. Louis, MO) (Jimenez-Urbieta et al., 2018).

8.2. PET scans and data acquisition

To study brain glucose metabolism, [^{18}F]-FDG radiotracer was used. Animals inoculated with the AAV-hα-syn (n = 9) and the AAV-EVV (n = 5) were treated with PPX (0.25 mg/kg, subcutaneous) 1 h before the image acquisition, and the [^{18}F]-FDG (30 ± 0.3 MBq, IBA Molypharma) was injected 30 min after PPX administration. The tail vein was catheterized with a 24-gauge catheter for intravenous administration of the radiotracer and animals were kept for an awake uptake period of 30 min to ensure the incorporation of the radiotracer. Blood samples were taken from the tail vein to obtain basal levels of serum glucose for posterior image normalization. The PET scans were performed under anesthesia with isoflurane in oxygen-enriched air (3-5% for induction and 1.5-2.0% for maintenance) using an eXploreVista-CT small animal PET-CT system (GE Healthcare) located at the Imaging Unit facilities of CICbiomaGUNE (San Sebastian, Spain). Each animal was positioned with the lungs at the center of the field of view of the PET camera to perform a static acquisition of 45 min in the 400-700 keV energetic window. During PET acquisition, rats were kept normothermic using a water-based heating blanket. After each PET scan, computed tomography (CT) acquisitions were also performed (140 μA intensity, 40 kV voltage), providing anatomical information of each animal as well as the attenuation map for the later image reconstruction. CT data were reconstructed using FeldKamp method with binning and PET data were reconstructed (random, scatter, decay, and CT-based attenuation corrected) with filtered back projection (FBP) method using a Ramp filter with a cut-off frequency of 0.5 mm^{-1}.

8.3. Image analysis

For whole-brain analysis, each CT image was normalized to a CT template created as a reference to a rat MRI template (Schweinhardt et al., 2003). Thereafter, all PET scans were exported and coregistered to their corresponding CT images using PMOD software (PMOD Technologies Lts.). For extracerebral regions, a mask was applied to eliminate the value of the voxels outside the brain. Then, image smoothing was applied with a Gaussian filter (4 mm FWHM) to minimize possible errors or spatial differences after the normalization process. Finally, to normalize the intensity of uptake within the images due to differences in administered doses, the uptake value of the white matter was considered in each animal as a reference region (Weber et al., 2002).

8.4. Statistical analysis

PET scans were statistically analyzed using Statistical Parametric Mapping 8 (SPM8) software (Welcome Department of Imaging Neuroscience, Institute of Neurology, London, UK). The groups of images belonging to the two experimental groups were compared using a t-test (one-sample t-test) introducing as a covariate a vector of blood glucose measurements performed before the PET acquisition. Once the design matrix was defined, hypothesis contrasts were applied to detect areas of hyper- or hypoactivity within the AAV-hα-syn group with respect to the AAV-EVV group, identifying the voxels with a significant change. The significance threshold was set at $p < 0.01$ (uncorrected), to obtain a map of statistically significant regions. The significant parametric maps were drawn as a 3D region on an MRI template eliminating the areas that did not exceed a size of 50 voxels. Finally, an anatomical rat brain atlas provided by the PMOD program was used to identify the affected regions.

9. Statistical Analyses

All statistical analyses were performed using GraphPad Prism 8.0 software (GraphPad Software Inc.). Data distribution for normality was assessed using the Kolmogorov-Smirnov (K–S) test and variance equality by Levene's test. For pair-wise comparisons between means of AAV-hα-syn and AAV-EVV groups, unpaired t-test or Mann–Whitney test was performed, when data were parametric or non-parametric, respectively. For multiple comparisons between means of different time points within the AAV-hα-syn group, Kruskal-Wallis test followed by Dunn´s *post-hoc* test was used, as data were non-parametric. For multiple comparisons between means of experimental groups and different conditions (basal/cLTP, treatment, time point) two-way ANOVA followed by Turkey's or Bonferroni's *post-hoc* tests were used. Group data are represented in graphs as mean ± SEM and statistically significant differences were set at $p < 0.05$.

Results

This doctoral thesis has been carried out using different experimental approaches to address the established objectives. Subsequent experiments were designed as the results of each experimental approach were known, varying the time points analyzed. The details for each set of experiments are described in the corresponding section.

1. Histological characterization of the mesolimbic pathway from the midbrain to the hippocampus

1.1. Experimental design

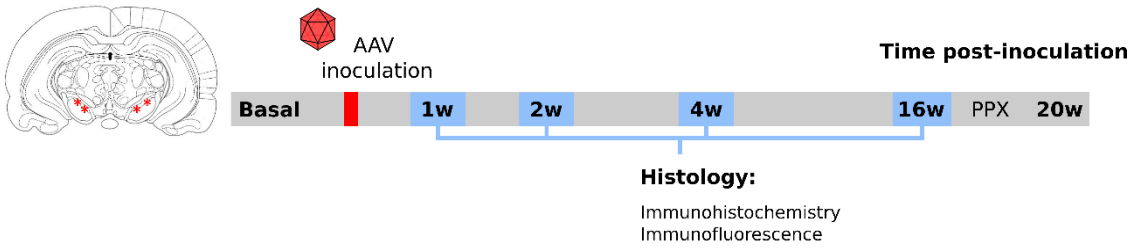

Figure 19. Experimental design for the histological characterization. Animals were inoculated with either AAV-hα-syn or AAV-EVV bilaterally in the SNpc and they were perfused at their corresponding final time point (1, 2, 4, and 16 weeks p.i.). Brains were removed and coronal slices were acquired for immunohistochemistry and immunofluorescence studies.

To study the mesolimbic pathway from the midbrain to the hippocampus, we performed a histological characterization of the SNpc, VTA, and hippocampus at different time points p.i. in the AAV-hα-syn animal model. For that purpose, animals were inoculated with the AAV-hα-syn and sacrificed at different time points p.i. (1, 2, 4, and 16 weeks p.i.; n = 4 for each time point). For the control group, animals were inoculated with the AAV-EVV (n = 4) and only the final time point (16 weeks p.i.) was studied to reduce the number of animals (Figure 19).

1.2. Histological characterization of the SNpc and VTA

1.2.1. Hα-syn overexpression in the SNpc and VTA

In the SNpc and VTA, inoculation of the AAV-hα-syn resulted in a robust and persistent expression of hα-syn from 1 week p.i. that expanded progressively and changed to a more diffuse pattern in later time points (Figure 20A-B). In both nuclei, hα-syn expression reached significance at 4 weeks p.i. (SNpc: $p < 0.001$ vs. 1w p.i., and $p < 0.05$ vs. 2w p.i.; VTA: $p < 0.05$ vs. 1w p.i. and

2w p.i.) and was maintained at 16 weeks p.i. (SNpc: $p < 0.05$ vs. 1w p.i.; VTA: $p < 0.01$ vs. 1w p.i., and $p < 0.05$ vs. 2w p.i.) (Figure 20C-D).

No hα-syn expression was observed in either the SNpc or the VTA in the AAV-EVV control group (Figure 20A).

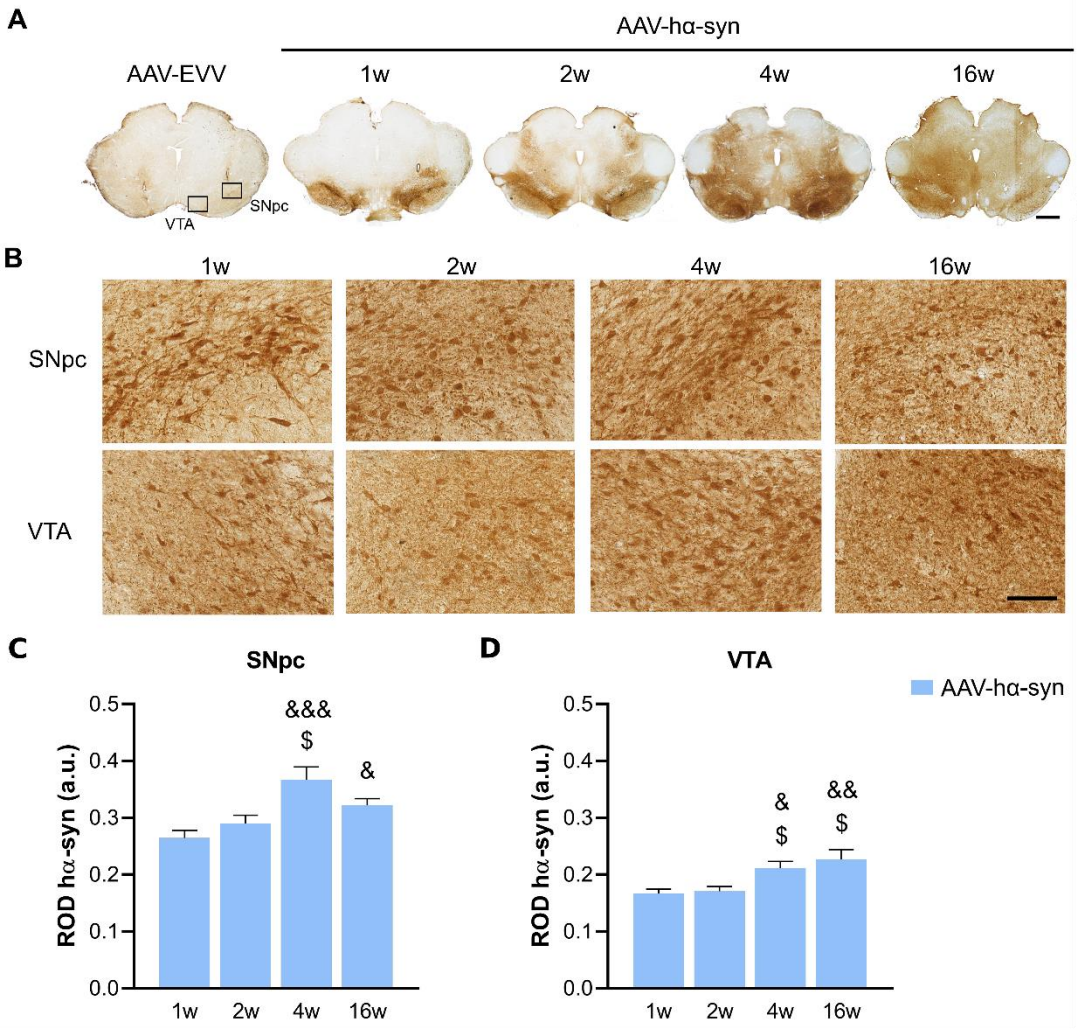

Figure 20. Hα-syn overexpression in the SNpc and VTA. A) Representative photomicrographs for hα-syn staining in coronal sections of the SNpc/VTA from AAV-EVV and AAV-hα-syn group at 1, 2, 4, and 16 weeks (w) p.i. Scale bar, 1 mm. **B)** Representative SNpc and VTA higher magnification photomicrographs for hα-syn staining from AAV-hα-syn group at their corresponding time points. Scale bar, 100 µm. Relative optical density (ROD) analysis of hα-syn expression in the **C)** SNpc and **D)** in the VTA from the AAV-hα-syn group at their corresponding time points p.i. Values are presented as the mean ± SEM. Kruskal-Wallis followed by Dunn´s post hoc test: & $p < 0.05$, && $p < 0.01$, &&& $p < 0.001$ vs. 1w p.i.; \$ $p < 0.05$ vs. 2w p.i. n = 4 for experimental group and time point evaluated.

1.2.2. Quantification of the dopaminergic neuronal loss in the SNpc and VTA

In the SNpc, the AAV-hα-syn group showed a significantly reduced number of TH^+ dopaminergic neurons from 4 weeks p.i. (31% reduction, $p < 0.05$ vs. AAV-EVV and AAV-hα-syn 1w p.i.) that was maintained at 16 weeks p.i. (33% reduction, $p < 0.05$ vs. AAV-EVV and $p < 0.01$ vs. AAV-hα-syn 1w p.i.) (Figure 21A-C).

In the VTA, the number of TH^+ dopaminergic neurons were significantly decreased from 1 week p.i. onwards (40% reduction, $p < 0.05$ vs. AAV-EVV for all time points p.i.) (Figure 21A, B, and D).

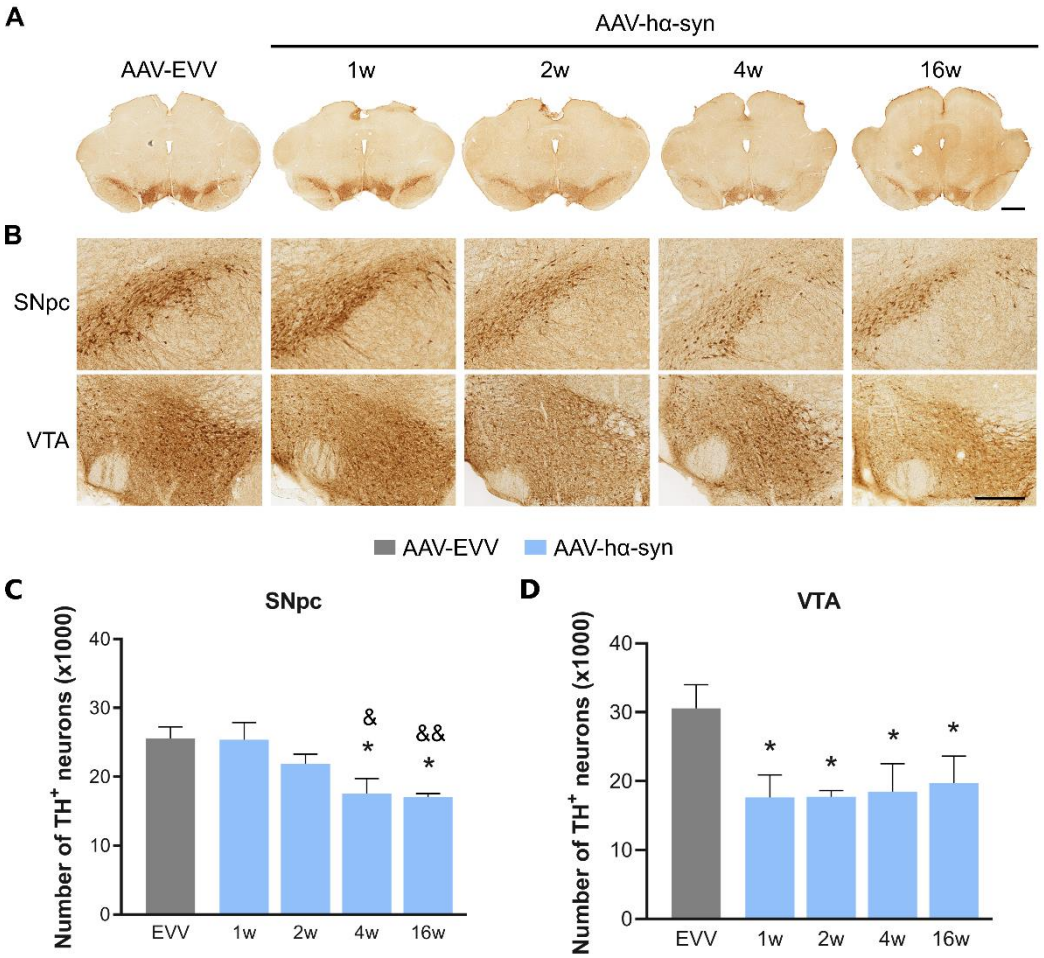

Figure 21. TH^+ neurons in the VTA and SNpc. A) Representative photomicrographs for TH staining in coronal sections of the SNpc/VTA from AAV-EVV and AAV-hα-syn group at 1, 2, 4, and 16 weeks (w) p.i. Scale bar, 1 mm. **B)** Representative SNpc and VTA higher magnification photomicrographs for TH staining from AAV-EVV and AAV-hα-syn groups at the corresponding time points. Scale bar, 300 µm. Quantification of TH^+ neurons in the **C)** SNpc and **D)** in the VTA from AAV-EVV and AAV-hα-syn group at the corresponding time points p.i. Values are presented as the mean ± SEM. Kruskal-Wallis followed by Dunn´s post hoc test: * $p < 0.05$ vs. AAV-EVV; & $p < 0.05$, && $p < 0.01$ vs. 1w p.i. $n = 4$ for experimental group and time point evaluated.

1.2.3. Hα-syn overexpression in dopaminergic and glutamatergic VTA neurons

The VTA has a central role in the neural processes that underlie motivation and behavioral reinforcement. Although thought to contain only dopaminergic and GABAergic neurons, the VTA also includes a population of glutamatergic neurons identified through the expression of the vesicular glutamate transporter 2 (vGlut2) (Yoo et al., 2016). This neuronal population remains poorly characterized, but they have been described to play a role in reward, aversion, and memory processing (Han et al., 2020; Root et al., 2018) as well as in dopaminergic neuron vulnerability and degeneration (Buck et al., 2021). Thus, in order to characterize this population and the specific cell type expressing hα-syn in the VTA, we performed triple immunofluorescence with hα-syn and the specific dopaminergic (TH) and glutamatergic (vGlut2) markers (Figure 22).

We observed positive hα-syn staining at all the time points p.i. and colocalizing abundantly with dopaminergic fibers. Colocalization of hα-syn in neuronal somas was only observed at 2 and 4 weeks p.i. (Figure 22A).

By contrast, colocalization of hα-syn with vGlut2 was restricted to a few glutamatergic fibers at 1 and 2 weeks p.i. Interestingly, at 4 weeks p.i. hα-syn$^+$ staining was observed in vGlut2$^+$ neuronal somas, suggesting that glutamatergic neurons overexpress hα-syn as well (Figure 22B). At 16 weeks p.i., few vGlut2$^+$ puncta colocalized with hα-syn staining (Figure 22B).

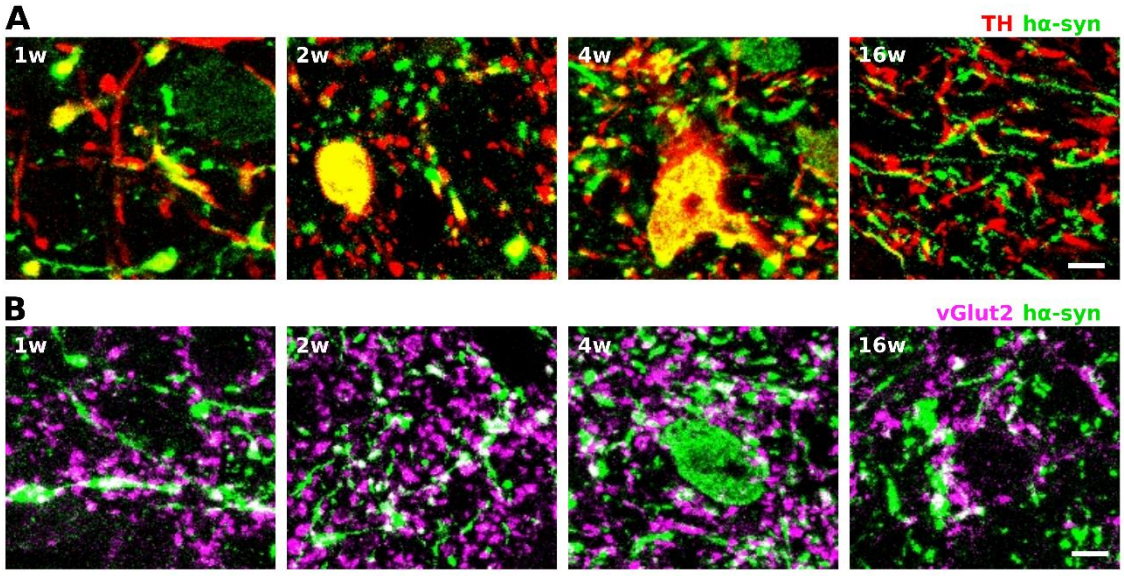

Figure 22. Expression of hα-syn in TH$^+$ and vGlut2$^+$ neurons in the VTA. Representative high magnification photomicrographs of hα-syn colocalization with **A)** TH staining, and **B)** vGlut2 staining, in the AAV-hα-syn group at 1, 2, 4, and 16 weeks (w) p.i. in the VTA. Scale bars, 5 µm.

1.3. Histological characterization of the hippocampus

1.3.1. Hα-syn overexpression in the hippocampus

In the hippocampus, intranigral inoculation of the AAV-hα-syn resulted in the progressive expression of hα-syn from 1 week p.i. (Figure 23A), reaching statistical significance at 4 weeks p.i. ($p < 0.01$ vs. 1w p.i., and $p < 0.05$ vs. 2w p.i.; Figure 23F) that was maintained at 16 weeks p.i. ($p < 0.001$ vs. 1w p.i., and $p < 0.01$ vs. 2w p.i.; Figure 23F). No hα-syn expression was observed in the hippocampus of the AAV-EVV control group (Figure 23B).

A different pattern of hα-syn overexpression was observed depending on the anatomical region of the hippocampus. In the DG (Figure 23C), hα-syn expression was observed since 1 week p.i. with punctate staining in the hilus, spreading towards CA3 at 2 weeks p.i. and changing to fibrillary staining at 4 and 16 weeks p.i. From 2 weeks p.i. onwards, hα-syn$^+$ fibers also appear in the granular cell layer. Overall, hα-syn levels in the DG increased significantly at 4 weeks p.i. ($p < 0.01$ vs. 1w p.i., and $p < 0.05$ vs. 2w p.i.; Figure 23G) and were maintained at 16 weeks p.i. ($p < 0.01$ vs. 1w p.i., and $p < 0.05$ vs. 2w p.i.; Figure 23G).

In the CA1 region (Figure 23D), hα-syn$^+$ fibers were observed mainly in the stratum oriens, stratum pyramidal, and stratum radiatum since 1 week p.i. Hα-syn$^+$ levels increased progressively at later time points reaching statistical significance at 4 weeks p.i. ($p < 0.01$ vs. 1w and 2w p.i.; Figure 23H), and 16 weeks p.i. ($p < 0.001$ vs. 1w p.i., and $p < 0.0001$ vs. 2w p.i.; Figure 23H). At 16 weeks p.i., immunostaining became more evident at the SLM (Figure 23D), thus, for the following experiments, the SLM will only be analyzed at the 16 weeks p.i. time point.

In the CA3 region (Figure 23E), although few puncta were observed at 2 weeks p.i. ($p < 0.05$ vs. 1w p.i.; Figure 23I), marked fiber immunostaining became evident particularly in the stratum lucidum at 4 weeks p.i. ($p < 0.0001$ vs. 1w p.i.; Figure 23I). At 16 weeks p.i., hα-syn staining expanded through the different layers of the CA3 region, and expression levels were maintained ($p < 0.0001$ vs. 1w p.i.; Figure 23I). For the following experiments, the CA3 region will only be analyzed at 4 and 16 weeks p.i. time points due to the low levels of hα-syn observed in the previous time-points.

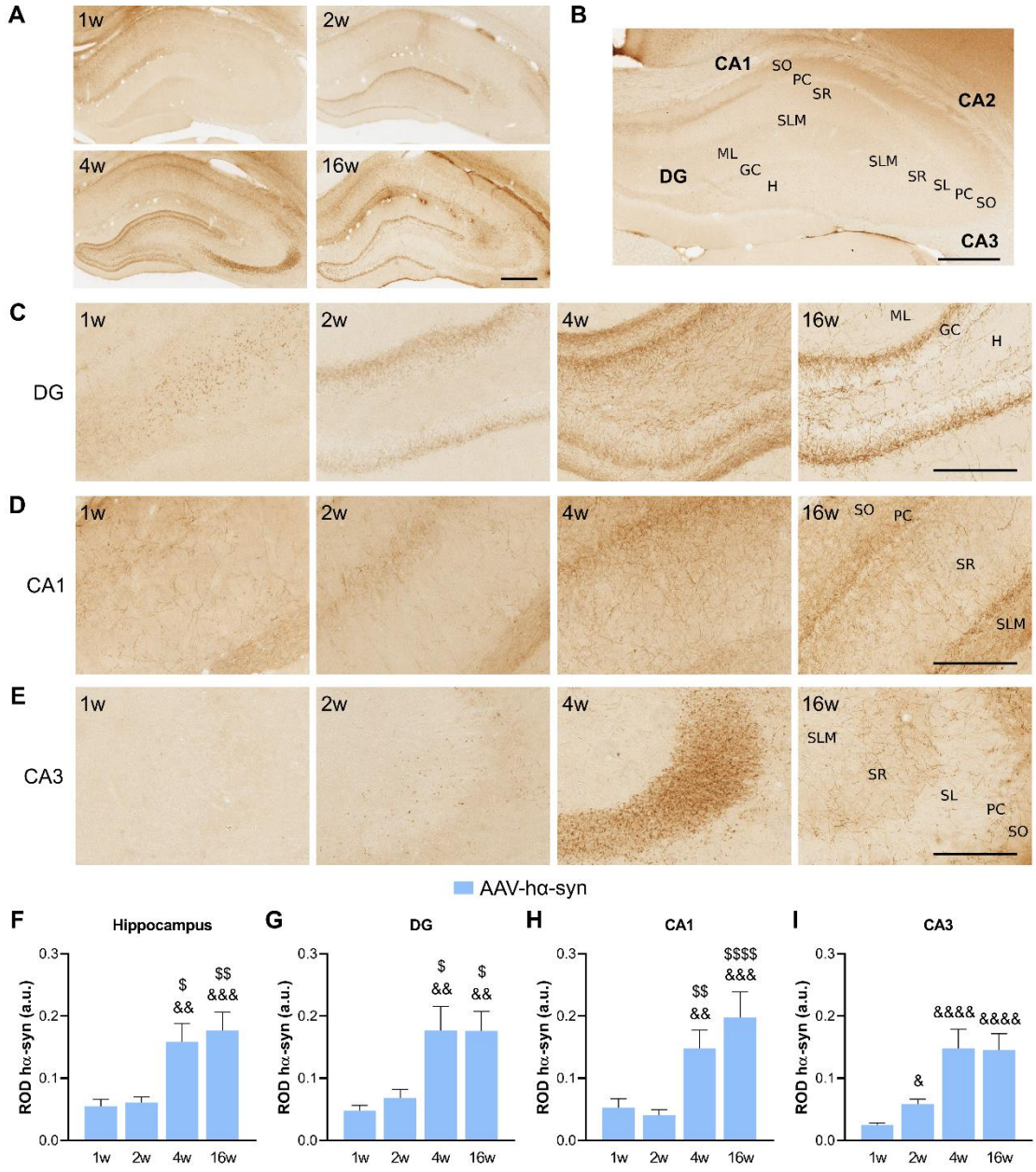

Figure 23. Hα-syn overexpression in the hippocampus. A) Representative photomicrographs for hα-syn staining in coronal sections of the hippocampus from the AAV-hα-syn group at 1, 2, 4, and 16 weeks (w) p.i. and **B)** the AAV-EVV group. Scale bars, 500 µm. Representative higher magnification photomicrographs for hα-syn staining from the **C)** DG, **D)** CA1 region, and **E)** CA3 region of the hippocampus from AAV-hα-syn group at the corresponding time points. Scale bars, 200 µm. The different anatomical regions and layers are indicated. DG: molecular layer (ML), granular cell layer (GC), and hilus (H); CA1: stratum oriens (SO), pyramidal cell layer (PC), stratum radiatum (SR), and stratum lacunosum-moleculare (SLM); CA3: SO, PC, stratum lucidum (SL), and SLM. **F)** Relative optical density (ROD) analysis of hα-syn expression in the whole hippocampus and specifically in **G)** DG, **H)** CA1 region, and **I)** CA3 region from the AAV-hα-syn group at the corresponding time points p.i. Values are presented as the mean ± SEM. Kruskal-Wallis followed by Dunn´s post hoc test: & $p < 0.05$, && $p < 0.01$, &&& $p < 0.001$, &&&& $p < 0.0001$ vs. 1w p.i.; $ $p < 0.05$, $$ $p < 0.01$, $$$$ $p < 0.0001$ vs. 2w p.i. n = 4 for experimental group and time point evaluated.

1.3.2. Localization of hα-syn$^+$ fibers in the different hippocampal afferents

In order to elucidate the distribution of hα-syn$^+$ fibers in the different afferent pathways from the VTA and its expression among the different anatomical subregions, we performed several double immunofluorescences with hα-syn and dopaminergic (TH), glutamatergic (vGlut2) or GABAergic (GABA) markers.

1.3.2.1. Dopaminergic pathway

TH staining showed a fibrillar pattern throughout the different regions of the hippocampus (Figure 24). Across the different time points, a general decrease of TH$^+$ fibers was observed, particularly at 16 weeks p.i. (Figure 24).

In the DG, TH$^+$ fibers were predominantly localized to the hilus (Figure 24A) while only a few fibers were present in the granular cell layer (Figure 24B). Specifically, in the hilus (Figure 24A) hα-syn$^+$ puncta widely colocalized with TH$^+$ fibers at 1 week p.i. Lower colocalization of hα-syn was observed in TH$^+$ fibers at 2 and 4 weeks p.i. although we observed a change in hα-syn to fibrillar staining. At 16 weeks p.i., some of the few remaining TH$^+$ fibers colocalized with hα-syn, although there was an overall decrease of both markers. In the granular cell layer of the DG, although hα-syn expression increased in later time points no colocalization with hα-syn was observed within the few TH$^+$ fibers at any of the time points analyzed (Figure 24B).

In the CA1 region, TH$^+$ fibers were found across the stratum oriens, pyramidal cell layer, and stratum radiatum (Figure 24C), and most abundantly in the SLM (Figure 24D). In the pyramidal cell layer and the adjacent stratum oriens and stratum radiatum (Figure 24C), although hα-syn expression was higher than TH$^+$ fibers at 1, 2, and 4 weeks p.i., minor colocalization was found. At 16 weeks p.i. no colocalization of hα-syn within TH$^+$ fibers was found along with an almost absent TH$^+$ staining in these regions. By contrast, in the SLM at 16 weeks p.i. (Figure 24D) we observed a strong colocalization of hα-syn within the TH$^+$ fibers.

In the CA3 region, TH$^+$ fibers were found around the stratum oriens, pyramidal cell layer, stratum ludicum, and stratum radiatum (Figure 24E). At 4 weeks p.i., few TH$^+$ fibers were observed in the CA3 area and they did not colocalize with hα-syn, which was present in the pyramidal cell layer, and most abundantly in the adjacent stratum lucidum. At 16 weeks p.i., a decrease in TH$^+$ fibers was observed, but no colocalization with hα-syn was found.

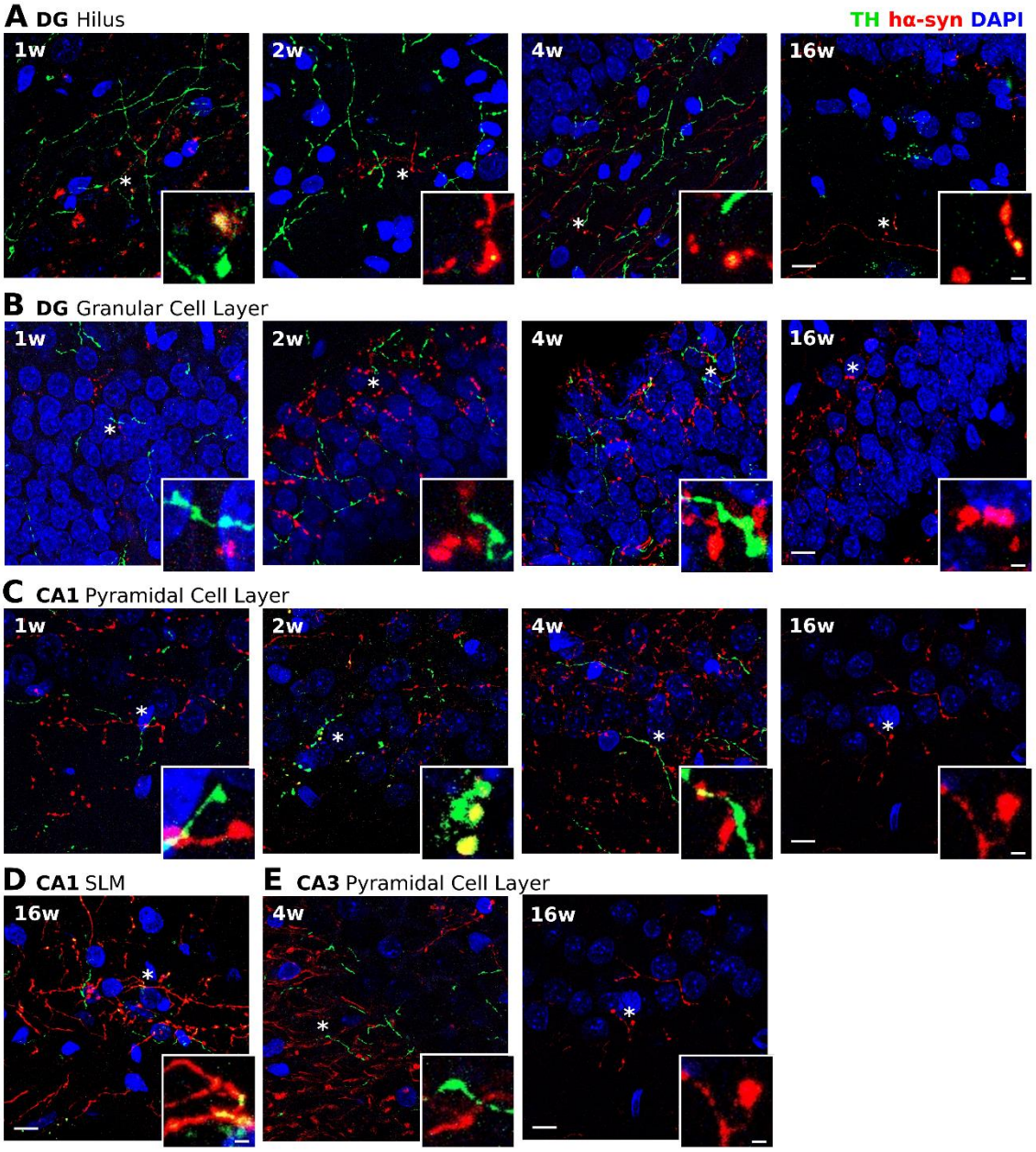

Figure 24. Expression of hα-syn in dopaminergic TH⁺ fibers of the hippocampus. Representative double immunofluorescence photomicrographs for TH and hα-syn in the hippocampus of the AAV-hα-syn group at 1w, 2w, 4w, and 16w p.i. in the DG **A)** hilus and **B)** granular cell layer; CA1 region **C)** pyramidal cell layer and **D)** stratum lacunosum moleculare (SLM); and CA3 region **E)** pyramidal cell layer. Scale bars, 10 µm. Higher magnification photomicrographs of areas pointed with an asterisk are detailed in the bottom right corner of each photo. Scale bars, 5 µm.

1.3.2.2. Glutamatergic pathway

The vGlut2 staining in the hippocampus showed punctate staining throughout all regions of the hippocampus in line with its abundant localization to synaptic vesicles at the glutamatergic terminals (Figure 25). Across the different time points, a general decrease of vGlut2$^+$ staining was observed, particularly at 16 weeks p.i. (Figure 25).

In the DG, vGlut2$^+$ staining was scarce in the hilus (Figure 25A) but particularly abundant in the granular cell layer (Figure 25B). In the hilus (Figure 25A), vGlut2$^+$ staining did not colocalize with hα-syn$^+$ puncta at 1 week p.i. but it did colocalize with fibrillar hα-syn at 2, 4, and 16 weeks p.i. In the granular cell layer of the DG (Figure 25B), a strong colocalization of hα-syn was observed within vGlut2$^+$ terminals from 2 weeks p.i. onwards, concomitant to the onset of hα-syn expression in this layer. Moreover, vGlut2 and hα-syn expression in the granular cell layer decreased over time, becoming more evident at 16 weeks p.i., although some hα-syn content was still observed in the few remaining vGlut2$^+$ terminals.

In the CA1 region, vGlut2$^+$ staining was found across the stratum oriens, pyramidal cell layer, stratum radiatum (Figure 25C), and SLM (Figure 25D), where it widely colocalized with hα-syn at all time points. In the pyramidal cell layer and the adjacent stratum oriens and stratum radiatum (Figure 25C), colocalization was present at 1, 2, and 4 weeks p.i. At 16 weeks p.i., both vGlut2 and hα-syn staining decreased in these regions, however, the remaining few vGlut2$^+$ fibers showed hα-syn$^+$ content. In the SLM at 16 weeks p.i. we also observed some vGlut2$^+$ fibers positive to hα-syn (Figure 25D).

In the CA3 region, vGlut2$^+$ staining was particularly abundant within the pyramidal cell layer, although it was found across all layers of CA3 (Figure 25E). At 4 weeks p.i., vGlut2$^+$ terminals strongly colocalized with hα-syn in the pyramidal cell layer and the adjacent stratum lucidum. At 16 weeks p.i. both markers were decreased, but hα-syn was observed within the remaining vGlut2$^+$ fibers.

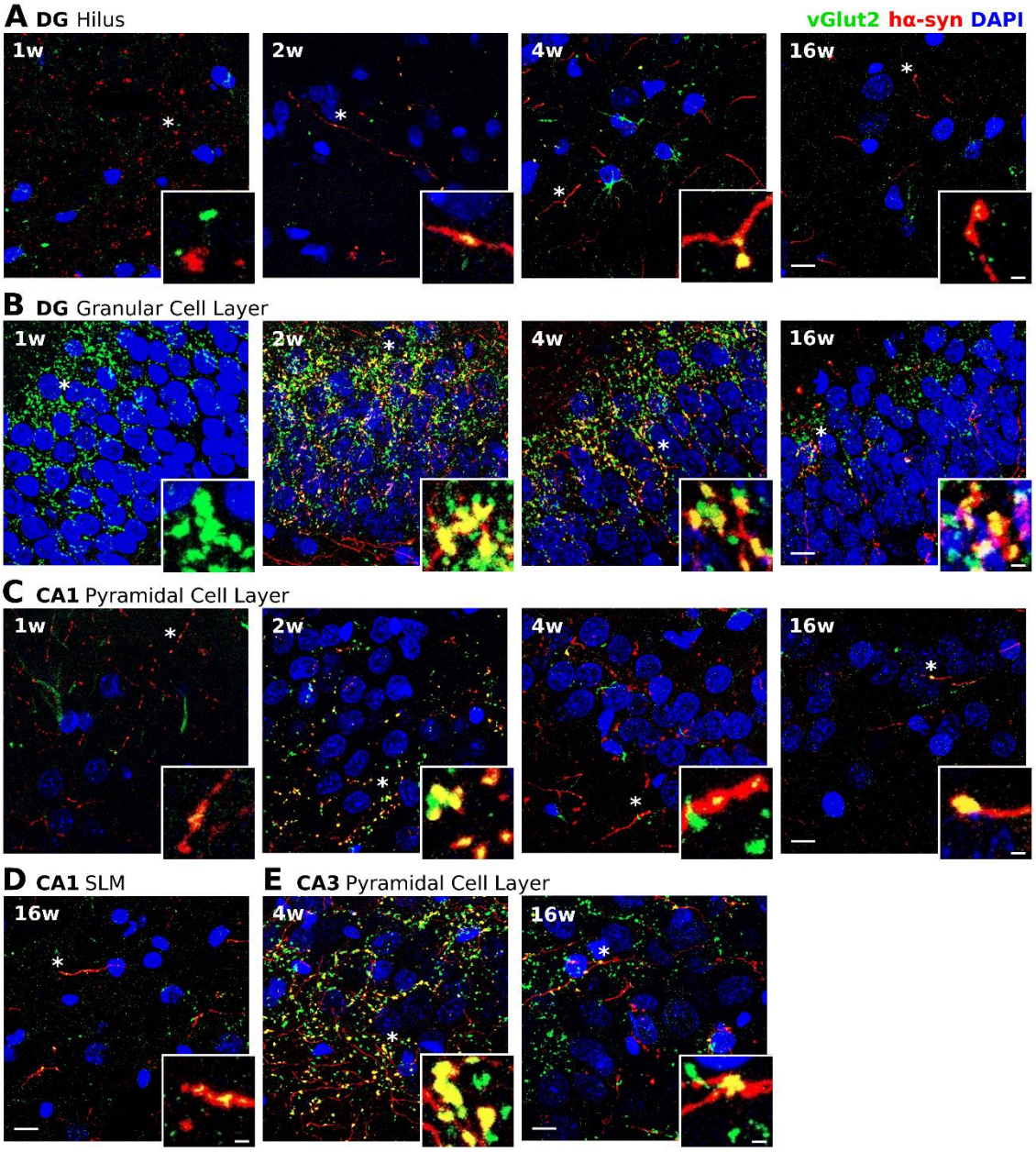

Figure 25. Expression of hα-syn in vGlut2⁺ terminals of the hippocampus. Representative double immunofluorescence photomicrographs for vGlut2 and hα-syn in the hippocampus of the AAV-hα-syn group at 1w, 2w, 4w, and 16w p.i. in the DG **A)** hilus and **B)** granular cell layer; CA1 region **C)** pyramidal cell layer and **D)** stratum lacunosum moleculare (SLM); and CA3 region **E)** pyramidal cell layer. Scale bar 10 µm. Higher magnification photomicrographs of areas pointed with an asterisk are detailed in the bottom right corner of each photo. Scale bars, 5 µm.

1.3.2.3. GABAergic pathway

GABA staining in the hippocampus showed a punctate pattern throughout all regions of the hippocampus in line with its abundant localization to GABAergic synaptic terminals (Figure 26). Moreover, several neuronal somas were also found throughout all regions of the hippocampus, corresponding to GABAergic interneurons. Of note, no hα-syn$^+$ staining was observed within these neurons evidencing the presence of hα-syn$^+$ only in GABAergic terminals. Across the different time points, a general decrease of GABA$^+$ staining was observed together with an increase of hα-syn$^+$ staining, particularly from 4 weeks p.i. onwards (Figure 26).

In the DG, GABA$^+$ staining was found across all layers, but it was particularly abundant in the granular cell layer (Figure 26A-B). In GABA$^+$ fibers from the hilus (Figure 26A) few hα-syn$^+$ puncta and fibers were observed at 1 and 2 weeks p.i. At 4 weeks p.i., GABA$^+$ staining decreased together with an increase in hα-syn expression and colocalized within some GABA$^+$ fibers. By contrast, at 16 weeks p.i., both GABA and hα-syn staining decreased and no colocalization was observed. In the granular cell layer of the DG (Figure 26B), hα-syn was observed within some GABA$^+$ terminals since 2 weeks p.i., concomitant with the onset of hα-syn expression in this region. At 4 and 16 weeks p.i., despite the decrease in GABA staining, some hα-syn$^+$ expression was still observed within GABA$^+$ fibers.

In the CA1 region, GABA$^+$ staining was particularly abundant in the pyramidal cell layer (Figure 26C), although it was found across all layers. In the pyramidal cell layer and the subjacent stratum oriens and stratum radiatum (Figure 26C), hα-syn colocalization with GABA$^+$ fibers was scarce at 1 week p.i., but more abundant at 2 weeks p.i. Together with an overall decrease of GABA staining at 4 weeks p.i., colocalization of both makers decreased and became almost absent at 16 weeks p.i. In the SLM at 16 weeks p.i. (Figure 26D) no hα-syn was observed within GABA$^+$ fibers.

In the CA3 region, again GABA$^+$ staining was particularly abundant within the pyramidal cell layer (Figure 26E), although it was found across all layers of CA3. However, no colocalization was observed between GABA and hα-syn at 4 weeks p.i. in the pyramidal cell layer and the adjacent stratum lucidum. At 16 weeks p.i., GABA staining was almost absent, and thus, there was no colocalization of hα-syn within GABA$^+$ fibers.

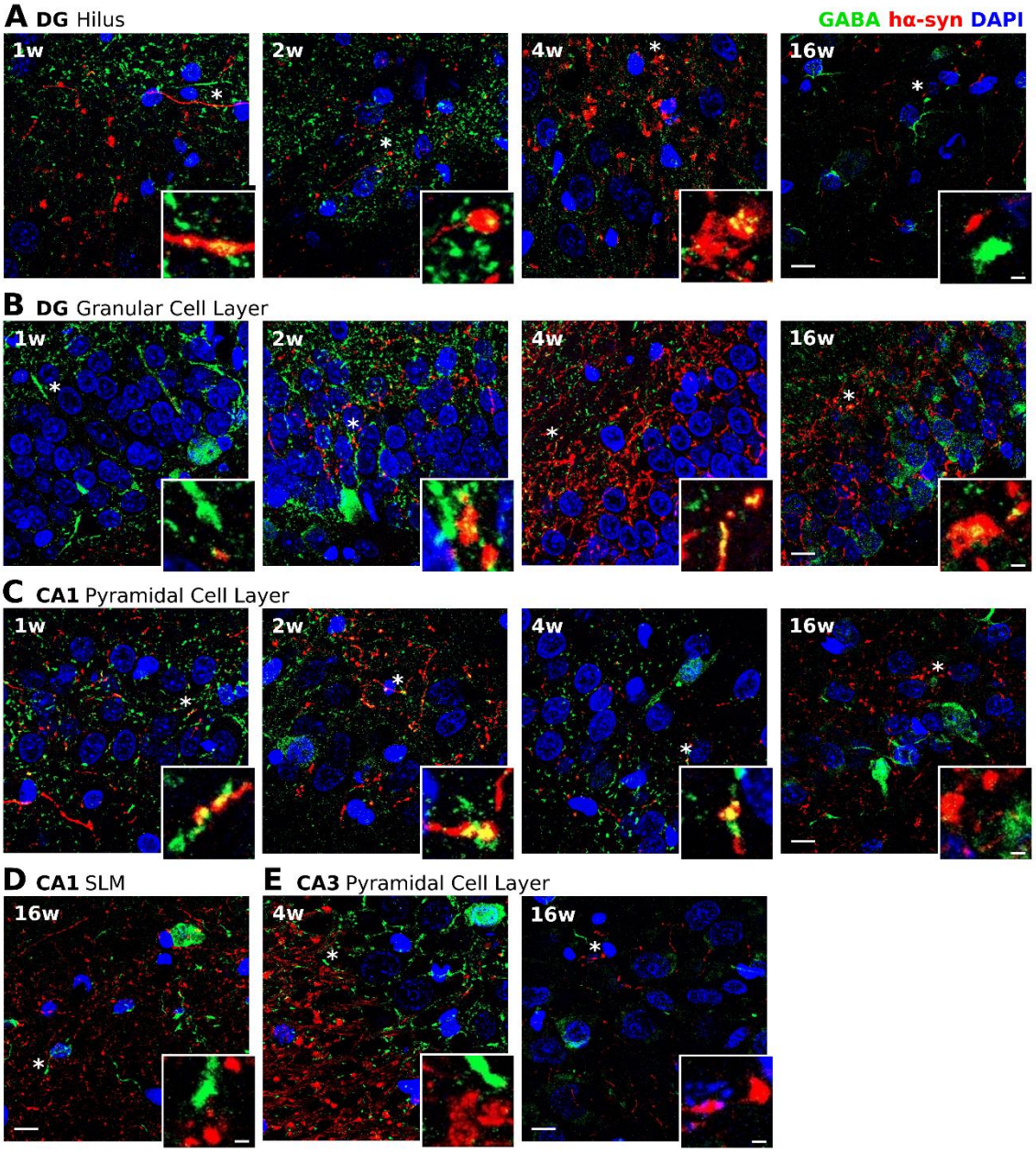

Figure 26. Expression of hα-syn in GABA⁺ terminals of the hippocampus. Representative double immunofluorescence photomicrographs for GABA and hα-syn in the hippocampus of the AAV-hα-syn group at 1w, 2w, 4w, and 16w p.i. in the DG **A)** hilus and **B)** granular cell layer; CA1 region **C)** pyramidal cell layer and **D)** stratum lacunosum moleculare (SLM); and CA3 region **E)** pyramidal cell layer. Scale bar 10 µm. Higher magnification photomicrographs of areas pointed with an asterisk are detailed in the bottom right corner of each photo. Scale bars, 5 µm.

2. Behavioral assessment and hippocampal cLTP

2.1. Experimental design

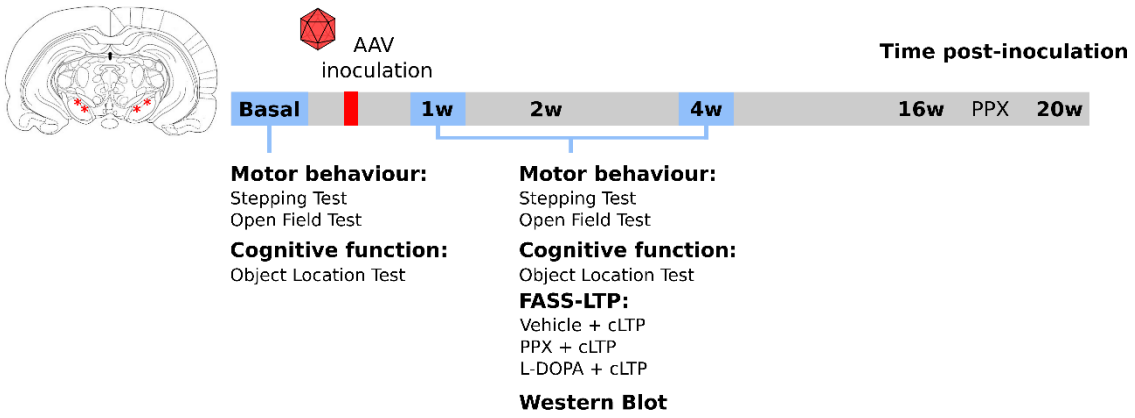

Figure 27. Experimental design for the behavioral evaluation and FASS-LTP. Animals were inoculated with either AAV-hα-syn or AAV-EVV bilaterally in the SNpc. Motor and memory tests were assessed before surgery (basal) and at the earliest time points of hα-syn overexpression (1 and 4 weeks p.i.). The time point of 16 weeks p.i. was omitted because the loss of TH^+ cells in the SNpc and VTA was similar to the one observed at 4 weeks p.i., with no further progression of the degeneration. Once animals were sacrificed at their corresponding final time point (1 and 4 weeks p.i.), brains were removed and synaptosomes were isolated from the hippocampi to perform FASS-LTP, while midbrains were used to confirm the expression of hα-syn by western blot.

This set of experiments aimed to determine the onset of memory and motor deficits as well as the impairment in synaptic plasticity. For that purpose, we only analyzed the earliest time points of hα-syn overexpression and dopaminergic degeneration. Specifically, we analyzed 1 week p.i. as it represents the onset of hα-syn expression in the hippocampus as well as the onset of a significant degeneration of VTA dopaminergic neurons; and 4 weeks p.i. because is the time point where it starts the significant dopaminergic neurodegeneration in the nigrostriatal pathway together with the maximum expression of hα-syn in the hippocampus. As we did not observed differences between 4 and 16 weeks p.i. regarding the loss of TH^+ cells in the SNpc/VTA, and since we are focused on the earliest changes during the onset of significant neurodegeneration, we decided not to include the 16 weeks p.i. time point in this experiment to reduce the number of animals.

For this purpose, behavioral tasks were assessed in the animals before surgery (basal) and at 1 and 4 weeks p.i. (n = 8 for each experimental group and time point) (Figure 27). On the other

hand, to determine whether hα-syn overexpression can influence LTP in synaptic terminals of the hippocampus, after behavioral tasks at 1 and 4 weeks p.i., animals were sacrificed and were used to perform the FASS-LTP in isolated synaptosomes. Additionally, the same samples were also tested with two dopaminergic drugs: PPX and L-DOPA. For that purpose, isolated synaptosomes were incubated with vehicle (water), PPX, or L-DOPA at basal unstimulated conditions and compared to cLTP stimulation conditions.

2.2. Behavioral assessment

2.2.1. Evaluation of motor activity

To evaluate forelimb bradykinesia, the stepping test was performed. In the AAV-hα-syn group, a 20% significant reduction was found in the number of adjusting steps at 4 weeks p.i. compared to the basal state ($p < 0.001$) and 1 week p.i. ($p < 0.0001$), as well as respect to their corresponding AAV-EVV group ($p < 0.01$) (Figure 28A). No differences were observed in the AAV-EVV at any time point evaluated (Figure 28A).

In the open field test, the AAV-hα-syn group showed a significant reduction of the distance traveled at 4 weeks p.i. compared to the basal state ($p < 0.001$) and 1 week p.i. ($p < 0.001$), as well as to their corresponding AAV-EVV group ($p < 0.05$) (Figure 28B). Additionally, a reduction in velocity of AAV-hα-syn animals was observed at 4 weeks p.i. compared to their basal state ($p < 0.01$; Figure 28C). No differences in both parameters were observed in the AAV-EVV at any time point evaluated (Figure 28B-C). Only a significant reduction in the time spent moving was observed in both AAV-hα-syn and AAV-EVV groups at 4 weeks p.i. compared to their corresponding basal state ($p < 0.01$ the AAV-hα-syn; $p < 0.05$ the AAV-EVV; Figure 28D).

Additionally, the time spent in the center of the arena, which is indicative of anxiety-like behavior, showed in the AAV-hα-syn and AAV-EVV groups an overall significant reduction at 4 weeks p.i. compared to their corresponding basal state ($p < 0.05$; Figure 28E). No differences were observed between experimental groups at any time point evaluated (Figure 28E).

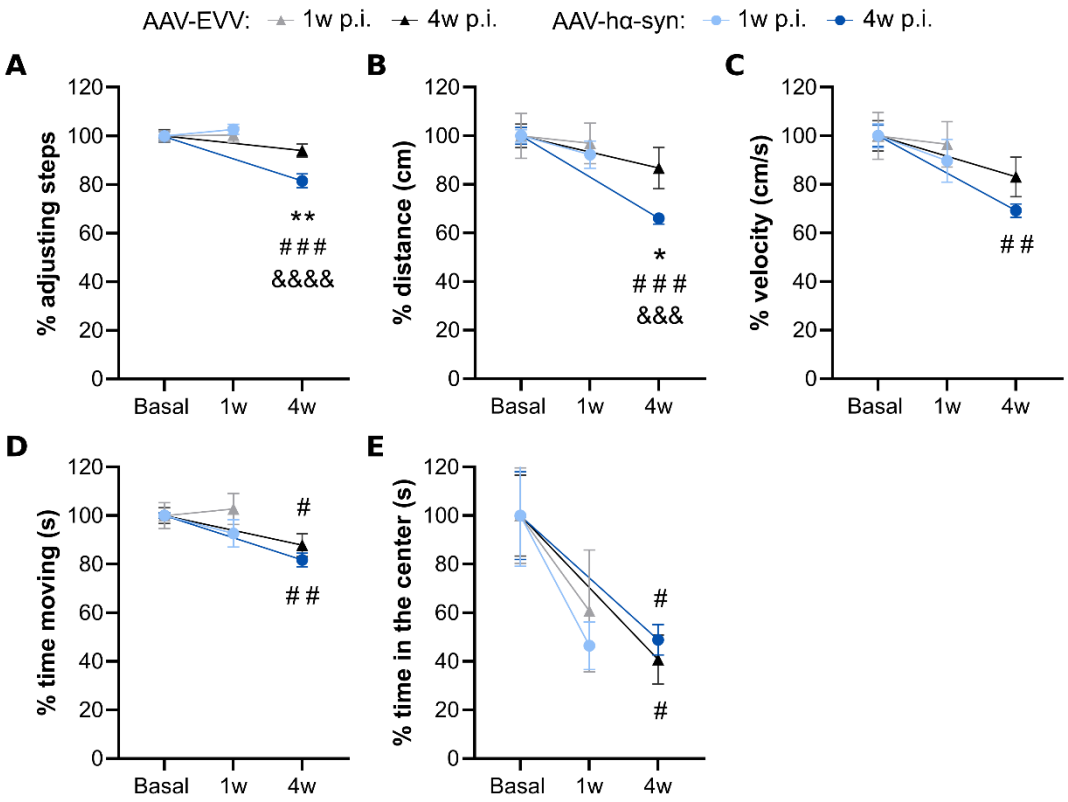

Figure 28. Evaluation of the motor activity. A) Stepping test and open field test: **B)** distance, **C)** velocity, **D)** time spent moving, and **E)** time spent in the center of the arena. Values at each time point were normalized to their corresponding basal values and represented as the mean ± SEM. Two-way ANOVA flowed by Tukey's post hoc test: # $p < 0.05$, ## $p < 0.01$, ### $p < 0.001$ vs. basal; * $p < 0.05$, ** $p < 0.01$ vs. AAV-EVV; & $p < 0.05$, &&&& $p < 0.0001$ vs. 1w p.i. n = 8 for each experimental group and time point evaluated.

2.2.2. Evaluation of hippocampal-dependent spatial memory

Spatial memory performance was assessed with the OLT. In the AAV-hα-syn group, a tendency towards reduced spatial memory was observed at 4 weeks p.i. compared to the corresponding AAV-EVV ($p = 0.0871$; Figure 29). No differences were observed when compared to basal or between time points in both groups at any time point evaluated (Figure 29).

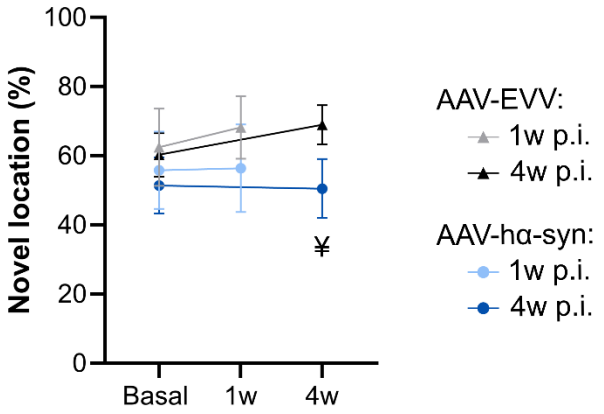

Figure 29. Evaluation of spatial memory. Object location test (OLT) was performed in the AAV-EVV and the AAV-hα-syn groups at 1 and 4 weeks (w) p.i. Time spent exploring the object in the novel location (%) was calculated and values are represented as the mean ± SEM. Two-way ANOVA flowed by Tukey's post hoc test: ¥ p = 0.0871 vs. AAV-EVV. n = 8 for each experimental group and time point evaluated.

2.3. cLTP in hippocampal synaptosomes

At 1 week p.i. and under vehicle conditions, the AAV-hα-syn group showed significantly decreased cLTP compared to their corresponding AAV-EVV ($p < 0.01$, Figure 30A). Interestingly, the dopaminergic agonist PPX increased significantly cLTP compared to the vehicle condition in the AAV-hα-syn group ($p < 0.05$; Figure 30A), whereas decreased cLTP was found in the AAV-EVV group ($p < 0.05$; Figure 30A). No differences were observed between groups under PPX conditions. By contrast, with the dopamine precursor L-DOPA, the AAV-hα-syn group showed decreased cLTP compared to the AAV-EVV control group ($p < 0.05$; Figure 30A). No differences were observed in cLTP in the AAV-EVV group with L-DOPA incubation (Figure 30A). No differences between treatments were observed in either of the experimental groups (Figure 30A).

At 4 weeks p.i. and under vehicle conditions, the AAV-hα-syn group showed a significantly decreased cLTP compared to their corresponding AAV-EVV ($p < 0.01$, Figure 30B). PPX increased significantly cLTP in the AAV-hα-syn group compared to the vehicle condition ($p < 0.05$; Figure 30B), while decreased cLTP was found in the AAV-EVV group ($p < 0.05$; Figure 30B). No differences were observed between groups under PPX conditions. L-DOPA increased significantly cLTP in the AAV-hα-syn group compared to the vehicle condition ($p < 0.05$; Figure 30B) and compared to PPX condition ($p < 0.05$, Figure 30B). No differences were observed in the AAV-EVV group or between groups (Figure 30B).

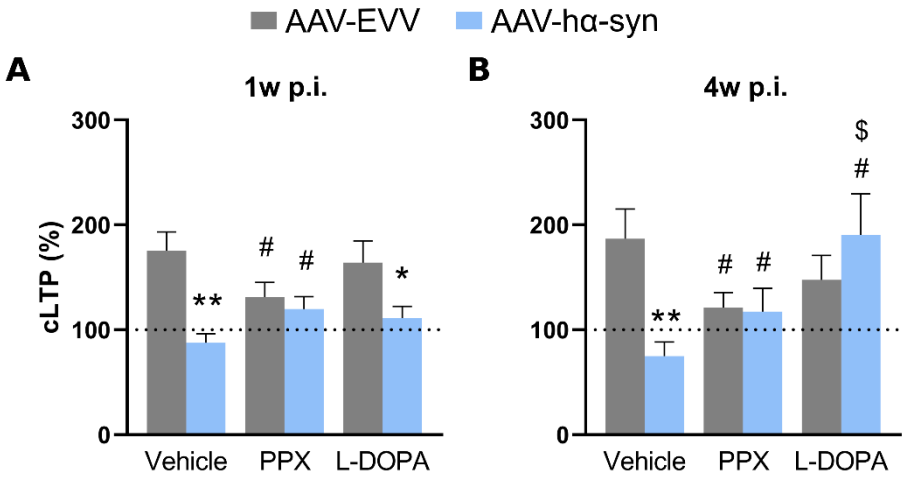

Figure 30. cLTP at hippocampal synaptosomes. cLTP (%) in synaptosomes isolated from the hippocampus of AAV-hα-syn and AAV-EVV groups in the presence of vehicle (water), PPX, and L-DOPA at **A)** 1 week p.i.; and **B)** 4 weeks p.i. Values are represented as the mean ± SEM. Two-way ANOVA flowed by Tukey's post hoc test: * $p < 0.05$, ** $p < 0.01$ vs. AAV-EVV; # $p < 0.05$ vs. vehicle; $ $p < 0.05$ vs PPX. n = 8 for each experimental group and time point evaluated.

A detailed analysis of GluA1/Nrx1β double staining showed significantly increased levels of these markers at the basal condition in the AAV-hα-syn group compared to their corresponding AAV-EVV at both time points (1w p.i.: $p < 0.01$; 4w p.i.: $p < 0.001$; Figure 31A, B, E). Moreover, at 4 weeks p.i., GluA1$^+$/Nrx1β$^+$ staining was significantly decreased in the cLTP condition compared to the basal condition ($p < 0.01$; Figure 31E). The AAV-EVV group showed a significant increase of these markers at cLTP condition compared to basal condition at 1 week p.i. ($p < 0.001$; Figure 31B), and a tendency towards significance at 4 weeks p.i. ($p = 0.0616$, Figure 31E), indicative of cLTP.

In the AAV-hα-syn group, preincubation of synaptosomes with PPX showed no differences compared to AAV-EVV, nor between basal and cLTP conditions at any time point (Figure 31C, F), although we found a tendency at 1 week p.i. towards decreased basal levels of GluA1$^+$/Nrx1β$^+$ compared to vehicle ($p = 0.0639$; Figure 31C). By contrast, increased basal levels of GluA1$^+$/Nrx1β$^+$ staining were observed in the AAV-EVV group compared to the vehicle at both time points ($p < 0.05$.; Figure 31C, F). In the AAV-EVV group, these markers remained significantly increased at the cLTP condition compared to the basal condition at 1 week p.i. ($p < 0.05$; Figure 31C), indicative of LTP.

In line with cLTP (%) results, L-DOPA raised different results depending on the time point. The AAV-hα-syn group showed increased basal GluA1^{+}/Nrx1β^{+} staining at 1 week p.i. compared to their corresponding AAV-EVV ($p < 0.01$; Figure 31D), without differences between basal and cLTP conditions, similar to results with the vehicle. By contrast, the AAV-hα-syn group showed significantly decreased basal levels of GluA1^{+}/Nrx1β^{+} at 4 weeks p.i. compared to vehicle ($p < 0.05$; Figure 31G), although there were no significant differences with the cLTP condition. In line with cLTP (%) results, the AAV-EVV group showed increased levels of the double-positive staining at cLTP conditions compared to basal at both time points ($p < 0.001$ at 1w and $p < 0.05$ at 4w p.i.; Figure 31D, G), without differences when compared to samples treated with vehicle. Comparison between the two dopaminergic drugs showed decreased basal levels of GluA1^{+}/Nrx1β^{+} with L-DOPA in the AAV-hα-syn group at 4 weeks p.i. ($p < 0.05$; Figure 31G), as well as in the AAV-EVV group at both time points ($p < 0.01$ at 1w p.i. and $p < 0.05$ at 4w p.i.; Figure 31D, G).

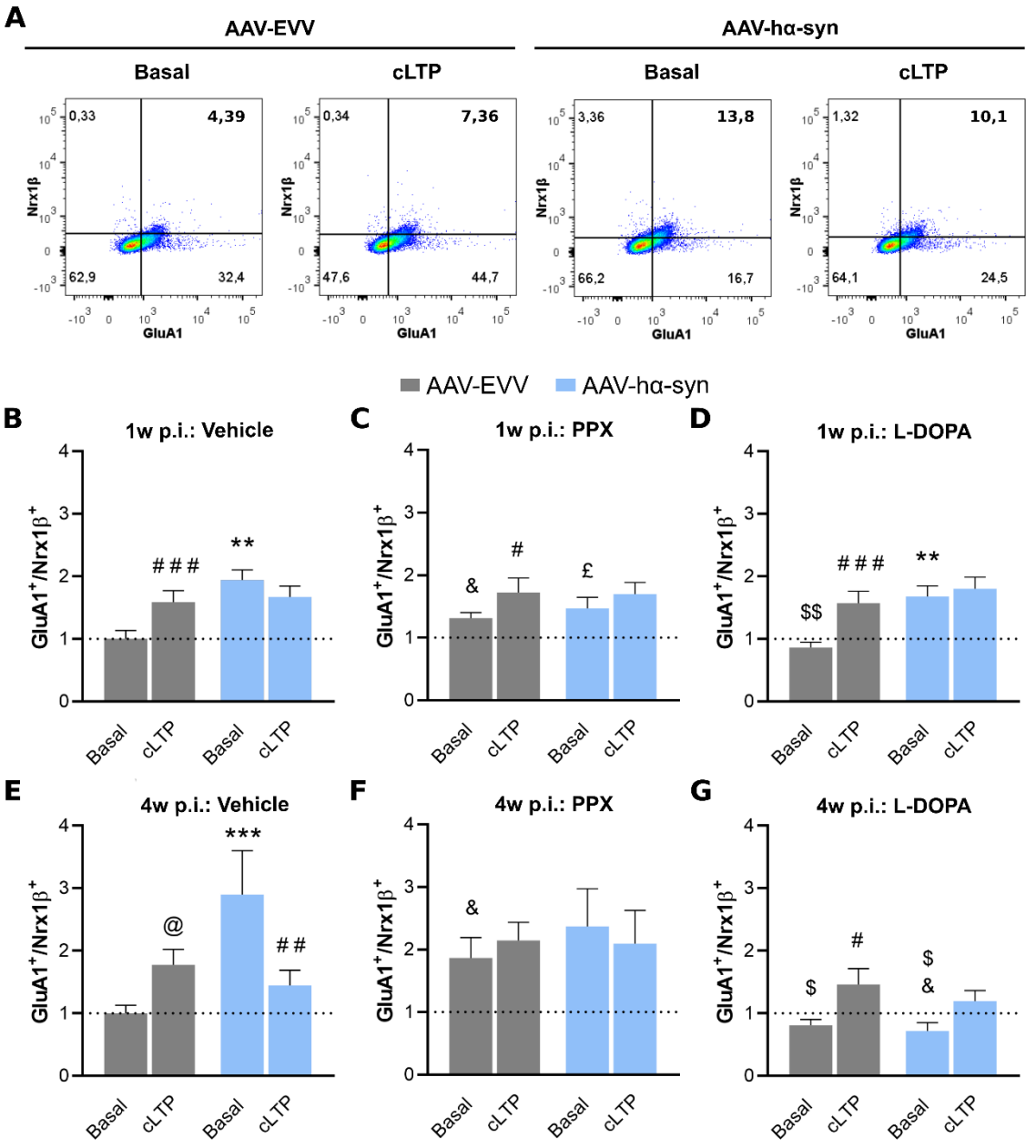

Figure 31. GluA1/Nrx1β staining in hippocampal synaptosomes. A) Representative GluA1/Nrx1β double staining in AAV-hα-syn and AAV-EVV at basal and cLTP conditions measured by flow cytometry. GluA1$^+$/Nrx1β$^+$ double-positive values in AAV-hα-syn and AAV-EVV at basal and cLTP stimulation condition at **B-D)** 1 week p.i. and **E-G)** 4 weeks p.i. in the presence of vehicle (**B, E**), pramipexole (PPX; **C, F**), and L-DOPA (**D, G**). Values were normalized to the AAV-EVV vehicle condition for each time point and are represented as the mean ± SEM. Two-way ANOVA flowed by Bonferroni's post hoc test: ** $p < 0.01$, *** $p < 0.001$ vs. AAV-EVV; # $p < 0.05$, ## $p < 0.01$, ### $p < 0.001$ vs. basal; & $p < 0.05$ vs. vehicle; $ $p < 0.05$, $$ $p < 0.01$ vs. PPX; @ $p=0.0616$ vs. basal; £ $p=0.0639$ vs. vehicle. n = 8 for each experimental group and time point evaluated.

Sujeto a confidencialidad por la autora

4. Glucose brain metabolism after chronic PPX treatment: [^{18}F]-FDG PET study

4.1. Experimental design

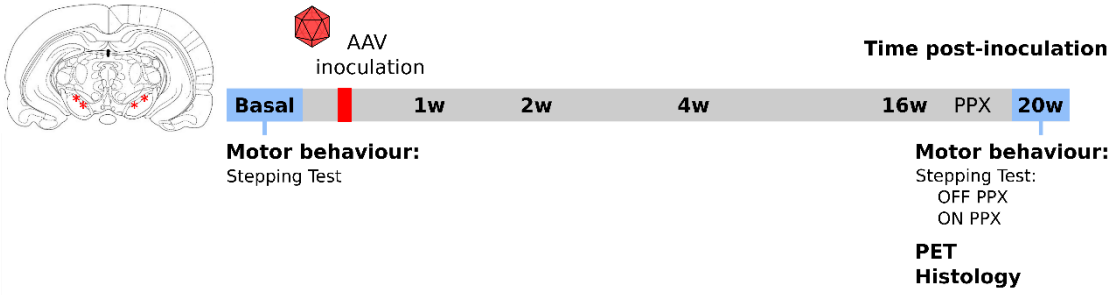

Figure 36. Experimental design for the PET study. Animals were inoculated with either AAV-hα-syn or AAV-EVV bilaterally in the SNpc. After 16 weeks p.i. animals underwent a chronic treatment with PPX (0.25 mg/kg/day, subcutaneous) for 4 weeks. Motor performance was assessed with the stepping test before surgery (basal) and at the final time point (20 weeks p.i.) before (OFF) and after (ON) the corresponding daily doses of PPX. [^{18}F]-FDG PET study was performed at the final time point (20 weeks p.i.) under the effect of the dopaminergic treatment. After the PET study, animals were perfused and brains were removed to obtain coronal slices for immunohistochemistry.

As [^{18}F]-FDG PET enables the assessment of brain activity *in vivo* and it is thought to be a marker of synaptic activity, in order to assess the effect of chronic PPX treatment at this level, we performed a [^{18}F]-FDG PET study in animals with an established dopaminergic degeneration and impaired motor function. For that purpose, animals were inoculated with either AAV-hα-syn (n = 9) or AAV-EVV (n = 5) and chronically treated with PPX for 4 weeks (0.25 mg/kg/day, subcutaneous) after 16 weeks p.i. to ensure a long-term dopaminergic lesion (Figure 36). Motor behavior was evaluated with the stepping test before surgery (basal) and at the final time point (20 weeks p.i.) before (OFF medication) and after (ON medication) the corresponding daily doses of PPX. After completion of the treatment (20 weeks p.i.), the [^{18}F]-FDG PET was performed under the effect of PPX and subsequently, animals were sacrificed and perfused for histological studies.

4.2. [^{18}F]-FDG PET study after PPX treatment

In the AAV-hα-syn group, significant hypometabolism in the anterodorsal hippocampus and the thalamus was observed within the right hemisphere compared to AAV-EVV ($p < 0.001$; uncorrected; Figure 37).

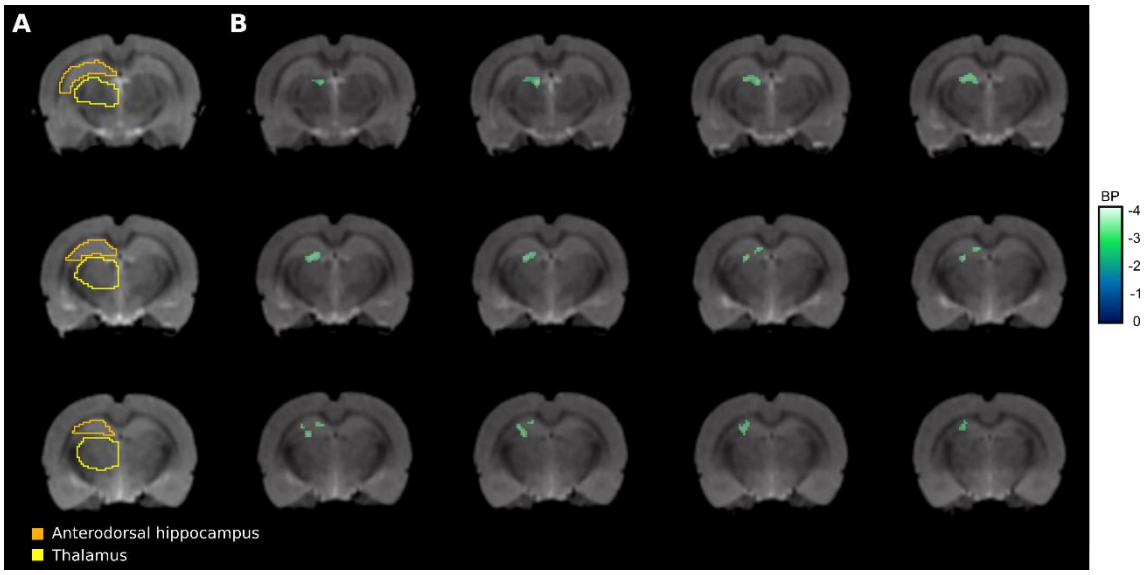

Figure 37. *In vivo* PET study with [^{18}F]-FDG after dopaminergic treatment with PPX. A) MRI images of the rat brain coronal sections showing the anteroposterior hippocampus (orange) and the thalamus (yellow). **B)** Hypometabolic areas in the AAV-hα-syn group compared to the AAV-EVV ($p < 0.001$, uncorrected). Binding potential (BP) values are color-coded and co-registered with MRI images.

4.3. Confirmation of the parkinsonian phenotype

The AAV-hα-syn animals showed motor impairment with a 60% significant reduction in the number of adjusting steps at 20 weeks p.i. before the daily doses of PPX (OFF medication) compared to the basal state ($p < 0.0001$; Figure 38A) and to their corresponding AAV-EVV group ($p < 0.0001$; Figure 38A). Following the daily administration of PPX (ON medication), although they were still significantly impaired compared to the basal state ($p < 0.0001$; Figure 38A), the AAV-hα-syn group significantly improved motor performance compared to the OFF state ($p < 0.001$; Figure 38A). However, the AAV-hα-syn animals were significantly impaired compared to their corresponding AAV-EVV group ($p < 0.01$; Figure 38A). No differences were observed in the AAV-EVV group between time points or PPX OFF/ON state (Figure 38A).

Regarding the histology, in the SNpc and VTA, hα-syn protein overexpression was confirmed in the AAV-hα-syn group at 20 weeks p.i. (Figure 38C) whereas no expression was observed in the AAV-EVV group (Figure 38C). In the striatum, a reduction of DAT expression was observed in the AAV-hα-syn group compared to the AAV-EVV group (50% reduction, $p < 0.05$; Figure 38B, D), indicative of dopaminergic degeneration.

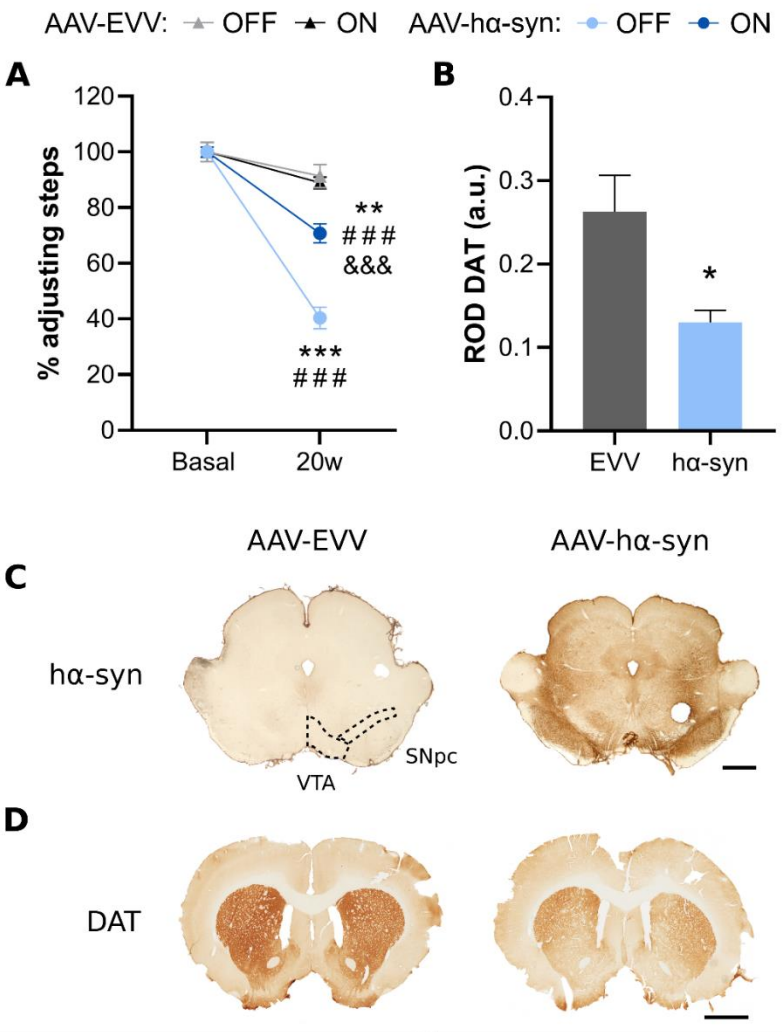

Figure 38. Confirmation of the parkinsonian phenotype in the AAV-hα-syn group used in the [^{18}F]-FDG PET study after the dopaminergic treatment with PPX. A) Stepping test of the AAV-EVV and the AAV-hα-syn groups at basal and 20 weeks p.i. At the latter time point, the number of adjusting steps were assessed before (OFF medication) and after (ON medication) the daily administration of PPX. Values at 20 weeks p.i. were normalized to their corresponding basal values and represented as the mean ± SEM. Two-way ANOVA flowed by Tukey's post hoc test: ### $p < 0.0001$ vs. basal; ** $p < 0.01$ vs. AAV-EVV; &&& $p < 0.0001$ vs. OFF medication. n = 5 for AAV-EVV group and n = 9 for AAV-hα-syn group. **B)** Relative optical density (ROD) analysis of DAT expression in the striatum from the AAV-EVV and the AAV-hα-syn groups at 20 weeks p.i. Values are presented as the mean ± SEM. Mann Whitney test: * $p < 0.05$ vs. AAV-EVV. n = 5 for AAV-EVV group and n = 9 for AAV-hα-syn group. **C)** Representative photomicrographs showing hα-syn overexpression in the SNpc/VTA in the AAV-hα-syn group at 20 weeks p.i. Scale bar, 1 mm. **D)** Representative photomicrographs showing DAT expression in the striatum of the AAV-EVV and the AAV-hα-syn groups at 20 weeks p.i. Scale bar, 2 mm.

Table 6. Summary of the main results obtained in this doctoral thesis in the AAV-hα-syn group. Significant increases are shown in green and significant decreases in red. Abbreviations: GA, GABAergic; Glu, glutamatergic; n.a., not available; n.s., not significant; TH, dopaminergic.

		AAV-hα-syn p.i. time points				
		1w	**2w**	**4w**	**16w**	**20w**
Histological characterization						
hα-syn in SNpc		↑	↑	↑↑↑	↑↑	n.a.
hα-syn in VTA		↑	↑	↑↑	↑↑	n.a.
TH in SNpc		-	-	↓	↓	n.a.
TH in VTA		↓	↓	↓	↓	n.a.
hα-syn in hippocampus		↑	↑	↑↑↑	↑↑↑	n.a.
hα-syn$^+$ afferents to the hippocampus						
DG Hilus		TH/GA	TH/Glu/GA	TH/Glu/GA	TH/Glu	n.a.
DG Granular		-	Glu/GA	Glu/GA	Glu/GA	n.a.
CA1 Pyramidal		Glu/GA	TH/Glu/GA	Glu/GA	Glu	n.a.
CA1 SLM		n.a.	n.a.	n.a.	TH/Glu	n.a.
CA3 Pyramidal		n.a.	n.a.	Glu	Glu	n.a.
Behavioral assessment						
Motor activity		-	n.a.	↓	n.a.	↓
Spatial memory		-	n.a.	↓ n.s.	n.a.	n.a.
FASS-LTP in hippocampal synaptosomes						
cLTP (%)	Vehicle	↓	n.a.	↓	n.a.	n.a.
	PPX	↑	n.a.	↑	n.a.	n.a.
	L-DOPA	↓	n.a.	↑	n.a.	n.a.
Basal GluA1/Nrx1β	Vehicle	↑	n.a.	↑	n.a.	n.a.
	PPX	↑ n.s.	n.a.	↑ n.s.	n.a.	n.a.
	L-DOPA	↑	n.a.	↓	n.a.	n.a.
Deregulated biological pathways in hippocampal synaptosomes						
ATP biosynthesis		Deregulated	n.s.	n.s.	n.s.	n.a.
Intracellular transport		Deregulated	Deregulated	n.s.	n.s.	n.a.
Actin cytoskeleton		n.s.	Deregulated	n.s.	n.s.	n.a.
SV trafficking		n.s.	Deregulated	n.s.	n.s.	n.a.
Lysosomal transport		n.s.	Deregulated	n.s.	n.s.	n.a.
Cation homeostasis		n.s.	n.s.	n.s.	Deregulated	n.a.
Membrane potential		n.s.	n.s.	n.s.	Deregulated	n.a.
Receptor signaling		n.s.	n.s.	n.s.	Deregulated	n.a.
tRNA metabolism		n.s.	n.s.	n.s.	Deregulated	n.a.
[^{18}F]-FDG PET study						
After chronic PPX treatment		n.a.	n.a.	n.a.	n.a.	↓ Thalamus & Hippocampus

Discussion

This doctoral thesis has focused on elucidating the early synaptic changes induced by the presence of hα-syn in the hippocampus, and its potential role in cognitive and behavioral manifestations in PD as well as the modulation of synaptic plasticity impairment by the dopaminergic therapy.

1. Pathological alterations in the mesolimbic pathway from the VTA to the hippocampus

Research on PD has classically been focused on the degeneration of the dopaminergic nigrostriatal pathway, leading to a dysregulation of the basal ganglia circuitry and, consequently, the onset of the cardinal motor features. However, PD is a multisystem disorder that affects many different regions in the brain, where dysregulation of other neurotransmitters such as noradrenaline, serotonin, or acetylcholine has been linked to the development of non-motor features of PD (Barone, 2010; Schapira et al., 2017), which have gained importance during the past decade.

The hippocampus has been suggested to play a role in the development of cognitive and behavioral alterations in PD (Calabresi et al., 2013) and thus, it has been our structure of interest in this doctoral thesis. The major source of DA to the hippocampus is the mesolimbic pathway from the VTA (Bentivoglio & Morelli, 2005; Björklund & Dunnett, 2007). Thus, we aimed to characterize the temporal sequence of dopaminergic neuronal loss and Lewy pathology in the VTA. Since the VTA also contains glutamatergic and GABAergic neurons, characterizing how these different neuronal populations influence the many different functions of the hippocampus is crucial for understanding their possible role in PD. Therefore, we also aimed to characterize Lewy pathology in these neurons and their corresponding projections to the hippocampus.

On the one hand, our results show that inoculation of the AAV-hα-syn into the SNpc triggers the overexpression of hα-syn in the SNpc as well as in the adjacent VTA since the earliest time point analyzed (1 week p.i.) and reaching its maximum at 4 weeks p.i. Moreover, we report a 40% degeneration of TH^+ dopaminergic neurons in the VTA starting 1 week p.i., which was maintained across time. This neuronal loss preceded the one in the SNpc, which was significant at 4 weeks p.i. with a 31% TH^+ cell loss. Since hα-syn expression was concomitant to a significant dopaminergic neuron loss in the VTA, we can speculate that aggregation of hα-syn plays a key role in the onset of dopaminergic neurodegeneration. Although the VTA has long been suggested to participate in PD pathogenesis, with neuronal cell loss ranging from 31% to 77% in *post mortem* PD brains (Alberico et al., 2015; Giguère et al., 2018), few studies on humans and animal models

have focused on this nucleus. Indeed, only one study has previously assessed the number of TH^+ dopaminergic cells in the VTA throughout different time points p.i. in an AAV-based animal model of PD (Alarcón-Arís et al., 2020). Unilaterally inoculated mice with the AAV5-hα-syn into the SNpc showed no degeneration in the VTA up to 16 weeks p.i. along with a modest TH^+ cell loss (15%) in the SNpc since 8 weeks p.i. (Alarcón-Arís et al., 2020). Another study showed a 30% degeneration of TH^+ dopaminergic neurons of the VTA at 8 weeks p.i. in AAV6-hα-syn inoculated rats (Caudal et al., 2015). Other studies with direct delivery of the AAVs into the VTA have shown a 22% and 24% TH^+ cell loss at 8 weeks p.i. (Alvarsson et al., 2016) and 23 weeks p.i. (H. Hall et al., 2013), respectively. In contrast, one study found no TH^+ cell degeneration in the VTA at 12 weeks p.i. of the direct delivery of the AAV-hα-syn into this nucleus, however, they pointed out that although VTA dopaminergic neurons survived hα-syn overexpression, they were functionally compromised as the animals developed a motor impairment (Maingay et al., 2006). Selective VTA dopaminergic degeneration, without affecting the SNpc, was shown to lower DA outflow in the hippocampus and NAcc, leading to impairments in synaptic plasticity, memory performance, and food reward processing (Nobili et al., 2017). Moreover, hα-syn expression specifically in the VTA neurons has previously been shown to lead to the motor as well as non-motor deficits in AAV-hα-syn inoculated animals (Alvarsson et al., 2016; H. Hall et al., 2013; Maingay et al., 2006). Our results support the influence that the VTA exerts on the dopaminergic system, being capable of modulating the motor and non-motor symptoms, as reflected by the impaired motor performance and a trend towards decreased cognitive functions when partial loss of VTA dopaminergic cells has started. Thus, our results highlight the relevance of the VTA in the progressive alterations that occur in the onset of parkinsonism.

Colocalization analysis revealed that not only dopaminergic but also glutamatergic neurons in the VTA overexpress hα-syn. Unfortunately, due to technical difficulties to stain GABAergic neurons in the VTA, it was not possible to confirm or exclude the presence of hα-syn in these neurons. The VTA is a heterogeneous nucleus with different neuronal populations including dopaminergic, GABAergic, and glutamatergic neurons, as well as small populations of DA-glutamate and GABA-glutamate co-releasing neurons (H. J. Kim et al., 2019; Morales & Margolis, 2017). VTA neurons play a range of different roles such as regulation of goal- and reward-directed behaviors as well as social behaviors, memory encoding, and wakefulness and sleep in target limbic regions (Bimpisidis & Wallén-Mackenzie, 2019; McNamara et al., 2014; Morales & Margolis, 2017; X. Yu et al., 2019). However, the contribution of each neuronal subpopulation to specific behaviors is still poorly understood. Recently, it has been shown that expression of vGlut2 in VTA neurons needs to be delicately balanced because perturbations in

either direction can have profound effects on dopaminergic neuron survival. In this sense, overexpression of vGlut2 has been associated with specific dopaminergic neuron loss (Steinkellner et al., 2018), while the absence of vGlut2 was related to a higher susceptibility of dopaminergic neurons to parkinsonian neurotoxins such as rotenone (Buck et al., 2021). However, α-syn pathology specifically in VTA non-DA neurons has not been studied before, and thus, their contribution to PD pathogenesis is still unknown. Our results suggest that hα-syn is overexpressed in VTA glutamatergic neurons, which could be inducing a dysregulation of the neuronal circuitry within the VTA, ultimately contributing to dopaminergic neuron vulnerability in the SNpc/VTA region since the earliest stages of the parkinsonism.

In the hippocampus, our results show that transduction of SNpc/VTA neurons leads to an overexpression of hα-syn since 1 week p.i., increasing progressively and reaching maximum levels at 4 weeks p.i. To date, few studies have distinguished between DA and non-DA projections from the VTA to the hippocampus. A detailed anatomical analysis showed that at the earliest time point of 1 week p.i., hα-syn is present in the hilus and the CA1 region, colocalizing within TH^+, $vGlut2^+$, and $GABA^+$ fibers. At 2 weeks p.i., apart from the already mentioned areas, hα-syn appears in the granular cell layer of the DG, where it colocalizes within $GABA^+$ and preferentially $vGlut2^+$ fibers. Of note, hα-syn staining in the hippocampus showed a fibrillar or punctate pattern, but no cell bodies were identified. Although we cannot rule out the spread of hα-syn to hippocampal neurons, these results suggest that hα-syn was not overexpressed in the hippocampal neurons but was rather spread from other affected brain areas (e.g., VTA). Moreover, our colocalization analysis is in line with the previously described anatomical distribution of VTA projections in the hippocampus, where VTA dopaminergic neurons project to the CA1 region and the hilus of the DG (Adeniyi et al., 2020; Edelmann & Lessmann, 2018; Lisman & Grace, 2005), VTA GABAergic neurons innervate preferentially the DG (Han et al., 2020; Ntamati & Lüscher, 2016), and VTA glutamatergic neurons project to all hippocampal regions (Adeniyi et al., 2020). Additionally, we found few TH^+ fibers in the granular cell layer of the DG and the CA3 region, without any associated hα-syn accumulation. These TH^+ fibers may arrive from other brain nuclei rather than the VTA as previously suggested (Adeniyi et al., 2020), or may belong to the noradrenergic system, which also expresses TH for the biosynthesis of noradrenaline and innervates these regions (Kempadoo et al., 2016; McNamara & Dupret, 2017). Regarding GABAergic innervation, although we found $GABA^+$ staining throughout the whole hippocampus, it has to be taken into consideration that GABA is not a specific marker for VTA afferents, and thus, the staining we observed also corresponds to afferents from other GABAergic brain regions as well as from hippocampal interneurons. However, we observe some colocalization of hα-syn within $GABA^+$

terminals, supporting the contribution of this neuronal population to hippocampal dysfunction. Interestingly, within the scarce colocalization of GABA with hα-syn, the granular cell layer of the DG is of special interest. In this area, VTA neurons have previously been described to co-release GABA and glutamate (Ntamati & Lüscher, 2016). Indeed, we also observed abundant colocalization of hα-syn within vGlut2$^+$ terminals in this hippocampal region, which could in part account for the co-releasing population. Of note, we noticed that hα-syn abundantly colocalized within vGlut2$^+$ terminals across the different layers and time points p.i., which is in line with the previously described predominant glutamatergic innervation compared to the scarce dopaminergic innervation from the VTA to the hippocampus (Adeniyi et al., 2020; Gasbarri et al., 1994; Han et al., 2020). Thus, our results evidence the implication of DA as well as non-DA (particularly glutamatergic) VTA neurons in the hippocampal dysfunction in our AAV-hα-syn-based animal model of PD.

Interestingly, α-syn was described to be differentially expressed in excitatory and inhibitory terminals throughout the hippocampus, with high levels of α-syn expression within excitatory terminals but weak or even absent expression of α-syn within inhibitory terminals (Taguchi et al., 2014). Similar results were found in cultured hippocampal neurons, where α-syn was shown to differentially modulate the synaptic machinery in excitatory and inhibitory neurons (Taguchi et al., 2014). Moreover, the same authors showed that in cultured hippocampal neurons, treatment with preformed fibrils was not associated with α-syn aggregation in inhibitory neurons, suggesting that intracellular aggregate formation might be related to the endogenous expression levels of α-syn. Thus, overexpression of hα-syn in SNpc/VTA neurons could be affecting differentially the synaptic machinery in excitatory and inhibitory neurons, thus, possibly impairing synaptic machinery in VTA glutamatergic terminals but not in GABAergic terminals, which could have a clear impact on hippocampal function.

Additionally, our AAV-hα-syn animals showed a tendency towards decreased performance in a hippocampal-dependent spatial memory task at 4 weeks p.i., preceded by impaired hippocampal cLTP starting at 1 week p.i. Despite the early alterations in synaptic plasticity, the immunofluorescence characterization of the hippocampus did not reveal any TH$^+$ or vGlut2$^+$ fiber degeneration until 16 weeks p.i., although it needs to be confirmed with more precise quantitative approaches. The results suggest that functional alterations impact behavioral performance and precede structural alterations. Importantly, our study shows that bilateral injection of hα-syn into the SNpc is sufficient to trigger α-syn pathology within the hippocampus leading to cognitive impairment, thus, providing additional proof that hα-syn may be one of the main neuronal substrates for cognitive impairment in synucleinopathies.

2. Impairment in synaptic plasticity and cognitive performance induced by hα-syn

2.1. The presence of hα-syn in the hippocampus impairs cLTP since 1 week p.i., preceding significant cognitive impairment

Hippocampal cLTP is impaired at 1 week p.i., concomitant to the onset of hα-syn expression in the hippocampus and the degeneration of TH^+ cells in the VTA, but without any associated motor and memory deficits. Moreover, impaired cLTP was maintained at 4 weeks p.i. when hα-syn reached its maximum expression in the hippocampus and the cognitive function was starting to fail as we found a tendency towards decreased spatial memory performance. Previous studies in transgenic animal models of hα-syn have described an age-dependent decline in LTP, particularly with the A53T mutation, accompanied by motor and cognitive alteration after several months of α-syn pathology development (Singh et al., 2019; Teravskis et al., 2018). Moreover, selective VTA dopaminergic neuron degeneration (without any α-syn pathology) was shown to result in lower DA outflow in the hippocampus along with impairments in CA1 region LTP, memory performance, and food reward processing, contributing to memory deficits and dysfunction of reward processing (Nobili et al., 2017). However, to the best of our knowledge, this is the first study to assess LTP in the hippocampus at the earliest stages of hα-syn expression, and specifically in the AAV-hα-syn-based animal model of PD. Our results evidence a functional hippocampal impairment in the early stages of PD preceding cognitive deficits.

According to our FASS-LTP experiments, cLTP impairment at both time points is associated with an increased basal expression of GluA1-AMPARs in the postsynaptic membrane. Indeed, α-syn has previously been shown to inhibit LTP by enhancing basal synaptic transmission through the overactivation of NMDAR (Diógenes et al., 2012), which is in line with our results as cLTP impairment appears concomitant to the onset of hα-syn expression in the hippocampus. According to Diógenes and coworkers, the enhanced NMDAR-mediated signaling under basal conditions led to a change in AMPAR subunit composition with increased contribution of GluA2-lacking AMPAR and increased GluA1 membrane expression, which resulted in LTP saturation (Diógenes et al., 2012). As suggested by these authors, an increased expression of GluA2-lacking AMPARs induced by α-syn could compromise AMPAR remodeling necessary for synaptic reinforcement, since a proper balance of GluA1 and GluA2 subunits is critical for LTP induction and maintenance. Moreover, the onset of cLTP impairment is also concomitant to the loss of TH^+ cells in the VTA, and thus, decreased levels of DA may also contribute to LTP impairment, as previously described in toxin-based as well as α-syn-based animal models of parkinsonism (Bonito-Oliva et al., 2014; Costa et al., 2012; Zhu et al., 2011).

It has been reported that deficits in learning and memory observed in α-syn transgenic mice are accompanied by alterations in both pre- and postsynaptic compartments (Lim et al., 2011; Masliah et al., 2011), suggesting that the toxicity of α-syn may be mediated by disturbances in synaptic transmission (Garcia-Reitböck et al., 2010; Larsen et al., 2006; Nemani et al., 2010). In our animal model, hα-syn-induced impaired cLTP preceded cognitive dysfunction for weeks, suggesting that sustained impaired synaptic transmission may be necessary for the development of cognitive deficits. Cardinal motor features in PD are estimated to appear with a 30–60% loss of dopaminergic neurons in the SNpc and a 70–80% loss of dopaminergic terminals in the striatum (Cheng et al., 2010). Similarly, cognitive deficits may also require a significant degeneration of dopaminergic neurons in the VTA and loss of synaptic terminals in target limbic areas. While we observe a 40% TH^+ cell loss in the VTA since 1 week p.i., concomitant to the cLTP failure, we do not appreciate any TH^+ fibers loss in the hippocampus until 16 weeks p.i. Since dopaminergic innervation to the hippocampus is scarce, subtle changes in TH^+ innervation may not be appreciated by the immunofluorescent approach, and thus, a more precise quantitative analysis would be desirable. Alternatively, these discrepancies may suggest that other neurotransmitter systems are also involved in hippocampal dysfunction. In this sense, VTA glutamatergic neurons may be of special interest as they also overexpress hα-syn and $vGlut2^+$ terminals abundantly colocalize with hα-syn in the hippocampus in our animal model. Moreover, VTA glutamatergic neurons have been described to modulate hippocampal LTP in the CA1 region (Adeniyi et al., 2020) and participate in memory processes (Han et al., 2020; Nordenankar et al., 2015).

2.2. Dopaminergic drugs functionally recover synaptic plasticity in the hippocampus

Our results show that both dopaminergic drugs, PPX and L-DOPA, restored cLTP in hippocampal synaptosomes. On the one hand, PPX restored cLTP in AAV-hα-syn rats at both time points, 1 and 4 weeks p.i. PPX is a dopaminergic agonist targeting the D2-like receptor family with higher selectivity for D3Rs (Beaulieu & Gainetdinov, 2011). Few studies have previously characterized the effect of this drug in LTP. A single *in vivo* dose of PPX in MPTP-lesioned mice restored LTP in the PFC, a different region of the limbic system (Okano et al., 2019), while bath application of PPX had no effect on the impaired LTP in the DG of 6-OHDA-lesioned mice (Bonito-Oliva et al., 2014). This is the first study, as far as we know, to assess the effect of PPX on hippocampal LTP in an α-syn-based animal model.

Despite the possible beneficial effects of PPX in AAV-hα-syn rats, this drug may be detrimental in the absence of underlying pathology, as we observed a decrease in cLTP in AAV-

EVV control animals. Previous studies have reported enhanced hippocampal LTP in healthy animals after *in vitro* incubation with PPX (Castro-Hernández et al., 2017) as well as 7-OH-DPAT, a D3R agonist (Swant & Wagner, 2006). The authors suggested that the enhancement could be mediated by a decrease in GABAergic interneuron activity and, thus, stimulation of glutamatergic activity (Hammad & Wagner, 2006; Swant et al., 2008). However, in line with our results, *in vivo* chronic PPX treatment in healthy animals resulted in decreased hippocampal LTP together with decreased spine density and glutamate release (Schepisi et al., 2016). Moreover, those animals developed a compulsive behavior, which is in line with the previously described reinforcing properties of PPX in healthy as well as in PD animal models (Engeln et al., 2013; Riddle et al., 2012). Furthermore, long-term treatment of dopaminergic agonists, particularly D3R-preferring agonists, in PD patients has been associated with the development of non-motor side effects such as ICD's and hallucinations as well as mild cognitive deficits (Fénelon et al., 2000; Voon et al., 2017). Thus, even though PPX may be beneficial to treat the motor signs and restore LTP in the hippocampus at least in short-term, the long-term therapy in PD patients may lead to maladaptive changes in synaptic transmission and the onset of non-motor side effects, possibly through the overstimulation of D3Rs (Black et al., 2002; Voon et al., 2011b). These receptors have more than 100-fold higher affinity for DA than D1Rs and D2Rs (P. Yang et al., 2020) and are abundant in the limbic system involved in memory, emotions, and behavior processing (Prieto, 2017).

On the other hand, L-DOPA was also able to restore cLTP in AAV-hα-syn animals without any detrimental effects in control animals, as previously reported in several electrophysiological studies performed in the CA1 region of the hippocampus of 6-OHDA-lesioned rats and hα-syn 1-120 transgenic mice (Costa et al., 2012), as well as in the DG of 6-OHDA-lesioned rats (Jalali et al., 2020) and mice (Bonito-Oliva et al., 2014). Interestingly, our results show that recovery of cLTP was statistically more significant with L-DOPA than PPX. L-DOPA is a DA precursor that after its conversion into DA activates both D1Rs and D2Rs (Trugman et al., 1991). Since the enhancement of DA in hippocampal LTP is thought to be mediated by D1-like receptors, while the role of D2-like receptors remains controversial (Jay, 2003; J. Lisman et al., 2011), the direct activation of D1-like receptors by L-DOPA may account for the difference observed between the two drugs. Moreover, in PD patients, L-DOPA also provides better control of motor signs than dopaminergic agonists (Group, 2014). By contrast, unlike PPX, L-DOPA showed differences between time points, restoring cLTP at 4 weeks p.i. but not at 1 week p.i. Agonists directly stimulate their corresponding receptors triggering a post-synaptic response while L-DOPA needs to be metabolized in the presynaptic compartment by the enzyme AADC into DA and then released to the synaptic cleft where it binds and activates the receptors (Aldred & Nutt, 2010). Impaired motor and cognitive function observed at 4 weeks p.i. may reflect a decrease in brain DA content, which could be

compensated by an exogenous administration of DA. However, at 1 week p.i., with no behavioral impairments, the onset of the pathological hα-syn in the presynaptic compartment may impair SV dynamics without decreasing DA content, as previously suggested (Garcia-Reitböck et al., 2010; Janezic et al., 2013; Nemani et al., 2010). Thus, exogenous administration of DA may not be successful in restoring synaptic function. Our proteomics results, which will be discussed in the following section, support the early impairment in intracellular trafficking and SV dynamics.

Finally, our results suggest that the recovery of cLTP may be associated with a rearrangement in basal postsynaptic AMPAR levels. D1-like and D2-like receptor agonists have previously been described to increase and decrease, respectively, the phosphorylation of GluA1 AMPAR subunits (Håkansson et al., 2006; Mangiavacchi & Wolf, 2004), essential for increasing AMPAR channel conductance and targeting them to the PSD (Kristensen et al., 2011; W. Lu et al., 2010). Additionally, Bagetta and coworkers reported that chronic PPX treatment was able to restore the enhanced synaptic transmission in the striatal SPNs of 6-OHDA-lesioned rats, which showed increased amplitude and frequency of EPSCs, decreased NMDAR/AMPAR ratio, and increased contribution of GluA2-lacking AMPARs (Bagetta et al., 2012).

3. Hα-syn overexpression induces proteostatic alterations in hippocampal synapses

In the hippocampus of PD patients, a recent proteomics study found deregulation of several proteins involved in synaptic function such as the structure of the synapse, ER, and mitochondrial function (Villar-Conde et al., 2021). Thus, to further characterize the synaptic alteration taking place in the hippocampus of our AAV-hα-syn animals, we performed a proteomic analysis in hippocampal synaptosomes. We were able to identify differentially expressed proteins in the AAV-hα-syn animals compared to the control AAV-EVV rats. Deregulated proteins were observed at all time points analyzed (1, 2, 4, and 16 weeks p.i.), although the number of proteins was particularly higher at 1 week p.i. and lower at 4 weeks p.i. Moreover, the bioinformatic analysis helped us elucidate the significantly enriched biological processes at 1, 2, and 16 weeks p.i. However, at 4 weeks p.i., the identified deregulated proteins did not share a common biological pathway that was significantly enriched. Individual proteins at 4 weeks p.i. participate in cellular processes such as synapse organization (CADM1), cation homeostasis (SLC25A23), lysosomal trafficking (Pip4p1), and protein folding (UGGT1). Despite the lack of significant quantitative changes in proteins involved in specific cellular processes, the synaptic function was impaired at

4 weeks p.i., with impaired cLTP at hippocampal synaptosomes together with a significant increase in hα-syn expression in this nucleus, as well as a deficient hippocampal-dependent cognitive performance.

Among all identified proteins, only a few of them overlapped between different time points. INPP4A, which was downregulated at 1 week p.i. and upregulated at 2 weeks p.i., is a negative modulator of the PI3K/AKT signaling pathway involved in multiple cellular functions. In neurons, INPP4A has been described to participate in NMDAR trafficking at the PSD, downregulating its surface expression (Sasaki et al., 2010). The protein UFSP2, downregulated at 1 week p.i. and upregulated at 4 weeks p.i. is also involved in receptor trafficking, particularly promoting the delivery of GPCRs from the ER to the plasma membrane (Chen et al., 2014). Another protein deregulated at both 1 and 4 weeks p.i. is TIMM21, which is upregulated and downregulated respectively. TIMM21 is a mitochondrial protein involved in the sorting and transfer of preproteins within the inner membrane (Srivastava et al., 2020). Among the proteins deregulated at 1 and 16 weeks p.i., MBP, which is downregulated at both time points p.i., is a major component of myelin and has been shown to interact with neuronal membranes interrupting their integrity and function (J. Zhang et al., 2014). Finally, ANXA7 was upregulated at both time points, and in neurons, it has been shown to participate in SNAP25-mediated presynaptic glutamate release and SNAP23-mediated postsynaptic NMDAR trafficking (Li et al., 2018). Thus, targeted therapies aimed to reduce ANXA7 may help recover a physiological balance in pre- and postsynaptic terminals restoring synaptic function and alleviating motor and non-motor signs.

Of note, several of the deregulated proteins across all time points are experimentally described interactors of human or rat α-syn (hα-syn: APP, CNP, INA, BCAS1, FBXO2, SNCB, MAP2, VPS52, MYO5A, COX5A, IARS, and MARK2; rat α-syn: MAP2K1 and BASP1) and will be discussed in the following section due to their relevant roles in the synapse.

3.1. The onset of hα-syn expression in hippocampal synapses is related to altered intracellular trafficking and impaired SV cycle at 1 and 2 weeks p.i.

The onset of hα-syn expression in the hilus and CA1 region at 1 week p.i. and in the granular cell layer of the DG at 2 weeks p.i. is associated with the emergence of deregulated proteins in the synaptic terminals. Several of the deregulated proteins participate in the assembly and organization of the synapse, particularly in the organization of the postsynaptic compartment

(1 week p.i.: INA, CNP, APP, OPALIN, MAP1K1; 2 weeks p.i.: RHEB, PPP1R9A, NEFH, LRP1), a biological process that is statistically enriched at 2 weeks p.i.

At these earliest time points, 1 and 2 weeks p.i., one of the cellular processes that were most affected by hα-syn expression is cytosolic transport (1 week p.i.: RAB6B, MAP2, MAP2K1; 2 weeks p.i.: VPS52, RDX) and its regulation (1 week p.i.: LCP1, MAP2, SLC4A8, MAP2K1; 2 weeks p.i.: VPS33B, MYO5A, PRRT2, SNAP29, NEFH, TM9SF4, RDX, TARDBP). Intracellular traffic is regulated by Rab GTPases, which control cargo mobility and tethering at target sites. Among this family, the brain-specific RAB6B, up-regulated in our synaptosomes at 1 week p.i., is a highly dynamic protein frequently transported in axons, delivering presynaptic cargo proteins to terminals (Nyitrai et al., 2020). The transport of cargos along the cytoskeleton is driven by motor proteins, such as the myosin family (Kneussel & Wagner, 2013). At 2 weeks p.i. we find a downregulation of two myosins in hippocampal synaptosomes, MYO5A and MYH14. MYO5A is a class V myosin, involved in presynaptic neuropeptide exocytosis as well as in postsynaptic plasticity (Rudolf et al., 2011). In the postsynaptic compartment, MYO5A participates in the tethering of the ER, a major intracellular Ca^{2+} store, within the spine head, crucial for proper Ca^{2+} signaling (Rudolf et al., 2011). Moreover, MYO5A plays also a prominent role in the activity-dependent, but not constitutive delivery of AMPARs to the spine head (Correia et al., 2008). MYH14 is a class II non-muscle myosin, which has been described to participate also in the trafficking of NMDARs and AMPARs into the PSD (Bu et al., 2015; Rubio et al., 2011).

The integrity of the cytoskeleton is crucial for neuronal maintenance and function and depends on a critical regulation of its components: actin filaments, microtubules, and intermediate filaments. The microtubule cytoskeleton is particularly altered at 1 week p.i. in our hippocampal synaptosomes (MBP, CNP, MAP2, APP, KLC2, RHOG, MAP2K1, NEFM, STMN1, PTPRG) and plays an important role in the transport of cargos along the axon as well as the dendrites (Kapitein & Hoogenraad, 2015). Indeed, KLC2, which is upregulated in our synaptosomes, is one of the adaptor proteins of the kinesin family involved in intracellular transport along the microtubule cytoskeleton of cargos including mitochondria and SV precursors containing presynaptic proteins in axons, as well as postsynaptic neurotransmitter receptors and messenger ribonucleoprotein complexes containing mRNAs in dendrites (Hirokawa et al., 2009). Taken together, these data strongly suggest the existence of disorganization of the axonal cytoskeleton that could impair the normal axonal transport, leading to the accumulation of autophagosomes/lysosomes, which could probably be mediated by hα-syn accumulation and the consequent proteostatic imbalance.

Recent evidence suggests that microtubules not only participate in transport along the axon or dendrites but also enter the synapse and regulate some synaptic functions such as

neurotransmitter release and synaptic plasticity (Waites et al., 2021). STMN1, up-regulated at 1 week p.i., is a member of the stathmin family involved in microtubule destabilization, which is critical for LTP induction in the hippocampus (Uchida & Shumyatsky, 2015). Furthermore, MAP2, a neuron-specific cytoskeletal protein, is found enriched in dendritic shafts and its translocation into the spines has recently been described to be critical for LTP induction, and the corresponding AMPAR surface delivery and spine enlargement (Y. Kim et al., 2020). According to these results, the upregulation of MAP2 observed in synaptosomes, may be related to the increased basal expression of GluA1-AMPARs. Of note, translocation of MAP2 into the spine depended not only on NMDAR activation but also on Ras-MAPK signaling (Y. Kim et al., 2020). Interestingly, we also find increased levels of MAP2K1 (also known as MEK1), a kinase that activates MAPKs. The activation of MAPK signaling is critical, among other cellular processes, for the maintenance of LTP through the activation of downstream enzymes and transcription factors that promote *de novo* mRNA and protein synthesis (Baltaci et al., 2019; Thomas & Huganir, 2004). Specifically, activation of MAP2K1 was described to be essential to trigger local protein synthesis after LTP induction (Kelleher III et al., 2004), similar to other proteins deregulated at 1 week p.i. (60S ribosomal protein L36, EIF3B, ATXN21, PAIP1).

Interestingly, APP, downregulated at 1 week p.i., codes for the precursor protein of amyloid β, the main constituents of senile plaques, which are one of the hallmarks of Alzheimer's disease. Although its physiological role is not completely understood, APP was shown to participate in Ca^{2+} homeostasis, neurotransmitter release, and mitochondrial function. APP is abundantly expressed within the active zone of the presynaptic membrane where it interacts with mediators rather than central players of the SV-machinery. Moreover, loss of APP causes an age-dependent phenotype with substantial changes of the active zone proteome without severe physiological impairments in younger mice and reduced total spine density as well as dysregulated bioenergetics along with impairments in learning and memory in the elderly (Weingarten et al., 2017). Thus, since the spread of concomitant β-amyloid and Lewy pathology is associated with cognitive decline in more advanced stages of PD (Irwin et al., 2013; C. Smith et al., 2019), therapies targeting early alterations in APP may potentially prevent the development of MCI and progression to dementia in this disease.

Apart from the microtubules, the actin cytoskeleton is particularly altered at 2 weeks p.i. with deregulated proteins participating in actin-filament based processes (VPS33B, MYO5A, MYH14, CSRP1, TPM1, PDE4D, PRRT2, SNAP29, PPP1R9A, NEFH, LRP1, RDX, SCN1B) and movement (MYO5A, MYH14, TPM1, PDE4D, SCN1B). The actin cytoskeleton plays a major role in synapse organization, regulation of SV pools, neurotransmitter release, transport, and synaptic

plasticity (Cingolani & Goda, 2008; Nelson et al., 2013). Indeed, following LTP induction, spines become larger and increase their actin contents, while after LTD induction spines shrink and depolymerize actin filaments (Hlushchenko et al., 2016). According to the prominent role of actin dynamics in the SV cycle and the trafficking of neurotransmitter receptors at the synapse, the biological processes of signal release (VPS33B, MYO5A, RHEB, PRRT2, SNAP29, PPP1R9A, LRP1, IQSEC2, TARDBP) and protein localization to the membrane (MYO5A, LRP1, IQSEC2, SRP54, TM9SF4, BCS1L, RDX) are significantly deregulated at 2 weeks p.i. Regarding signal release processes, PRRT2 and SNAP29, two downregulated proteins at 2 weeks p.i., are of special interest. Recently, PRRT2 was described to participate in actin cytoskeleton dynamics at the synapse (Savino et al., 2020), further supporting the role of actin dynamics in the SV cycle. Loss of PRRT2 function was associated with impaired synaptic transmission due to a decrease in the density of excitatory synapses as well as a decrease in neurotransmitter release probability (Valente et al., 2016). On the other hand, SNAP29 was shown to act as a negative modulator of neurotransmitter release by decreasing the turnover of SVs (Pan et al., 2005). The downregulation of these two proteins at 2 weeks p.i. suggests that hα-syn impairs the SV cycle at different steps including the exocytosis process as well as the turnover of SVs, thus, probably impairing neurotransmission.

Endosome trafficking within the synapse is crucial for the proper recycling of SVs as well as for the correct delivery and retrieval of membrane proteins such as neurotransmitter receptors. LRP1, one of the most downregulated proteins at 2 weeks p.i., is a member of the lipoprotein receptor family that acts as a cargo receptor at the synaptic membrane for the subsequent endocytosis of its ligands including APP and TAU (Herz & Strickland, 2001; Rauch et al., 2020) and probably α-syn (Sui et al., 2014). Among its many functions, we highlight that LRP1 deletion was associated with decreased LTP in the hippocampus and impaired motor function and memory performance (Liu et al., 2010). In line with this evidence, LRP1 has been associated with decreased levels in *post-mortem* brain studies of patients with several neurodegenerative disorders such as amnesic MCI (Sultana et al., 2010) and Alzheimer's disease (Shinohara et al., 2014). Despite the role of LRP1 in the synaptic processing of key proteins associated with neurodegenerative processes, particularly with amyloid β processing in Alzheimer's Disease, only a few studies have assessed LRP1 in PD. One study found increased levels of LRP1 in the SN of incidental PD and PD patients (Wilhelmus et al., 2011), and another study reported increased levels of LRP1 in the CSF of PD patients (M. Shi et al., 2015). However, this is the first study to find altered LRP1 in the hippocampus of an animal model of PD, and thus, we suggest that LRP1 may as well be an interesting target for early synaptic-based therapies.

One of the major regulators of endosome trafficking is the ARF protein signaling pathway, which is also altered in hippocampal synaptosomes at 2 weeks p.i. (PSD, RHEB, RALGAPA1, PSD3, IQSEC2). Among these proteins, IQSEC2, an activator of ARF6, is of special interest. IQSEC2, through the activation of ARF6, was shown to be crucial for surface AMPAR removal and maintenance of LTD (Brown et al., 2016). Moreover, the same study described that IQSEC2, independently from ARF6 activity, increased AMPAR-mediated responses by rising GluA2-containing AMPAR expression, without acting on NMDARs and the consequent insertion of GluA1-containing AMPAR into the synapse. However, although it may regulate basal excitatory transmission, IQSEC2 did not interfere with LTP expression (Brown et al., 2016).

Additionally, endosomes can be directed towards the degradation of their cargo proteins through the lysosomal pathway. The biological process of lysosomal transport is impaired at 2 weeks p.i. as well (VPS33B, CSRP1, TPM1, VPS52, NEFH, LRP1). Of note, we observed a downregulation of VPS52, a protein of the Golgi-associated retrograde protein complex described to regulate protein sorting to lysosomes (Homma & Fukuda, 2021; Pérez-Victoria et al., 2008). Interestingly, another protein involved in retrograde transport of cargos to the trans-Golgi network is VPS35, of which loss-of-function mutations have been associated with inherited autosomal dominant PD cases. Moreover, another PD-related protein, LRRK2, was shown to interact with VPS52 promoting efficient vesicle trafficking (Beilina et al., 2020).

The aforementioned cytoskeleton dynamics, SV trafficking, and protein sorting in the synapse require a great amount of energy. In line with this, at 1 week p.i., several of the deregulated proteins are involved in ATP biosynthesis (INNP4A, MTMR9, APP, ATP5MF, MAP2K1). Among the deregulated proteins, ATP5MF encoding one of the subunits of the mitochondrial ATP synthase, which is downregulated in our synaptosomes, is of special interest. The unfolded monomeric form of α-syn was described to interact with the ATP synthase to improve the efficiency of ATP production (Ludtmann et al., 2016). By contrast, the oligomeric α-syn was shown to induce oxidative modifications in the ATP synthase affecting mitochondrial function and inducing cell death (Ludtmann et al., 2018). Thus, the presence of hα-syn in hippocampal synaptic terminals may interfere with normal mitochondrial function and decrease ATP production, although additional experiments should be conducted to confirm this. To further support the relationship between hα-syn expression and altered mitochondrial function, several other mitochondrial proteins were also found deregulated at 1 and 2 weeks p.i. At 1 week p.i., deregulated proteins included TIMM21, involved in sorting and transfer of preproteins in mitochondria, the ribosomal protein MRPS30 involved in mitochondrial translation, and the CLIC4 chloride channel involved in the regulation of the mitochondrial membrane potential.

Additionally, at 2 weeks p.i., we found a downregulation of COX5A and an upregulation of BCS1L, components of complex III and IV of the mitochondrial respiratory chain, respectively. In a recent study, COX5A was found downregulated in the dopaminergic neurons of a novel animal model of parkinsonism based on the genetic deletion of an essential subunit of the mitochondrial complex I catalytic core specifically in these neurons (González-Rodríguez et al., 2021). Disruption of the mitochondrial function in dopaminergic neurons was associated with decreased striatal TH levels and an almost complete absence of evoked DA release, highlighting the importance of mitochondria in synaptic function.

Finally, other biological processes significantly enriched at the earliest time points following hα-syn overexpression are related to water homeostasis (ANXA7, KRT1, CLIC4, MAP2K1, STMN1) and SN development (INA, CNP, MBP) at 1 week p.i., and the regulation of vascular associated smooth muscle cell migration (MYO5A, TPM1, PDE4D, PRRT2, PPP1R9A, SRP54, LRP1, TM9SF4, IQSEC2, RDX, BCS1L, TARDBP) at 2 weeks p.i. However, most of these proteins are related to the cytoskeleton and participate in other cellular functions already discussed above.

3.2. Accumulation of hα-syn in hippocampal synapses leads to ion dyshomeostasis and impaired intracellular signaling at 16 weeks p.i.

Prolonged hα-syn accumulation in the hippocampus leads to a deregulation of neuronal homeostatic processes such as membrane potential and intracellular Ca^{2+} levels, as well as altered receptor-activated molecular signaling pathways. On the one hand, since neurons are excitable cells with polarized plasma membranes, extra- and intracellular levels of different ions need to be tightly regulated. At 16 weeks p.i. there is a significant alteration particularly in cation homeostatic processes (ANXA7, MBP, ATP6AP2, KCNA1, KRT10, GRIK2, CALM3). In neurons, Ca^{2+} acts as a second messenger in multiple intracellular signaling pathways involved in morphology, synapse formation, excitability, neurotransmitter release, and synaptic plasticity, among others (Berridge, 1998; Mateos-Aparicio & Rodríguez-Moreno, 2020; Südhof, 2012a). One of the adaptor proteins for downstream Ca^{2+} signaling is calmodulin, which is encoded by three different genes (CALM1-3) that give rise to the same protein (Berchtold et al., 1993). Interestingly, CALM3 is downregulated in our hippocampal synaptosomes at 16 weeks p.i. Calmodulin is a Ca^{2+}-binding protein that orchestrates the activation of a family of Ca^{2+}-regulated proteins involved in Ca^{2+} homeostasis as well as Ca^{2+}-signaling pathways. It regulates several types of Ca^{2+} channels that provide Ca^{2+} influx into the cytoplasm including voltage-gated Ca^{2+} channels and NMDARs (Villalobo et al., 2018). Moreover, calmodulin activates several enzymes involved in synaptic plasticity processes such as CaMKII and calcineurin, which are essential for LTP and LTD, respectively, as well as adenylyl

cyclases, which increase cAMP levels and activate the PKA signal transduction pathway (Xia & Storm, 2005). Additionally, calmodulin may regulate neuronal excitability and neurotransmitter release by interacting with small-conductance Ca^{2+}-activated K^+ channels (Villalobo et al., 2018). Interestingly, several of these calmodulin binding proteins have been related to neurodegenerative disorders, including Alzheimer's disease (O'Day et al., 2015) and PD (Bohush et al., 2021). Thus, the decreased expression of CALM3 suggests that prolonged accumulation of hα-syn within the synapse may lead to overall synaptic dysfunction by impairing not only presynaptic SV release but also impairing postsynaptic response. Importantly, recovering the balance among downstream Ca^{2+} effector proteins may be beneficial for overall synaptic function and neuronal homeostasis, and targeting calmodulin, which orchestrates many of these Ca^{2+}-related signaling events, may represent a potential therapeutic approach.

Other cations such as Na^+ and K^+ play a major role in the regulation of membrane potential and the initiation and conduction of action potentials throughout the axons (Purves et al., 2004), ultimately regulating neurotransmitter release at the synaptic level (Meir et al., 1999). Interestingly, at 16 weeks p.i., some of the deregulated proteins participate in the regulation of membrane potential (ANXA7, KCNA1, DDX39B, AFDN, GRIK2, CALM3). Among these proteins, KCNA1 encoding a voltage-gated K^+ channel of the A subfamily, which has been related to dystonia, is of special interest. One study showed that several dystonia-associated genes, including KCNA1, converge in similar intracellular pathways and contribute to the pathogenesis of the disease by dysregulating synaptic functions (Mencacci et al., 2020). Moreover, the authors also showed that these dystonia-associated genes were related to the heritability of several neuropsychiatric disorders, including major depressive disorder and obsessive-compulsive disorder. These findings suggest that maybe the non-motor signs of PD are not simply a reaction to the disability derived from the disease itself, but rather, the underlying molecular pathophysiology of PD, including decreased KCNA1 expression and other proteins, which could increase the risk of developing non-motor symptoms in patients.

Furthermore, another biological process significantly deregulated at 16 weeks p.i., included the cell surface receptor-activated signaling pathways (ATP6AP2, MARK2, AFDN, GRIK2), particularly those mediated by Gi-coupled GPCRs (PRKACB, HEBP1, ATP6AP2, GRM3, RGS12, PLD3, ACTR10, AFDN, GRIK2, CALM3). Among them, two different glutamate receptors, GRIK2 and GRM3, are downregulated. GRIK2 codes for the GluK2 subunit of the kainate receptors, which is essential for membrane delivery of the receptors. In general, kainate receptors participate in the regulation of presynaptic neurotransmitter release as well as postsynaptic excitatory neurotransmission, controlling both short and longer-term plasticity (Evans et al., 2019). GRM3

codes for the mGluR3 that belongs to the group II mGluRs together with mGluR2, which are coupled to Gi/o, thus inhibiting adenylyl cyclase and PKA activity. mGluR3 is predominantly expressed presynaptically, but it can also be expressed postsynaptically. Although the physiological role remains largely unknown, mGluR3 was shown to be required for LTD in the DG of the hippocampus, while it reduced LTP probably through reducing presynaptic neurotransmitter release (Pöschel et al., 2005). Interestingly, group II mGluRs agonists or positive allosteric modulators have been suggested to contribute to PD treatment due to their presynaptic reduction of glutamate transmission, which is overstimulated in PD models (Zhu Zhang et al., 2019). Moreover, a group II mGluRs agonist was recently shown to alleviate dyskinesia and psychosis-like behavior while simultaneously enhancing L-DOPA therapeutic benefit in 6-OHDA rats and MPTP-marmosets (Frouni et al., 2019).

Apart from membrane receptors, downstream intracellular proteins were also deregulated in hippocampal synaptosomes at 16 weeks p.i. Indeed, the most downregulated protein at this time point was RGS12, a member of the 'regulators of G protein signaling' protein superfamily involved in the inactivation of the Gα subunit (Woodard et al., 2015). Another downregulated major intracellular player is PRKACB, the catalytic subunit β of PKA. Within synapses, PKA is found expressed both pre- and postsynaptically, where it participates in the regulation of SV pools and the maintenance of long-term synaptic plasticity, respectively. In the presynaptic terminal, activation of PKA enhances neurotransmitter release by promoting the formation of the SNARE complex and increasing the size of the readily releasable pool (Baba et al., 2005). In the postsynaptic compartment, PKA is critical for the late phase of LTP, by enhancing the transcription of genes related to synaptic plasticity (Baltaci et al., 2019; Waltereit & Weller, 2003).

Interestingly, local protein synthesis in hippocampal synapses is also deregulated at 16 weeks p.i. The translation initiation factor EIF2S3 is upregulated and several proteins involved in the metabolism of tRNAs (MRI1, IARS, EPRS, ELP1) are also deregulated. MRI1 codes for methylthioribose-1-phosphate isomerase involved in methionine biosynthesis, while IARS and EPRS code for isoleucyl-tRNA synthetase and glutamyl-prolyl-tRNA synthetase, respectively, which catalyze the binding of tRNAs to their corresponding amino acid. These results further support the impairment in the long-term maintenance of synaptic plasticity, as local protein translation is triggered after LTP induction and is critical to sustaining long-term changes (Baltaci et al., 2019; Holt et al., 2019).

4. Long-term hα-syn expression leads to decreased hippocampal glucose metabolism despite dopaminergic treatment

Glucose metabolism studies using [^{18}F]-FDG PET, which is thought to be a marker of synaptic activity, have been successfully carried out in PD patients (Ma & Eidelberg, 2007; Matthews et al., 2018), identifying specific patterns of deficit in PD brains (Buchert et al., 2019). Specifically, several studies in our research group have found hippocampal hypometabolism in association with cognitive deficits in PD patients (Gasca-Salas et al., 2016) and hypometabolism in the entorhinal cortex, the input and output structure of the hippocampal circuit, related to ICDs in PD patients (Navalpotro-Gomez et al., 2019). Thus, we performed a [^{18}F]-FDG PET study in an animal model of parkinsonism in an attempt to understand the alterations in the brain metabolism associated with dopaminergic depletion and chronic dopaminergic treatment. Our [^{18}F]-FDG PET study showed reduced glucose metabolism in the hippocampus of rats overexpressing mutated A53T hα-syn with an established dopaminergic degeneration (50% striatal DAT denervation) and after chronic treatment with PPX. Recent studies using α-syn animal models have shown similar findings. In an AAV-based rat model with a different serotype (AAV2/7-A53T-hα-syn), a decreased hippocampal glucose metabolism was found at 9 weeks p.i., corresponding to a near-complete and stable dopaminergic degeneration (Devrome et al., 2019; Mondal et al., 2021). Similarly, hippocampal [^{18}F]-FDG uptake was also significantly reduced in A53T transgenic mice at 9 months of age, concomitant to the onset of dopaminergic degeneration.

However, differentially from these previous studies, our [^{18}F]-FDG PET study was carried out after chronic PPX treatment, and surprisingly, loss of hippocampal glucose metabolic function was observed despite the dopamine replacement therapy. In contrast to our results, in advanced PD patients, significant metabolic changes were observed after 6 months of apomorphine treatment, another dopaminergic agonist used as standard therapy in clinical practice (Auffret et al., 2017). In this study, the authors observed an overall increase in [^{18}F]-FDG uptake in the hippocampus among other structures, alongside beneficial effects on the motor as well as non-motor symptoms such as apathy and cognition. However, despite the dopaminergic therapy, multiple [^{18}F]-FDG PET and structural MRI studies have previously established an association of hippocampal hypometabolism and atrophy with memory impairment and progression into dementia in PD patients (Filippi et al., 2020; Gasca-Salas et al., 2016; González-Redondo et al., 2014; Jokinen et al., 2010; Kandiah et al., 2014; Mak et al., 2015; Martín-Bastida et al., 2021; Pereira et al., 2013). The impaired hippocampal cLTP we observe since 1 week p.i. and the tendency towards decreased cognitive performance in the hippocampal-dependent memory task at 4 weeks p.i. support a progressive cognitive dysfunction in our AAV-hα-syn animals. Thus, the

hippocampal hypometabolism observed in our study supports the progressive development of cognitive deficits associated with parkinsonism. Moreover, since hypometabolism is observed despite the chronic dopaminergic therapy, the cognitive decline may be independent of DA, suggesting the involvement of other neurotransmitter systems. As suggested by our histological characterization, glutamatergic and GABAergic neurons from the VTA may participate in this hippocampal dysfunction. Alternatively, other neurotransmitter systems such as the cholinergic system may contribute to the development of cognitive deficits. The septohippocampal cholinergic pathways, together with the dopaminergic system, were shown to regulate certain aspects of memory in rats, such as working memory (H. Hall et al., 2013; Wisman et al., 2008). Moreover, loss of acetylcholine in the hippocampus has been described in PDD patients (Bohnen et al., 2003; H. Hall et al., 2014) as well as in patients with DLB (Tiraboschi et al., 2000). Overall, our [^{18}F]-FDG PET results suggest the development of hippocampal dysfunction in the treated AAV-hα-syn animal model, which is probably, at least in part, independent from the dopaminergic degeneration.

In summary, combined evidence from the present work shows that hippocampal dysfunction participates in PD pathogenesis since the earliest stages of the disease, with associated alterations in the dopaminergic as well as glutamatergic mesolimbic systems from the VTA to the hippocampus. This study demonstrates that overexpression of hα-syn can lead to hippocampal synaptic plasticity alterations, as observed by reduced cLTP, which preceded the onset of memory impairments, suggesting that cognitive deficits are a consequence of prolonged synaptic plasticity dysfunction. Furthermore, the impaired synaptic function was initially associated with altered neurotransmitter release and basal hyperexcitability, with deregulated proteins involved in major biological processes such as intracellular transport, SV dynamics, and protein sorting to the membrane. However, prolonged hα-syn accumulation led to deregulation in crucial cellular processes such as ion homeostasis, particularly Ca^{2+}, and impaired intracellular signaling. In addition, dopaminergic drugs were able to restore synaptic function, although with some differences. The dopaminergic agonist PPX, despite being less efficient, restored cLTP at all time points. By contrast, the DA precursor L-DOPA efficiently rescued LTP but only at 4 weeks p.i. when no alterations in SV dynamics were observed. Since both dopaminergic therapies are related to the long-term development of side effects, novel therapies aimed to restore specific synaptic functions may help with motor and non-motor signs of PD.

Conclusions

1. Bilateral inoculation of the AAV-hα-syn into the SNpc induces a progressive hα-syn expression in the SNpc and VTA, causing a mild dopaminergic neuronal loss firstly in the VTA and later in the SNpc before the onset of motor manifestations.

2. Hα-syn overexpression is observed in the dopaminergic and glutamatergic neurons of the VTA, increasing progressively and spreading to their axonal terminals in the hippocampus. The presence of hα-syn is observed in the dopaminergic, glutamatergic, and GABAergic fibers of the hippocampus mainly in the DG and CA1 region, which are the main input and output areas of the intrinsic hippocampal circuit. Thus, we demonstrate that the accumulation of hα-syn in DA and non-DA VTA neurons, which could differentially affect the synaptic machinery predominating its impact in the excitatory inputs, accounts for an alteration of hippocampal function.

3. The hippocampal changes observed in this model cause a tendency to impairment in the hippocampal-dependent spatial memory performance, concomitant to the onset of motor deficits.

4. Hα-syn impairs synaptic plasticity in the hippocampus since early stages by increasing basal excitability, which may impair further potentiation of the synaptic transmission, leading to defective plasticity and hippocampal-dependent cognitive deficits.

5. Abnormal synaptic plasticity at the earliest stages may be a consequence of the deregulation of microtubule- and actin-based intracellular transport crucial for synaptic morphology, plasticity, and communication with the neuronal soma, as well as of the defective SV trafficking crucial for the release of neurotransmitters from the presynaptic terminal, ultimately regulating synaptic transmission and plasticity.

6. The dopaminergic agonist PPX, although partially effective in rescuing synaptic plasticity, may eventually lead to maladaptive synaptic changes in the limbic system associated with the onset of non-motor side effects.

7. The dopamine precursor L-DOPA rescues synaptic plasticity probably by increasing DA levels, however, it may not be efficient to restore synaptic function at the earliest stages as it depends on its synaptic conversion into DA and proper neurotransmitter release, the latter deregulated concomitant to hα-syn overexpression.

8. Sustained pathology along the mesolimbic pathway leads to a homeostatic imbalance in hippocampal synapses, impairing crucial functions such as the regulation of the membrane potential, intracellular signaling, and protein synthesis, exacerbating the proteotoxic stress and contributing to the maintenance of aberrant synaptic activity, probably causative of the emergence of neurocognitive deficits in PD.

9. *In vivo* decreased glucose metabolism in the anterodorsal hippocampus despite chronic dopaminergic treatment with PPX further supports the impairment of the synaptic function in the hippocampus and its role in the development of cognitive and behavioral signs.

10. This doctoral thesis demonstrates the working hypothesis that synaptic dysfunction in the hippocampus is an early event triggered by hα-syn overexpression, which may ultimately lead to cognitive and behavioral deficits associated with parkinsonism. Moreover, the present work highlights the relevance of pathological cellular processes beyond the nigrostriatal dopaminergic pathway in the expression of cognitive deficits in PD, where glutamatergic and GABAergic mesolimbic projections from the VTA may play a role in hippocampal dysfunction.

References

Aarsland, D., Creese, B., Politis, M., Chaudhuri, K. R., Ffytche, D. H., Weintraub, D., & Ballard, C. (2017). Cognitive decline in Parkinson disease. *Nature Reviews. Neurology*, *13*(4), 217–231. https://doi.org/10.1038/nrneurol.2017.27

Aarsland, D., Marsh, L., & Schrag, A. (2009). Neuropsychiatric symptoms in Parkinson's disease. *Movement Disorders : Official Journal of the Movement Disorder Society*, *24*(15), 2175–2186. https://doi.org/10.1002/mds.22589

Adcock, R. A., Thangavel, A., Whitfield-Gabrieli, S., Knutson, B., & Gabrieli, J. D. E. (2006). Reward-motivated learning: mesolimbic activation precedes memory formation. *Neuron*, *50*(3), 507–517. https://doi.org/10.1016/j.neuron.2006.03.036

Adeniyi, P. A., Shrestha, A., & Ogundele, O. M. (2020). Distribution of VTA Glutamate and Dopamine Terminals, and their Significance in CA1 Neural Network Activity. *Neuroscience*, *446*, 171–198. https://doi.org/https://doi.org/10.1016/j.neuroscience.2020.06.045

Alarcón-Arís, D., Pavia-Collado, R., Miquel-Rio, L., Coppola-Segovia, V., Ferrés-Coy, A., Ruiz-Bronchal, E., Galofré, M., Paz, V., Campa, L., Revilla, R., Montefeltro, A., Kordower, J. H., Vila, M., Artigas, F., & Bortolozzi, A. (2020). Anti-α-synuclein ASO delivered to monoamine neurons prevents α-synuclein accumulation in a Parkinson's disease-like mouse model and in monkeys. *EBioMedicine*, *59*. https://doi.org/10.1016/j.ebiom.2020.102944

Alberico, S. L., Cassell, M. D., & Narayanan, N. S. (2015). The Vulnerable Ventral Tegmental Area in Parkinson's Disease. *Basal Ganglia*, *5*(2–3), 51–55. https://doi.org/10.1016/j.baga.2015.06.001

Albin, R. L., Young, A. B., & Penney, J. B. (1989). The functional anatomy of basal ganglia disorders. *Trends in Neurosciences*, *12*(10), 366–375. https://doi.org/10.1016/0166-2236(89)90074-x

Alcamí, P., & Pereda, A. E. (2019). Beyond plasticity: the dynamic impact of electrical synapses on neural circuits. *Nature Reviews Neuroscience*, *20*(5), 253–271. https://doi.org/10.1038/s41583-019-0133-5

Aldred, J., & Nutt, J. G. (2010). *Levodopa* (K. Kompoliti & L. V. B. T.-E. of M. D. Metman (Eds.); pp. 132–137). Academic Press. https://doi.org/https://doi.org/10.1016/B978-0-12-374105-9.00340-3

Aldrin-Kirk, P., Davidsson, M., Holmqvist, S., Li, J.-Y., & Björklund, T. (2014). Novel AAV-Based Rat Model of Forebrain Synucleinopathy Shows Extensive Pathologies and Progressive Loss of Cholinergic Interneurons. *PLOS ONE*, *9*(7), e100869. https://doi.org/10.1371/journal.pone.0100869

Alessi, D. R., & Sammler, E. (2018). LRRK2 kinase in Parkinson's disease. *Science*, *360*(6384), 36 LP – 37. https://doi.org/10.1126/science.aar5683

Alexander, G. E., DeLong, M. R., & Strick, P. L. (1986). Parallel organization of functionally segregated circuits linking basal ganglia and cortex. *Annual Review of Neuroscience*, *9*, 357–381. https://doi.org/10.1146/annurev.ne.09.030186.002041

Alvarsson, A., Caudal, D., Björklund, A., & Svenningsson, P. (2016). Emotional memory impairments induced by AAV-mediated overexpression of human α-synuclein in dopaminergic neurons of the ventral tegmental area. *Behavioural Brain Research*, *296*, 129–133. https://doi.org/10.1016/j.bbr.2015.08.034

Alza, N. P., Iglesias González, P. A., Conde, M. A., Uranga, R. M., & Salvador, G. A. (2019). Lipids at the Crossroad of α-Synuclein Function and Dysfunction: Biological and Pathological Implications . In *Frontiers in Cellular Neuroscience* (Vol. 13, p. 175). https://www.frontiersin.org/article/10.3389/fncel.2019.00175

Angot, E., Steiner, J. A., Hansen, C., Li, J.-Y., & Brundin, P. (2010). Are synucleinopathies prion-like disorders? *The Lancet. Neurology*, *9*(11), 1128–1138. https://doi.org/10.1016/S1474-4422(10)70213-1

Arias-Carrión, O., Stamelou, M., Murillo-Rodríguez, E., Menéndez-González, M., & Pöppel, E. (2010). Dopaminergic reward system: a short integrative review. *International Archives of Medicine*, *3*, 24. https://doi.org/10.1186/1755-7682-3-24

Arotcarena, M.-L., Dovero, S., Prigent, A., Bourdenx, M., Camus, S., Porras, G., Thiolat, M.-L., Tasselli, M., Aubert, P., Kruse, N., Mollenhauer, B., Trigo Damas, I., Estrada, C., Garcia-Carrillo, N., Vaikath, N. N., El-Agnaf, O. M. A., Herrero, M. T., Vila, M., Obeso, J. A., … Bezard, E. (2020). Bidirectional gut-to-brain and brain-to-gut propagation of synucleinopathy in non-human primates. *Brain*, *143*(5), 1462–1475. https://doi.org/10.1093/brain/awaa096

Arranz, A. M., Delbroek, L., Van Kolen, K., Guimarães, M. R., Mandemakers, W., Daneels, G., Matta, S., Calafate, S., Shaban, H., Baatsen, P., De Bock, P.-J., Gevaert, K., Vanden Berghe, P., Verstreken, P., De Strooper, B., & Moechars, D. (2015). LRRK2 functions in synaptic vesicle endocytosis through a kinase-dependent mechanism. *Journal of Cell Science*, *128*(3), 541–552. https://doi.org/10.1242/jcs.158196

Auffret, M., Le Jeune, F., Maurus, A., Drapier, S., Houvenaghel, J.-F., Robert, G. H., Sauleau, P., & Vérin, M. (2017). Apomorphine pump in advanced Parkinson's disease: Effects on motor and nonmotor symptoms with brain metabolism correlations. *Journal of the Neurological Sciences*, *372*, 279–287.

https://doi.org/https://doi.org/10.1016/j.jns.2016.11.080

Avchalumov, Y., & Mandyam, C. D. (2021). Plasticity in the Hippocampus, Neurogenesis and Drugs of Abuse. In *Brain Sciences* (Vol. 11, Issue 3). https://doi.org/10.3390/brainsci11030404

Awasthi, J. R., Tamada, K., Overton, E. T. N., & Takumi, T. (2020). Comprehensive Topographical Map of the Serotonergic Fibers in the Mouse Brain. *BioRxiv*, 2020.03.18.997775. https://doi.org/10.1101/2020.03.18.997775

Baba, T., Sakisaka, T., Mochida, S., & Takai, Y. (2005). PKA-catalyzed phosphorylation of tomosyn and its implication in Ca2+-dependent exocytosis of neurotransmitter. *The Journal of Cell Biology*, *170*(7), 1113–1125. https://doi.org/10.1083/jcb.200504055

Bagetta, V., Sgobio, C., Pendolino, V., Del Papa, G., Tozzi, A., Ghiglieri, V., Giampà, C., Zianni, E., Gardoni, F., Calabresi, P., & Picconi, B. (2012). Rebalance of striatal NMDA/AMPA receptor ratio underlies the reduced emergence of dyskinesia during D2-like dopamine agonist treatment in experimental Parkinson's disease. *The Journal of Neuroscience : The Official Journal of the Society for Neuroscience*, *32*(49), 17921–17931. https://doi.org/10.1523/JNEUROSCI.2664-12.2012

Ball, N., Teo, W.-P., Chandra, S., & Chapman, J. (2019). Parkinson's Disease and the Environment . In *Frontiers in Neurology* (Vol. 10, p. 218). https://www.frontiersin.org/article/10.3389/fneur.2019.00218

Baltaci, S. B., Mogulkoc, R., & Baltaci, A. K. (2019). Molecular Mechanisms of Early and Late LTP. *Neurochemical Research*, *44*(2), 281–296. https://doi.org/10.1007/s11064-018-2695-4

Barbour, R., Kling, K., Anderson, J. P., Banducci, K., Cole, T., Diep, L., Fox, M., Goldstein, J. M., Soriano, F., Seubert, P., & Chilcote, T. J. (2008). Red blood cells are the major source of alpha-synuclein in blood. *Neuro-Degenerative Diseases*, *5*(2), 55–59. https://doi.org/10.1159/000112832

Barker, G. R. I., & Warburton, E. C. (2011). When is the hippocampus involved in recognition memory? *Journal of Neuroscience*, *31*(29), 10721–10731. https://doi.org/10.1523/JNEUROSCI.6413-10.2011

Barone, P. (2010). Neurotransmission in Parkinson's disease: beyond dopamine. *European Journal of Neurology*, *17*(3), 364–376. https://doi.org/10.1111/j.1468-1331.2009.02900.x

Barone, P., Antonini, A., Colosimo, C., Marconi, R., Morgante, L., Avarello, T. P., Bottacchi, E., Cannas, A., Ceravolo, G., Ceravolo, R., Cicarelli, G., Gaglio, R. M., Giglia, R. M., Iemolo, F., Manfredi, M., Meco, G., Nicoletti, A., Pederzoli, M., Petrone, A., … Dotto, P. Del. (2009). The PRIAMO study: A multicenter assessment of nonmotor symptoms and their impact on quality of life in Parkinson's disease. *Movement Disorders : Official Journal of the Movement Disorder Society*, *24*(11), 1641–1649. https://doi.org/10.1002/mds.22643

Bastide, M. F., Meissner, W. G., Picconi, B., Fasano, S., Fernagut, P.-O., Feyder, M., Francardo, V., Alcacer, C., Ding, Y., Brambilla, R., Fisone, G., Jon Stoessl, A., Bourdenx, M., Engeln, M., Navailles, S., De Deurwaerdère, P., Ko, W. K. D., Simola, N., Morelli, M., … Bézard, E. (2015). Pathophysiology of L-dopa-induced motor and non-motor complications in Parkinson's disease. *Progress in Neurobiology*, *132*, 96–168. https://doi.org/https://doi.org/10.1016/j.pneurobio.2015.07.002

Beaulieu, J.-M., & Gainetdinov, R. R. (2011). The Physiology, Signaling, and Pharmacology of Dopamine Receptors. *Pharmacological Reviews*, *63*(1), 182 LP – 217. https://doi.org/10.1124/pr.110.002642

Behl, T., Kaur, G., Fratila, O., Buhas, C., Judea-Pusta, C. T., Negrut, N., Bustea, C., & Bungau, S. (2021). Cross-talks among GBA mutations, glucocerebrosidase, and α-synuclein in GBA-associated Parkinson's disease and their targeted therapeutic approaches: a comprehensive review. *Translational Neurodegeneration*, *10*(1), 4. https://doi.org/10.1186/s40035-020-00226-x

Beilina, A., Bonet-Ponce, L., Kumaran, R., Kordich, J. J., Ishida, M., Mamais, A., Kaganovich, A., Saez-Atienzar, S., Gershlick, D. C., Roosen, D. A., Pellegrini, L., Malkov, V., Fell, M. J., Harvey, K., Bonifacino, J. S., Moore, D. J., & Cookson, M. R. (2020). The Parkinson’s Disease Protein LRRK2 Interacts with the GARP Complex to Promote Retrograde Transport to the trans-Golgi Network. *Cell Reports*, *31*(5). https://doi.org/10.1016/j.celrep.2020.107614

Bell, M. E., Bourne, J. N., Chirillo, M. A., Mendenhall, J. M., Kuwajima, M., & Harris, K. M. (2014). Dynamics of nascent and active zone ultrastructure as synapses enlarge during long-term potentiation in mature hippocampus. *Journal of Comparative Neurology*, *522*(17), 3861–3884. https://doi.org/https://doi.org/10.1002/cne.23646

Belvisi, D., Pellicciari, R., Fabbrini, G., Tinazzi, M., Berardelli, A., & Defazio, G. (2020). Modifiable risk and protective factors in disease development, progression and clinical subtypes of Parkinson's disease: What do prospective studies suggest? *Neurobiology of Disease*, *134*, 104671. https://doi.org/https://doi.org/10.1016/j.nbd.2019.104671

Benskey, M. J., Perez, R. G., & Manfredsson, F. P. (2016). The contribution of alpha synuclein to neuronal survival and function - Implications for Parkinson's disease. *Journal of Neurochemistry*, *137*(3), 331–359.

https://doi.org/10.1111/jnc.13570

Bentivoglio, M., & Morelli, M. (2005). Chapter I The organization and circuits of mesencephalic dopaminergic neurons and the distribution of dopamine receptors in the brain. In S. B. Dunnett, M. Bentivoglio, A. Björklund, & T. B. T.-H. of C. N. Hökfelt (Eds.), *Dopamine* (Vol. 21, pp. 1–107). Elsevier. https://doi.org/https://doi.org/10.1016/S0924-8196(05)80005-3

Berardelli, A., Rothwell, J. C., Thompson, P. D., & Hallett, M. (2001). Pathophysiology of bradykinesia in Parkinson's disease. *Brain : A Journal of Neurology*, *124*(Pt 11), 2131–2146. https://doi.org/10.1093/brain/124.11.2131

Berchtold, M. W., Egli, R., Rhyner, J. A., Hameister, H., & Strehler, E. E. (1993). Localization of the human bona fide calmodulin genes CALM1, CALM2, and CALM3 to chromosomes 14q24-q31, 2p21.1-p21.3, and 19q13.2-q13.3. *Genomics*, *16*(2), 461–465. https://doi.org/10.1006/geno.1993.1211

Bereczki, E., Bogstedt, A., Höglund, K., Tsitsi, P., Brodin, L., Ballard, C., Svenningsson, P., & Aarsland, D. (2017). Synaptic proteins in CSF relate to Parkinson's disease stage markers. *NPJ Parkinson's Disease*, *3*, 7. https://doi.org/10.1038/s41531-017-0008-2

Bereczki, E., Branca, R. M., Francis, P. T., Pereira, J. B., Baek, J.-H., Hortobágyi, T., Winblad, B., Ballard, C., Lehtiö, J., & Aarsland, D. (2018). Synaptic markers of cognitive decline in neurodegenerative diseases: a proteomic approach. *Brain : A Journal of Neurology*, *141*(2), 582–595. https://doi.org/10.1093/brain/awx352

Berg, D., Postuma, R. B., Adler, C. H., Bloem, B. R., Chan, P., Dubois, B., Gasser, T., Goetz, C. G., Halliday, G., Joseph, L., Lang, A. E., Liepelt-Scarfone, I., Litvan, I., Marek, K., Obeso, J., Oertel, W., Olanow, C. W., Poewe, W., Stern, M., & Deuschl, G. (2015). MDS research criteria for prodromal Parkinson's disease. *Movement Disorders : Official Journal of the Movement Disorder Society*, *30*(12), 1600–1611. https://doi.org/10.1002/mds.26431

Berridge, M. J. (1998). Neuronal Calcium Signaling. *Neuron*, *21*(1), 13–26. https://doi.org/10.1016/S0896-6273(00)80510-3

Beyer, M. K., Bronnick, K. S., Hwang, K. S., Bergsland, N., Tysnes, O. B., Larsen, J. P., Thompson, P. M., Somme, J. H., & Apostolova, L. G. (2013). Verbal memory is associated with structural hippocampal changes in newly diagnosed Parkinson's disease. *Journal of Neurology, Neurosurgery & Psychiatry*, *84*(1), 23 LP – 28. https://doi.org/10.1136/jnnp-2012-303054

Bezard, E., Yue, Z., Kirik, D., & Spillantini, M. G. (2013). Animal models of Parkinson's disease: limits and relevance to neuroprotection studies. *Movement Disorders : Official Journal of the Movement Disorder Society*, *28*(1), 61–70. https://doi.org/10.1002/mds.25108

Bido, S., Soria, F. N., Fan, R. Z., Bezard, E., & Tieu, K. (2017). Mitochondrial division inhibitor-1 is neuroprotective in the A53T-α-synuclein rat model of Parkinson's disease. *Scientific Reports*, *7*(1). https://doi.org/10.1038/s41598-017-07181-0

Bimpisidis, Z., & Wallén-Mackenzie, Å. (2019). Neurocircuitry of Reward and Addiction: Potential Impact of Dopamine-Glutamate Co-release as Future Target in Substance Use Disorder. *Journal of Clinical Medicine*, *8*(11). https://doi.org/10.3390/jcm8111887

Binotti, B., Jahn, R., & Chua, J. J. E. (2016). Functions of Rab Proteins at Presynaptic Sites. *Cells*, *5*(1). https://doi.org/10.3390/cells5010007

Björklund, A., & Dunnett, S. B. (2007). Dopamine neuron systems in the brain: an update. *Trends in Neurosciences*, *30*(5), 194–202. https://doi.org/10.1016/j.tins.2007.03.006

Black, K. J., Hershey, T., Koller, J. M., Videen, T. O., Mintun, M. A., Price, J. L., & Perlmutter, J. S. (2002). A possible substrate for dopamine-related changes in mood and behavior: prefrontal and limbic effects of a D3-preferring dopamine agonist. *Proceedings of the National Academy of Sciences of the United States of America*, *99*(26), 17113–17118. https://doi.org/10.1073/pnas.012260599

Blesa, J., Trigo-Damas, I., Quiroga-Varela, A., & Jackson-Lewis, V. R. (2015). Oxidative stress and Parkinson's disease . In *Frontiers in Neuroanatomy* (Vol. 9, p. 91). https://www.frontiersin.org/article/10.3389/fnana.2015.00091

Bliss, T. V, & Lomo, T. (1973). Long-lasting potentiation of synaptic transmission in the dentate area of the anaesthetized rabbit following stimulation of the perforant path. *The Journal of Physiology*, *232*(2), 331–356. https://doi.org/10.1113/jphysiol.1973.sp010273

Bohnen, N. I., Kaufer, D. I., Ivanco, L. S., Lopresti, B., Koeppe, R. A., Davis, J. G., Mathis, C. A., Moore, R. Y., & DeKosky, S. T. (2003). Cortical Cholinergic Function Is More Severely Affected in Parkinsonian Dementia Than in Alzheimer Disease: An In Vivo Positron Emission Tomographic Study. *Archives of Neurology*, *60*(12), 1745–1748. https://doi.org/10.1001/archneur.60.12.1745

Bohush, A., Leśniak, W., Weis, S., & Filipek, A. (2021). Calmodulin and Its Binding Proteins in Parkinson's Disease.

International Journal of Molecular Sciences, *22*(6), 3016. https://doi.org/10.3390/ijms22063016

Bonito-Oliva, A., Pignatelli, M., Spigolon, G., Yoshitake, T., Seiler, S., Longo, F., Piccinin, S., Kehr, J., Mercuri, N. B., Nisticò, R., & Fisone, G. (2014). Cognitive impairment and dentate gyrus synaptic dysfunction in experimental parkinsonism. *Biological Psychiatry*, *75*(9), 701–710. https://doi.org/10.1016/j.biopsych.2013.02.015

Bosch, M., Castro, J., Saneyoshi, T., Matsuno, H., Sur, M., & Hayashi, Y. (2014). Structural and Molecular Remodeling of Dendritic Spine Substructures during Long-Term Potentiation. *Neuron*, *82*(2), 444–459. https://doi.org/10.1016/j.neuron.2014.03.021

Bourdenx, M., Dovero, S., Engeln, M., Bido, S., Bastide, M. F., Dutheil, N., Vollenweider, I., Baud, L., Piron, C., Grouthier, V., Boraud, T., Porras, G., Li, Q., Baekelandt, V., Scheller, D., Michel, A., Fernagut, P., Georges, F., Courtine, G., … Dehay, B. (2015). Lack of additive role of ageing in nigrostriatal neurodegeneration triggered by α -synuclein overexpression. *Acta Neuropathologica Communications*, 1–15. https://doi.org/10.1186/s40478-015-0222-2

Bové, J., Prou, D., Perier, C., & Przedborski, S. (2005). Toxin-induced models of Parkinson's disease. *NeuroRx : The Journal of the American Society for Experimental NeuroTherapeutics*, *2*(3), 484–494. https://doi.org/10.1602/neurorx.2.3.484

Braak, H., Del Tredici, K., Rüb, U., de Vos, R. A. I., Jansen Steur, E. N. H., & Braak, E. (2003). Staging of brain pathology related to sporadic Parkinson's disease. *Neurobiology of Aging*, *24*(2), 197–211. https://doi.org/10.1016/s0197-4580(02)00065-9

Braak, H., Sandmann-Keil, D., Gai, W., & Braak, E. (1999). Extensive axonal Lewy neurites in Parkinson's disease: a novel pathological feature revealed by alpha-synuclein immunocytochemistry. *Neuroscience Letters*, *265*(1), 67–69. https://doi.org/10.1016/s0304-3940(99)00208-6

Bras, J., Verloes, A., Schneider, S. A., Mole, S. E., & Guerreiro, R. J. (2012). Mutation of the parkinsonism gene ATP13A2 causes neuronal ceroid-lipofuscinosis. *Human Molecular Genetics*, *21*(12), 2646–2650. https://doi.org/10.1093/hmg/dds089

Bridi, J. C., & Hirth, F. (2018). Mechanisms of α-Synuclein Induced Synaptopathy in Parkinson's Disease . In *Frontiers in Neuroscience* (Vol. 12, p. 80). https://www.frontiersin.org/article/10.3389/fnins.2018.00080

Brown, J. C., Petersen, A., Zhong, L., Himelright, M. L., Murphy, J. A., Walikonis, R. S., & Gerges, N. Z. (2016). Bidirectional regulation of synaptic transmission by BRAG1/IQSEC2 and its requirement in long-term depression. *Nature Communications*, *7*(1), 11080. https://doi.org/10.1038/ncomms11080

Brück, A., Kurki, T., Kaasinen, V., Vahlberg, T., & Rinne, J. O. (2004). Hippocampal and prefrontal atrophy in patients with early non-demented Parkinson's disease is related to cognitive impairment. *Journal of Neurology, Neurosurgery, and Psychiatry*, *75*(10), 1467–1469. https://doi.org/10.1136/jnnp.2003.031237

Brundin, P., Melki, R., & Kopito, R. (2010). Prion-like transmission of protein aggregates in neurodegenerative diseases. *Nature Reviews. Molecular Cell Biology*, *11*(4), 301–307. https://doi.org/10.1038/nrm2873

Bu, Y., Wang, N., Wang, S., Sheng, T., Tian, T., Chen, L., Pan, W., Zhu, M., Luo, J., & Lu, W. (2015). Myosin IIb-dependent Regulation of Actin Dynamics Is Required for N-Methyl-D-aspartate Receptor Trafficking during Synaptic Plasticity. *The Journal of Biological Chemistry*, *290*(42), 25395–25410. https://doi.org/10.1074/jbc.M115.644229

Buchert, R., Buhmann, C., Apostolova, I., Meyer, P. T., & Gallinat, J. (2019). Nuclear Imaging in the Diagnosis of Clinically Uncertain Parkinsonian Syndromes. *Deutsches Arzteblatt International*, *116*(44), 747–754. https://doi.org/10.3238/arztebl.2019.0747

Buck, S. A., De Miranda, B. R., Logan, R. W., Fish, K. N., Greenamyre, J. T., & Freyberg, Z. (2021). VGLUT2 Is a Determinant of Dopamine Neuron Resilience in a Rotenone Model of Dopamine Neurodegeneration. *The Journal of Neuroscience*, *41*(22), 4937 LP – 4947. https://doi.org/10.1523/JNEUROSCI.2770-20.2021

Burke, D. A., Rotstein, H. G., & Alvarez, V. A. (2017). Striatal Local Circuitry: A New Framework for Lateral Inhibition. *Neuron*, *96*(2), 267–284. https://doi.org/10.1016/j.neuron.2017.09.019

Burré, J., Sharma, M., & Südhof, T. C. (2014). α-Synuclein assembles into higher-order multimers upon membrane binding to promote SNARE complex formation. *Proceedings of the National Academy of Sciences*, *111*(40), E4274 LP-E4283. https://doi.org/10.1073/pnas.1416598111

Burré, J., Sharma, M., & Südhof, T. C. (2018). Cell Biology and Pathophysiology of α-Synuclein. *Cold Spring Harbor Perspectives in Medicine*, *8*(3). https://doi.org/10.1101/cshperspect.a024091

Burré, J., Sharma, M., Tsetsenis, T., Buchman, V., Etherton, M. R., & Südhof, T. C. (2010). Alpha-synuclein promotes SNARE-complex assembly in vivo and in vitro. *Science (New York, N.Y.)*, *329*(5999), 1663–1667. https://doi.org/10.1126/science.1195227

Calabresi, P., Castrioto, A., Di Filippo, M., & Picconi, B. (2013). New experimental and clinical links between the hippocampus and the dopaminergic system in Parkinson's disease. In *The Lancet Neurology* (Vol. 12, Issue 8, pp. 811–821). https://doi.org/10.1016/S1474-4422(13)70118-2

Calabresi, P., Maj, R., Pisani, A., Mercuri, N. B., & Bernardi, G. (1992). Long-term synaptic depression in the striatum: physiological and pharmacological characterization. *The Journal of Neuroscience : The Official Journal of the Society for Neuroscience*, *12*(11), 4224–4233.

Calabresi, P., Picconi, B., Tozzi, A., & Di Filippo, M. (2007). Dopamine-mediated regulation of corticostriatal synaptic plasticity. *Trends in Neurosciences*, *30*(5), 211–219. https://doi.org/10.1016/j.tins.2007.03.001

Calabresi, P., Pisani, A., Mercuri, N. B., & Bernardi, G. (1992). Long-term Potentiation in the Striatum is Unmasked by Removing the Voltage-dependent Magnesium Block of NMDA Receptor Channels. *The European Journal of Neuroscience*, *4*(10), 929–935.

Calo, L., Wegrzynowicz, M., Santivañez-Perez, J., & Grazia Spillantini, M. (2016). Synaptic failure and α-synuclein. *Movement Disorders : Official Journal of the Movement Disorder Society*, *31*(2), 169–177. https://doi.org/10.1002/mds.26479

Camicioli, R., Moore, M. M., Kinney, A., Corbridge, E., Glassberg, K., & Kaye, J. A. (2003). Parkinson's disease is associated with hippocampal atrophy. *Movement Disorders*, *18*(7), 784–790. https://doi.org/https://doi.org/10.1002/mds.10444

Caminiti, S. P., Presotto, L., Baroncini, D., Garibotto, V., Moresco, R. M., Gianolli, L., Volonté, M. A., Antonini, A., & Perani, D. (2017). Axonal damage and loss of connectivity in nigrostriatal and mesolimbic dopamine pathways in early Parkinson's disease. *NeuroImage. Clinical*, *14*, 734–740. https://doi.org/10.1016/j.nicl.2017.03.011

Campêlo, C. L. das C., & Silva, R. H. (2017). Genetic Variants in SNCA and the Risk of Sporadic Parkinson's Disease and Clinical Outcomes: A Review. *Parkinson's Disease*, *2017*, 4318416. https://doi.org/10.1155/2017/4318416

Campos, F., Carvalho, M., Cristovão, A., Je, G., Baltazar, G., Salgado, A., Kim, Y.-S., & Sousa, N. (2013). Rodent models of Parkinson's disease: beyond the motor symptomatology . In *Frontiers in Behavioral Neuroscience* (Vol. 7, p. 175). https://www.frontiersin.org/article/10.3389/fnbeh.2013.00175

Carriere, N., Lopes, R., Defebvre, L., Delmaire, C., & Dujardin, K. (2015). Impaired corticostriatal connectivity in impulse control disorders in Parkinson disease. *Neurology*, *84*(21), 2116 LP – 2123. https://doi.org/10.1212/WNL.0000000000001619

Carta, A. R., Boi, L., Pisanu, A., Palmas, M. F., Carboni, E., & De Simone, A. (2020). Advances in modelling alpha-synuclein-induced Parkinson's diseases in rodents: Virus-based models versus inoculation of exogenous preformed toxic species. *Journal of Neuroscience Methods*, *338*, 108685. https://doi.org/https://doi.org/10.1016/j.jneumeth.2020.108685

Castillo, P. E. (2012). Presynaptic LTP and LTD of excitatory and inhibitory synapses. *Cold Spring Harbor Perspectives in Biology*, *4*(2), a005728. https://doi.org/10.1101/cshperspect.a005728

Castro-Hernández, J., Adlard, P. A., & Finkelstein, D. I. (2017). Pramipexole restores depressed transmission in the ventral hippocampus following MPTP-lesion. *Scientific Reports*, *7*, 44426. https://doi.org/10.1038/srep44426

Catani, M., Dell'acqua, F., & Thiebaut de Schotten, M. (2013). A revised limbic system model for memory, emotion and behaviour. *Neuroscience and Biobehavioral Reviews*, *37*(8), 1724–1737. https://doi.org/10.1016/j.neubiorev.2013.07.001

Caudal, D., Alvarsson, A., Björklund, A., & Svenningsson, P. (2015). Depressive-like phenotype induced by AAV-mediated overexpression of human α-synuclein in midbrain dopaminergic neurons. *Experimental Neurology*, *273*, 243–252. https://doi.org/https://doi.org/10.1016/j.expneurol.2015.09.002

Cerri, S., Mus, L., & Blandini, F. (2019). Parkinson's Disease in Women and Men: What's the Difference? *Journal of Parkinson's Disease*, *9*(3), 501–515. https://doi.org/10.3233/JPD-191683

Chahine, L. M., Amara, A. W., & Videnovic, A. (2017). A systematic review of the literature on disorders of sleep and wakefulness in Parkinson's disease from 2005 to 2015. *Sleep Medicine Reviews*, *35*, 33–50. https://doi.org/10.1016/j.smrv.2016.08.001

Chahine, L. M., Weintraub, D., Hawkins, K. A., Siderowf, A., Eberly, S., Oakes, D., Seibyl, J., Stern, M. B., Marek, K., & Jennings, D. (2016). Cognition in individuals at risk for Parkinson's: Parkinson associated risk syndrome (PARS) study findings. *Movement Disorders : Official Journal of the Movement Disorder Society*, *31*(1), 86–94. https://doi.org/10.1002/mds.26373

Chartier-Harlin, M.-C., Kachergus, J., Roumier, C., Mouroux, V., Douay, X., Lincoln, S., Levecque, C., Larvor, L., Andrieux, J., Hulihan, M., Waucquier, N., Defebvre, L., Amouyel, P., Farrer, M., & Destée, A. (2004). Alpha-synuclein locus

duplication as a cause of familial Parkinson's disease. *Lancet (London, England)*, *364*(9440), 1167–1169. https://doi.org/10.1016/S0140-6736(04)17103-1

Chen, C., Itakura, E., Weber, K. P., Hegde, R. S., & de Bono, M. (2014). An ER Complex of ODR-4 and ODR-8/Ufm1 Specific Protease 2 Promotes GPCR Maturation by a Ufm1-Independent Mechanism. *PLOS Genetics*, *10*(3), e1004082. https://doi.org/10.1371/journal.pgen.1004082

Cheng, H.-C., Ulane, C. M., & Burke, R. E. (2010). Clinical progression in Parkinson disease and the neurobiology of axons. *Annals of Neurology*, *67*(6), 715–725. https://doi.org/10.1002/ana.21995

Cherian, A., & Divya, K. P. (2020). Genetics of Parkinson's disease. *Acta Neurologica Belgica*, *120*(6), 1297–1305. https://doi.org/10.1007/s13760-020-01473-5

Chou, J.-S., Chen, C.-Y., Chen, Y.-L., Weng, Y.-H., Yeh, T.-H., Lu, C.-S., Chang, Y.-M., & Wang, H.-L. (2014). (G2019S) LRRK2 causes early-phase dysfunction of SNpc dopaminergic neurons and impairment of corticostriatal long-term depression in the PD transgenic mouse. *Neurobiology of Disease*, *68*, 190–199. https://doi.org/https://doi.org/10.1016/j.nbd.2014.04.021

Chu, Y., & Kordower, J. H. (2007). Age-associated increases of alpha-synuclein in monkeys and humans are associated with nigrostriatal dopamine depletion: Is this the target for Parkinson's disease? *Neurobiology of Disease*, *25*(1), 134–149. https://doi.org/10.1016/j.nbd.2006.08.021

Chu, Y., Muller, S., Tavares, A., Barret, O., Alagille, D., Seibyl, J., Tamagnan, G., Marek, K., Luk, K. C., Trojanowski, J. Q., Lee, V. M. Y., & Kordower, J. H. (2019). Intrastriatal alpha-synuclein fibrils in monkeys: spreading, imaging and neuropathological changes. *Brain : A Journal of Neurology*, *142*(11), 3565–3579. https://doi.org/10.1093/brain/awz296

Chung, C. Y., Koprich, J. B., Siddiqi, H., & Isacson, O. (2009). Dynamic changes in presynaptic and axonal transport proteins combined with striatal neuroinflammation precede dopaminergic neuronal loss in a rat model of AAV alpha-synucleinopathy. *The Journal of Neuroscience : The Official Journal of the Society for Neuroscience*, *29*(11), 3365–3373. https://doi.org/10.1523/JNEUROSCI.5427-08.2009

Cilia, R., Ko, J. H., Cho, S. S., van Eimeren, T., Marotta, G., Pellecchia, G., Pezzoli, G., Antonini, A., & Strafella, A. P. (2010). Reduced dopamine transporter density in the ventral striatum of patients with Parkinson's disease and pathological gambling. *Neurobiology of Disease*, *39*(1), 98–104. https://doi.org/10.1016/j.nbd.2010.03.013

Cilia, R., Siri, C., Marotta, G., Isaias, I. U., De Gaspari, D., Canesi, M., Pezzoli, G., & Antonini, A. (2008). Functional Abnormalities Underlying Pathological Gambling in Parkinson Disease. *Archives of Neurology*, *65*(12), 1604–1611. https://doi.org/10.1001/archneur.65.12.1604

Cingolani, L. A., & Goda, Y. (2008). Actin in action: the interplay between the actin cytoskeleton and synaptic efficacy. *Nature Reviews Neuroscience*, *9*(5), 344–356. https://doi.org/10.1038/nrn2373

Citri, A., & Malenka, R. C. (2008). Synaptic plasticity: multiple forms, functions, and mechanisms. *Neuropsychopharmacology : Official Publication of the American College of Neuropsychopharmacology*, *33*(1), 18–41. https://doi.org/10.1038/sj.npp.1301559

Conte, A., Khan, N., Defazio, G., Rothwell, J. C., & Berardelli, A. (2013). Pathophysiology of somatosensory abnormalities in Parkinson disease. *Nature Reviews. Neurology*, *9*(12), 687–697. https://doi.org/10.1038/nrneurol.2013.224

Cools, R., Barker, R. A., Sahakian, B. J., & Robbins, T. W. (2001). Enhanced or impaired cognitive function in Parkinson's disease as a function of dopaminergic medication and task demands. *Cerebral Cortex (New York, N.Y. : 1991)*, *11*(12), 1136–1143. https://doi.org/10.1093/cercor/11.12.1136

Correia, S. S., Bassani, S., Brown, T. C., Lisé, M.-F., Backos, D. S., El-Husseini, A., Passafaro, M., & Esteban, J. A. (2008). Motor protein–dependent transport of AMPA receptors into spines during long-term potentiation. *Nature Neuroscience*, *11*(4), 457–466. https://doi.org/10.1038/nn2063

Costa, C., Sgobio, C., Siliquini, S., Tozzi, A., Tantucci, M., Ghiglieri, V., Di Filippo, M., Pendolino, V., de Iure, A., Marti, M., Morari, M., Spillantini, M. G., Latagliata, E. C., Pascucci, T., Puglisi-Allegra, S., Gardoni, F., Di Luca, M., Picconi, B., & Calabresi, P. (2012). Mechanisms underlying the impairment of hippocampal long-term potentiation and memory in experimental Parkinson's disease. *Brain : A Journal of Neurology*, *135*(Pt 6), 1884–1899. https://doi.org/10.1093/brain/aws101

Crowley, E. K., Nolan, Y. M., & Sullivan, A. M. (2018). Neuroprotective effects of voluntary running on cognitive dysfunction in an α-synuclein rat model of Parkinson's disease. *Neurobiology of Aging*, *65*, 60–68. https://doi.org/10.1016/j.neurobiolaging.2018.01.011

Dai, J., Aoto, J., & Südhof, T. C. (2019). Alternative Splicing of Presynaptic Neurexins Differentially Controls Postsynaptic NMDA and AMPA Receptor Responses. *Neuron*, *102*(5), 993-1008.e5. https://doi.org/10.1016/j.neuron.2019.03.032

Dalfó, E., Portero-Otín, M., Ayala, V., Martínez, A., Pamplona, R., & Ferrer, I. (2005). Evidence of oxidative stress in the neocortex in incidental Lewy body disease. *Journal of Neuropathology and Experimental Neurology*, *64*(9), 816–830. https://doi.org/10.1097/01.jnen.0000179050.54522.5a

Davidson, W. S., Jonas, A., Clayton, D. F., & George, J. M. (1998). Stabilization of alpha-synuclein secondary structure upon binding to synthetic membranes. *The Journal of Biological Chemistry*, *273*(16), 9443–9449. https://doi.org/10.1074/jbc.273.16.9443

de Bie, R. M. A., Clarke, C. E., Espay, A. J., Fox, S. H., & Lang, A. E. (2020). Initiation of pharmacological therapy in Parkinson's disease: when, why, and how. *The Lancet. Neurology*, *19*(5), 452–461. https://doi.org/10.1016/S1474-4422(20)30036-3

Decressac, M., Mattsson, B., Lundblad, M., Weikop, P., & Björklund, A. (2012). Progressive neurodegenerative and behavioural changes induced by AAV-mediated overexpression of α-synuclein in midbrain dopamine neurons. *Neurobiology of Disease*, *45*(3), 939–953. https://doi.org/https://doi.org/10.1016/j.nbd.2011.12.013

Del Rey, N. L.-G., Quiroga-Varela, A., Garbayo, E., Carballo-Carbajal, I., Fernández-Santiago, R., Monje, M. H. G., Trigo-Damas, I., Blanco-Prieto, M. J., & Blesa, J. (2018). Advances in Parkinson's Disease: 200 Years Later . In *Frontiers in Neuroanatomy* (Vol. 12, p. 113). https://www.frontiersin.org/article/10.3389/fnana.2018.00113

Delgado-Alvarado, M., Gago, B., Navalpotro-Gomez, I., Jiménez-Urbieta, H., & Rodriguez-Oroz, M. C. (2016). Biomarkers for dementia and mild cognitive impairment in Parkinson's disease. *Movement Disorders : Official Journal of the Movement Disorder Society*, *31*(6), 861–881. https://doi.org/10.1002/mds.26662

DeMaagd, G., & Philip, A. (2015). Parkinson's Disease and Its Management: Part 1: Disease Entity, Risk Factors, Pathophysiology, Clinical Presentation, and Diagnosis. *P & T : A Peer-Reviewed Journal for Formulary Management*, *40*(8), 504–532.

Denninger, J. K., Smith, B. M., & Kirby, E. D. (2018). Novel object recognition and object location behavioral testing in mice on a budget. *Journal of Visualized Experiments*, *2018*(141). https://doi.org/10.3791/58593

Devrome, M., Casteels, C., Van der Perren, A., Van Laere, K., Baekelandt, V., & Koole, M. (2019). Identifying a glucose metabolic brain pattern in an adeno-associated viral vector based rat model for Parkinson's disease using 18F-FDG PET imaging. *Scientific Reports*, *9*(1), 12368. https://doi.org/10.1038/s41598-019-48713-0

Dickson, D. W., Braak, H., Duda, J. E., Duyckaerts, C., Gasser, T., Halliday, G. M., Hardy, J., Leverenz, J. B., Del Tredici, K., Wszolek, Z. K., & Litvan, I. (2009). Neuropathological assessment of Parkinson's disease: refining the diagnostic criteria. *The Lancet. Neurology*, *8*(12), 1150–1157. https://doi.org/10.1016/S1474-4422(09)70238-8

Diering, G. H., & Huganir, R. L. (2018). The AMPA Receptor Code of Synaptic Plasticity. *Neuron*, *100*(2), 314–329. https://doi.org/10.1016/j.neuron.2018.10.018

Dijkstra, A. A., Ingrassia, A., de Menezes, R. X., van Kesteren, R. E., Rozemuller, A. J. M., Heutink, P., & van de Berg, W. D. J. (2015). Evidence for Immune Response, Axonal Dysfunction and Reduced Endocytosis in the Substantia Nigra in Early Stage Parkinson's Disease. *PLOS ONE*, *10*(6), e0128651. https://doi.org/10.1371/journal.pone.0128651

Diógenes, M. J., Dias, R. B., Rombo, D. M., Vicente Miranda, H., Maiolino, F., Guerreiro, P., Näsström, T., Franquelim, H. G., Oliveira, L. M. A., Castanho, M. A. R. B., Lannfelt, L., Bergström, J., Ingelsson, M., Quintas, A., Sebastião, A. M., Lopes, L. V, & Outeiro, T. F. (2012). Extracellular alpha-synuclein oligomers modulate synaptic transmission and impair LTP via NMDA-receptor activation. *The Journal of Neuroscience : The Official Journal of the Society for Neuroscience*, *32*(34), 11750–11762. https://doi.org/10.1523/JNEUROSCI.0234-12.2012

Dolgacheva, L. P., Berezhnov, A. V, Fedotova, E. I., Zinchenko, V. P., & Abramov, A. Y. (2019). Role of DJ-1 in the mechanism of pathogenesis of Parkinson's disease. *Journal of Bioenergetics and Biomembranes*, *51*(3), 175–188. https://doi.org/10.1007/s10863-019-09798-4

Dorsey, E. R., Constantinescu, R., Thompson, J. P., Biglan, K. M., Holloway, R. G., Kieburtz, K., Marshall, F. J., Ravina, B. M., Schifitto, G., Siderowf, A., & Tanner, C. M. (2007). Projected number of people with Parkinson disease in the most populous nations, 2005 through 2030. *Neurology*, *68*(5), 384–386. https://doi.org/10.1212/01.wnl.0000247740.47667.03

Dosemeci, A., Weinberg, R. J., Reese, T. S., & Tao-Cheng, J.-H. (2016). The Postsynaptic Density: There Is More than Meets the Eye . In *Frontiers in Synaptic Neuroscience* (Vol. 8, p. 23). https://www.frontiersin.org/article/10.3389/fnsyn.2016.00023

Doty, R. L. (2012). Olfactory dysfunction in Parkinson disease. *Nature Reviews. Neurology*, *8*(6), 329–339. https://doi.org/10.1038/nrneurol.2012.80

Drøjdahl, N., Nielsen, H. H., Gardi, J. E., Wree, A., Peterson, A. C., Nyengaard, J. R., Eyer, J., & Finsen, B. (2010). Axonal plasticity elicits long-term changes in oligodendroglia and myelinated fibers. *GLIA*, *58*(1), 29–42.

https://doi.org/10.1002/glia.20897

Durante, V., de Iure, A., Loffredo, V., Vaikath, N., De Risi, M., Paciotti, S., Quiroga-Varela, A., Chiasserini, D., Mellone, M., Mazzocchetti, P., Calabrese, V., Campanelli, F., Mechelli, A., Di Filippo, M., Ghiglieri, V., Picconi, B., El-Agnaf, O. M., De Leonibus, E., Gardoni, F., … Calabresi, P. (2019). Alpha-synuclein targets GluN2A NMDA receptor subunit causing striatal synaptic dysfunction and visuospatial memory alteration. *Brain*, *142*(5), 1365–1385. https://doi.org/10.1093/brain/awz065

Edelmann, E., & Lessmann, V. (2018). Dopaminergic innervation and modulation of hippocampal networks. *Cell and Tissue Research*, *373*(3), 711–727. https://doi.org/10.1007/s00441-018-2800-7

Engeln, M., Ahmed, S. H., Vouillac, C., Tison, F., Bezard, E., & Fernagut, P.-O. (2013). Reinforcing properties of Pramipexole in normal and parkinsonian rats. *Neurobiology of Disease*, *49*, 79–86. https://doi.org/https://doi.org/10.1016/j.nbd.2012.08.005

Esmaeili-Mahani, S., Haghparast, E., Nezhadi, A., Abbasnejad, M., & Sheibani, V. (2021). Apelin-13 prevents hippocampal synaptic plasticity impairment in Parkinsonism rats. *Journal of Chemical Neuroanatomy*, *111*, 101884. https://doi.org/10.1016/j.jchemneu.2020.101884

Espa, E., Clemensson, E. K. H., Luk, K. C., Heuer, A., Björklund, T., & Cenci, M. A. (2019). Seeding of protein aggregation causes cognitive impairment in rat model of cortical synucleinopathy. *Movement Disorders : Official Journal of the Movement Disorder Society*, *34*(11), 1699–1710. https://doi.org/10.1002/mds.27810

Evans, A. J., Gurung, S., Henley, J. M., Nakamura, Y., & Wilkinson, K. A. (2019). Exciting Times: New Advances Towards Understanding the Regulation and Roles of Kainate Receptors. *Neurochemical Research*, *44*(3), 572–584. https://doi.org/10.1007/s11064-017-2450-2

Fasano, A., Visanji, N. P., Liu, L. W. C., Lang, A. E., & Pfeiffer, R. F. (2015). Gastrointestinal dysfunction in Parkinson's disease. *The Lancet. Neurology*, *14*(6), 625–639. https://doi.org/10.1016/S1474-4422(15)00007-1

Fastenrath, M., Coynel, D., Spalek, K., Milnik, A., Gschwind, L., Roozendaal, B., Papassotiropoulos, A., & de Quervain, D. J. F. (2014). Dynamic Modulation of Amygdala–Hippocampal Connectivity by Emotional Arousal. *The Journal of Neuroscience*, *34*(42), 13935 LP – 13947. https://doi.org/10.1523/JNEUROSCI.0786-14.2014

Feligioni, M., Mango, D., Piccinin, S., Imbriani, P., Iannuzzi, F., Caruso, A., De Angelis, F., Blandini, F., Mercuri, N. B., Pisani, A., & Nisticò, R. (2016). Subtle alterations of excitatory transmission are linked to presynaptic changes in the hippocampus of PINK1-deficient mice. *Synapse (New York, N.Y.)*, *70*(6), 223–230. https://doi.org/10.1002/syn.21894

Fénelon, G., Mahieux, F., Huon, R., & Ziégler, M. (2000). Hallucinations in Parkinson's disease: Prevalence, phenomenology and risk factors. *Brain*, *123*(4), 733–745. https://doi.org/10.1093/brain/123.4.733

Ferreira, D. G., Batalha, V. L., Vicente Miranda, H., Coelho, J. E., Gomes, R., Gonçalves, F. Q., Real, J. I., Rino, J., Albino-Teixeira, A., Cunha, R. A., Outeiro, T. F., & Lopes, L. V. (2017). Adenosine A2A Receptors Modulate α-Synuclein Aggregation and Toxicity. *Cerebral Cortex (New York, N.Y. : 1991)*, *27*(1), 718–730. https://doi.org/10.1093/cercor/bhv268

Ffytche, D. H., Creese, B., Politis, M., Chaudhuri, K. R., Weintraub, D., Ballard, C., & Aarsland, D. (2017). The psychosis spectrum in Parkinson disease. *Nature Reviews. Neurology*, *13*(2), 81–95. https://doi.org/10.1038/nrneurol.2016.200

Filippi, M., Sarasso, E., Piramide, N., Stojkovic, T., Stankovic, I., Basaia, S., Fontana, A., Tomic, A., Markovic, V., Stefanova, E., Kostic, V. S., & Agosta, F. (2020). Progressive brain atrophy and clinical evolution in Parkinson's disease. *NeuroImage. Clinical*, *28*, 102374. https://doi.org/10.1016/j.nicl.2020.102374

Foster, M., & Sherrington, C. S. (1897). *A Textbook of Physiology, Part Three: The Central Nervous System* (Seventh Ed). MacMillan Co Ltd.

Frank, M. J., Seeberger, L. C., & O'reilly, R. C. (2004). By carrot or by stick: cognitive reinforcement learning in parkinsonism. *Science (New York, N.Y.)*, *306*(5703), 1940–1943. https://doi.org/10.1126/science.1102941

Frey, U., Schroeder, H., & Matthies, H. (1990). Dopaminergic antagonists prevent long-term maintenance of posttetanic LTP in the CA1 region of rat hippocampal slices. *Brain Research*, *522*(1), 69–75. https://doi.org/https://doi.org/10.1016/0006-8993(90)91578-5

Frezza, C., Cipolat, S., & Scorrano, L. (2007). Organelle isolation: Functional mitochondria from mouse liver, muscle and cultured filroblasts. *Nature Protocols*, *2*(2), 287–295. https://doi.org/10.1038/nprot.2006.478

Frotscher, M., & Léránth, C. (1985). Cholinergic innervation of the rat hippocampus as revealed by choline acetyltransferase immunocytochemistry: A combined light and electron microscopic study. *Journal of Comparative Neurology*, *239*(2), 237–246. https://doi.org/https://doi.org/10.1002/cne.902390210

Frouni, I., Hamadjida, A., Kwan, C., Bédard, D., Nafade, V., Gaudette, F., Nuara, S. G., Gourdon, J. C., Beaudry, F., & Huot, P.

(2019). Activation of mGlu(2/3) receptors, a novel therapeutic approach to alleviate dyskinesia and psychosis in experimental parkinsonism. *Neuropharmacology*, *158*, 107725. https://doi.org/10.1016/j.neuropharm.2019.107725

García-Ramos, R., López Valdés, E., Ballesteros, L., Jesús, S., & Mir, P. (2016). The social impact of Parkinson's disease in Spain: Report by the Spanish Foundation for the Brain. *Neurologia (Barcelona, Spain)*, *31*(6), 401–413. https://doi.org/10.1016/j.nrl.2013.04.008

Garcia-Reitböck, P., Anichtchik, O., Bellucci, A., Iovino, M., Ballini, C., Fineberg, E., Ghetti, B., Della Corte, L., Spano, P., Tofaris, G. K., Goedert, M., & Spillantini, M. G. (2010). SNARE protein redistribution and synaptic failure in a transgenic mouse model of Parkinson's disease. *Brain : A Journal of Neurology*, *133*(Pt 7), 2032–2044. https://doi.org/10.1093/brain/awq132

Gasbarri, A., Verney, C., Innocenzi, R., Campana, E., & Pacitti, C. (1994). Mesolimbic dopaminergic neurons innervating the hippocampal formation in the rat: a combined retrograde tracing and immunohistochemical study. *Brain Research*, *668*(1), 71–79. https://doi.org/https://doi.org/10.1016/0006-8993(94)90512-6

Gasca-Salas, C., Clavero, P., García-García, D., Obeso, J. A., & Rodríguez-Oroz, M. C. (2016). Significance of visual hallucinations and cerebral hypometabolism in the risk of dementia in Parkinson's disease patients with mild cognitive impairment. *Human Brain Mapping*, *37*(3), 968–977. https://doi.org/10.1002/hbm.23080

Gaugler, M. N., Genc, O., Bobela, W., Mohanna, S., Ardah, M. T., El-Agnaf, O. M., Cantoni, M., Bensadoun, J.-C., Schneggenburger, R., Knott, G. W., Aebischer, P., & Schneider, B. L. (2012). Nigrostriatal overabundance of α-synuclein leads to decreased vesicle density and deficits in dopamine release that correlate with reduced motor activity. *Acta Neuropathologica*, *123*(5), 653–669. https://doi.org/10.1007/s00401-012-0963-y

Gauthier, J. L., & Tank, D. W. (2018). A Dedicated Population for Reward Coding in the Hippocampus. *Neuron*, *99*(1), 179-193.e7. https://doi.org/https://doi.org/10.1016/j.neuron.2018.06.008

Ge, P., Dawson, V. L., & Dawson, T. M. (2020). PINK1 and Parkin mitochondrial quality control: a source of regional vulnerability in Parkinson's disease. *Molecular Neurodegeneration*, *15*(1), 20. https://doi.org/10.1186/s13024-020-00367-7

Gerfen, C R. (2000). Molecular effects of dopamine on striatal-projection pathways. *Trends in Neurosciences*, *23*(10 Suppl), S64-70. https://doi.org/10.1016/s1471-1931(00)00019-7

Gerfen, C R, Engber, T. M., Mahan, L. C., Susel, Z., Chase, T. N., Monsma, F. J. J., & Sibley, D. R. (1990). D1 and D2 dopamine receptor-regulated gene expression of striatonigral and striatopallidal neurons. *Science (New York, N.Y.)*, *250*(4986), 1429–1432. https://doi.org/10.1126/science.2147780

Gerfen, Charles R, & Surmeier, D. J. (2011). Modulation of striatal projection systems by dopamine. *Annual Review of Neuroscience*, *34*, 441–466. https://doi.org/10.1146/annurev-neuro-061010-113641

Gerlach, M., Double, K., Arzberger, T., Leblhuber, F., Tatschner, T., & Riederer, P. (2003). Dopamine receptor agonists in current clinical use: comparative dopamine receptor binding profiles defined in the human striatum. *Journal of Neural Transmission (Vienna, Austria : 1996)*, *110*(10), 1119–1127. https://doi.org/10.1007/s00702-003-0027-5

Ghanbarian, E., & Motamedi, F. (2013). Ventral tegmental area inactivation suppresses the expression of CA1 long term potentiation in anesthetized rat. *PloS One*, *8*(3), e58844. https://doi.org/10.1371/journal.pone.0058844

Ghiglieri, V., Calabrese, V., & Calabresi, P. (2018). Alpha-Synuclein: From Early Synaptic Dysfunction to Neurodegeneration. *Frontiers in Neurology*, *9*, 295. https://doi.org/10.3389/fneur.2018.00295

Giasson, B. I., Duda, J. E., Quinn, S. M., Zhang, B., Trojanowski, J. Q., & Lee, V. M.-Y. (2002). Neuronal α-Synucleinopathy with Severe Movement Disorder in Mice Expressing A53T Human α-Synuclein. *Neuron*, *34*(4), 521–533. https://doi.org/10.1016/S0896-6273(02)00682-7

Giguère, N., Burke Nanni, S., & Trudeau, L.-E. (2018). On Cell Loss and Selective Vulnerability of Neuronal Populations in Parkinson's Disease . In *Frontiers in Neurology* (Vol. 9, p. 455). https://www.frontiersin.org/article/10.3389/fneur.2018.00455

Gillet, L. C., Navarro, P., Tate, S., Röst, H., Selevsek, N., Reiter, L., Bonner, R., & Aebersold, R. (2012). Targeted data extraction of the MS/MS spectra generated by data-independent acquisition: a new concept for consistent and accurate proteome analysis. *Molecular & Cellular Proteomics : MCP*, *11*(6), O111.016717. https://doi.org/10.1074/mcp.O111.016717

Giordano, N., Iemolo, A., Mancini, M., Cacace, F., De Risi, M., Latagliata, E. C., Ghiglieri, V., Bellenchi, G. C., Puglisi-Allegra, S., Calabresi, P., Picconi, B., & De Leonibus, E. (2018). Motor learning and metaplasticity in striatal neurons: relevance for Parkinson's disease. *Brain*, *141*(2), 505–520. https://doi.org/10.1093/brain/awx351

Gitler, A. D., Bevis, B. J., Shorter, J., Strathearn, K. E., Hamamichi, S., Su, L. J., Caldwell, K. A., Caldwell, G. A., Rochet, J.-C.,

McCaffery, J. M., Barlowe, C., & Lindquist, S. (2008). The Parkinson's disease protein α-synuclein disrupts cellular Rab homeostasis. *Proceedings of the National Academy of Sciences*, *105*(1), 145 LP – 150. https://doi.org/10.1073/pnas.0710685105

Global, regional, and national burden of Parkinson's disease, 1990-2016: a systematic analysis for the Global Burden of Disease Study 2016. (2018). *The Lancet. Neurology*, *17*(11), 939–953. https://doi.org/10.1016/S1474-4422(18)30295-3

Gómez-Benito, M., Granado, N., García-Sanz, P., Michel, A., Dumoulin, M., & Moratalla, R. (2020). Modeling Parkinson's Disease With the Alpha-Synuclein Protein. *Frontiers in Pharmacology*, *11*, 356. https://doi.org/10.3389/fphar.2020.00356

González-Redondo, R., García-García, D., Clavero, P., Gasca-Salas, C., García-Eulate, R., Zubieta, J. L., Arbizu, J., Obeso, J. A., & Rodríguez-Oroz, M. C. (2014). Grey matter hypometabolism and atrophy in Parkinson's disease with cognitive impairment: a two-step process. *Brain : A Journal of Neurology*, *137*(Pt 8), 2356–2367. https://doi.org/10.1093/brain/awu159

González-Rodríguez, P., Zampese, E., Stout, K. A., Guzman, J. N., Ilijic, E., Yang, B., Tkatch, T., Stavarache, M. A., Wokosin, D. L., Gao, L., Kaplitt, M. G., López-Barneo, J., Schumacker, P. T., & Surmeier, D. J. (2021). Disruption of mitochondrial complex I induces progressive parkinsonism. *Nature*. https://doi.org/10.1038/s41586-021-04059-0

Gorbatyuk, O. S., Li, S., Sullivan, L. F., Chen, W., Kondrikova, G., Manfredsson, F. P., Mandel, R. J., & Muzyczka, N. (2008). The phosphorylation state of Ser-129 in human α-synuclein determines neurodegeneration in a rat model of Parkinson disease. *Proceedings of the National Academy of Sciences*, *105*(2), 763 LP – 768. https://doi.org/10.1073/pnas.0711053105

Goto, Y., & Grace, A. A. (2005). Dopaminergic modulation of limbic and cortical drive of nucleus accumbens in goal-directed behavior. *Nature Neuroscience*, *8*(6), 805–812. https://doi.org/10.1038/nn1471

Goto, Y., & Grace, A. A. (2008). Limbic and cortical information processing in the nucleus accumbens. *Trends in Neurosciences*, *31*(11), 552–558. https://doi.org/10.1016/j.tins.2008.08.002

Grace, A. A., Floresco, S. B., Goto, Y., & Lodge, D. J. (2007). Regulation of firing of dopaminergic neurons and control of goal-directed behaviors. *Trends in Neurosciences*, *30*(5), 220–227. https://doi.org/10.1016/j.tins.2007.03.003

Granado, N., Ortiz, O., Suárez, L. M., Martín, E. D., Ceña, V., Solís, J. M., & Moratalla, R. (2008). D1 but not D5 dopamine receptors are critical for LTP, spatial learning, and LTP-Induced arc and zif268 expression in the hippocampus. *Cerebral Cortex (New York, N.Y. : 1991)*, *18*(1), 1–12. https://doi.org/10.1093/cercor/bhm026

Gratwicke, J., Jahanshahi, M., & Foltynie, T. (2015). Parkinson's disease dementia: a neural networks perspective. *Brain : A Journal of Neurology*, *138*(Pt 6), 1454–1476. https://doi.org/10.1093/brain/awv104

Groenewegen, H. J. (2003). The basal ganglia and motor control. *Neural Plasticity*, *10*(1–2), 107–120. https://doi.org/10.1155/NP.2003.107

Groenewegen, H. J., & Uylings, H. B. M. (2010). Chapter 20 - Organization of Prefrontal-Striatal Connections. In H. Steiner & K. Y. B. T.-H. of B. N. Tseng (Eds.), *Handbook of Basal Ganglia Structure and Function* (Vol. 20, pp. 353–365). Elsevier. https://doi.org/https://doi.org/10.1016/B978-0-12-374767-9.00020-2

Gross, O. P., & von Gersdorff, H. (2016). Endocytosis: Recycling at synapses. *ELife*, *5*, e17692. https://doi.org/10.7554/eLife.17692

Group, P. D. M. E. D. C. (2014). Long-term effectiveness of dopamine agonists and monoamine oxidase B inhibitors compared with levodopa as initial treatment for Parkinson's disease (PD MED): a large, open-label, pragmatic randomised trial. *The Lancet*, *384*(9949), 1196–1205. https://doi.org/10.1016/S0140-6736(14)60683-8

Grubbs, R. D. (2008). Presynaptic and Postsynaptic Receptors. In P. M. Conn (Ed.), *Neuroscience in Medicine* (pp. 111–130). Humana Press. https://doi.org/10.1007/978-1-60327-455-5_6

Gundersen, H. J., & Jensen, E. B. (1987). The efficiency of systematic sampling in stereology and its prediction. *Journal of Microscopy*, *147*(Pt 3), 229–263.

Guo, F., Zhao, J., Zhao, D., Wang, J., Wang, X., Feng, Z., Vreugdenhil, M., & Lu, C. (2017). Dopamine D4 receptor activation restores CA1 LTP in hippocampal slices from aged mice. *Aging Cell*, *16*(6), 1323–1333. https://doi.org/10.1111/acel.12666

Guo, J. T., Chen, A. Q., Kong, Q., Zhu, H., Ma, C. M., & Qin, C. (2008). Inhibition of Vesicular Monoamine Transporter-2 Activity in α-Synuclein Stably Transfected SH-SY5Y Cells. *Cellular and Molecular Neurobiology*, *28*(1), 35–47. https://doi.org/10.1007/s10571-007-9227-0

Gupta, R., Duff, M. C., Denburg, N. L., Cohen, N. J., Bechara, A., & Tranel, D. (2009). Declarative memory is critical for sustained advantageous complex decision-making. *Neuropsychologia*, *47*(7), 1686–1693. https://doi.org/https://doi.org/10.1016/j.neuropsychologia.2009.02.007

Gureviciene, I., Gurevicius, K., & Tanila, H. (2007). Role of α-synuclein in synaptic glutamate release. *Neurobiology of Disease*, *28*(1), 83–89. https://doi.org/https://doi.org/10.1016/j.nbd.2007.06.016

Gureviciene, I., Gurevicius, K., & Tanila, H. (2009). Aging and alpha-synuclein affect synaptic plasticity in the dentate gyrus. *Journal of Neural Transmission (Vienna, Austria : 1996)*, *116*(1), 13–22. https://doi.org/10.1007/s00702-008-0149-x

Håkansson, K., Galdi, S., Hendrick, J., Snyder, G., Greengard, P., & Fisone, G. (2006). Regulation of phosphorylation of the GluR1 AMPA receptor by dopamine D2 receptors. *Journal of Neurochemistry*, *96*(2), 482–488. https://doi.org/https://doi.org/10.1111/j.1471-4159.2005.03558.x

Hall, H., Jewett, M., Landeck, N., Nilsson, N., Schagerlöf, U., Leanza, G., & Kirik, D. (2013). Characterization of Cognitive Deficits in Rats Overexpressing Human Alpha-Synuclein in the Ventral Tegmental Area and Medial Septum Using Recombinant Adeno-Associated Viral Vectors. *PLOS ONE*, *8*(5), e64844. https://doi.org/10.1371/journal.pone.0064844

Hall, H., Reyes, S., Landeck, N., Bye, C., Leanza, G., Double, K., Thompson, L., Halliday, G., & Kirik, D. (2014). Hippocampal Lewy pathology and cholinergic dysfunction are associated with dementia in Parkinson's disease. *Brain*, *137*(9), 2493–2508. https://doi.org/10.1093/brain/awu193

Hall, S., Janelidze, S., Zetterberg, H., Brix, B., Mattsson, N., Surova, Y., Blennow, K., & Hansson, O. (2020). Cerebrospinal Fluid Levels of Neurogranin in Parkinsonian Disorders. *Movement Disorders*, *35*(3), 513–518. https://doi.org/https://doi.org/10.1002/mds.27950

Halliday, G. M., Leverenz, J. B., Schneider, J. S., & Adler, C. H. (2014). The neurobiological basis of cognitive impairment in Parkinson's disease. *Movement Disorders*, *29*(5), 634–650. https://doi.org/https://doi.org/10.1002/mds.25857

Hammad, H., & Wagner, J. J. (2006). Dopamine-Mediated Disinhibition in the CA1 Region of Rat Hippocampus via D₃ Receptor Activation. *Journal of Pharmacology and Experimental Therapeutics*, *316*(1), 113 LP – 120. https://doi.org/10.1124/jpet.105.091579

Han, Y., Zhang, Y., Kim, H., Grayson, V. S., Jovasevic, V., Ren, W., Centeno, M. V, Guedea, A. L., Meyer, M. A. A., Wu, Y., Gutruf, P., Surmeier, D. J., Gao, C., Martina, M., Apkarian, A. V, Rogers, J. A., & Radulovic, J. (2020). Excitatory VTA to DH projections provide a valence signal to memory circuits. *Nature Communications*, *11*(1), 1466. https://doi.org/10.1038/s41467-020-15035-z

Hansen, K. B., Yi, F., Perszyk, R. E., Furukawa, H., Wollmuth, L. P., Gibb, A. J., & Traynelis, S. F. (2018). Structure, function, and allosteric modulation of NMDA receptors. *Journal of General Physiology*, *150*(8), 1081–1105. https://doi.org/10.1085/jgp.201812032

Hayashi, Y., Shi, S.-H., Esteban, J. A., Piccini, A., Poncer, J.-C., & Malinow, R. (2000). Driving AMPA Receptors into Synapses by LTP and CaMKII: Requirement for GluR1 and PDZ Domain Interaction. *Science*, *287*(5461), 2262 LP – 2267. https://doi.org/10.1126/science.287.5461.2262

Hebb, D. O. (1949). The organization of behavior; a neuropsychological theory. In *The organization of behavior; a neuropsychological theory*. Wiley.

Hely, M. A., Morris, J. G. L., Reid, W. G. J., & Trafficante, R. (2005). Sydney Multicenter Study of Parkinson's disease: non-L-dopa-responsive problems dominate at 15 years. *Movement Disorders : Official Journal of the Movement Disorder Society*, *20*(2), 190–199. https://doi.org/10.1002/mds.20324

Herz, J., & Strickland, D. K. (2001). LRP: a multifunctional scavenger and signaling receptor. *The Journal of Clinical Investigation*, *108*(6), 779–784. https://doi.org/10.1172/JCI13992

Hirokawa, N., Noda, Y., Tanaka, Y., & Niwa, S. (2009). Kinesin superfamily motor proteins and intracellular transport. *Nature Reviews Molecular Cell Biology*, *10*(10), 682–696. https://doi.org/10.1038/nrm2774

Hirsch, L., Jette, N., Frolkis, A., Steeves, T., & Pringsheim, T. (2016). The Incidence of Parkinson's Disease: A Systematic Review and Meta-Analysis. *Neuroepidemiology*, *46*(4), 292–300. https://doi.org/10.1159/000445751

Hlushchenko, I., Koskinen, M., & Hotulainen, P. (2016). Dendritic spine actin dynamics in neuronal maturation and synaptic plasticity. *Cytoskeleton*, *73*(9), 435–441. https://doi.org/https://doi.org/10.1002/cm.21280

Ho, V. M., Lee, J.-A., & Martin, K. C. (2011). The cell biology of synaptic plasticity. *Science (New York, N.Y.)*, *334*(6056), 623–628. https://doi.org/10.1126/science.1209236

Holt, C. E., Martin, K. C., & Schuman, E. M. (2019). Local translation in neurons: visualization and function. *Nature Structural*

& Molecular Biology, *26*(7), 557–566. https://doi.org/10.1038/s41594-019-0263-5

Holtmaat, A., & Caroni, P. (2016). Functional and structural underpinnings of neuronal assembly formation in learning. *Nature Neuroscience*, *19*(12), 1553–1562. https://doi.org/10.1038/nn.4418

Homma, Y., & Fukuda, M. (2021). Knockout analysis of Rab6 effector proteins revealed the role of VPS52 in the secretory pathway. *Biochemical and Biophysical Research Communications*, *561*, 151–157. https://doi.org/https://doi.org/10.1016/j.bbrc.2021.05.009

Horak, M., Seabold, G. K., & Petralia, R. S. (2014). *Chapter Eight - Trafficking of Glutamate Receptors and Associated Proteins in Synaptic Plasticity* (V. Pickel & M. B. T.-T. S. Segal (Eds.); pp. 221–279). Academic Press. https://doi.org/https://doi.org/10.1016/B978-0-12-418675-0.00008-0

Hou, Y., Dan, X., Babbar, M., Wei, Y., Hasselbalch, S. G., Croteau, D. L., & Bohr, V. A. (2019). Ageing as a risk factor for neurodegenerative disease. *Nature Reviews Neurology*, *15*(10), 565–581. https://doi.org/10.1038/s41582-019-0244-7

Hu, Q., Ren, X., Liu, Y., Li, Z., Zhang, L., Chen, X., He, C., & Chen, J.-F. (2016). Aberrant adenosine A2A receptor signaling contributes to neurodegeneration and cognitive impairments in a mouse model of synucleinopathy. *Experimental Neurology*, *283*, 213–223. https://doi.org/https://doi.org/10.1016/j.expneurol.2016.05.040

Huang, Y. Y., & Kandel, E. R. (1995). D1/D5 receptor agonists induce a protein synthesis-dependent late potentiation in the CA1 region of the hippocampus. *Proceedings of the National Academy of Sciences*, *92*(7), 2446 LP – 2450. https://doi.org/10.1073/pnas.92.7.2446

Imbriani, P., Sciamanna, G., Santoro, M., Schirinzi, T., & Pisani, A. (2018). Promising rodent models in Parkinson's disease. *Parkinsonism & Related Disorders*, *46*, S10–S14. https://doi.org/https://doi.org/10.1016/j.parkreldis.2017.07.027

Incontro, S., Díaz-Alonso, J., Iafrati, J., Vieira, M., Asensio, C. S., Sohal, V. S., Roche, K. W., Bender, K. J., & Nicoll, R. A. (2018). The CaMKII/NMDA receptor complex controls hippocampal synaptic transmission by kinase-dependent and independent mechanisms. *Nature Communications*, *9*(1), 2069. https://doi.org/10.1038/s41467-018-04439-7

Irizarry, M. C., Growdon, W., Gomez-Isla, T., Newell, K., George, J. M., Clayton, D. F., & Hyman, B. T. (1998). Nigral and cortical Lewy bodies and dystrophic nigral neurites in Parkinson's disease and cortical Lewy body disease contain alpha-synuclein immunoreactivity. *Journal of Neuropathology and Experimental Neurology*, *57*(4), 334–337. https://doi.org/10.1097/00005072-199804000-00005

Irwin, D. J., Lee, V. M.-Y., & Trojanowski, J. Q. (2013). Parkinson's disease dementia: convergence of α-synuclein, tau and amyloid-β pathologies. *Nature Reviews Neuroscience*, *14*(9), 626–636. https://doi.org/10.1038/nrn3549

Jagmag, S. A., Tripathi, N., Shukla, S. D., Maiti, S., & Khurana, S. (2016). Evaluation of Models of Parkinson's Disease . In *Frontiers in Neuroscience* (Vol. 9, p. 503). https://www.frontiersin.org/article/10.3389/fnins.2015.00503

Jalali, M. S., Sarkaki, A., Farbood, Y., Azandeh, S. S., Mansouri, E., Ghasemi Dehcheshmeh, M., & Saki, G. (2020). Transplanted Wharton's jelly mesenchymal stem cells improve memory and brain hippocampal electrophysiology in rat model of Parkinson's disease. *Journal of Chemical Neuroanatomy*, *110*, 101865. https://doi.org/10.1016/j.jchemneu.2020.101865

Janezic, S., Threlfell, S., Dodson, P. D., Dowie, M. J., Taylor, T. N., Potgieter, D., Parkkinen, L., Senior, S. L., Anwar, S., Ryan, B., Deltheil, T., Kosillo, P., Cioroch, M., Wagner, K., Ansorge, O., Bannerman, D. M., Bolam, J. P., Magill, P. J., Cragg, S. J., & Wade-Martins, R. (2013). Deficits in dopaminergic transmission precede neuron loss and dysfunction in a new Parkinson model. *Proceedings of the National Academy of Sciences of the United States of America*, *110*(42), E4016-25. https://doi.org/10.1073/pnas.1309143110

Jankovic, J. (2008). Parkinson's disease: clinical features and diagnosis. *Journal of Neurology, Neurosurgery, and Psychiatry*, *79*(4), 368–376. https://doi.org/10.1136/jnnp.2007.131045

Jay, T. M. (2003). Dopamine: a potential substrate for synaptic plasticity and memory mechanisms. *Progress in Neurobiology*, *69*(6), 375–390.

Jellinger, K. A. (2009). Formation and development of Lewy pathology: a critical update. *Journal of Neurology*, *256*(3), 270–279. https://doi.org/10.1007/s00415-009-5243-y

Jimenez-Urbieta, H., Gago, B., Quiroga-Varela, A., Rodriguez-Chinchilla, T., Merino-Galan, L., Oregi, A., Belloso-Iguerategui, A., Delgado-Alvarado, M., Navalpotro-Gomez, I., Marin, C., Fernagut, P.-O., & Rodriguez-Oroz, M. C. (2018). Pramipexole-induced impulsivity in mildparkinsonian rats: a model of impulse control disorders in Parkinson's disease. *Neurobiology of Aging*, *75*, 126–135. https://doi.org/10.1016/j.neurobiolaging.2018.11.021

Joel, D., & Weiner, I. (2000). The connections of the dopaminergic system with the striatum in rats and primates: an analysis with respect to the functional and compartmental organization of the striatum. *Neuroscience*, *96*(3), 451–474.

https://doi.org/https://doi.org/10.1016/S0306-4522(99)00575-8

Jokinen, P., Scheinin, N. M., Aalto, S., Någren, K., Savisto, N., Parkkola, R., Rokka, J., Haaparanta, M., Röyttä, M., & Rinne, J. O. (2010). [11C]PIB-, [18F]FDG-PET and MRI imaging in patients with Parkinson's disease with and without dementia. *Parkinsonism & Related Disorders*, *16*(10), 666–670. https://doi.org/https://doi.org/10.1016/j.parkreldis.2010.08.021

Jones, E. G. (1999). Colgi, Cajal and the Neuron Doctrine. *Journal of the History of the Neurosciences*, *8*(2), 170–178. https://doi.org/10.1076/jhin.8.2.170.1838

Joseph, S., Schulz, J. B., & Stegmüller, J. (2018). Mechanistic contributions of FBXO7 to Parkinson disease. *Journal of Neurochemistry*, *144*(2), 118–127. https://doi.org/https://doi.org/10.1111/jnc.14253

Ju, W., Morishita, W., Tsui, J., Gaietta, G., Deerinck, T. J., Adams, S. R., Garner, C. C., Tsien, R. Y., Ellisman, M. H., & Malenka, R. C. (2004). Activity-dependent regulation of dendritic synthesis and trafficking of AMPA receptors. *Nature Neuroscience*, *7*(3), 244–253. https://doi.org/10.1038/nn1189

Kandiah, N., Zainal, N. H., Narasimhalu, K., Chander, R. J., Ng, A., Mak, E., Au, W. L., Sitoh, Y. Y., Nadkarni, N., & Tan, L. C. S. (2014). Hippocampal volume and white matter disease in the prediction of dementia in Parkinson's disease. *Parkinsonism & Related Disorders*, *20*(11), 1203–1208. https://doi.org/https://doi.org/10.1016/j.parkreldis.2014.08.024

Kapitein, L. C., & Hoogenraad, C. C. (2015). Building the Neuronal Microtubule Cytoskeleton. *Neuron*, *87*(3), 492–506. https://doi.org/10.1016/j.neuron.2015.05.046

Kasongo, D. W., de Leo, G., Vicario, N., Leanza, G., & Legname, G. (2020). Chronic α-Synuclein Accumulation in Rat Hippocampus Induces Lewy Bodies Formation and Specific Cognitive Impairments. *Eneuro*, *7*(3), ENEURO.0009-20.2020. https://doi.org/10.1523/ENEURO.0009-20.2020

Keable, R., Leshchyns'ka, I., & Sytnyk, V. (2020). Trafficking and Activity of Glutamate and GABA Receptors: Regulation by Cell Adhesion Molecules. *The Neuroscientist*, *26*(5–6), 415–437. https://doi.org/10.1177/1073858420921117

Kehagia, A. A., Barker, R. A., & Robbins, T. W. (2010). Neuropsychological and clinical heterogeneity of cognitive impairment and dementia in patients with Parkinson's disease. *The Lancet. Neurology*, *9*(12), 1200–1213. https://doi.org/10.1016/S1474-4422(10)70212-X

Kelleher III, R. J., Govindarajan, A., Jung, H.-Y., Kang, H., & Tonegawa, S. (2004). Translational Control by MAPK Signaling in Long-Term Synaptic Plasticity and Memory. *Cell*, *116*(3), 467–479. https://doi.org/10.1016/S0092-8674(04)00115-1

Kempadoo, K. A., Mosharov, E. V, Choi, S. J., Sulzer, D., & Kandel, E. R. (2016). Dopamine release from the locus coeruleus to the dorsal hippocampus promotes spatial learning and memory. *Proceedings of the National Academy of Sciences*, *113*(51), 14835 LP – 14840. https://doi.org/10.1073/pnas.1616515114

Kim, H. J., Kim, M., Kang, B., Yun, S., Ryeo, S. E., Hwang, D., & Kim, J.-H. (2019). Systematic analysis of expression signatures of neuronal subpopulations in the VTA. *Molecular Brain*, *12*(1), 110. https://doi.org/10.1186/s13041-019-0530-8

Kim, Y., Jang, Y.-N., Kim, J.-Y., Kim, N., Noh, S., Kim, H., Queenan, B. N., Bellmore, R., Mun, J. Y., Park, H., Rah, J. C., Pak, D. T. S., & Lee, K. J. (2020). Microtubule-associated protein 2 mediates induction of long-term potentiation in hippocampal neurons. *The FASEB Journal*, *34*(5), 6965–6983. https://doi.org/https://doi.org/10.1096/fj.201902122RR

Kirik, D., Rosenblad, C., Burger, C., Lundberg, C., Johansen, T. E., Muzyczka, N., Mandel, R. J., & Björklund, A. (2002). Parkinson-Like Neurodegeneration Induced by Targeted Overexpression of α-Synuclein in the Nigrostriatal System. *The Journal of Neuroscience*, *22*(7), 2780 LP – 2791. https://doi.org/10.1523/JNEUROSCI.22-07-02780.2002

Kitada, T., Pisani, A., Karouani, M., Haburcak, M., Martella, G., Tscherter, A., Platania, P., Wu, B., Pothos, E. N., & Shen, J. (2009). Impaired dopamine release and synaptic plasticity in the striatum of Parkin−/− mice. *Journal of Neurochemistry*, *110*(2), 613–621. https://doi.org/https://doi.org/10.1111/j.1471-4159.2009.06152.x

Kitada, T., Pisani, A., Porter, D. R., Yamaguchi, H., Tscherter, A., Martella, G., Bonsi, P., Zhang, C., Pothos, E. N., & Shen, J. (2007). Impaired dopamine release and synaptic plasticity in the striatum of PINK1-deficient mice. *Proceedings of the National Academy of Sciences*, *104*(27), 11441 LP – 11446. https://doi.org/10.1073/pnas.0702717104

Klein, R. L., King, M. A., Hamby, M. E., & Meyer, E. M. (2002). Dopaminergic Cell Loss Induced by Human A30P α-Synuclein Gene Transfer to the Rat Substantia Nigra. *Human Gene Therapy*, *13*(5), 605–612. https://doi.org/10.1089/10430340252837206

Knecht, S., Breitenstein, C., Bushuven, S., Wailke, S., Kamping, S., Flöel, A., Zwitserlood, P., & Ringelstein, E. B. (2004).

Levodopa: faster and better word learning in normal humans. *Annals of Neurology*, *56*(1), 20–26. https://doi.org/10.1002/ana.20125

Kneussel, M., & Wagner, W. (2013). Myosin motors at neuronal synapses: drivers of membrane transport and actin dynamics. *Nature Reviews Neuroscience*, *14*(4), 233–247. https://doi.org/10.1038/nrn3445

Koopmans, F., van Nierop, P., Andres-Alonso, M., Byrnes, A., Cijsouw, T., Coba, M. P., Cornelisse, L. N., Farrell, R. J., Goldschmidt, H. L., Howrigan, D. P., Hussain, N. K., Imig, C., de Jong, A. P. H., Jung, H., Kohansalnodehi, M., Kramarz, B., Lipstein, N., Lovering, R. C., MacGillavry, H., … Verhage, M. (2019). SynGO: An Evidence-Based, Expert-Curated Knowledge Base for the Synapse. *Neuron*, *103*(2), 217-234.e4. https://doi.org/10.1016/j.neuron.2019.05.002

Koprich, J. B., Johnston, T. H., Reyes, M. G., Sun, X., & Brotchie, J. M. (2010). Expression of human A53T alpha-synuclein in the rat substantia nigra using a novel AAV1/2 vector produces a rapidly evolving pathology with protein aggregation, dystrophic neurite architecture and nigrostriatal degeneration with potential to model the pat. *Molecular Neurodegeneration*, *5*(1), 43. https://doi.org/10.1186/1750-1326-5-43

Koprich, J. B., Kalia, L. V, & Brotchie, J. M. (2017). Animal models of α-synucleinopathy for Parkinson disease drug development. *Nature Reviews. Neuroscience*, *18*(9), 515–529. https://doi.org/10.1038/nrn.2017.75

Kordower, J. H., Olanow, C. W., Dodiya, H. B., Chu, Y., Beach, T. G., Adler, C. H., Halliday, G. M., & Bartus, R. T. (2013). Disease duration and the integrity of the nigrostriatal system in Parkinson's disease. *Brain : A Journal of Neurology*, *136*(Pt 8), 2419–2431. https://doi.org/10.1093/brain/awt192

Kramer, M. L., & Schulz-Schaeffer, W. J. (2007). Presynaptic α-Synuclein Aggregates, Not Lewy Bodies, Cause Neurodegeneration in Dementia with Lewy Bodies. *The Journal of Neuroscience*, *27*(6), 1405 LP – 1410. https://doi.org/10.1523/JNEUROSCI.4564-06.2007

Kravitz, A. V, Freeze, B. S., Parker, P. R. L., Kay, K., Thwin, M. T., Deisseroth, K., & Kreitzer, A. C. (2010). Regulation of parkinsonian motor behaviours by optogenetic control of basal ganglia circuitry. *Nature*, *466*(7306), 622–626. https://doi.org/10.1038/nature09159

Kristensen, A. S., Jenkins, M. A., Banke, T. G., Schousboe, A., Makino, Y., Johnson, R. C., Huganir, R., & Traynelis, S. F. (2011). Mechanism of Ca2+/calmodulin-dependent kinase II regulation of AMPA receptor gating. *Nature Neuroscience*, *14*(6), 727–735. https://doi.org/10.1038/nn.2804

La Vitola, P., Balducci, C., Cerovic, M., Santamaria, G., Brandi, E., Grandi, F., Caldinelli, L., Colombo, L., Morgese, M. G., Trabace, L., Pollegioni, L., Albani, D., & Forloni, G. (2018). Alpha-synuclein oligomers impair memory through glial cell activation and via Toll-like receptor 2. *Brain, Behavior, and Immunity*, *69*, 591–602. https://doi.org/https://doi.org/10.1016/j.bbi.2018.02.012

Lai, Y., Kim, S., Varkey, J., Lou, X., Song, J.-K., Diao, J., Langen, R., & Shin, Y.-K. (2014). Nonaggregated α-synuclein influences SNARE-dependent vesicle docking via membrane binding. *Biochemistry*, *53*(24), 3889–3896. https://doi.org/10.1021/bi5002536

Lanciego, J. L., Luquin, N., & Obeso, J. A. (2012). Functional neuroanatomy of the basal ganglia. *Cold Spring Harbor Perspectives in Medicine*, *2*(12), a009621–a009621. https://doi.org/10.1101/cshperspect.a009621

Larsen, K. E., Schmitz, Y., Troyer, M. D., Mosharov, E., Dietrich, P., Quazi, A. Z., Savalle, M., Nemani, V., Chaudhry, F. A., Edwards, R. H., Stefanis, L., & Sulzer, D. (2006). α-Synuclein Overexpression in PC12 and Chromaffin Cells Impairs Catecholamine Release by Interfering with a Late Step in Exocytosis. *The Journal of Neuroscience*, *26*(46), 11915 LP – 11922. https://doi.org/10.1523/JNEUROSCI.3821-06.2006

Lee, F. J. S., Xue, S., Pei, L., Vukusic, B., Chéry, N., Wang, Y., Wang, Y. T., Niznik, H. B., Yu, X., & Liu, F. (2002). Dual Regulation of NMDA Receptor Functions by Direct Protein-Protein Interactions with the Dopamine D1 Receptor. *Cell*, *111*(2), 219–230. https://doi.org/10.1016/S0092-8674(02)00962-5

LeGates, T. A., Kvarta, M. D., Tooley, J. R., Francis, T. C., Lobo, M. K., Creed, M. C., & Thompson, S. M. (2018). Reward behaviour is regulated by the strength of hippocampus–nucleus accumbens synapses. *Nature*, *564*(7735), 258–262. https://doi.org/10.1038/s41586-018-0740-8

Lehr, A. B., Kumar, A., Tetzlaff, C., Hafting, T., Fyhn, M., & Stöber, T. M. (2021). CA2 beyond social memory: Evidence for a fundamental role in hippocampal information processing. *Neuroscience & Biobehavioral Reviews*, *126*, 398–412. https://doi.org/https://doi.org/10.1016/j.neubiorev.2021.03.020

Lemon, N., & Manahan-Vaughan, D. (2006). Dopamine D₁/D₅ Receptors Gate the Acquisition of Novel Information through Hippocampal Long-Term Potentiation and Long-Term Depression. *The Journal of Neuroscience*, *26*(29), 7723 LP – 7729. https://doi.org/10.1523/JNEUROSCI.1454-06.2006

Lepeta, K., Lourenco, M. V, Schweitzer, B. C., Martino Adami, P. V, Banerjee, P., Catuara-Solarz, S., de La Fuente Revenga,

M., Guillem, A. M., Haidar, M., Ijomone, O. M., Nadorp, B., Qi, L., Perera, N. D., Refsgaard, L. K., Reid, K. M., Sabbar, M., Sahoo, A., Schaefer, N., Sheean, R. K., … Seidenbecher, C. (2016). Synaptopathies: synaptic dysfunction in neurological disorders – A review from students to students. *Journal of Neurochemistry*, *138*(6), 785–805. https://doi.org/https://doi.org/10.1111/jnc.13713

Lerche, S., Sjödin, S., Brinkmalm, A., Blennow, K., Wurster, I., Roeben, B., Zimmermann, M., Hauser, A.-K., Liepelt-Scarfone, I., Waniek, K., Lachmann, I., Gasser, T., Zetterberg, H., & Brockmann, K. (2021). CSF Protein Level of Neurotransmitter Secretion, Synaptic Plasticity, and Autophagy in PD and DLB. *Movement Disorders*, *n/a*(n/a). https://doi.org/https://doi.org/10.1002/mds.28704

Lesage, S., Drouet, V., Majounie, E., Deramecourt, V., Jacoupy, M., Nicolas, A., Cormier-Dequaire, F., Hassoun, S. M., Pujol, C., Ciura, S., Erpapazoglou, Z., Usenko, T., Maurage, C.-A., Sahbatou, M., Liebau, S., Ding, J., Bilgic, B., Emre, M., Erginel-Unaltuna, N., … Brice, A. (2016). Loss of VPS13C Function in Autosomal-Recessive Parkinsonism Causes Mitochondrial Dysfunction and Increases PINK1/Parkin-Dependent Mitophagy. *The American Journal of Human Genetics*, *98*(3), 500–513. https://doi.org/10.1016/j.ajhg.2016.01.014

Lesage, S., Dürr, A., Tazir, M., Lohmann, E., Leutenegger, A.-L., Janin, S., Pollak, P., & Brice, A. (2006). LRRK2 G2019S as a cause of Parkinson's disease in North African Arabs. In *The New England journal of medicine* (Vol. 354, Issue 4, pp. 422–423). https://doi.org/10.1056/NEJMc055540

LeWitt, P. A., & Fahn, S. (2016). Levodopa therapy for Parkinson disease. *Neurology*, *86*(14 Supplement 1), S3 LP-S12. https://doi.org/10.1212/WNL.0000000000002509

Lewy, F. H. (1912). Handbuch der Neurologie. *Berlin: Julius Springer*.

Li, H., Liu, S., Sun, X., Yang, J., Yang, Z., Shen, H., Li, X., Liu, Y., & Chen, G. (2018). Critical role for Annexin A7 in secondary brain injury mediated by its phosphorylation after experimental intracerebral hemorrhage in rats. *Neurobiology of Disease*, *110*, 82–92. https://doi.org/https://doi.org/10.1016/j.nbd.2017.11.012

Liauw, J., Wu, L.-J., & Zhuo, M. (2005). Calcium-Stimulated Adenylyl Cyclases Required for Long-Term Potentiation in the Anterior Cingulate Cortex. *Journal of Neurophysiology*, *94*(1), 878–882. https://doi.org/10.1152/jn.01205.2004

Licker, V., Turck, N., Kövari, E., Burkhardt, K., Côte, M., Surini-Demiri, M., Lobrinus, J. A., Sanchez, J.-C., & Burkhard, P. R. (2014). Proteomic analysis of human substantia nigra identifies novel candidates involved in Parkinson's disease pathogenesis. *PROTEOMICS*, *14*(6), 784–794. https://doi.org/https://doi.org/10.1002/pmic.201300342

Lim, Y., Kehm, V. M., Lee, E. B., Soper, J. H., Li, C., Trojanowski, J. Q., & Lee, V. M.-Y. (2011). α-Syn Suppression Reverses Synaptic and Memory Defects in a Mouse Model of Dementia with Lewy Bodies. *The Journal of Neuroscience*, *31*(27), 10076 LP – 10087. https://doi.org/10.1523/JNEUROSCI.0618-11.2011

Lin, G., Lee, P.-T., Chen, K., Mao, D., Tan, K. L., Zuo, Z., Lin, W.-W., Wang, L., & Bellen, H. J. (2018). Phospholipase PLA2G6, a Parkinsonism-Associated Gene, Affects Vps26 and Vps35, Retromer Function, and Ceramide Levels, Similar to α-Synuclein Gain. *Cell Metabolism*, *28*(4), 605-618.e6. https://doi.org/10.1016/j.cmet.2018.05.019

Lisman, J. E., & Grace, A. A. (2005). The hippocampal-VTA loop: controlling the entry of information into long-term memory. *Neuron*, *46*(5), 703–713. https://doi.org/10.1016/j.neuron.2005.05.002

Lisman, J., Grace, A. A., & Duzel, E. (2011). A neoHebbian framework for episodic memory; role of dopamine-dependent late LTP. *Trends in Neurosciences*, *34*(10), 536–547. https://doi.org/10.1016/j.tins.2011.07.006

Lisman, J., Yasuda, R., & Raghavachari, S. (2012). Mechanisms of CaMKII action in long-term potentiation. *Nature Reviews Neuroscience*, *13*(3), 169–182. https://doi.org/10.1038/nrn3192

Liu, Q., Trotter, J., Zhang, J., Peters, M. M., Cheng, H., Bao, J., Han, X., Weeber, E. J., & Bu, G. (2010). Neuronal LRP1 Knockout in Adult Mice Leads to Impaired Brain Lipid Metabolism and Progressive, Age-Dependent Synapse Loss and Neurodegeneration. *The Journal of Neuroscience*, *30*(50), 17068 LP – 17078. https://doi.org/10.1523/JNEUROSCI.4067-10.2010

Longhena, F., Faustini, G., Spillantini, M. G., & Bellucci, A. (2019). Living in Promiscuity: The Multiple Partners of Alpha-Synuclein at the Synapse in Physiology and Pathology. *International Journal of Molecular Sciences*, *20*(1), 141. https://doi.org/10.3390/ijms20010141

Lou, X., Kim, J., Hawk, B. J., & Shin, Y.-K. (2017). α-Synuclein may cross-bridge v-SNARE and acidic phospholipids to facilitate SNARE-dependent vesicle docking. *The Biochemical Journal*, *474*(12), 2039–2049. https://doi.org/10.1042/BCJ20170200

Lu, J., Sun, F., Ma, H., Qing, H., & Deng, Y. (2015). Comparison between α-synuclein wild-type and A53T mutation in a progressive Parkinson's disease model. *Biochemical and Biophysical Research Communications*, *464*(4), 988–993.

https://doi.org/10.1016/j.bbrc.2015.07.007

Lu, K.-W., Yang, J., Hsieh, C.-L., Hsu, Y.-C., & Lin, Y.-W. (2017). Electroacupuncture restores spatial learning and downregulates phosphorylated N-methyl-D-aspartate receptors in a mouse model of Parkinson's disease. *Acupuncture in Medicine : Journal of the British Medical Acupuncture Society*, *35*(2), 133–141. https://doi.org/10.1136/acupmed-2015-011041

Lu, W., Isozaki, K., Roche, K. W., & Nicoll, R. A. (2010). Synaptic targeting of AMPA receptors is regulated by a CaMKII site in the first intracellular loop of GluA1. *Proceedings of the National Academy of Sciences*, *107*(51), 22266 LP – 22271. https://doi.org/10.1073/pnas.1016289107

Lu, W., Shi, Y., Jackson, A. C., Bjorgan, K., During, M. J., Sprengel, R., Seeburg, P. H., & Nicoll, R. A. (2009). Subunit Composition of Synaptic AMPA Receptors Revealed by a Single-Cell Genetic Approach. *Neuron*, *62*(2), 254–268. https://doi.org/https://doi.org/10.1016/j.neuron.2009.02.027

Ludtmann, M. H. R., Angelova, P. R., Horrocks, M. H., Choi, M. L., Rodrigues, M., Baev, A. Y., Berezhnov, A. V, Yao, Z., Little, D., Banushi, B., Al-Menhali, A. S., Ranasinghe, R. T., Whiten, D. R., Yapom, R., Dolt, K. S., Devine, M. J., Gissen, P., Kunath, T., Jaganjac, M., … Gandhi, S. (2018). α-synuclein oligomers interact with ATP synthase and open the permeability transition pore in Parkinson's disease. *Nature Communications*, *9*(1), 2293. https://doi.org/10.1038/s41467-018-04422-2

Ludtmann, M. H. R., Angelova, P. R., Ninkina, N. N., Gandhi, S., Buchman, V. L., & Abramov, A. Y. (2016). Monomeric Alpha-Synuclein Exerts a Physiological Role on Brain ATP Synthase. *The Journal of Neuroscience*, *36*(41), 10510 LP – 10521. https://doi.org/10.1523/JNEUROSCI.1659-16.2016

Luk, K. C., Kehm, V., Carroll, J., Zhang, B., O'Brien, P., Trojanowski, J. Q., & Lee, V. M.-Y. (2012a). Pathological α-Synuclein Transmission Initiates Parkinson-like Neurodegeneration in Nontransgenic Mice. *Science*, *338*(6109), 949 LP – 953. https://doi.org/10.1126/science.1227157

Luk, K. C., Kehm, V. M., Zhang, B., O'Brien, P., Trojanowski, J. Q., & Lee, V. M. Y. (2012b). Intracerebral inoculation of pathological α-synuclein initiates a rapidly progressive neurodegenerative α-synucleinopathy in mice. *The Journal of Experimental Medicine*, *209*(5), 975–986. https://doi.org/10.1084/jem.20112457

Lundblad, M., Decressac, M., Mattsson, B., & Björklund, A. (2012). Impaired neurotransmission caused by overexpression of α-synuclein in nigral dopamine neurons. *Proceedings of the National Academy of Sciences*, *109*(9), 3213 LP – 3219. https://doi.org/10.1073/pnas.1200575109

Ma, Y., & Eidelberg, D. (2007). Functional imaging of cerebral blood flow and glucose metabolism in Parkinson's disease and Huntington's disease. *Molecular Imaging and Biology*, *9*(4), 223–233. https://doi.org/10.1007/s11307-007-0085-4

Madeo, G., Schirinzi, T., Martella, G., Latagliata, E. C., Puglisi, F., Shen, J., Valente, E. M., Federici, M., Mercuri, N. B., Puglisi-Allegra, S., Bonsi, P., & Pisani, A. (2014). PINK1 heterozygous mutations induce subtle alterations in dopamine-dependent synaptic plasticity. *Movement Disorders : Official Journal of the Movement Disorder Society*, *29*(1), 41–53. https://doi.org/10.1002/mds.25724

Maingay, M., Romero-Ramos, M., Carta, M., & Kirik, D. (2006). Ventral tegmental area dopamine neurons are resistant to human mutant alpha-synuclein overexpression. *Neurobiology of Disease*, *23*(3), 522–532. https://doi.org/https://doi.org/10.1016/j.nbd.2006.04.007

Mak, E., Su, L., Williams, G. B., Firbank, M. J., Lawson, R. A., Yarnall, A. J., Duncan, G. W., Owen, A. M., Khoo, T. K., Brooks, D. J., Rowe, J. B., Barker, R. A., Burn, D. J., & O'Brien, J. T. (2015). Baseline and longitudinal grey matter changes in newly diagnosed Parkinson's disease: ICICLE-PD study. *Brain*, *138*(10), 2974–2986. https://doi.org/10.1093/brain/awv211

Mangiavacchi, S., & Wolf, M. E. (2004). D1 dopamine receptor stimulation increases the rate of AMPA receptor insertion onto the surface of cultured nucleus accumbens neurons through a pathway dependent on protein kinase A. *Journal of Neurochemistry*, *88*(5), 1261–1271. https://doi.org/https://doi.org/10.1046/j.1471-4159.2003.02248.x

Marmion, D. J., & Kordower, J. H. (2018). α-Synuclein nonhuman primate models of Parkinson's disease. *Journal of Neural Transmission (Vienna, Austria : 1996)*, *125*(3), 385–400. https://doi.org/10.1007/s00702-017-1720-0

Martín-Bastida, A., Delgado-Alvarado, M., Navalpotro-Gómez, I., & Rodríguez-Oroz, M. C. (2021). Imaging Cognitive Impairment and Impulse Control Disorders in Parkinson's Disease. In *Frontiers in neurology* (Vol. 12, p. 733570). https://doi.org/10.3389/fneur.2021.733570

Martin, Z. S., Neugebauer, V., Dineley, K. T., Kayed, R., Zhang, W., Reese, L. C., & Taglialatela, G. (2012). α-Synuclein oligomers oppose long-term potentiation and impair memory through a calcineurin-dependent mechanism: relevance to human synucleopathic diseases. *Journal of Neurochemistry*, *120*(3), 440–452. https://doi.org/https://doi.org/10.1111/j.1471-4159.2011.07576.x

Martínez-Fernández, R., Rodríguez-Rojas, R., Del Álamo, M., Hernández-Fernández, F., Pineda-Pardo, J. A., Dileone, M., Alonso-Frech, F., Foffani, G., Obeso, I., Gasca-Salas, C., de Luis-Pastor, E., Vela, L., & Obeso, J. A. (2018). Focused ultrasound subthalamotomy in patients with asymmetric Parkinson's disease: a pilot study. *The Lancet. Neurology*, *17*(1), 54–63. https://doi.org/10.1016/S1474-4422(17)30403-9

Masliah, E., Rockenstein, E., Mante, M., Crews, L., Spencer, B., Adame, A., Patrick, C., Trejo, M., Ubhi, K., Rohn, T. T., Mueller-Steiner, S., Seubert, P., Barbour, R., McConlogue, L., Buttini, M., Games, D., & Schenk, D. (2011). Passive Immunization Reduces Behavioral and Neuropathological Deficits in an Alpha-Synuclein Transgenic Model of Lewy Body Disease. *PLOS ONE*, *6*(4), e19338. https://doi.org/10.1371/journal.pone.0019338

Masliah, E., Rockenstein, E., Veinbergs, I., Mallory, M., Hashimoto, M., Takeda, A., Sagara, Y., Sisk, A., & Mucke, L. (2000). Dopaminergic Loss and Inclusion Body Formation in α-Synuclein Mice: Implications for Neurodegenerative Disorders. *Science*, *287*(5456), 1265 LP – 1269. https://doi.org/10.1126/science.287.5456.1265

Masuda-Suzukake, M., Nonaka, T., Hosokawa, M., Oikawa, T., Arai, T., Akiyama, H., Mann, D. M. A., & Hasegawa, M. (2013). Prion-like spreading of pathological α-synuclein in brain. *Brain*, *136*(4), 1128–1138. https://doi.org/10.1093/brain/awt037

Mateos-Aparicio, P., & Rodríguez-Moreno, A. (2020). *Calcium Dynamics and Synaptic Plasticity BT - Calcium Signaling* (M. S. Islam (Ed.); pp. 965–984). Springer International Publishing. https://doi.org/10.1007/978-3-030-12457-1_38

Matikainen-Ankney, B. A., Kezunovic, N., Menard, C., Flanigan, M. E., Zhong, Y., Russo, S. J., Benson, D. L., & Huntley, G. W. (2018). Parkinson's Disease-Linked LRRK2-G2019S Mutation Alters Synaptic Plasticity and Promotes Resilience to Chronic Social Stress in Young Adulthood. *The Journal of Neuroscience*, *38*(45), 9700 LP – 9711. https://doi.org/10.1523/JNEUROSCI.1457-18.2018

Matthews, D. C., Lerman, H., Lukic, A., Andrews, R. D., Mirelman, A., Wernick, M. N., Giladi, N., Strother, S. C., Evans, K. C., Cedarbaum, J. M., & Even-Sapir, E. (2018). FDG PET Parkinson's disease-related pattern as a biomarker for clinical trials in early stage disease. *NeuroImage. Clinical*, *20*, 572–579. https://doi.org/10.1016/j.nicl.2018.08.006

Matuskey, D., Tinaz, S., Wilcox, K. C., Naganawa, M., Toyonaga, T., Dias, M., Henry, S., Pittman, B., Ropchan, J., Nabulsi, N., Suridjan, I., Comley, R. A., Huang, Y., Finnema, S. J., & Carson, R. E. (2020). Synaptic Changes in Parkinson Disease Assessed with in vivo Imaging. *Annals of Neurology*, *87*(3), 329–338. https://doi.org/https://doi.org/10.1002/ana.25682

McNamara, C. G., & Dupret, D. (2017). Two sources of dopamine for the hippocampus. *Trends in Neurosciences*, *40*(7), 383–384. https://doi.org/10.1016/j.tins.2017.05.005

McNamara, C. G., Tejero-Cantero, Á., Trouche, S., Campo-Urriza, N., & Dupret, D. (2014). Dopaminergic neurons promote hippocampal reactivation and spatial memory persistence. *Nature Neuroscience*, *17*(12), 1658–1660. https://doi.org/10.1038/nn.3843

Meir, A., Ginsburg, S., Butkevich, A., Kachalsky, S. G., Kaiserman, I., Ahdut, R., Demirgoren, S., & Rahamimoff, R. (1999). Ion Channels in Presynaptic Nerve Terminals and Control of Transmitter Release. *Physiological Reviews*, *79*(3), 1019–1088. https://doi.org/10.1152/physrev.1999.79.3.1019

Meiser, J., Weindl, D., & Hiller, K. (2013). Complexity of dopamine metabolism. *Cell Communication and Signaling*, *11*(1), 34. https://doi.org/10.1186/1478-811X-11-34

Mencacci, N. E., Reynolds, R. H., Ruiz, S. G., Vandrovcova, J., Forabosco, P., Sánchez-Ferrer, A., Volpato, V., Weale, M. E., Bhatia, K. P., Webber, C., Hardy, J., Botía, J. A., & Ryten, M. (2020). Dystonia genes functionally converge in specific neurons and share neurobiology with psychiatric disorders. *Brain*, *143*(9), 2771–2787. https://doi.org/10.1093/brain/awaa217

Miller, S., Yasuda, M., Coats, J. K., Jones, Y., Martone, M. E., & Mayford, M. (2002). Disruption of Dendritic Translation of CaMKIIα Impairs Stabilization of Synaptic Plasticity and Memory Consolidation. *Neuron*, *36*(3), 507–519. https://doi.org/10.1016/S0896-6273(02)00978-9

Mondal, R., Campoy, A.-D. T., Liang, C., & Mukherjee, J. (2021). [18F]FDG PET/CT Studies in Transgenic Hualpha-Syn (A53T) Parkinson's Disease Mouse Model of α-Synucleinopathy . In *Frontiers in Neuroscience* (Vol. 15, p. 718). https://www.frontiersin.org/article/10.3389/fnins.2021.676257

Moraga-Amaro, R., González, H., Ugalde, V., Donoso-Ramos, J. P., Quintana-Donoso, D., Lara, M., Morales, B., Rojas, P., Pacheco, R., & Stehberg, J. (2016). Dopamine receptor D5 deficiency results in a selective reduction of hippocampal NMDA receptor subunit NR2B expression and impaired memory. *Neuropharmacology*, *103*, 222–235. https://doi.org/10.1016/j.neuropharm.2015.12.018

Morales, M., & Margolis, E. B. (2017). Ventral tegmental area: cellular heterogeneity, connectivity and behaviour. *Nature Reviews Neuroscience*, *18*(2), 73–85. https://doi.org/10.1038/nrn.2016.165

Moriguchi, S., Yabuki, Y., & Fukunaga, K. (2012). Reduced calcium/calmodulin-dependent protein kinase II activity in the hippocampus is associated with impaired cognitive function in MPTP-treated mice. *Journal of Neurochemistry*, *120*(4), 541–551. https://doi.org/10.1111/j.1471-4159.2011.07608.x

Murakoshi, H., Wang, H., & Yasuda, R. (2011). Local, persistent activation of Rho GTPases during plasticity of single dendritic spines. *Nature*, *472*(7341), 100–104. https://doi.org/10.1038/nature09823

Mutluay, S. U., Çınar, E., Yalçın Çakmaklı, G., Ulusoy, A., Elibol, B., & Tel, B. C. (2020). Modelling Non-motor Symptoms of Parkinson's Disease: AAV Mediated Overexpression of Alpha-synuclein in Rat Hippocampus and Basal Ganglia. *Turkish Journal of Neurology*, *26*(4), 322–329. https://doi.org/10.4274/tnd.2020.22308

Nagata, T., Redman, R. S., & Lakshman, R. (2010). Isolation of intact nuclei of high purity from mouse liver. *Analytical Biochemistry*, *398*(2), 178–184. https://doi.org/10.1016/j.ab.2009.11.017

Navakkode, S., Chew, K. C. M., Tay, S. J. N., Lin, Q., Behnisch, T., & Soong, T. W. (2017). Bidirectional modulation of hippocampal synaptic plasticity by Dopaminergic D4-receptors in the CA1 area of hippocampus. *Scientific Reports*, *7*(1), 15571. https://doi.org/10.1038/s41598-017-15917-1

Navalpotro-Gomez, I., Dacosta-Aguayo, R., Molinet-Dronda, F., Martin-Bastida, A., Botas-Peñin, A., Jimenez-Urbieta, H., Delgado-Alvarado, M., Gago, B., Quiroga-Varela, A., & Rodriguez-Oroz, M. C. (2019). Nigrostriatal dopamine transporter availability, and its metabolic and clinical correlates in Parkinson's disease patients with impulse control disorders. *European Journal of Nuclear Medicine and Molecular Imaging*, *46*(10), 2065–2076. https://doi.org/10.1007/s00259-019-04396-3

Navalpotro-Gomez, I., Kim, J., Paz-Alonso, P. M., Delgado-Alvarado, M., Quiroga-Varela, A., Jimenez-Urbieta, H., Carreiras, M., Strafella, A. P., & Rodriguez-Oroz, M. C. (2020). Disrupted salience network dynamics in Parkinson's disease patients with impulse control disorders. *Parkinsonism & Related Disorders*, *70*, 74–81. https://doi.org/10.1016/j.parkreldis.2019.12.009

Nelson, J. C., Stavoe, A. K. H., & Colón-Ramos, D. A. (2013). The actin cytoskeleton in presynaptic assembly. *Cell Adhesion & Migration*, *7*(4), 379–387. https://doi.org/10.4161/cam.24803

Nemani, V. M., Lu, W., Berge, V., Nakamura, K., Onoa, B., Lee, M. K., Chaudhry, F. A., Nicoll, R. A., & Edwards, R. H. (2010). Increased expression of alpha-synuclein reduces neurotransmitter release by inhibiting synaptic vesicle reclustering after endocytosis. *Neuron*, *65*(1), 66–79. https://doi.org/10.1016/j.neuron.2009.12.023

Nguyen, M., Wong, Y. C., Ysselstein, D., Severino, A., & Krainc, D. (2019). Synaptic, Mitochondrial, and Lysosomal Dysfunction in Parkinson's Disease. *Trends in Neurosciences*, *42*(2), 140–149. https://doi.org/10.1016/j.tins.2018.11.001

Nicoll, R. A., & Schmitz, D. (2005). Synaptic plasticity at hippocampal mossy fibre synapses. *Nature Reviews Neuroscience*, *6*(11), 863–876. https://doi.org/10.1038/nrn1786

Niu, H., Shen, L., Li, T., Ren, C., Ding, S., Wang, L., Zhang, Z., Liu, X., Zhang, Q., Geng, D., Wu, X., & Li, H. (2018). Alpha-synuclein overexpression in the olfactory bulb initiates prodromal symptoms and pathology of Parkinson's disease. *Translational Neurodegeneration*, *7*(1), 25. https://doi.org/10.1186/s40035-018-0128-6

Nobili, A., Latagliata, E. C., Viscomi, M. T., Cavallucci, V., Cutuli, D., Giacovazzo, G., Krashia, P., Rizzo, F. R., Marino, R., Federici, M., De Bartolo, P., Aversa, D., Dell'Acqua, M. C., Cordella, A., Sancandi, M., Keller, F., Petrosini, L., Puglisi-Allegra, S., Mercuri, N. B., … D'Amelio, M. (2017). Dopamine neuronal loss contributes to memory and reward dysfunction in a model of Alzheimer's disease. *Nature Communications*, *8*(1), 14727. https://doi.org/10.1038/ncomms14727

Nordenankar, K., Smith-Anttila, C. J. A., Schweizer, N., Viereckel, T., Birgner, C., Mejia-Toiber, J., Morales, M., Leao, R. N., & Wallén-Mackenzie, Å. (2015). Increased hippocampal excitability and impaired spatial memory function in mice lacking VGLUT2 selectively in neurons defined by tyrosine hydroxylase promoter activity. *Brain Structure and Function*, *220*(4), 2171–2190. https://doi.org/10.1007/s00429-014-0778-9

Noyce, A. J., Bestwick, J. P., Silveira-Moriyama, L., Hawkes, C. H., Giovannoni, G., Lees, A. J., & Schrag, A. (2012). Meta-analysis of early nonmotor features and risk factors for Parkinson disease. *Annals of Neurology*, *72*(6), 893–901. https://doi.org/10.1002/ana.23687

Ntamati, N. R., & Lüscher, C. (2016). VTA Projection Neurons Releasing GABA and Glutamate in the Dentate Gyrus. *Eneuro*, *3*(4), ENEURO.0137-16.2016. https://doi.org/10.1523/ENEURO.0137-16.2016

Nyitrai, H., Wang, S. S. H., & Kaeser, P. S. (2020). ELKS1 Captures Rab6-Marked Vesicular Cargo in Presynaptic Nerve Terminals. *Cell Reports*, *31*(10). https://doi.org/10.1016/j.celrep.2020.107712

O'Callaghan, C., & Lewis, S. J. G. (2017). Chapter Eighteen - Cognition in Parkinson's Disease. In K. R. Chaudhuri & N. B. T.-I. R. of N. Titova (Eds.), *Nonmotor Parkinson's: The Hidden Face* (Vol. 133, pp. 557–583). Academic Press. https://doi.org/https://doi.org/10.1016/bs.irn.2017.05.002

O'Carroll, C. M., & Morris, R. G. M. (2004). Heterosynaptic co-activation of glutamatergic and dopaminergic afferents is required to induce persistent long-term potentiation. *Neuropharmacology*, *47*(3), 324–332. https://doi.org/10.1016/j.neuropharm.2004.04.005

O'Day, D. H., Eshak, K., & Myre, M. A. (2015). Calmodulin Binding Proteins and Alzheimer's Disease. *Journal of Alzheimer's Disease : JAD*, *46*(3), 553–569. https://doi.org/10.3233/JAD-142772

Oades, R. D., & Halliday, G. M. (1987). Ventral tegmental (A10) system: neurobiology. 1. Anatomy and connectivity. *Brain Research*, *434*(2), 117–165. https://doi.org/10.1016/0165-0173(87)90011-7

Obeso, J. A., Rodríguez-Oroz, M. C., Rodríguez, M., Arbizu, J., & Giménez-Amaya, J. M. (2002). The Basal Ganglia and Disorders of Movement: Pathophysiological Mechanisms. *Physiology*, *17*(2), 51–55. https://doi.org/10.1152/nips.01363.2001

Oh, B. H., Moon, H. C., Kim, A., Kim, H. J., Cheong, C. J., & Park, Y. S. (2021). Prefrontal and hippocampal atrophy using 7-tesla magnetic resonance imaging in patients with Parkinson's disease. *Acta Radiologica Open*, *10*(2), 2058460120988097–2058460120988097. https://doi.org/10.1177/2058460120988097

Okano, M., Takahata, K., Sugimoto, J., & Muraoka, S. (2019). Selegiline Recovers Synaptic Plasticity in the Medial Prefrontal Cortex and Improves Corresponding Depression-Like Behavior in a Mouse Model of Parkinson's Disease . In *Frontiers in Behavioral Neuroscience* (Vol. 13, p. 176). https://www.frontiersin.org/article/10.3389/fnbeh.2019.00176

Oliveras-Salvá, M., Van der Perren, A., Casadei, N., Stroobants, S., Nuber, S., D'Hooge, R., Van den Haute, C., & Baekelandt, V. (2013). rAAV2/7 vector-mediated overexpression of alpha-synuclein in mouse substantia nigra induces protein aggregation and progressive dose-dependent neurodegeneration. *Molecular Neurodegeneration*, *8*(1), 44. https://doi.org/10.1186/1750-1326-8-44

Otmakhova, N. A., & Lisman, J. E. (1996). D1/D5 dopamine receptor activation increases the magnitude of early long-term potentiation at CA1 hippocampal synapses. *The Journal of Neuroscience : The Official Journal of the Society for Neuroscience*, *16*(23), 7478–7486. https://doi.org/10.1523/JNEUROSCI.16-23-07478.1996

Oughtred, R., Stark, C., Breitkreutz, B.-J., Rust, J., Boucher, L., Chang, C., Kolas, N., O'Donnell, L., Leung, G., McAdam, R., Zhang, F., Dolma, S., Willems, A., Coulombe-Huntington, J., Chatr-Aryamontri, A., Dolinski, K., & Tyers, M. (2019). The BioGRID interaction database: 2019 update. *Nucleic Acids Research*, *47*(D1), D529–D541. https://doi.org/10.1093/nar/gky1079

Ozelius, L. J., Senthil, G., Saunders-Pullman, R., Ohmann, E., Deligtisch, A., Tagliati, M., Hunt, A. L., Klein, C., Henick, B., Hailpern, S. M., Lipton, R. B., Soto-Valencia, J., Risch, N., & Bressman, S. B. (2006). LRRK2 G2019S as a Cause of Parkinson's Disease in Ashkenazi Jews. *New England Journal of Medicine*, *354*(4), 424–425. https://doi.org/10.1056/NEJMc055509

Pacelli, C., Giguère, N., Bourque, M.-J., Lévesque, M., Slack, R. S., & Trudeau, L.-É. (2015). Elevated Mitochondrial Bioenergetics and Axonal Arborization Size Are Key Contributors to the Vulnerability of Dopamine Neurons. *Current Biology*, *25*(18), 2349–2360. https://doi.org/10.1016/j.cub.2015.07.050

Pagonabarraga, J., Martinez-Horta, S., Fernández de Bobadilla, R., Pérez, J., Ribosa-Nogué, R., Marín, J., Pascual-Sedano, B., García, C., Gironell, A., & Kulisevsky, J. (2016). Minor hallucinations occur in drug-naive Parkinson's disease patients, even from the premotor phase. *Movement Disorders : Official Journal of the Movement Disorder Society*, *31*(1), 45–52. https://doi.org/10.1002/mds.26432

Paille, V., Picconi, B., Bagetta, V., Ghiglieri, V., Sgobio, C., Di Filippo, M., Viscomi, M. T., Giampa, C., Fusco, F. R., Gardoni, F., Bernardi, G., Greengard, P., Di Luca, M., & Calabresi, P. (2010). Distinct levels of dopamine denervation differentially alter striatal synaptic plasticity and NMDA receptor subunit composition. *The Journal of Neuroscience : The Official Journal of the Society for Neuroscience*, *30*(42), 14182–14193. https://doi.org/10.1523/JNEUROSCI.2149-10.2010

Pan, P.-Y., Cai, Q., Lin, L., Lu, P.-H., Duan, S., & Sheng, Z.-H. (2005). SNAP-29-mediated Modulation of Synaptic Transmission in CulturedHippocampalNeurons *. *Journal of Biological Chemistry*, *280*(27), 25769–25779. https://doi.org/10.1074/jbc.M502356200

Pang, S. Y.-Y., Ho, P. W.-L., Liu, H.-F., Leung, C.-T., Li, L., Chang, E. E. S., Ramsden, D. B., & Ho, S.-L. (2019). The interplay of aging, genetics and environmental factors in the pathogenesis of Parkinson's disease. *Translational Neurodegeneration*, *8*, 23. https://doi.org/10.1186/s40035-019-0165-9

Paoletti, P., Bellone, C., & Zhou, Q. (2013). NMDA receptor subunit diversity: impact on receptor properties, synaptic plasticity and disease. *Nature Reviews Neuroscience*, *14*(6), 383–400. https://doi.org/10.1038/nrn3504

Parkinson, J. (2002). An essay on the shaking palsy. 1817. *The Journal of Neuropsychiatry and Clinical Neurosciences*, *14*(2), 223–236; discussion 222. https://doi.org/10.1176/jnp.14.2.223

Patterson, J. R., Duffy, M. F., Kemp, C. J., Howe, J. W., Collier, T. J., Stoll, A. C., Miller, K. M., Patel, P., Levine, N., Moore, D. J., Luk, K. C., Fleming, S. M., Kanaan, N. M., Paumier, K. L., El-Agnaf, O. M. A., & Sortwell, C. E. (2019). Time course and magnitude of alpha-synuclein inclusion formation and nigrostriatal degeneration in the rat model of synucleinopathy triggered by intrastriatal α-synuclein preformed fibrils. *Neurobiology of Disease*, *130*, 104525. https://doi.org/https://doi.org/10.1016/j.nbd.2019.104525

Paumier, K. L., Luk, K. C., Manfredsson, F. P., Kanaan, N. M., Lipton, J. W., Collier, T. J., Steece-Collier, K., Kemp, C. J., Celano, S., Schulz, E., Sandoval, I. M., Fleming, S., Dirr, E., Polinski, N. K., Trojanowski, J. Q., Lee, V. M., & Sortwell, C. E. (2015). Intrastriatal injection of pre-formed mouse α-synuclein fibrils into rats triggers α-synuclein pathology and bilateral nigrostriatal degeneration. *Neurobiology of Disease*, *82*, 185–199. https://doi.org/10.1016/j.nbd.2015.06.003

Paumier, K. L., Sukoff Rizzo, S. J., Berger, Z., Chen, Y., Gonzales, C., Kaftan, E., Li, L., Lotarski, S., Monaghan, M., Shen, W., Stolyar, P., Vasilyev, D., Zaleska, M., D Hirst, W., & Dunlop, J. (2013). Behavioral characterization of A53T mice reveals early and late stage deficits related to Parkinson's disease. *PloS One*, *8*(8), e70274. https://doi.org/10.1371/journal.pone.0070274

Paxinos, G., & Watson, C. (1998). *The Rat Brain in Stereotaxic Coordinates, 4th Ed*. https://doi.org/10.1017/CBO9781107415324.004

Peelaerts, W., Bousset, L., Baekelandt, V., & Melki, R. (2018). α-Synuclein strains and seeding in Parkinson's disease, incidental Lewy body disease, dementia with Lewy bodies and multiple system atrophy: similarities and differences. *Cell and Tissue Research*, *373*(1), 195–212. https://doi.org/10.1007/s00441-018-2839-5

Peelaerts, W., Bousset, L., Van der Perren, A., Moskalyuk, A., Pulizzi, R., Giugliano, M., Van den Haute, C., Melki, R., & Baekelandt, V. (2015). α-Synuclein strains cause distinct synucleinopathies after local and systemic administration. *Nature*, *522*(7556), 340–344. https://doi.org/10.1038/nature14547

Pei, L., Lee, F. J. S., Moszczynska, A., Vukusic, B., & Liu, F. (2004). Regulation of Dopamine D1 Receptor Function by Physical Interaction with the NMDA Receptors. *The Journal of Neuroscience*, *24*(5), 1149 LP – 1158. https://doi.org/10.1523/JNEUROSCI.3922-03.2004

Pendolino, V., Bagetta, V., Ghiglieri, V., Sgobio, C., Morelli, E., Poggini, S., Branchi, I., Latagliata, E. C., Pascucci, T., Puglisi-Allegra, S., Calabresi, P., & Picconi, B. (2014). l-DOPA reverses the impairment of Dentate Gyrus LTD in experimental parkinsonism via β-adrenergic receptors. *Experimental Neurology*, *261*, 377–385. https://doi.org/10.1016/j.expneurol.2014.07.006

Pereira, J. B., Junqué, C., Bartrés-Faz, D., Ramírez-Ruiz, B., Marti, M.-J., & Tolosa, E. (2013). Regional vulnerability of hippocampal subfields and memory deficits in Parkinson's disease. *Hippocampus*, *23*(8), 720–728. https://doi.org/10.1002/hipo.22131

Pérez-Victoria, F. J., Mardones, G. A., & Bonifacino, J. S. (2008). Requirement of the Human GARP Complex for Mannose 6-phosphate-receptor-dependent Sorting of Cathepsin D to Lysosomes. *Molecular Biology of the Cell*, *19*(6), 2350–2362. https://doi.org/10.1091/mbc.e07-11-1189

Perez, R. G., Waymire, J. C., Lin, E., Liu, J. J., Guo, F., & Zigmond, M. J. (2002). A Role for α-Synuclein in the Regulation of Dopamine Biosynthesis. *The Journal of Neuroscience*, *22*(8), 3090 LP – 3099. https://doi.org/10.1523/JNEUROSCI.22-08-03090.2002

Pfeiffer, R. F. (2020). Autonomic Dysfunction in Parkinson's Disease. *Neurotherapeutics*, *17*(4), 1464–1479. https://doi.org/10.1007/s13311-020-00897-4

Phan, J.-A., Stokholm, K., Zareba-Paslawska, J., Jakobsen, S., Vang, K., Gjedde, A., Landau, A. M., & Romero-Ramos, M. (2017). Early synaptic dysfunction induced by α-synuclein in a rat model of Parkinson's disease. *Scientific Reports*, *7*(1), 6363. https://doi.org/10.1038/s41598-017-06724-9

Phelps, E. A. (2004). Human emotion and memory: interactions of the amygdala and hippocampal complex. *Current Opinion in Neurobiology*, *14*(2), 198–202. https://doi.org/https://doi.org/10.1016/j.conb.2004.03.015

Pifl, C., Rajput, A., Reither, H., Blesa, J., Cavada, C., Obeso, J. A., Rajput, A. H., & Hornykiewicz, O. (2014). Is Parkinson's disease a vesicular dopamine storage disorder? Evidence from a study in isolated synaptic vesicles of human and nonhuman primate striatum. *The Journal of Neuroscience : The Official Journal of the Society for Neuroscience*, *34*(24), 8210–8218. https://doi.org/10.1523/JNEUROSCI.5456-13.2014

Pissadaki, E., & Bolam, J. P. (2013). The energy cost of action potential propagation in dopamine neurons: clues to susceptibility in Parkinson's disease . In *Frontiers in Computational Neuroscience* (Vol. 7, p. 13). https://www.frontiersin.org/article/10.3389/fncom.2013.00013

Poewe, W., Seppi, K., Tanner, C. M., Halliday, G. M., Brundin, P., Volkmann, J., Schrag, A.-E., & Lang, A. E. (2017). Parkinson disease. *Nature Reviews. Disease Primers*, *3*, 17013. https://doi.org/10.1038/nrdp.2017.13

Polymeropoulos, M. H., Lavedan, C., Leroy, E., Ide, S. E., Dehejia, A., Dutra, A., Pike, B., Root, H., Rubenstein, J., Boyer, R., Stenroos, E. S., Chandrasekharappa, S., Athanassiadou, A., Papapetropoulos, T., Johnson, W. G., Lazzarini, A. M., Duvoisin, R. C., Di Iorio, G., Golbe, L. I., & Nussbaum, R. L. (1997). Mutation in the α-Synuclein Gene Identified in Families with Parkinson's Disease. *Science*, *276*(5321), 2045 LP – 2047. https://doi.org/10.1126/science.276.5321.2045

Pöschel, B., Wroblewska, B., Heinemann, U., & Manahan-Vaughan, D. (2005). The Metabotropic Glutamate Receptor mGluR3 is Critically Required for Hippocampal Long-term Depression and Modulates Long-term Potentiation in the Dentate Gyrus of Freely Moving Rats. *Cerebral Cortex*, *15*(9), 1414–1423. https://doi.org/10.1093/cercor/bhi022

Postuma, R. B., Aarsland, D., Barone, P., Burn, D. J., Hawkes, C. H., Oertel, W., & Ziemssen, T. (2012). Identifying prodromal Parkinson's disease: pre-motor disorders in Parkinson's disease. *Movement Disorders : Official Journal of the Movement Disorder Society*, *27*(5), 617–626. https://doi.org/10.1002/mds.24996

Postuma, R. B., & Berg, D. (2019). Prodromal Parkinson's Disease: The Decade Past, the Decade to Come. *Movement Disorders : Official Journal of the Movement Disorder Society*, *34*(5), 665–675. https://doi.org/10.1002/mds.27670

Postuma, R. B., Berg, D., Stern, M., Poewe, W., Olanow, C. W., Oertel, W., Obeso, J., Marek, K., Litvan, I., Lang, A. E., Halliday, G., Goetz, C. G., Gasser, T., Dubois, B., Chan, P., Bloem, B. R., Adler, C. H., & Deuschl, G. (2015). MDS clinical diagnostic criteria for Parkinson's disease. *Movement Disorders : Official Journal of the Movement Disorder Society*, *30*(12), 1591–1601. https://doi.org/10.1002/mds.26424

Prieto, G. A. (2017). Abnormalities of Dopamine D3 Receptor Signaling in the Diseased Brain. *Journal of Central Nervous System Disease*, *9*, 1179573517726335. https://doi.org/10.1177/1179573517726335

Prieto, G. A., Trieu, B. H., Dang, C. T., Bilousova, T., Gylys, K. H., Berchtold, N. C., Lynch, G., & Cotman, C. W. (2017). Pharmacological Rescue of Long-Term Potentiation in Alzheimer Diseased Synapses. *The Journal of Neuroscience : The Official Journal of the Society for Neuroscience*, *37*(5), 1197–1212. https://doi.org/10.1523/JNEUROSCI.2774-16.2016

Puighermanal, E., Biever, A., Espallergues, J., Gangarossa, G., De Bundel, D., & Valjent, E. (2015). drd2-cre:ribotag mouse line unravels the possible diversity of dopamine d2 receptor-expressing cells of the dorsal mouse hippocampus. *Hippocampus*, *25*(7), 858–875. https://doi.org/10.1002/hipo.22408

Purves, D., Augustine, G., Fitzpatrick, D., Hall, W. C., LaMantia, A., McNamara, J., & Williams, S. M. (2004). *Neuroscience, 3rd ed.*

Rahman, A. A., & Morrison, B. E. (2019). Contributions of VPS35 Mutations to Parkinson's Disease. *Neuroscience*, *401*, 1–10. https://doi.org/https://doi.org/10.1016/j.neuroscience.2019.01.006

Raj, K., Kaur, P., Gupta, G. D., & Singh, S. (2021). Metals associated neurodegeneration in Parkinson's disease: Insight to physiological, pathological mechanisms and management. *Neuroscience Letters*, *753*, 135873. https://doi.org/10.1016/j.neulet.2021.135873

Rajput, A. H., Rozdilsky, B., & Ang, L. (1991). Occurrence of resting tremor in Parkinson's disease. *Neurology*, *41*(8), 1298–1299. https://doi.org/10.1212/wnl.41.8.1298

Raslau, F. D., Mark, L. P., Sabsevitz, D. S., & Ulmer, J. L. (2015). Imaging of Functional and Dysfunctional Episodic Memory. *Seminars in Ultrasound, CT and MRI*, *36*(3), 260–274. https://doi.org/https://doi.org/10.1053/j.sult.2015.05.010

Rathore, A. S., Birla, H., Singh, S. Sen, Zahra, W., Dilnashin, H., Singh, R., Keshri, P. K., & Singh, S. P. (2021). Epigenetic Modulation in Parkinson's Disease and Potential Treatment Therapies. *Neurochemical Research*. https://doi.org/10.1007/s11064-021-03334-w

Rauch, J. N., Luna, G., Guzman, E., Audouard, M., Challis, C., Sibih, Y. E., Leshuk, C., Hernandez, I., Wegmann, S., Hyman, B. T., Gradinaru, V., Kampmann, M., & Kosik, K. S. (2020). LRP1 is a master regulator of tau uptake and spread. *Nature*, *580*(7803), 381–385. https://doi.org/10.1038/s41586-020-2156-5

Recasens, A., Dehay, B., Bové, J., Carballo-Carbajal, I., Dovero, S., Pérez-Villalba, A., Fernagut, P.-O., Blesa, J., Parent, A., Perier, C., Fariñas, I., Obeso, J. A., Bezard, E., & Vila, M. (2014). Lewy body extracts from Parkinson disease brains trigger α-synuclein pathology and neurodegeneration in mice and monkeys. *Annals of Neurology*, *75*(3), 351–362. https://doi.org/10.1002/ana.24066

Redgrave, P., Prescott, T. J., & Gurney, K. (1999). The basal ganglia: a vertebrate solution to the selection problem? *Neuroscience*, *89*(4), 1009–1023. https://doi.org/https://doi.org/10.1016/S0306-4522(98)00319-4

Rey, S., Marra, V., Smith, C., & Staras, K. (2020). Nanoscale Remodeling of Functional Synaptic Vesicle Pools in Hebbian Plasticity. *Cell Reports*, *30*(6), 2006-2017.e3. https://doi.org/10.1016/j.celrep.2020.01.051

Rial, D., Castro, A. A., Machado, N., Garção, P., Gonçalves, F. Q., Silva, H. B., Tomé, A. R., Köfalvi, A., Corti, O., Raisman-Vozari,

R., Cunha, R. A., & Prediger, R. D. (2014). Behavioral phenotyping of Parkin-deficient mice: looking for early preclinical features of Parkinson's disease. *PloS One*, *9*(12), e114216. https://doi.org/10.1371/journal.pone.0114216

Riddle, J. L., Rokosik, S. L., & Napier, T. C. (2012). Pramipexole- and methamphetamine-induced reward-mediated behavior in a rodent model of Parkinson's disease and controls. *Behavioural Brain Research*, *233*(1), 15–23. https://doi.org/https://doi.org/10.1016/j.bbr.2012.04.027

Rocchetti, J., Isingrini, E., Dal Bo, G., Sagheby, S., Menegaux, A., Tronche, F., Levesque, D., Moquin, L., Gratton, A., Wong, T. P., Rubinstein, M., & Giros, B. (2015). Presynaptic D2 dopamine receptors control long-term depression expression and memory processes in the temporal hippocampus. *Biological Psychiatry*, *77*(6), 513–525. https://doi.org/10.1016/j.biopsych.2014.03.013

Rodríguez-Chinchilla, T., Quiroga-Varela, A., Molinet-Dronda, F., Belloso-Iguerategui, A., Merino-Galan, L., Jimenez-Urbieta, H., Gago, B., & Rodriguez-Oroz, M. C. (2020). [(18)F]-DPA-714 PET as a specific in vivo marker of early microglial activation in a rat model of progressive dopaminergic degeneration. *European Journal of Nuclear Medicine and Molecular Imaging*, *47*(11), 2602–2612. https://doi.org/10.1007/s00259-020-04772-4

Rodriguez-Oroz, M. C. (2010). Deep brain stimulation for advanced Parkinson's disease. In *The Lancet. Neurology* (Vol. 9, Issue 6, pp. 558–559). https://doi.org/10.1016/S1474-4422(10)70108-3

Rodriguez-Oroz, M. C., Jahanshahi, M., Krack, P., Litvan, I., Macias, R., Bezard, E., & Obeso, J. A. (2009). Initial clinical manifestations of Parkinson's disease: features and pathophysiological mechanisms. *The Lancet. Neurology*, *8*(12), 1128–1139. https://doi.org/10.1016/S1474-4422(09)70293-5

Rolls, E. T. (2015). Limbic systems for emotion and for memory, but no single limbic system. *Cortex; a Journal Devoted to the Study of the Nervous System and Behavior*, *62*, 119–157. https://doi.org/10.1016/j.cortex.2013.12.005

Root, D. H., Estrin, D. J., & Morales, M. (2018). Aversion or Salience Signaling by Ventral Tegmental Area Glutamate Neurons. *IScience*, *2*, 51–62. https://doi.org/https://doi.org/10.1016/j.isci.2018.03.008

Rosborough, K., Patel, N., & Kalia, L. V. (2017). α-Synuclein and Parkinsonism: Updates and Future Perspectives. *Current Neurology and Neuroscience Reports*, *17*(4), 31. https://doi.org/10.1007/s11910-017-0737-y

Rosenbusch, K. E., & Kortholt, A. (2016). Activation Mechanism of LRRK2 and Its Cellular Functions in Parkinson's Disease. *Parkinson's Disease*, *2016*, 7351985. https://doi.org/10.1155/2016/7351985

Rubin, R. D., Watson, P. D., Duff, M. C., & Cohen, N. J. (2014). The role of the hippocampus in flexible cognition and social behavior . In *Frontiers in Human Neuroscience* (Vol. 8, p. 742). https://www.frontiersin.org/article/10.3389/fnhum.2014.00742

Rubio, M. D., Johnson, R., Miller, C. A., Huganir, R. L., & Rumbaugh, G. (2011). Regulation of synapse structure and function by distinct myosin II motors. *The Journal of Neuroscience : The Official Journal of the Society for Neuroscience*, *31*(4), 1448–1460. https://doi.org/10.1523/JNEUROSCI.3294-10.2011

Rudenko, G. (2017). Dynamic Control of Synaptic Adhesion and Organizing Molecules in Synaptic Plasticity. *Neural Plasticity*, *2017*, 6526151. https://doi.org/10.1155/2017/6526151

Rudolf, R., Bittins, C. M., & Gerdes, H.-H. (2011). The role of myosin V in exocytosis and synaptic plasticity. *Journal of Neurochemistry*, *116*(2), 177–191. https://doi.org/https://doi.org/10.1111/j.1471-4159.2010.07110.x

Ruiz-Martínez, J., Gorostidi, A., Ibañez, B., Alzualde, A., Otaegui, D., Moreno, F., de Munain, A. L., Bergareche, A., Gómez-Esteban, J. C., & Massó, J. F. M. (2010). Penetrance in Parkinson's disease related to the LRRK2 R1441G mutation in the Basque country (Spain). *Movement Disorders*, *25*(14), 2340–2345. https://doi.org/https://doi.org/10.1002/mds.23278

Sacktor, T. C. (2011). How does PKMζ maintain long-term memory? *Nature Reviews Neuroscience*, *12*(1), 9–15. https://doi.org/10.1038/nrn2949

Saheki, Y., & De Camilli, P. (2012). Synaptic vesicle endocytosis. *Cold Spring Harbor Perspectives in Biology*, *4*(9), a005645. https://doi.org/10.1101/cshperspect.a005645

Sanjari Moghaddam, H., Zare-Shahabadi, A., Rahmani, F., & Rezaei, N. (2017). Neurotransmission systems in Parkinson's disease. *Reviews in the Neurosciences*, *28*(5), 509–536. https://doi.org/10.1515/revneuro-2016-0068

Sarantis, K., Matsokis, N., & Angelatou, F. (2009). Synergistic interactions of dopamine D1 and glutamate NMDA receptors in rat hippocampus and prefrontal cortex: Involvement of ERK1/2 signaling. *Neuroscience*, *163*(4), 1135–1145. https://doi.org/https://doi.org/10.1016/j.neuroscience.2009.07.056

Sasaki, J., Kofuji, S., Itoh, R., Momiyama, T., Takayama, K., Murakami, H., Chida, S., Tsuya, Y., Takasuga, S., Eguchi, S., Asanuma, K., Horie, Y., Miura, K., Davies, E. M., Mitchell, C., Yamazaki, M., Hirai, H., Takenawa, T., Suzuki, A., & Sasaki,

T. (2010). The PtdIns(3,4)P2 phosphatase INPP4A is a suppressor of excitotoxic neuronal death. *Nature*, *465*(7297), 497–501. https://doi.org/10.1038/nature09023

Savino, E., Cervigni, R. I., Povolo, M., Stefanetti, A., Ferrante, D., Valente, P., Corradi, A., Benfenati, F., Guarnieri, F. C., & Valtorta, F. (2020). Proline-rich transmembrane protein 2 (PRRT2) regulates the actin cytoskeleton during synaptogenesis. *Cell Death & Disease*, *11*(10), 856. https://doi.org/10.1038/s41419-020-03073-w

Schapira, A. H. V. (2009). Neurobiology and treatment of Parkinson's disease. *Trends in Pharmacological Sciences*, *30*(1), 41–47. https://doi.org/10.1016/j.tips.2008.10.005

Schapira, A. H. V, Chaudhuri, K. R., & Jenner, P. (2017). Non-motor features of Parkinson disease. In *Nature reviews. Neuroscience* (Vol. 18, Issue 8, p. 509). https://doi.org/10.1038/nrn.2017.91

Scharfman, H., & Myers, C. (2013). Hilar mossy cells of the dentate gyrus: a historical perspective . In *Frontiers in Neural Circuits* (Vol. 6, p. 106). https://www.frontiersin.org/article/10.3389/fncir.2012.00106

Scheefhals, N., & MacGillavry, H. D. (2018). Functional organization of postsynaptic glutamate receptors. *Molecular and Cellular Neuroscience*, *91*, 82–94. https://doi.org/https://doi.org/10.1016/j.mcn.2018.05.002

Schepisi, C., Pignataro, A., Doronzio, S. S., Piccinin, S., Ferraina, C., Di Prisco, S., Feligioni, M., Pittaluga, A., Mercuri, N. B., Ammassari-Teule, M., Nisticò, R., & Nencini, P. (2016). Inhibition of hippocampal plasticity in rats performing contrafreeloading for water under repeated administrations of pramipexole. *Psychopharmacology*, *233*(4), 727–737. https://doi.org/10.1007/s00213-015-4150-4

Schneider, S. A., & Alcalay, R. N. (2017). Neuropathology of genetic synucleinopathies with parkinsonism: Review of the literature. *Movement Disorders : Official Journal of the Movement Disorder Society*, *32*(11), 1504–1523. https://doi.org/10.1002/mds.27193

Schultz, C., & Engelhardt, M. (2014). Anatomy of the hippocampal formation. *Frontiers of Neurology and Neuroscience*, *34*, 6–17. https://doi.org/10.1159/000360925

Schultz, W. (2002). Getting formal with dopamine and reward. *Neuron*, *36*(2), 241–263. https://doi.org/10.1016/s0896-6273(02)00967-4

Schulz-Schaeffer, W. J. (2010). The synaptic pathology of alpha-synuclein aggregation in dementia with Lewy bodies, Parkinson's disease and Parkinson's disease dementia. *Acta Neuropathologica*, *120*(2), 131–143. https://doi.org/10.1007/s00401-010-0711-0

Schweinhardt, P., Fransson, P., Olson, L., Spenger, C., & Andersson, J. L. R. (2003). A template for spatial normalisation of MR images of the rat brain. *Journal of Neuroscience Methods*, *129*(2), 105–113. https://doi.org/10.1016/s0165-0270(03)00192-4

Scott, D., & Roy, S. (2012). α-Synuclein Inhibits Intersynaptic Vesicle Mobility and Maintains Recycling-Pool Homeostasis. *The Journal of Neuroscience*, *32*(30), 10129 LP – 10135. https://doi.org/10.1523/JNEUROSCI.0535-12.2012

Seegobin, S. P., Heaton, G. R., Liang, D., Choi, I., Blanca Ramirez, M., Tang, B., & Yue, Z. (2020). Progress in LRRK2-Associated Parkinson's Disease Animal Models . In *Frontiers in Neuroscience* (Vol. 14, p. 674). https://www.frontiersin.org/article/10.3389/fnins.2020.00674

Sesack, S. R., & Grace, A. A. (2010). Cortico-Basal Ganglia reward network: microcircuitry. *Neuropsychopharmacology : Official Publication of the American College of Neuropsychopharmacology*, *35*(1), 27–47. https://doi.org/10.1038/npp.2009.93

Shahmoradian, S. H., Lewis, A. J., Genoud, C., Hench, J., Moors, T. E., Navarro, P. P., Castaño-Díez, D., Schweighauser, G., Graff-Meyer, A., Goldie, K. N., Sütterlin, R., Huisman, E., Ingrassia, A., Gier, Y. de, Rozemuller, A. J. M., Wang, J., Paepe, A. De, Erny, J., Staempfli, A., … Lauer, M. E. (2019). Lewy pathology in Parkinson's disease consists of crowded organelles and lipid membranes. *Nature Neuroscience*, *22*(7), 1099–1109. https://doi.org/10.1038/s41593-019-0423-2

Sheng, M., & Kim, E. (2011). The postsynaptic organization of synapses. *Cold Spring Harbor Perspectives in Biology*, *3*(12). https://doi.org/10.1101/cshperspect.a005678

Shepherd, J. D., & Huganir, R. L. (2007). The Cell Biology of Synaptic Plasticity: AMPA Receptor Trafficking. *Annual Review of Cell and Developmental Biology*, *23*(1), 613–643. https://doi.org/10.1146/annurev.cellbio.23.090506.123516

Shevchenko, A., Tomas, H., Havlis, J., Olsen, J. V, & Mann, M. (2006). In-gel digestion for mass spectrometric characterization of proteins and proteomes. *Nature Protocols*, *1*(6), 2856–2860. https://doi.org/10.1038/nprot.2006.468

Shi, M.-M., Shi, C.-H., & Xu, Y.-M. (2017). Rab GTPases: The Key Players in the Molecular Pathway of Parkinson's Disease.

Frontiers in Cellular Neuroscience, *11*, 81. https://doi.org/10.3389/fncel.2017.00081

Shi, M., Movius, J., Dator, R., Aro, P., Zhao, Y., Pan, C., Lin, X., Bammler, T. K., Stewart, T., Zabetian, C. P., Peskind, E. R., Hu, S.-C., Quinn, J. F., Galasko, D. R., & Zhang, J. (2015). Cerebrospinal Fluid Peptides as Potential Parkinson Disease Biomarkers: A Staged Pipeline for Discovery and Validation *[S]. *Molecular & Cellular Proteomics*, *14*(3), 544–555. https://doi.org/10.1074/mcp.M114.040576

Shilov, I. V, Seymour, S. L., Patel, A. A., Loboda, A., Tang, W. H., Keating, S. P., Hunter, C. L., Nuwaysir, L. M., & Schaeffer, D. A. (2007). The Paragon Algorithm, a next generation search engine that uses sequence temperature values and feature probabilities to identify peptides from tandem mass spectra. *Molecular & Cellular Proteomics : MCP*, *6*(9), 1638–1655. https://doi.org/10.1074/mcp.T600050-MCP200

Shinohara, M., Fujioka, S., Murray, M. E., Wojtas, A., Baker, M., Rovelet-Lecrux, A., Rademakers, R., Das, P., Parisi, J. E., Graff-Radford, N. R., Petersen, R. C., Dickson, D. W., & Bu, G. (2014). Regional distribution of synaptic markers and APP correlate with distinct clinicopathological features in sporadic and familial Alzheimer's disease. *Brain*, *137*(5), 1533–1549. https://doi.org/10.1093/brain/awu046

Shohamy, D., & Adcock, R. A. (2010). Dopamine and adaptive memory. *Trends in Cognitive Sciences*, *14*(10), 464–472. https://doi.org/10.1016/j.tics.2010.08.002

Siderowf, A., & Lang, A. E. (2012). Premotor Parkinson's disease: concepts and definitions. *Movement Disorders : Official Journal of the Movement Disorder Society*, *27*(5), 608–616. https://doi.org/10.1002/mds.24954

Sidransky, E., & Lopez, G. (2012). The link between the GBA gene and parkinsonism. *The Lancet. Neurology*, *11*(11), 986–998. https://doi.org/10.1016/S1474-4422(12)70190-4

Simon, D. K., Tanner, C. M., & Brundin, P. (2020). Parkinson Disease Epidemiology, Pathology, Genetics, and Pathophysiology. *Clinics in Geriatric Medicine*, *36*(1), 1–12. https://doi.org/10.1016/j.cger.2019.08.002

Singh, B., Covelo, A., Martell-Martínez, H., Nanclares, C., Sherman, M. A., Okematti, E., Meints, J., Teravskis, P. J., Gallardo, C., Savonenko, A. V, Benneyworth, M. A., Lesné, S. E., Liao, D., Araque, A., & Lee, M. K. (2019). Tau is required for progressive synaptic and memory deficits in a transgenic mouse model of α-synucleinopathy. *Acta Neuropathologica*, *138*(4), 551–574. https://doi.org/10.1007/s00401-019-02032-w

Singleton, A. B., Farrer, M., Johnson, J., Singleton, A., Hague, S., Kachergus, J., Hulihan, M., Peuralinna, T., Dutra, A., Nussbaum, R., Lincoln, S., Crawley, A., Hanson, M., Maraganore, D., Adler, C., Cookson, M. R., Muenter, M., Baptista, M., Miller, D., … Gwinn-Hardy, K. (2003). alpha-Synuclein locus triplication causes Parkinson's disease. *Science (New York, N.Y.)*, *302*(5646), 841. https://doi.org/10.1126/science.1090278

Smith, C., Malek, N., Grosset, K., Cullen, B., Gentleman, S., & Grosset, D. G. (2019). Neuropathology of dementia in patients with Parkinson's disease: a systematic review of autopsy studies. *Journal of Neurology, Neurosurgery & Psychiatry*, *90*(11), 1234 LP – 1243. https://doi.org/10.1136/jnnp-2019-321111

Smith, W. B., Starck, S. R., Roberts, R. W., & Schuman, E. M. (2005). Dopaminergic Stimulation of Local Protein Synthesis Enhances Surface Expression of GluR1 and Synaptic Transmission in Hippocampal Neurons. *Neuron*, *45*(5), 765–779. https://doi.org/10.1016/j.neuron.2005.01.015

Soukup, S.-F., Vanhauwaert, R., & Verstreken, P. (2018). Parkinson's disease: convergence on synaptic homeostasis. *The EMBO Journal*, *37*(18), e98960. https://doi.org/https://doi.org/10.15252/embj.201898960

Spillantini, M. G., Crowther, R. A., Jakes, R., Hasegawa, M., & Goedert, M. (1998). α-Synuclein in filamentous inclusions of Lewy bodies from Parkinson's disease and dementia with Lewy bodies. *Proceedings of the National Academy of Sciences*, *95*(11), 6469 LP – 6473. https://doi.org/10.1073/pnas.95.11.6469

Squire, L. R., Stark, C. E. L., & Clark, R. E. (2004). THE MEDIAL TEMPORAL LOBE. *Annual Review of Neuroscience*, *27*(1), 279–306. https://doi.org/10.1146/annurev.neuro.27.070203.144130

Srivastava, A., Bala, S., Motomura, H., Kohda, D., Tama, F., & Miyashita, O. (2020). Conformational ensemble of an intrinsically flexible loop in mitochondrial import protein Tim21 studied by modeling and molecular dynamics simulations. *Biochimica et Biophysica Acta. General Subjects*, *1864*(2), 129417. https://doi.org/10.1016/j.bbagen.2019.129417

Steeves, T. D. L., Miyasaki, J., Zurowski, M., Lang, A. E., Pellecchia, G., Van Eimeren, T., Rusjan, P., Houle, S., & Strafella, A. P. (2009). Increased striatal dopamine release in Parkinsonian patients with pathological gambling: a [11C] raclopride PET study. *Brain : A Journal of Neurology*, *132*(Pt 5), 1376–1385. https://doi.org/10.1093/brain/awp054

Steinkellner, T., Zell, V., Farino, Z. J., Sonders, M. S., Villeneuve, M., Freyberg, R. J., Przedborski, S., Lu, W., Freyberg, Z., & Hnasko, T. S. (2018). Role for VGLUT2 in selective vulnerability of midbrain dopamine neurons. *The Journal of Clinical Investigation*, *128*(2), 774–788. https://doi.org/10.1172/JCI95795

Steulet, A.-F., Bemasconi, R., Leonhardt, T., Martin, P., Grünenwald, C., Bischoff, S., Heinrich, M., Bandelier, V., & Maître, L. (1990). Effects of selective dopamine D1 and D2 receptor agonists on the rate of GABA synthesis in mouse brain. *European Journal of Pharmacology*, *191*(1), 19–27. https://doi.org/https://doi.org/10.1016/0014-2999(90)94092-C

Südhof, T. C. (2012a). Calcium control of neurotransmitter release. *Cold Spring Harbor Perspectives in Biology*, *4*(1), a011353–a011353. https://doi.org/10.1101/cshperspect.a011353

Südhof, T. C. (2012b). The presynaptic active zone. *Neuron*, *75*(1), 11–25. https://doi.org/10.1016/j.neuron.2012.06.012

Südhof, T. C. (2013). Neurotransmitter release: the last millisecond in the life of a synaptic vesicle. *Neuron*, *80*(3), 675–690. https://doi.org/10.1016/j.neuron.2013.10.022

Südhof, T. C. (2017). Synaptic Neurexin Complexes: A Molecular Code for the Logic of Neural Circuits. *Cell*, *171*(4), 745–769. https://doi.org/10.1016/j.cell.2017.10.024

Südhof, T. C. (2018). Towards an Understanding of Synapse Formation. *Neuron*, *100*(2), 276–293. https://doi.org/https://doi.org/10.1016/j.neuron.2018.09.040

Südhof, T. C., & Rizo, J. (2011). Synaptic vesicle exocytosis. *Cold Spring Harbor Perspectives in Biology*, *3*(12). https://doi.org/10.1101/cshperspect.a005637

Sui, Y.-T., Bullock, K. M., Erickson, M. A., Zhang, J., & Banks, W. A. (2014). Alpha synuclein is transported into and out of the brain by the blood–brain barrier. *Peptides*, *62*, 197–202. https://doi.org/https://doi.org/10.1016/j.peptides.2014.09.018

Sultana, R., Banks, W. A., & Butterfield, D. A. (2010). Decreased levels of PSD95 and two associated proteins and increased levels of BCl2 and caspase 3 in hippocampus from subjects with amnestic mild cognitive impairment: Insights into their potential roles for loss of synapses and memory, accumulation of Aβ,. *Journal of Neuroscience Research*, *88*(3), 469–477. https://doi.org/https://doi.org/10.1002/jnr.22227

Sulzer, D., & Surmeier, D. J. (2013). Neuronal vulnerability, pathogenesis, and Parkinson's disease. *Movement Disorders : Official Journal of the Movement Disorder Society*, *28*(1), 41–50. https://doi.org/10.1002/mds.25095

Surguchov, A. (2021). Invertebrate Models Untangle the Mechanism of Neurodegeneration in Parkinson's Disease. *Cells*, *10*(2). https://doi.org/10.3390/cells10020407

Surmeier, D. J., Obeso, J. A., & Halliday, G. M. (2017). Selective neuronal vulnerability in Parkinson disease. *Nature Reviews. Neuroscience*, *18*(2), 101–113. https://doi.org/10.1038/nrn.2016.178

Swant, J., Goodwin, J. S., North, A., Ali, A. A., Gamble-George, J., Chirwa, S., & Khoshbouei, H. (2011). α-Synuclein Stimulates a Dopamine Transporter-dependent Chloride Current and Modulates the Activity of the Transporter * . *Journal of Biological Chemistry*, *286*(51), 43933–43943. https://doi.org/10.1074/jbc.M111.241232

Swant, J., Stramiello, M., & Wagner, J. J. (2008). Postsynaptic dopamine D3 receptor modulation of evoked IPSCs via GABA(A) receptor endocytosis in rat hippocampus. *Hippocampus*, *18*(5), 492–502. https://doi.org/10.1002/hipo.20408

Swant, J., & Wagner, J. J. (2006). Dopamine transporter blockade increases LTP in the CA1 region of the rat hippocampus via activation of the D3 dopamine receptor. *Learning & Memory (Cold Spring Harbor, N.Y.)*, *13*(2), 161–167. https://doi.org/10.1101/lm.63806

Sweet, E. S., Saunier-Rebori, B., Yue, Z., & Blitzer, R. D. (2015). The Parkinson's Disease-Associated Mutation LRRK2-G2019S Impairs Synaptic Plasticity in Mouse Hippocampus. *The Journal of Neuroscience*, *35*(32), 11190 LP – 11195. https://doi.org/10.1523/JNEUROSCI.0040-15.2015

Tagliaferro, P., & Burke, R. E. (2016). Retrograde Axonal Degeneration in Parkinson Disease. *Journal of Parkinson's Disease*, *6*(1), 1–15. https://doi.org/10.3233/JPD-150769

Taguchi, K., Watanabe, Y., Tsujimura, A., Tatebe, H., Miyata, S., Tokuda, T., Mizuno, T., & Tanaka, M. (2014). Differential Expression of Alpha-Synuclein in Hippocampal Neurons. *PLOS ONE*, *9*(2), e89327. https://doi.org/10.1371/journal.pone.0089327

Takeuchi, T., Duszkiewicz, A. J., Sonneborn, A., Spooner, P. A., Yamasaki, M., Watanabe, M., Smith, C. C., Fernández, G., Deisseroth, K., Greene, R. W., & Morris, R. G. M. (2016). Locus coeruleus and dopaminergic consolidation of everyday memory. *Nature*, *537*(7620), 357–362. https://doi.org/10.1038/nature19325

Tang, W. H., Shilov, I. V, & Seymour, S. L. (2008). Nonlinear fitting method for determining local false discovery rates from decoy database searches. *Journal of Proteome Research*, *7*(9), 3661–3667. https://doi.org/10.1021/pr070492f

Tanji, K., Mori, F., Mimura, J., Itoh, K., Kakita, A., Takahashi, H., & Wakabayashi, K. (2010). Proteinase K-resistant alpha-

synuclein is deposited in presynapses in human Lewy body disease and A53T alpha-synuclein transgenic mice. *Acta Neuropathologica*, *120*(2), 145–154. https://doi.org/10.1007/s00401-010-0676-z

Tatulli, G., Mitro, N., Cannata, S. M., Audano, M., Caruso, D., D'Arcangelo, G., Lettieri-Barbato, D., & Aquilano, K. (2018). Intermittent Fasting Applied in Combination with Rotenone Treatment Exacerbates Dopamine Neurons Degeneration in Mice . In *Frontiers in Cellular Neuroscience* (Vol. 12, p. 4). https://www.frontiersin.org/article/10.3389/fncel.2018.00004

Taylor, S. R., Badurek, S., Dileone, R. J., Nashmi, R., Minichiello, L., & Picciotto, M. R. (2014). GABAergic and glutamatergic efferents of the mouse ventral tegmental area. *Journal of Comparative Neurology*, *522*(14), 3308–3334. https://doi.org/https://doi.org/10.1002/cne.23603

Teravskis, P. J., Covelo, A., Miller, E. C., Singh, B., Martell-Martínez, H. A., Benneyworth, M. A., Gallardo, C., Oxnard, B. R., Araque, A., Lee, M. K., & Liao, D. (2018). A53T Mutant Alpha-Synuclein Induces Tau-Dependent Postsynaptic Impairment Independently of Neurodegenerative Changes. *The Journal of Neuroscience : The Official Journal of the Society for Neuroscience*, *38*(45), 9754–9767. https://doi.org/10.1523/JNEUROSCI.0344-18.2018

Thakur, P., Breger, L. S., Lundblad, M., Wan, O. W., Mattsson, B., Luk, K. C., Lee, V. M. Y., Trojanowski, J. Q., & Björklund, A. (2017). Modeling Parkinson's disease pathology by combination of fibril seeds and α-synuclein overexpression in the rat brain. *Proceedings of the National Academy of Sciences of the United States of America*, *114*(39), E8284–E8293. https://doi.org/10.1073/pnas.1710442114

Thomas, G. M., & Huganir, R. L. (2004). MAPK cascade signalling and synaptic plasticity. *Nature Reviews Neuroscience*, *5*(3), 173–183. https://doi.org/10.1038/nrn1346

Tiraboschi, P., Hansen, L. A., Alford, M., Sabbagh, M. N., Schoos, B., Masliah, E., Thal, L. J., & Corey-Bloom, J. (2000). Cholinergic dysfunction in diseases with Lewy bodies. *Neurology*, *54*(2), 407 LP – 407. https://doi.org/10.1212/WNL.54.2.407

Tolosa, E., Vila, M., Klein, C., & Rascol, O. (2020). LRRK2 in Parkinson disease: challenges of clinical trials. *Nature Reviews Neurology*, *16*(2), 97–107. https://doi.org/10.1038/s41582-019-0301-2

Tozzi, A., Costa, C., Siliquini, S., Tantucci, M., Picconi, B., Kurz, A., Gispert, S., Auburger, G., & Calabresi, P. (2012). Mechanisms underlying altered striatal synaptic plasticity in old A53T-α synuclein overexpressing mice. *Neurobiology of Aging*, *33*(8), 1792–1799. https://doi.org/10.1016/j.neurobiolaging.2011.05.002

Tozzi, A., de Iure, A., Bagetta, V., Tantucci, M., Durante, V., Quiroga-Varela, A., Costa, C., Di Filippo, M., Ghiglieri, V., Latagliata, E. C., Wegrzynowicz, M., Decressac, M., Giampa, C., Dalley, J. W., Xia, J., Gardoni, F., Mellone, M., El-Agnaf, O. M., Ardah, M. T., … Calabresi, P. (2016). Alpha-Synuclein Produces Early Behavioral Alterations via Striatal Cholinergic Synaptic Dysfunction by Interacting With GluN2D N-Methyl-D-Aspartate Receptor Subunit. *Biological Psychiatry*, *79*(5), 402–414. https://doi.org/10.1016/j.biopsych.2015.08.013

Traynelis, S. F., Wollmuth, L. P., McBain, C. J., Menniti, F. S., Vance, K. M., Ogden, K. K., Hansen, K. B., Yuan, H., Myers, S. J., & Dingledine, R. (2010). Glutamate Receptor Ion Channels: Structure, Regulation, and Function. *Pharmacological Reviews*, *62*(3), 405 LP – 496. https://doi.org/10.1124/pr.109.002451

Trugman, J. M., James, C. L., & Wooten, G. F. (1991). D1/D2 dopamine receptor stimulation by L-dopa. A [14C]-2-deoxyglucose autoradiographic study. *Brain : A Journal of Neurology*, *114 (Pt 3*, 1429–1440. https://doi.org/10.1093/brain/114.3.1429

Uchida, S., & Shumyatsky, G. P. (2015). Deceivingly dynamic: Learning-dependent changes in stathmin and microtubules. *Neurobiology of Learning and Memory*, *124*, 52–61. https://doi.org/https://doi.org/10.1016/j.nlm.2015.07.011

Uemura, N., Ueda, J., Yoshihara, T., Ikuno, M., Uemura, M. T., Yamakado, H., Asano, M., Trojanowski, J. Q., & Takahashi, R. (2021). α-Synuclein Spread from Olfactory Bulb Causes Hyposmia, Anxiety, and Memory Loss in BAC-SNCA Mice. *Movement Disorders*, *n/a*(n/a). https://doi.org/https://doi.org/10.1002/mds.28512

Ulusoy, A., Bjorklund, T., Hermening, S., & Kirik, D. (2008). In vivo gene delivery for development of mammalian models for Parkinson's disease. *Experimental Neurology*, *209*(1), 89–100. https://doi.org/https://doi.org/10.1016/j.expneurol.2007.09.011

Ulusoy, A., Decressac, M., Kirik, D., & Björklund, A. (2010). Viral vector-mediated overexpression of α-synuclein as a progressive model of Parkinson's disease. In *Progress in Brain Research* (Vol. 184, Issue C). Elsevier B.V. https://doi.org/10.1016/S0079-6123(10)84005-1

Valente, P., Castroflorio, E., Rossi, P., Fadda, M., Sterlini, B., Cervigni, R. I., Prestigio, C., Giovedì, S., Onofri, F., Mura, E., Guarnieri, F. C., Marte, A., Orlando, M., Zara, F., Fassio, A., Valtorta, F., Baldelli, P., Corradi, A., & Benfenati, F. (2016). PRRT2 Is a Key Component of the Ca^{2+}-Dependent Neurotransmitter Release Machinery. *Cell Reports*, *15*(1), 117–131. https://doi.org/10.1016/j.celrep.2016.03.005

van de Berg, W. D. J., Hepp, D. H., Dijkstra, A. A., Rozemuller, J. A. M., Berendse, H. W., & Foncke, E. (2012). Patterns of alpha-synuclein pathology in incidental cases and clinical subtypes of Parkinson's disease. *Parkinsonism & Related Disorders*, *18*, S28–S30. https://doi.org/https://doi.org/10.1016/S1353-8020(11)70011-6

van der Putten, H., Wiederhold, K. H., Probst, A., Barbieri, S., Mistl, C., Danner, S., Kauffmann, S., Hofele, K., Spooren, W. P., Ruegg, M. A., Lin, S., Caroni, P., Sommer, B., Tolnay, M., & Bilbe, G. (2000). Neuropathology in mice expressing human alpha-synuclein. *The Journal of Neuroscience : The Official Journal of the Society for Neuroscience*, *20*(16), 6021–6029. https://doi.org/10.1523/JNEUROSCI.20-16-06021.2000

van Diggelen, F., Hrle, D., Apetri, M., Christiansen, G., Rammes, G., Tepper, A., & Otzen, D. E. (2019). Two conformationally distinct α-synuclein oligomers share common epitopes and the ability to impair long-term potentiation. *PLOS ONE*, *14*(3), e0213663. https://doi.org/10.1371/journal.pone.0213663

Van Kampen, J. M., & Robertson, H. A. (2017). The BSSG rat model of Parkinson's disease: progressing towards a valid, predictive model of disease. *The EPMA Journal*, *8*(3), 261–271. https://doi.org/10.1007/s13167-017-0114-6

Vanni, S., Colini Baldeschi, A., Zattoni, M., & Legname, G. (2020). Brain aging: A Ianus-faced player between health and neurodegeneration. *Journal of Neuroscience Research*, *98*(2), 299–311. https://doi.org/10.1002/jnr.24379

Vargas, K. J., Makani, S., Davis, T., Westphal, C. H., Castillo, P. E., & Chandra, S. S. (2014). Synucleins Regulate the Kinetics of Synaptic Vesicle Endocytosis. *The Journal of Neuroscience*, *34*(28), 9364 LP – 9376. https://doi.org/10.1523/JNEUROSCI.4787-13.2014

Vargas, K. J., Schrod, N., Davis, T., Fernandez-Busnadiego, R., Taguchi, Y. V, Laugks, U., Lucic, V., & Chandra, S. S. (2017). Synucleins Have Multiple Effects on Presynaptic Architecture. *Cell Reports*, *18*(1), 161–173. https://doi.org/10.1016/j.celrep.2016.12.023

Varkey, J., Isas, J. M., Mizuno, N., Jensen, M. B., Bhatia, V. K., Jao, C. C., Petrlova, J., Voss, J. C., Stamou, D. G., Steven, A. C., & Langen, R. (2010). Membrane curvature induction and tubulation are common features of synucleins and apolipoproteins. *The Journal of Biological Chemistry*, *285*(42), 32486–32493. https://doi.org/10.1074/jbc.M110.139576

Vermilyea, S. C., & Emborg, M. E. (2015). α-Synuclein and nonhuman primate models of Parkinson's disease. *Journal of Neuroscience Methods*, *255*, 38–51. https://doi.org/https://doi.org/10.1016/j.jneumeth.2015.07.025

Vermilyea, S. C., Guthrie, S., Hernandez, I., Bondarenko, V., & Emborg, M. E. (2019). α-Synuclein Expression Is Preserved in Substantia Nigra GABAergic Fibers of Young and Aged Neurotoxin-Treated Rhesus Monkeys. *Cell Transplantation*, *28*(4), 379–387. https://doi.org/10.1177/0963689719835794

Vickers, C. A., Dickson, K. S., & Wyllie, D. J. A. (2005). Induction and maintenance of late-phase long-term potentiation in isolated dendrites of rat hippocampal CA1 pyramidal neurones. *The Journal of Physiology*, *568*(Pt 3), 803–813. https://doi.org/10.1113/jphysiol.2005.092924

Vila, M. (2019). Neuromelanin, aging, and neuronal vulnerability in Parkinson's disease. *Movement Disorders : Official Journal of the Movement Disorder Society*, *34*(10), 1440–1451. https://doi.org/10.1002/mds.27776

Villalobo, A., Ishida, H., Vogel, H. J., & Berchtold, M. W. (2018). Calmodulin as a protein linker and a regulator of adaptor/scaffold proteins. *Biochimica et Biophysica Acta. Molecular Cell Research*, *1865*(3), 507–521. https://doi.org/10.1016/j.bbamcr.2017.12.004

Villar-Conde, S., Astillero-Lopez, V., Gonzalez-Rodriguez, M., Villanueva-Anguita, P., Saiz-Sanchez, D., Martinez-Marcos, A., Flores-Cuadrado, A., & Ubeda-Bañon, I. (2021). The Human Hippocampus in Parkinson's Disease: An Integrative Stereological and Proteomic Study. *Journal of Parkinson's Disease*, *Preprint*, 1–20. https://doi.org/10.3233/JPD-202465

Volpicelli-Daley, L. A., Kirik, D., Stoyka, L. E., Standaert, D. G., & Harms, A. S. (2016). How can rAAV-alpha-synuclein and the fibril alpha-synuclein models advance our understanding of Parkinson disease? *Journal of Neurochemistry*. https://doi.org/10.1111/jnc.13627

Volta, M., Cataldi, S., Beccano-Kelly, D., Munsie, L., Tatarnikov, I., Chou, P., Bergeron, S., Mitchell, E., Lim, R., Khinda, J., Lloret, A., Bennett, C. F., Paradiso, C., Morari, M., Farrer, M. J., & Milnerwood, A. J. (2015). Chronic and acute LRRK2 silencing has no long-term behavioral effects, whereas wild-type and mutant LRRK2 overexpression induce motor and cognitive deficits and altered regulation of dopamine release. *Parkinsonism & Related Disorders*, *21*(10), 1156–1163. https://doi.org/https://doi.org/10.1016/j.parkreldis.2015.07.025

Voon, V., Gao, J., Brezing, C., Symmonds, M., Ekanayake, V., Fernandez, H., Dolan, R. J., & Hallett, M. (2011a). Dopamine agonists and risk: impulse control disorders in Parkinson's; disease. *Brain*, *134*(5), 1438–1446. https://doi.org/10.1093/brain/awr080

Voon, V., Mehta, A. R., & Hallett, M. (2011b). Impulse control disorders in Parkinson's disease: recent advances. *Current Opinion in Neurology*, *24*(4), 324–330. https://doi.org/10.1097/WCO.0b013e3283489687

Voon, V., Napier, T. C., Frank, M. J., Sgambato-Faure, V., Grace, A. A., Rodriguez-Oroz, M., Obeso, J., Bezard, E., & Fernagut, P.-O. (2017). Impulse control disorders and levodopa-induced dyskinesias in Parkinson's disease: an update. *The Lancet. Neurology*, *16*(3), 238–250. https://doi.org/10.1016/S1474-4422(17)30004-2

Voon, V., Rizos, A., Chakravartty, R., Mulholland, N., Robinson, S., Howell, N. A., Harrison, N., Vivian, G., & Ray Chaudhuri, K. (2014). Impulse control disorders in Parkinson's disease: decreased striatal dopamine transporter levels. *Journal of Neurology, Neurosurgery &Amp; Psychiatry*, *85*(2), 148 LP – 152. https://doi.org/10.1136/jnnp-2013-305395

Wagner, L. M., Nathwani, S. M., Ten Eyck, P. P., & Aldridge, G. M. (2020). Local cortical overexpression of human wild-type alpha-synuclein leads to increased dendritic spine density in mouse. *Neuroscience Letters*, *733*, 135051. https://doi.org/10.1016/j.neulet.2020.135051

Waites, C., Qu, X., & Bartolini, F. (2021). The synaptic life of microtubules. *Current Opinion in Neurobiology*, *69*, 113–123. https://doi.org/https://doi.org/10.1016/j.conb.2021.03.004

Waldeyer, W. von. (1891). Uber einige neuere Forshungen im Gebiete der Anatomie des centralen Nervensystems. *Deutsch. Med. Wochenschr*, *17*, 1213–1218; 1244–1246; 1267–1269; 1331–1332; 1352–1.

Waltereit, R., & Weller, M. (2003). Signaling from cAMP/PKA to MAPK and synaptic plasticity. *Molecular Neurobiology*, *27*(1), 99–106. https://doi.org/10.1385/MN:27:1:99

Wang, C., Zhao, C., Li, D., Tian, Z., Lai, Y., Diao, J., & Liu, C. (2016). Versatile Structures of α-Synuclein . In *Frontiers in Molecular Neuroscience* (Vol. 9, p. 48). https://www.frontiersin.org/article/10.3389/fnmol.2016.00048

Wang, Y., Chandran, J. S., Cai, H., & Mattson, M. P. (2008). DJ-1 is essential for long-term depression at hippocampal CA1 synapses. *Neuromolecular Medicine*, *10*(1), 40–45. https://doi.org/10.1007/s12017-008-8023-4

Weber, B., Fouad, K., Burger, C., & Buck, A. (2002). White matter glucose metabolism during intracortical electrostimulation: a quantitative [(18)F]Fluorodeoxyglucose autoradiography study in the rat. *NeuroImage*, *16*(4), 993–998. https://doi.org/10.1006/nimg.2002.1104

Weingarten, J., Weingarten, M., Wegner, M., & Volknandt, W. (2017). APP—A Novel Player within the Presynaptic Active Zone Proteome . In *Frontiers in Molecular Neuroscience* (Vol. 10, p. 43). https://www.frontiersin.org/article/10.3389/fnmol.2017.00043

Weintraub, D., & Claassen, D. O. (2017). Impulse Control and Related Disorders in Parkinson's Disease. *International Review of Neurobiology*, *133*, 679–717. https://doi.org/10.1016/bs.irn.2017.04.006

Weintraub, D., Koester, J., Potenza, M. N., Siderowf, A. D., Stacy, M., Voon, V., Whetteckey, J., Wunderlich, G. R., & Lang, A. E. (2010). Impulse control disorders in Parkinson disease: a cross-sectional study of 3090 patients. *Archives of Neurology*, *67*(5), 589–595. https://doi.org/10.1001/archneurol.2010.65

Wellington, H., Paterson, R. W., Portelius, E., Törnqvist, U., Magdalinou, N., Fox, N. C., Blennow, K., Schott, J. M., & Zetterberg, H. (2016). Increased CSF neurogranin concentration is specific to Alzheimer disease. *Neurology*, *86*(9), 829–835. https://doi.org/10.1212/WNL.0000000000002423

Wenthold, R. J., Petralia, R. S., Blahos J, I. I., & Niedzielski, A. S. (1996). Evidence for multiple AMPA receptor complexes in hippocampal CA1/CA2 neurons. *The Journal of Neuroscience*, *16*(6), 1982 LP – 1989. https://doi.org/10.1523/JNEUROSCI.16-06-01982.1996

West, M. J. (1999). Stereological methods for estimating the total number of neurons and synapses: Issues of precision and bias. *Trends in Neurosciences*, *22*(2), 51–61. https://doi.org/10.1016/S0166-2236(98)01362-9

Wigström, H., & Gustafsson, B. (1983). Facilitated induction of hippocampal long-lasting potentiation during blockade of inhibition. *Nature*, *301*(5901), 603–604. https://doi.org/10.1038/301603a0

Wilhelmus, M. M. M., Bol, J. G. J. M., Van Haastert, E. S., Rozemuller, A. J. M., Bu, G., Drukarch, B., & Hoozemans, J. J. M. (2011). Apolipoprotein E and LRP1 Increase Early in Parkinson's Disease Pathogenesis. *The American Journal of Pathology*, *179*(5), 2152–2156. https://doi.org/10.1016/j.ajpath.2011.07.021

Wilson, H., Pagano, G., de Natale, E. R., Mansur, A., Caminiti, S. P., Polychronis, S., Middleton, L. T., Price, G., Schmidt, K. F., Gunn, R. N., Rabiner, E. A., & Politis, M. (2020). Mitochondrial Complex 1, Sigma 1, and Synaptic Vesicle 2A in Early Drug-Naive Parkinson's Disease. *Movement Disorders : Official Journal of the Movement Disorder Society*, *35*(8), 1416–1427. https://doi.org/10.1002/mds.28064

Wisman, L. A. B., Sahin, G., Maingay, M., Leanza, G., & Kirik, D. (2008). Functional Convergence of Dopaminergic and

Cholinergic Input Is Critical for Hippocampus-Dependent Working Memory. *The Journal of Neuroscience*, *28*(31), 7797 LP – 7807. https://doi.org/10.1523/JNEUROSCI.1885-08.2008

Wittmann, B. C., Schott, B. H., Guderian, S., Frey, J. U., Heinze, H.-J., & Düzel, E. (2005). Reward-related FMRI activation of dopaminergic midbrain is associated with enhanced hippocampus-dependent long-term memory formation. *Neuron*, *45*(3), 459–467. https://doi.org/10.1016/j.neuron.2005.01.010

Wong, Y. C., Luk, K., Purtell, K., Burke Nanni, S., Stoessl, A. J., Trudeau, L.-E., Yue, Z., Krainc, D., Oertel, W., Obeso, J. A., & Volpicelli-Daley, L. A. (2019). Neuronal vulnerability in Parkinson disease: Should the focus be on axons and synaptic terminals? *Movement Disorders : Official Journal of the Movement Disorder Society*, *34*(10), 1406–1422. https://doi.org/10.1002/mds.27823

Woodard, G. E., Jardín, I., Berna-Erro, A., Salido, G. M., & Rosado, J. A. (2015). *Chapter Three - Regulators of G-Protein-Signaling Proteins: Negative Modulators of G-Protein-Coupled Receptor Signaling* (K. W. B. T.-I. R. of C. and M. B. Jeon (Ed.); Vol. 317, pp. 97–183). Academic Press. https://doi.org/https://doi.org/10.1016/bs.ircmb.2015.02.001

Xia, Z., & Storm, D. R. (2005). The role of calmodulin as a signal integrator for synaptic plasticity. *Nature Reviews Neuroscience*, *6*(4), 267–276. https://doi.org/10.1038/nrn1647

Xicoy, H., Brouwers, J. F., Wieringa, B., & Martens, G. J. M. (2020). Explorative Combined Lipid and Transcriptomic Profiling of Substantia Nigra and Putamen in Parkinson's Disease. *Cells*, *9*(9). https://doi.org/10.3390/cells9091966

Xiong, Y., Neifert, S., Karuppagounder, S. S., Liu, Q., Stankowski, J. N., Lee, B. D., Ko, H. S., Lee, Y., Grima, J. C., Mao, X., Jiang, H., Kang, S.-U., Swing, D. A., Iacovitti, L., Tessarollo, L., Dawson, T. M., & Dawson, V. L. (2018). Robust kinase- and age-dependent dopaminergic and norepinephrine neurodegeneration in LRRK2 G2019S transgenic mice. *Proceedings of the National Academy of Sciences*, *115*(7), 1635 LP – 1640. https://doi.org/10.1073/pnas.1712648115

Xu, R., Hu, X., Jiang, X., Zhang, Y., Wang, J., & Zeng, X. (2020). Longitudinal volume changes of hippocampal subfields and cognitive decline in Parkinson's disease. *Quantitative Imaging in Medicine and Surgery*, *10*(1), 220–232. https://doi.org/10.21037/qims.2019.10.17

Yang, P., Perlmutter, J. S., Benzinger, T. L. S., Morris, J. C., & Xu, J. (2020). Dopamine D3 receptor: A neglected participant in Parkinson Disease pathogenesis and treatment? *Ageing Research Reviews*, *57*, 100994. https://doi.org/https://doi.org/10.1016/j.arr.2019.100994

Yang, Y., & Wang, J.-Z. (2017). From Structure to Behavior in Basolateral Amygdala-Hippocampus Circuits . In *Frontiers in Neural Circuits* (Vol. 11, p. 86). https://www.frontiersin.org/article/10.3389/fncir.2017.00086

Yoo, J. H., Zell, V., Gutierrez-Reed, N., Wu, J., Ressler, R., Shenasa, M. A., Johnson, A. B., Fife, K. H., Faget, L., & Hnasko, T. S. (2016). Ventral tegmental area glutamate neurons co-release GABA and promote positive reinforcement. *Nature Communications*, *7*(1), 13697. https://doi.org/10.1038/ncomms13697

Yu, Q., Liu, Y.-Z., Zhu, Y.-B., Wang, Y.-Y., Li, Q., & Yin, D.-M. (2019). Genetic labeling reveals temporal and spatial expression pattern of D2 dopamine receptor in rat forebrain. *Brain Structure and Function*, *224*(3), 1035–1049. https://doi.org/10.1007/s00429-018-01824-2

Yu, X., Li, W., Ma, Y., Tossell, K., Harris, J. J., Harding, E. C., Ba, W., Miracca, G., Wang, D., Li, L., Guo, J., Chen, M., Li, Y., Yustos, R., Vyssotski, A. L., Burdakov, D., Yang, Q., Dong, H., Franks, N. P., & Wisden, W. (2019). GABA and glutamate neurons in the VTA regulate sleep and wakefulness. *Nature Neuroscience*, *22*(1), 106–119. https://doi.org/10.1038/s41593-018-0288-9

Zaja-Milatovic, S., Milatovic, D., Schantz, A. M., Zhang, J., Montine, K. S., Samii, A., Deutch, A. Y., & Montine, T. J. (2005). Dendritic degeneration in neostriatal medium spiny neurons in Parkinson disease. *Neurology*, *64*(3), 545–547. https://doi.org/10.1212/01.WNL.0000150591.33787.A4

Zarei, M., Ibarretxe-Bilbao, N., Compta, Y., Hough, M., Junque, C., Bargallo, N., Tolosa, E., & Martí, M. J. (2013). Cortical thinning is associated with disease stages and dementia in Parkinson's disease. *Journal of Neurology, Neurosurgery, and Psychiatry*, *84*(8), 875–881. https://doi.org/10.1136/jnnp-2012-304126

Zhang, J., Sun, X., Zheng, S., Liu, X., Jin, J., Ren, Y., & Luo, J. (2014). Myelin Basic Protein Induces Neuron-Specific Toxicity by Directly Damaging the Neuronal Plasma Membrane. *PLOS ONE*, *9*(9), e108646. https://doi.org/10.1371/journal.pone.0108646

Zhang, Zhentao, Kang, S. S., Liu, X., Ahn, E. H., Zhang, Z., He, L., Iuvone, P. M., Duong, D. M., Seyfried, N. T., Benskey, M. J., Manfredsson, F. P., Jin, L., Sun, Y. E., Wang, J.-Z., & Ye, K. (2017). Asparagine endopeptidase cleaves α-synuclein and mediates pathologic activities in Parkinson's disease. *Nature Structural & Molecular Biology*, *24*(8), 632–642. https://doi.org/10.1038/nsmb.3433

Zhang, Zhu, Zhang, S., Fu, P., Zhang, Z., Lin, K., Ko, J. K., & Yung, K. K. (2019). Roles of Glutamate Receptors in Parkinson's

Disease. In *International Journal of Molecular Sciences* (Vol. 20, Issue 18). https://doi.org/10.3390/ijms20184391

Zhou, Y., Zhou, B., Pache, L., Chang, M., Khodabakhshi, A. H., Tanaseichuk, O., Benner, C., & Chanda, S. K. (2019). Metascape provides a biologist-oriented resource for the analysis of systems-level datasets. *Nature Communications*, *10*(1), 1523. https://doi.org/10.1038/s41467-019-09234-6

Zhu, G., Chen, Y., Huang, Y., Li, Q., & Behnisch, T. (2011). MPTP-meditated hippocampal dopamine deprivation modulates synaptic transmission and activity-dependent synaptic plasticity. *Toxicology and Applied Pharmacology*, *254*(3), 332–341. https://doi.org/10.1016/j.taap.2011.05.007

Zou, L., Zhang, X., Xiong, M., Meng, L., Tian, Y., Pan, L., Yuan, X., Chen, G., Wang, Z., Bu, L., Yao, Z., Zhang, Z., Ye, K., & Zhang, Z. (2021). Asparagine endopeptidase cleaves synaptojanin 1 and triggers synaptic dysfunction in Parkinson's disease. *Neurobiology of Disease*, *154*, 105326. https://doi.org/10.1016/j.nbd.2021.105326

Zucker, R. S., & Regehr, W. G. (2002). Short-term synaptic plasticity. *Annual Review of Physiology*, *64*, 355–405. https://doi.org/10.1146/annurev.physiol.64.092501.114547

Annex

Antibodies

The antibodies used for the detection of proteins in immunohistochemistry and immunofluorescence studies are listed in Tables 7 and 8, those used in flow cytometry studies in Tables 9 and 10, and those used for Western Blots are listed in Tables 11 and 12. All of them specify the antigen against which they react, the host species, the species reactivity, the clone, the isotype, the conjugate, the dilution used in the experiments, and the reference of the commercial company.

Table 7. Primary antibodies used for immunohistochemistry (IHC) and immunofluorescence (IF).

Antigen	Host species	Species reactivity*	Clone	Isotype	Dilution	Reference
α-syn	Mouse	H	Monoclonal (LB509)	IgG1k	IHC: 1:500 IF: 1:1000	Invitrogen, #180215
DAT	Goat	H, M, R	Polyclonal	IgG	1:100	Santa Cruz Biotechnology, sc-1433
GABA	Rabbit	H, M, R	Polyclonal	IgG	1:3000	GeneTex, #GTX125988
TH	Mouse	R	Monoclonal (2/40/15)	IgG2a	1:1000	Millipore, #MAB5280
TH	Rabbit	H, M, R	Polyclonal	IgG	1:1000	Merck, #AB152
vGlut2	Guinea pig	M, R	Polyclonal	IgG	1:500	Synaptic Systems, #135-404

*We only show the following species: H, human; M, mouse; R, rat.

Table 8. Secondary antibodies used for immunohistochemistry (IHC) and immunofluorescence (IF).

Target	Production species	Conjugate	Isotype	Dilution	Reference
Goat	Rabbit	Biotinylated	IgG	1:500	Vector Laboratories, #BA5000
Mouse	Horse	Biotinylated	IgG	hα-syn: 1:300 TH: 1:500	Vector Laboratories, #BA2000
Guinea pig	Goat	Alexa Fluor 594	IgG	1:1000	Invitrogen, #A11076
Mouse	Donkey	Alexa Fluor 546	IgG	1:1000	Invitrogen, #A10036
Mouse	Donkey	Alexa Fluor 647	IgG	1:1000	Invitrogen, #A31571
Rabbit	Goat	Alexa Fluor 488	IgG	1:1000	Invitrogen, #A11034

Table 9. Primary antibodies used for flow cytometry.

Antigen	Host species	Species reactivity*	Clone	Isotype	Dilution	Reference
GluA1	Rabbit	M, R	Monoclonal (D4N9V)	IgG	1:1500	Cell Signaling Technology, #13185S
Nrx1β	Mouse	H, M, R	Monoclonal (N170A/1)	IgG1	1:400	NeuroMab, #75-216

*We only show the following species: H, human; M, mouse; R, rat.

Table 10. Secondary antibodies used for flow cytometry.

Target	Production species	Conjugate	Isotype	Dilution	Reference
Mouse	Goat	Alexa Fluor 647	IgG	1:800	Invitrogen, #A21240
Rabbit	Goat	Brilliant Violet 421	IgG	1:400	Jackson ImmunoResearch, #111-675-144

Table 11. Primary antibodies used for Western Blot.

Antigen	Host species	Species reactivity*	Clone	Isotype	Dilution	Reference
α-syn	Mouse	H	Monoclonal (Syn211)	IgG1k	1:2000	Invitrogen, #32-8100
GAPDH	Mouse	H, M, R	Monoclonal (6C5)	IgG1	1:10000	Merck, #MAB374

*We only show the following species: H, human; M, mouse; R, rat.

Table 12. Secondary antibodies used for Western Blot.

Target	Production species	Conjugate	Isotype	Dilution	Reference
Mouse	Goat	HRP	IgG	hα-syn: 1:2000 GAPDH: 1:10000	Cell Signaling Technology, #7076

Buffers

The following section summarizes the composition of buffers used in the different experiments of this work, arranged by techniques.

General buffers

0.1 M Phosphate Buffer (0.1 M PB)

25 mM NaH_2PO_4-H_2O and 75 mM Na_2HPO_4-$2H_2O$; pH 7.4

0.01 M Phosphate Buffer (0.01 M PB)

2.5 mM NaH_2PO_4-H_2O and 7.5 mM Na_2HPO_4-$2H_2O$; pH 7.4

0.1 M Phosphate Buffer Saline (0.1 M PBS)

150 mM NaCl; diluted in 0.1 M PB, pH 7.4

Histology

4% Paraformaldehyde (4% PFA)

4% PFA; dissolved in 0.1 M PB, pH 7.4

Cryoprotectant solution (fixed brains)

30% sucrose and 3 mM sodium azide; diluted in 0.1 M PBS, pH 7.4

Cryoprotectant solution (fixed coronal sections)

30% ethylene glycol, 30% glycerol and 0.01 M PB; pH 7.4

FASS-LTP

Sucrose Buffer

320 mM sucrose, 10 mM HEPES, [1:1000] protease inhibitor cocktail (Sigma-Aldrich, #P8340), and [1:100] phosphatase inhibitor cocktail (Thermo Fisher Scientific, #78420); pH 7.4

Extracellular Solution

120 mM NaCl, 3 mM KCl, 2 mM $CaCl_2$, 2 mM $MgCl_2$, 15 mM glucose, and 15 mM HEPES; pH 7.4

cLTP solution

125 mM NaCl, 5 mM KCl, 2 mM $CaCl_2$, 30 mM glucose, and 10 mM HEPES; pH 7.4

Buffer A

250 mM sucrose, 5 mM $MgCl_2$, and 10 mM Tris; pH 7.4

Buffer B

2 M sucrose, 1 mM $MgCl_2$, and 10 mM Tris; pH 7.4

Buffer C

200 mM sucrose, 10 mM Tris, 1 mM EGTA, and [1:1000] protease inhibitor cocktail (Sigma-Aldrich, #P8340); pH 7.4

Glycine Solution

5 mM glycine, 0.01 mM strychnine (Sigma-Aldrich, #S0532), and 0.2 mM bicuculline methiodide (Sigma-Aldrich, #14343); diluted in cLTP solution

KCl solution

50 mM NaCl, 100 mM KCl, 2 mM $CaCl_2$, 30 mM glucose, 0.5 mM glycine, 10 mM HEPES, 0.001 mM strychnine (Sigma-Aldrich, #S0532), and 0.02 mM bicuculline methiodide (Sigma-Aldrich, #14343); pH 7.4

Western Blot

2% Sodium Dodecyl Sulfate Buffer (2% SDS buffer)

10 mM Tris, 2% SDS, [1:1000] protease inhibitor cocktail (Sigma-Aldrich, #P8340), and [1:100] phosphatase inhibitor cocktail (Thermo Fisher Scientific, #78420); pH 7.4

Loading Buffer 4x

1.25 M Tris, 40% glycerol, 8% SDS, 0.04% bromophenol blue, and 5% 2-mercaptoethanol; pH 6.8

Lysis Buffer

25 mM HEPES, 150 mM NaCl, 1% Triton X-100, and 5 mM EDTA; pH 7.4

Electrophoresis Buffer

25 mM Tris, 190 mM glycine, and 0.15% SDS

Transfer buffer 1X (Trans-Blot Turbo RTA Mini PVDF Transfer Kit)

20% Bio-Rad's Transfer buffer 5X and 20% ethanol

Tris Buffer Saline (TBS)

20 mM Tris and 140 mM NaCl; pH 7.6

Proteomics

Buffer D

10 mM HEPES, 320 mM sucrose, 1 mM $MgCl_2$, 1 mM EGTA, [1:1000] protease inhibitor cocktail (Sigma-Aldrich, #P8340), and [1:100] phosphatase inhibitor cocktail (Thermo Fisher Scientific, #78420); pH 7.4

Buffer E

10 mM HEPES, 1.4 M sucrose, and phenol red; pH 7.4

Lysis Buffer

7 M urea, 2 M thiourea, and 50 mM DTT

MS Buffer

2% acetonitrile, and 0.5% formic acid; diluted in MilliQ-water

** All buffers were diluted in distilled water, unless otherwise specified.*

biodonostia
osasun ikerketa institutua
instituto de investigación sanitaria

eman ta zabal zazu
Universidad del País Vasco
Euskal Herriko Unibertsitatea

Cima Universidad de Navarra